Synthesis and characterisation of polythersulphone poly(dimethyl siloxane) block copolymers.

NORTHERN, Michael A.

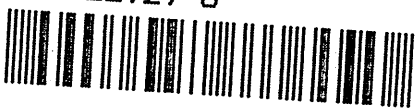

ProQuest LLC.
789 East Eisenhower Parkway
P.O. Box 1346
Ann Arbor, MI 48106 – 1346

SYNTHESIS AND CHARACTERISATION OF POLYETHERSULPHONE-POLY(DIMETHYL SILOXANE) BLOCK COPOLYMERS.

by

Michael Antony Northern BSc, CChem, MRSC.

A thesis submitted in partial fulfilment of the requirements of the Council for National Academic Awards for the degree of Doctor of Philosophy.

June 1991.

Sponsoring Establishment: Sheffield City Polytechnic,
(School of Science,
Division of Chemistry).

Collaborating Establishment: Imperial Chemical Industries plc,
Wilton.

SYNTHESIS AND CHARACTERISATION OF POLYETHERSULPHONE - POLY(DIMETHYL SILOXANE) BLOCK COPOLYMERS.

M A Northern, School of Science, Sheffield City Polytechnic.

ABSTRACT.

The objectives of this project were to investigate synthetic routes to form block copolymers of polyethersulphone and polydimethylsiloxane, linked through ≡Si-C≡ bonds.

The work carried out has included the synthesis and characterisation of hydroxyl terminated polyethersulphone oligomers (PES). This material has then been quantitatively functionalised to give vinyl ended PES.

A number of hydride terminated polydimethylsiloxane oligomers (PDMS) have also been synthesised and characterised. These materials have been successfully functionalised with epoxy groups through a vinyl addition reaction in the presence of chloroplatinic acid catalyst, incorporating the ≡Si-C≡ bond into the PDMS.

These polymers, along with purchased carboxy propyl PDMS allowed the investigation of three principle routes to PES/PDMS copolymers:-

(i) the catalysed addition reaction of vinyl PES with hydride terminated PDMS.

(ii) the reaction of hydroxyl terminated PES with epoxy functionalised PDMS.

(iii) the condensation reaction of hydroxyl terminated PES with carboxy propyl PDMS in the presence of stannous octoate catalyst.

All three routes produce $(A\text{-}B)_n$ PES/PDMS block copolymers linked through ≡Si-C≡ bonds.

Due to the large difference in solubility parameters between PES and PDMS homopolymers, there is great difficulty in producing a homogeneous solution of the reacting polymers. A wide range of solvent systems were investigated before 1,1,2,2-tetrachloroethane (TCE) was found to be the most suitable. Routes (i) and (ii) were investigated as solution reactions in TCE and the reaction products characterised by proton nuclear magnetic resonance spectroscopy (^{1}H nmr) and differential scanning calorimetry (dsc). Both reactions showed only limited success. Route (iii) could not be investigated in solution as a homogeneous solution of the oligomers could not be formed.

All three synthetic routes were investigated as reactions in the melt and the products characterised by ^{1}H nmr and dsc. Routes (ii) and (iii) proving to be the more successful.

All three reaction schemes were examined extensively using model compounds and short chain polymeric oligomers and were shown to be suitable routes to form the required block copolymers.

ACKNOWLEDGEMENTS.

The author wishes to thank Dr K Dodgson and Dr DW Clegg for their advice and guidance during the period of study for this thesis.

He is also grateful to all the members of the Department of Chemistry, Sheffield City Polytechnic for their help and generous assistance and to Dr AA Collyer for his encouragement throughout this project.

The author also wishes to thank the staff of ICI (Advanced Materials Group), Wilton, in particular Dr DG Parker, Mr B Spence and Mr A Bunn for their technical and material support throughout the project and for making my visits to Wilton most rewarding.

Thanks are also due to the members of the reasearch staff of Sheffield City Polytechnic, in particular Mr I Walker, Mr S Cockett, Mr S Marsden and Mr R Broughton for many happy hours of lively discussion and help in the laboratory.

Many thanks are also due to Mrs S Northern for all her encouragement and practical help throughout the preparation of this thesis.

The author would like to acknowledge the funding provided by SERC and ICI plc for this project.

INDEX.

This thesis presents a survey of the literature in Chapters 2 and 3 following a general introduction to the project. Chapter 4 contains the experimental work and discusses the results, the conclusions of which are in Chapter 5. The references cited in this thesis are listed on pages 203-213 and the figures referred to in the experimental work are presented together sequentially on pages 214-315.

1. INTRODUCTION.

ICI (Chemicals and Polymers) currently market poly(oxy-1,4-phenylenesulphonyl-1,4-phenylene) under the trade name "Victrex" polyethersulphone (PES).

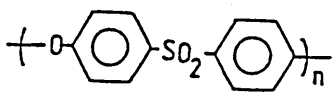

As a member of the aromatic sulphone group of engineering thermoplastics, it is composed of aromatic rings giving high thermal stability and rigidity (1). These rings are joined by sulphone and ether links introducing sufficient flexibility to the polymer chains that PES shows thermoplasticity below the decomposition temperature without the loss of thermal stability (2).

As well as high thermal stability, PES exhibits low flammability and smoke emission, but like most other thermoplastics it is notch sensitive. To extend its applications in the aerospace industry, a better notched response is required, but there must be no loss of the thermal stability or low gas and smoke emission properties for which PES is well within the specifications given by the aerospace industry (3). Obviously the development of a toughened grade of PES would provide further inroads into the important automotive and aerospace markets.

The impact strength may be improved by incorporating additional groups into the backbone of the polymer, but this

would result in changes in the polymer properties, not all of which would be beneficial e.g. any increase or decrease in the glass transition temperature. A better method of improving the notch sensitivity of the polymer would be to blend PES with an impact modifier. Blending rubber materials with brittle plastics can create huge improvements in the toughness of the brittle plastic if a number of criteria are met; the most important of these being the problem of compatibility. Simply blending two polymers together usually results in delamination of the ploymers due to the incompatibility of the polymers involved.

The most suitable method of improving the impact strength and reducing the notch sensitivity of PES, is to introduce an additive to the PES matrix in which the impact modifier is chemically bonded to some material compatible with the PES matrix. In this way, it should be possible to improve the dispersity and adhesion of the modifier within the matrix, so resulting in an improved, toughened product.

Work of this type has been carried out to toughen many different brittle polymers including polysulphone (4-18) and polyethersulphone (19). This work has been based upon copolymers of the arylenesulphone and poly(dimethylsiloxane). The siloxane provides the rubber toughening properties of the copolymers and the arylenesulphone the adhesion to the host matrix. The link between the siloxane and the arylenesulphone has been through silicon-oxygen-carbon bonds (≡Si-O-C≡) which

are extremely hydrolytically unstable in the presence of moisture and both acids and alkalis, especially at the high temperatures required to process these polymers (19-26). Consequently, this thesis reports the examination of synthetic routes to form block copolymers linked via more hydrolytically stable bonds in order to prepare a material with which to rubber toughen polyethersulphone.

This has involved the synthesis and characterisation of a number of polyethersulphone and siloxane rubber samples. These materials have been functionalised and characterised in order to investigate the principle synthetic routes to prepare hydrolytically stable block copoloymers. Model reactions were carried out to demonstrate that each route would be suitable to prepare the required copolymers and to help characterise the resultant copolymeric products.

Coplymerisations were investigated as reactions in both solution and in the melt. The products were characterised to determine the success of the reactions.

2. RUBBER TOUGHENING OF POLYMERS.

2.1 Polyethersulphones.

In recent years there has been a considerable amount of interest in polyarylenesulphone polymers as a source of "high performance" engineering thermoplastics (27-29). Their development stemmed from the requirement of materials which displayed the high temperature stability of thermosets as well as the ease of processing of thermoplastics. These materials would ideally be processed in conventional injection moulding equipment and have properties superior to polycarbonate.

The search for plastics of this type led to polymers composed of linked aromatic rings which possess the required high thermal and oxidative stability. The aromatic rings have to be linked by a group which is sufficiently flexible to allow themoplasticity below the decomposition temperature, but without any loss of the thermal stability. The sulphone group provides these properties to some extent, but a polymer consisting of phenylene rings linked by sulphone groups alone would be too rigid to exhibit thermoplasticity (30,31).

Three routes to polyethersulphones were discovered independently and almost simultaneously by the 3M Corporation, Union Carbide Corporation and ICI Plastics Division UK.

Product	Repeat Unit
Astrel 360M (3M)	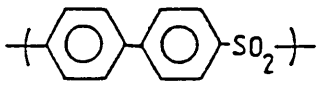 and 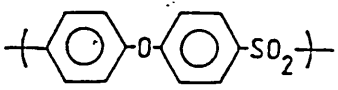
Tg=285°C	First repeat unit predominates
Udel Polysulphone (Union Carbide) Tg=190°C	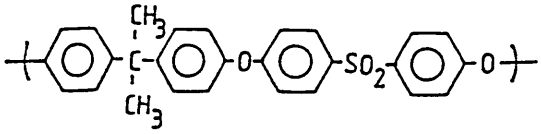
Victrex PES (ICI) Tg=230°C	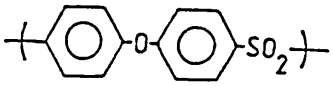

The introduction of ether linkages (and isopropylidene linkages in the case of Udel Polysulphone) reduces the softening temperature of the polymers. As the proportion of these linkages increases, there is a progressive reduction in the Tg of the polymer and therefore an increase in thermoplasticity. The Tg of Astrel 360 is significantly higher than the Victrex or Udel material because it contains less ether linkages per repeat unit. Astrel 360 cannot be processed by conventional injection moulding machinary and is no longer available commercially.

These amorphous polymers all contain a highly resonant diarylsulphone group in the para position. The sulphur atom is in its highest oxidation state which enables these polymers to exhibit the required oxidation resistance, high thermal

stability and rigidity. The phenyl rings also give the structure high strength, temperature resistance and structural rigidity (32). This high temperature stability is required for high temperature moulding and extrusion processes as well as during its end use. The ether linkages permit rotation of the backbone chain, allowing processing at usable temperatures below the degradation temperature of the arylsulphone groups; which is >500°C (28). The incorporation of the isopropylidene group in Udel polysulphone improves the melt processing by increasing the flexibility of the backbone chain and hence reducing the Tg (33).

ICI Victrex polyethersulphone has found uses in many fields, replacing ceramics, metals and thermosetting plastics. At room temperature it is typical of engineering thermoplastics being rigid, strong tough and has excellent load bearing properties. It has very good electrical insulation properties coupled with heat resistance, flame resistance, non-burning behaviour and low smoke emission (27,28). These properties have led to Victrex PES being used as coil formers, connectors, terminal blocks, printed circuit boards (which resist soldering heat), passenger cabin components, radomes, pump housings, reflectors, bearings, microwave ovens, chemical pump linings, metal coatings, medical components and matrices for composite materials (27,28,34). Victrex PES possesses the strengths and weaknesses of amorphous thermoplastics including notch sensitivity, particularly when in use as a structural adhesive

or as a composite matrix. Failure is mainly governed by flaw growth and subsequent crack propagation (27,31,35). An improvement in this physical property would be a major advantage over competitive materials and would lead to increased use in the substantial aerospace and automotive markets, where materials such as polycarbonate-co-polydimethylsiloxane/polyimide blends are already being used in window frames, air vents and luggage compartments.

One way this could be achieved would be to modify the backbone structure of the material or introduce crystallites to the structure. This would change the balance between high temperature stability and processability as shown by comparing Astrel 360 polysulphone and Victrex PES. The introduction of the extra phenylene groups in Astrel 360 increases the impact strength, but at the expense of increasing the Tg by 70°C and rendering the material unprocessable by normal injection moulding equipment (27).

It has been known for many years that brittle thermoplastics in the glassy state may be toughened by incorporating a dispersed elastomeric phase into the thermoplastic matrix. Toughened forms of high temperature engineering thermoplastics are rare, because the chemistry involved is difficult and the incorporation of rubber in the matrix of these materials generally reduces temperature resistance (3). The production of a toughened grade of Victrex PES would not only have the potential for substantial

commercial success, but would prove easier to launch as a toughened grade of an existing product already in the market place, rather than a totally new product. Other promising commercial advantages of a rubber toughened grade of Victrex PES would be that the production requirements may be similar to those already existing for Victrex PES and the development costs for a totally new polymer are prohibitively high.

Increasingly the modification of existing polymers has attracted widespread commercial interest, particularly through the blending of two or more existing polymers to obtain new products. This approach has proved successful for example in the production of toughened PVC, a blend of PVC and rubber. High impact polystyrene (HIPS) and acrylonitrile-butadiene-styrene (ABS) are both commercial plastics whose properties are attributed to the combination of rubber with a more brittle thermoplastic (36).

2.2 Toughening Mechanisms.

Various theories have been proposed to explain the toughening of polymers with rubber particles, including energy absorption by the rubber (37), crack termination at the rubber particles (36), matrix crazing (36,38-40), shear yielding (41,42), and combinations of crazing and yielding (36,39,41,43,44). It is apparent from these studies that the form of specimen failure varies between different polymers and polymer blends. Generally, brittle polymers such as

crazing is that it is an energy absorbing process and therefore leads to a toughened material response through increased energy absorption. Crazing is frequently a precursor to brittle fracture of a polymer through the crazes coalescing to produce a crack in the material (48). It is important to realise that the initiation of a large number of small, stable crazes throughout the polymer specimen leads to a toughened material response, whereas a small number of large crazes lead to crack failure in the polymer (49).

Shear yielding is also a source of energy absorption and shear bands are possible termination points for crazes. When a polymer is under an applied stress, it may deform without a significant change in volume. Under these circumstances the polymer is said to have undergone shear yielding. This is also an energy absorbing process and is therefore an important contribution to the toughening mechanism of polymers. The rubber-matrix interface is a stress concentrator and is known to initiate shear bands. If a polymer is to suppress brittle fracture, it must have a high yield stress in order to be strong and prevent bulk yielding which would lead to fracture.

It can be seen, that both crazing and shear yielding have much in common. They are both important sources of energy absorption in the toughening mechanism of polymers, both involve plastic yielding arising from stress-strain concentrations and so dissipate energy in the vicinity of a crack tip. The main difference between the two, is that

polystyrene and polymethylmethacrylate undergo crazing as the source of crack initiation and propagation, whereas a comparatively ductile polymer such as polycarbonate undergoes shear yielding and ductile fracture (45). However, it is acknowledged that both shear yielding and craze formation will take place during specimen failure of unmodified PES (46).

Not surprisingly, none of the theories proposed for the toughening of polymers applies rigidly to all polymers nor explains completely the theory of rubber toughening. As expected, the relative contribution of each proposed toughening mechanism differs for each polymer system and the different test conditions used. For example, Petrich (47) studying PVC modified with methacrylate-butadiene-styrene copolymers concluded that there was no evidence of voids or crazes present on failure. The theory proposed that the rubber particles were reducing the yield stress, allowing cold drawing to take place and thereby increase the energy absorption. This resulted in higher impact resistance. No crazing was observed even though this is a major cause of specimen failure.

Merz et al (37) first proposed the idea of rubber particles absorbing energy in order to toughen polymers. They concluded that the fibrils of styrene-butadiene copolymer stretched across the fracture surface of a developing crack in polystyrene held the void together and in doing so absorbed more than an equivalent volume of polystyrene matrix.

This theory has been shown to be only partly true by Newman and Strella (42) since the energy absorbed by the rubber phase is only one tenth of the total energy absorbed by the composite matrix. This work also presented the important theory that the rubber particles present initiate shear yielding in the matrix and that enhanced toughness could be attributed to the increased energy absorption taking place due to cold-drawing of the matrix. A triaxial stress field around the rubber particles results in sufficient lowering of the Tg to allow cold-drawing of the matrix. This work also suggested that the rubber particles stop crack growth and so enhances toughening.

Another important toughening model was proposed by Bucknall and Smith (38). The multiple craze theory was suggested to explain the phenomenon of "stress-whitening" in high impact polystyrene (HIPS). Stress-whitening was attributed to crazes in the matrix as opposed to the formation of actual cracks. Crazes are microvoids formed when stress concentrates at flaws, scratches or molecular heterogeneities in the polymer. These localised yielded regions have a lower refractive index than the matrix and for example, in polystyrene, appear as white or opaque regions of polymer. In rubber toughened materials, the rubber particles are localised stress centres and therefore a source of craze initiation. These crazes are prevented from growing sufficiently in size to form cracks, by termination at other rubber particles or at shear bands (45). The importance of

crazing is that it is an energy absorbing process and therefore leads to a toughened material response through increased energy absorption. Crazing is frequently a precursor to brittle fracture of a polymer through the crazes coalescing to produce a crack in the material (48). It is important to realise that the initiation of a large number of small, stable crazes throughout the polymer specimen leads to a toughened material response, whereas a small number of large crazes lead to crack failure in the polymer (49).

Shear yielding is also a source of energy absorption and shear bands are possible termination points for crazes. When a polymer is under an applied stress, it may deform without a significant change in volume. Under these circumstances the polymer is said to have undergone shear yielding. This is also an energy absorbing process and is therefore an important contribution to the toughening mechanism of polymers. The rubber-matrix interface is a stress concentrator and is known to initiate shear bands. If a polymer is to suppress brittle fracture, it must have a high yield stress in order to be strong and prevent bulk yielding which would lead to fracture.

It can be seen, that both crazing and shear yielding have much in common. They are both important sources of energy absorption in the toughening mechanism of polymers, both involve plastic yielding arising from stress-strain concentrations and so dissipate energy in the vicinity of a crack tip. The main difference between the two, is that

crazing involves an increase in volume as microvoids are formed and shear yielding is a constant volume process.

The controlled initiation of both or either crazing and shear yielding in a polymer can increase it's toughness by increasing the energy absorbing processes. This can prevent a crack initiated at a surface notch developing to a critical length beyond which it would cause the failure of the polymer (50).

2.3 Rubber Particle Size.

It is now generally accepted that the energy absorption of rubber toughened polymer blends during impact occurs principally in the polymer matrix. The role of the rubber particles seems to be to provide a large number of stress concentration sites by which the deformation processes of the polymer may be controlled. A polymer may fracture through multiple crazing or shear yielding, leading to a terminal crack, but the presence of rubber particles may control this through a combination if the following:-

Matrix.

(i) dissipation of energy near the crack tip.

(ii) strain induced crystallisation.

(iii) development of high orientation.

Rubber.

(i) increased dissipation of energy.

(ii) deflection of cracks.

(iii) cavitation (crazes).

(iv) shear yielding.

Notch sensitive polymers fail due to the localised nature of the crazing and shear yielding (45). To increase toughness in these materials, it is necessary to ensure that the dissipation of energy occurs throughout the polymer matrix, rather than in concentrated areas where a small number of crazes can break down into catastrophic cracks or where shear yielding leads to specimen failure (39).

Numerous attempts to explain the importance of the particle size of rubber inclusions in toughened plastics have concentrated mainly upon their ability to initiate crazes or shear bands (36,38,44) as well as the interaction between crazes and shear bands (36,45,51).

One important observation which emerges from the literature is that for toughened polymer systems there appears to be a critical particle size below which no effective toughening is observed. The critical particle size is different for each polymer system (52). For example, a particle size of >1μm is required to toughen HIPS (45), 0.2μm for toughened PVC (52), <0.6μm for poly(ethylene-co-propylene) and HDPE in polypropylene (53), >0.08μm for styrene-

acrylonitrile toughened by olefinic rubber (54) and 0.3μm particles are required to rubber toughen nylon (55).

These studies have also shown that there is an optimum rubber particle size required in order to achieve the maximum toughening of the matrix polymer. Beyond this size, toughening decreases. This can be related to the different sizes of crazes generated by larger rubber particles. The larger the rubber particles, the larger the crazes formed. There is a point at which the crazes formed can grow into cracks and therefore the toughening contribution of these particles is greatly reduced (54). This accounts for the observed figure of <0.6μm for the optimum particle size required to toughen polypropylene (53).

The possible explanations for critical particle size effects are that small rubber particles are unable to either control craze growth directly or initiate crazes effectively. This results in a situation where the large number of energy absorbing crazes required for toughening the polymer are not produced. This would certainly be the case for brittle polymers. In more ductile materials, craze growth is inhibited by shear yielding, so small particles unable to control craze growth directly may be able to do so indirectly, by initiating more shear bands. This explains why increasingly more ductile polymers require decreasingly smaller particles for effective toughening. The increased level of shear yielding compensates for the lower level of

crazing and at the same time prevents the crazes formed becoming catastrophically large (39).

By altering the size of the rubber particles in a polymer, the comparison of the toughening results will also reflect the effects of the change in volume of the rubber inclusions and also the interparticle distance. Wu (55) proposed that increasing the critical particle size also increases the rubber volume fraction i.e. if the rubber particles are large, then a larger amount of rubber is required to toughen the polymer than for small particles. It was also established that the transition between a brittle and a toughened plastic is controlled by the interparticle distance. The blend will be toughened if the interparticle distance is smaller than the observed critical value and the blend will be brittle if the interparticle distance is greater than this critical value. These conclusions were formed after studying rubber toughened nylon blends. The rubber volume fraction and rubber-matrix adhesion were held constant and the particle size varied. A sharp tough-brittle transition was observed at a critical particle size. The critical particle size increased with increasing rubber volume fraction according to the equation:-

$$d_c = T_c\{(\pi/(6\phi_r))^{-1/3}-1\}^{-1}$$

d_c = critical partical diameter

T_c = critical interparticle distance

Φ_r = rubber volume fraction

From studies of polystyrene grafted onto rubber spheres, Matsuo et al (56) observed that crazes are initiated at the equator of the rubber spheres. Crazes are easier to initiate and more stable if another rubber sphere is within a critical distance from the surface of the sphere.

The importance of the number of rubber particles present is emphasised by the observation that an increase in the number of particles increases the sites at which energy absorbing processes can take place. This is effected by the amount of rubber added, the efficiency of the dispersion of the rubber and the important matter of rubber-matrix adhesion. If the rubber does not adhere sufficiently to the matrix, then it will fail to sustain stress and absorb energy during the fracturing process due to inefficient energy transfer across the rubber-matrix interface (38). A propagating crack can tear a rubber particle from the matrix (57), or just bypass the particle altogether and therefore reduce any potential toughening effects (58). Merz et al (37) and Bucknall (59) claim adhesion has a greater influence upon the "toughening" of a polymer than the size of the rubber particles dispersed in the polymer matrix.

2.4 Polymer-Polymer Miscibility.

From a preparative point of view, the easiest way to introduce rubber to toughen a polymer would be to physically blend the two materials together. However, instances of compatible polymers are very rare and in most cases a two phase blend is formed. One aspect of rubber toughening is to form a blend of discreet particles uniformally dispersed through the polymer matrix. If however, the two polymers are so incompatible that a uniform dispersion cannot be obtained, then toughening will not be achieved and a decrease in impact strength will be observed as the polymers delaminate. As mentioned previously, the discreet rubber particles have to adhere sufficiently to the matrix polymer in order to toughen the matrix, but not so easily that the two-phase nature of the system is lost. These two factors have to be balanced in order to produce a rubber toughened polymer.

Phase separation and miscibility can be predicted when considering the thermodynamics of mixing:-

$$\Delta Gm = \Delta Hm - T\Delta Sm \qquad \text{Equation 2.1}$$

Gm = Gibb's free energy of mixing.

Hm = enthalpy of mixing .

T = temperature.

Sm = entropy of mixing.

In general, the entropy of the system is positive since mixing increases the disorder of the system. If the enthalpy of mixing is negative, then the system would be miscible, however, the enthalpy of mixing is usually positive making the polymer blends immiscible in most cases. Miscibility between polymers is usually controlled by the entropy rather than the enthalpy effects.

The entropy of mixing one polymer with another polymer, or with a solvent consists of two main terms; the configurational entropy of mixing and the local pair entropy. The configurational entropy of mixing arises from the increased number of ways of arranging the polymer units and is given by the Flory-Huggins equation (60):-

$$\Delta S_m = -R(n_1 ln X_1 + n_2 ln X_2) \qquad \text{Equation 2.2}$$

R = Gas constant.

n_1 = mole fraction of polymer 1.

X_1 = volume fraction of polymer 1.

n_2 = mole fraction of polymer 2.

X_2 = volume fraction of polymer 2.

For high molecular weight polymers, the number of configurations is less than for free units (solvents) or short chain polymers. Therefore, the entropy of mixing is a function of molecular weight and is less than in simple cases; approaching zero at high molecular weights (61). For ΔGm to

adopt the negative value required for spontaneous miscibility or mixing, ΔHm must be either zero or negative. However, it has been shown by Hildebrand (62) that the enthalpy of mixing can be expressed as follows:-

$$\Delta H_m = V(\delta_1-\delta_2)^2 X_1 X_2 \qquad \text{Equation 2.3}$$

V = molar volume of the blend.

δ_1 = solubility parameter of polymer 1.

δ_2 = solubility parameter of polymer 2.

The contribution of the enthalpy of mixing is largely due to the interactions of the polymer chains and is related to the tendency of the like molecules to attract each other rather than dissimilar molecules.

Combining the three equations 2.1-2.3 gives:-

$$\Delta G_m = V(\delta_1-\delta_2)^2 X_1 X_2 + RT(n_1 \ln X_1 - n_2 \ln X_2) \qquad \text{Equation 2.4}$$

This equation based upon the solubility parameter approach predicts an increase in the free energy of mixing as the molecular masses of the polymer increases. The simplicity of the equation is useful in relating the miscibility of polymers to the solubility parameters of the individual polymers: $(\delta_1-\delta_2)^2$.

It has already been stated that two requirements for rubber toughening are that the rubber forms a separate phase and still maintains good adhesion to the matrix. Stehling et al (53) attempted to put these considerations on a more quantitative basis. Following the work of Krause (63) and assuming a molecular weight of 10^5 for each component, they calculated that $(\delta_1-\delta_2)$ must not exceed $0.84(MJ^{-3})^{\frac{1}{2}}$ for phase separation to occur. $(\delta_1-\delta_2)$ must be $< 1.7(MJ^{-3})^{\frac{1}{2}}$ for there to be adhesion in a toughened polymer containing 5-10% rubber at 25°C.

This work also considered adhesion between polymer pairs with the aid of Helfand's theory for the thickness of the interface between two polymer phases (64). This theory states that the interfacial distance increases as $(\delta_1-\delta_2)$ decreases. Stehling et al introduced the theory that good adhesion between polymers required physical entanglements between the two different molecular species at the interface. Taking the number of chain bonds between entanglements as 500, a bond distance of 0.15nm (65) and assuming freely jointed bonds, they calculated the root mean squared distance between entanglements to be greater than 3nm for good adhesion. This work showed that $(\delta_1-\delta_2)$ should be less than 1.7 $(MJ^{-3})^{\frac{1}{2}}$ for good polymer adhesion.

Experimental work toughening polypropylene with high density polypropylene and poly(ethylene-co-propylene) has

found to be in good agreement with the predictions from this work.

Using these results and the known values of polymer solubility parameters, it is relatively easy to judge whether a polymer blend will be miscible and have good adhesion.

2.5 Polymer Compatiblisation.

Ideally, two or more polymers may be blended together to form a wide range of products that offer desirable combinations of properties, rubber toughening being one of these. However, it may be difficult or even impossible in practise to achieve these aims through simple blending due to the high probability that the polymers are thermodynamically immiscible and will form a two phase blend. For rubber toughening, a two phase morphology is quite useful except at the interface between the two polymers, where high interfacial tension leads to difficulties imparting the required degree of dispersion throughout the blend. This causes a subsequent lack of stability from delamination within the blend (66,67). Poor adhesion leads to very weak and brittle mechanical behaviour, quite the opposite to the rubber toughening effects that may be the aim of blending in the first place.

The problem of incompatible polymers demixing can be overcome by the careful choice of an additive to improve the interfacial interactions and promote adhesion of the polymers

(68,69). The ideal additive for toughening a brittle polymer, is a rubber which is neither compatible nor incompatible with the host matrix. These requirements are satisfied by graft and block copolymers, consisting of a rubber and a material which will promote compatibility at the interface with the matrix polymer. These materials may resist phase separation on a macro scale through having sufficient compatibility at the interface even though they are thermodynamically immiscible, whilst the rubber is still sufficiently incompatible to form small particles capable of rubber toughening when dispersed throughout the host matrix polymer. Materials which alter the interfacial situation in such a way are referred to as "compatiblisers" and if properly chosen, preferentially locate themselves at the interface between the two phases as shown here:

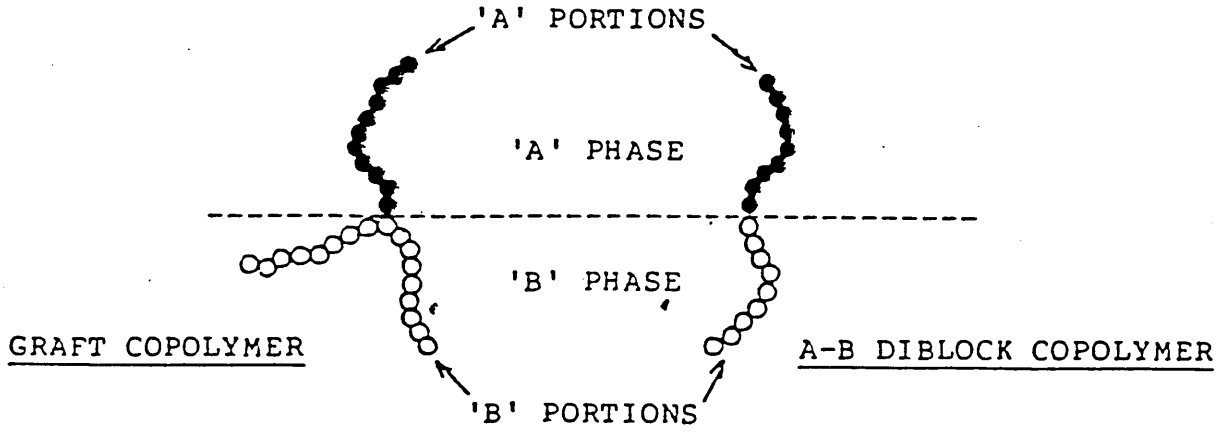

For a copolymer to act as a toughening agent in a blend with a more brittle polymer, it should be comprised of a rubbery polymer chemically bonded to a material which is miscible with the host matrix, enabling the copolymer to be

intimately mixed with the host matrix at the interface. This will provide the following improvements over a simple physical blend:-

(i) reduced interfacial energy between the phases.
(ii) permit a finer dispersion during mixing.
(iii) provide stability against macrophase separation.
(iv) gives greater interfacial adhesion.

For this to occur, ideally one component of the copolymer should be chemically identical to the host matrix polymer. In this way, a copolymer containing two immiscible materials chemically linked will locate at the interface in the phase in which they are miscible (70). Referring to the previous diagram, the affinity of the "A" segments of the copolymer for the "A" phase and the "B" segments for the "B" phase serves to locate the copolymer at the interface of the blend, with the chemical bonding maintaining the adhesion across the interface (71). The result is improved adhesion between the two phases and an improvement in the blend properties, such as elongation and tensile strength as well as providing a fine dispersion of the rubber component throughout the host matrix (72).

A mixture of two completely compatible polymers has properties intermediate between those of its constituents, but to rubber toughen a polymer, no loss of the properties of either the rubber or the host matrix is required. Therefore,

a phase separated system is required with good adhesion at the interface, as provided by a copolymer located at the interface and preventing gross phase separation (73,74). The properties of the copolymer and the ultimate performance of the additive are also strongly related to the molecular weight of the copolymer segments, which will be considered in more detail later on (4). The dependance of the coplymer properties upon molecular weight is to be expected after studying equation 2.2.

The conformational restraints are important for a blend of a copolymer in a host matrix. The different segments of polymer are required to locate in their respective phases. Depending upon the conditions and materials used to synthesise the copolymers, different copolymer architectures can be formed. Restricting the copolymer to two different homopolymers results in the architectures described below.

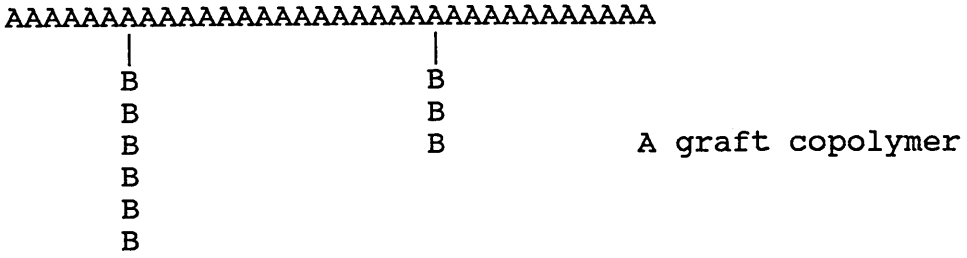

AAAAAAAAAAAAAAAAAAAAAA-BBBBBBBBBBBBBBBBB

A diblock or AB coplymer

AAAAAAAAAA-BBBBBBBBBB-AAAAAAAAAA

A triblock or ABA block copolymer

AAAAAA-BBBBB-AAAAA-BBBBB-AAAAA-BBBBB-AAAAA-BBBBB

An $(AB)_n$ block copolymer

In addition to these architectures, there are random block copolymers, where the backbone chain of the polymer consists of comonomer repeat units placed statistically or "randomly". This cannot be controlled during synthesis.

Considering the graft copolymer, there is obviously great difficulty in placing the backbone of the polymer in one phase and the many different graft branches in their respective phases, as the multiple branches would restrict the backbone from being totally located in only one phase. This is partly dependant upon the number of grafts, but the lower the degree of grafting, the less adhesion there is between the two phases. Increasing the grafting reduces the freedom of the main backbone to locate itself in one phase.

Considering these problems, an AB or ABA block copolymer would be able to locate itself across an interface much more easily (72). However, by analogy with the graft, a diblock copolymer would be more effective than a triblock copolymer (66). The choice of copolymer architecture can be selected only after consideration of the required effect after blending. Although copolymers are suitable as interfacial agents, they are also used purely as impact modifiers (75). Diblock copolymers are suitable as compatiblisers, but would

be less useful solely as impact modifiers, as they would form only a few comparatively large dispersed domains instead of the large number of small domains required to produce rubber toughening (76). Toughening may be improved by blending the compatibliser with a rubber as well as the brittle matrix polymer.

A great amount of work has been carried out to establish that copolymers do act as compatiblisers and separate into two phases. A recent example of this has been the emulsifying effect of poly(hydrogenated butadiene-b-styrene) diblock copolymers in LDPE/polystyrene blends (74). The copolymer was identified as locating preferentially at the LDPE/polystyrene interface and was more effective as a compatibliser than similar graft or triblock copolymers. Simple blends of LDPE and polystyrene produced phase separation on a large scale, with pronounced coalescence. The addition of 2-10% copolymer produced a much smaller particle size. This work also emphasised the importance the molecular weight of the coplymer has upon its performance as a compatibliser.

There are many commercial examples of copolymers being used as impact modifiers, the first was polystyrene modified by a rubber graft (HIPS) (36). A rubber solution is polymerised in styrene monomer. It is recognised that although discrete particles of rubber are formed, some degree of grafting takes place and it is this graft copolymer which

improves the adhesion between the glassy and rubbery phases by acting as an interfacial compatibliser.

This was followed by acrylonitrile-butadiene-styrene (ABS), brittle acrylonitrile-styrene copolymer melt blended with acrylonitrile-butadiene rubber. The process was replaced by an emulsion graft process. Brittle PVC has been toughened by melt blending with acrylonitrile-butadiene rubber in the presence of a small percentage of ABS. A grafting process is impossible with PVC, so blending PVC with a rubber and ABS is the easiest way to improve its toughness. Styrene is compatible with PVC and so ABS is able to provide the interfacial adhesion between PVC and acrylonitrile-butadiene rubber (66).

2.6 Phase Separation in Block Coplymers and their Blends.

Although it has been shown that copolymers can be used as compatiblisers in the rubber toughening of polymers by acting as a bridge between the rubber particles and the host matrix, there has been much work to produce copolymers that can act as impact modifiers themselves when blended with a brittle homopolymer (75). If the blending process is properly controlled and the correct copolymer employed, a fine dispersion of rubber particles can be introduced to the homopolymer matrix and so can improve the toughness of the homopolymer. The blending of polymers thermodynamically causes macrophase separation, but can be compatiblised by the

use of copolymers. For a copolymer to be compatible with the homopolymer and produce rubber toughening itself requires phase separation within the copolymer segments. The rubber segments and the segments of material compatible with the host matrix must phase separate on a micro scale i.e. microphase separation must take place. As the copolymer is usually formed from two incompatible materials, phase separation is predicted thermodynamically, but the two materials are covalently bonded so that gross macrophase separation within the copolymer is overcome, leaving phase separation on a micro scale which can produce a substantial increase in the mechanical properties when blended with a brittle homopolymer.

Considerable work has been carried out to establish that copolymers do undergo microphase separation. Meier (77) studied A-B block copolymers and established the thermodynamic criteria for domain formation. The study identified the basic thermodynamic difference between block copolymers and simple blends as the constraints placed upon the copolymer chains at the interface between the two phases. The coplymer is constrained to stay within the region of the interface and this causes a reduction in entropy relative to random placement of the chains. This is called "placement entropy".

Restricting the polymer to a position only spanning an interface causes a further reduction in entropy and this is called "restricted volume entropy". These restrictions in the interfacial region also reduce the number of available

configurations and volume the polymer chains can adopt, so reducing the entropy of the system even further. This third term is called "elastic entropy" and is found to be negligable. The interactions of the A-B segments at the domain surface were also considered and were treated as causes of surface free energy.

This theory relies heavily upon Flory's interaction parameter χ_{AB}, but the critical molecular weights required for polystyrene and polybutadiene segments of an A-B copolymer could be predicted. These molecular weights were between 2.5-5 times larger than for a simple homopolymer blend due to the configurational constraints placed upon the domain system. Experimental work based upon these predictions showed that microscopic domains were formed above these critical molecular weights.

Leary and Williams (78) studied ABA triblock copolymers and included in their calculations a diffuse region of mixed A and B segments. They suggested the existance of 3 phases, a pure A phase, a pure B phase, and a mixed A-B region. The calculations enabled them to predict the morphology of the coplymer system by considering the enthalpy of demixing (based upon the Scatchard-Hildebrand regular solution theory) and the entropy of phase separation. The entropy of phase separation was thought to arise due to three separate contributions. The first change in entropy is due to forcing one of the A-B junctions per molecule to occupy a position somewhere in the

A-B mixed region. The second entropy change is due to restricting the A segments entirely to within the A phase and the mixed region. The third enthalpy term is due to forcing the B segments to start at an A-B bond in the A-B mixed region, with the B segments always remaining outside the A phase. By minimising the free energy for these contributions, Leary and Williams were able to predict the favoured morphology of styrene-butadiene-styrene ABA block copolymers and later confirmed these predictions using differential scanning calorimetry (dsc), light scattering and transmission electron microscopy (tem). This work again relies upon the solubility parameter for each polymer in the accuracy of its predictions (79).

Inoue et al (80) studied polystyrene-isoprene A-B block copolymers and described their solution behaviour in terms of micelle formation. The studies of these materials involved casting films of the copolymers from different solvents and then examining the two phase structure by an osmium tetraoxide fixation technique. The different morphologies were examined as the weight fractions of polystyrene and isoprene were changed. The work suggested that as the solvent dried during film casting, a critical concentration is reached at which each section of the copolymer undergoes phase separation and forms its own characteristic molecular micelle. This can be compared with soap molecules forming micelles in aqueous solution at the critical micelle concentration. It is assumed that there is no change in morphology on complete drying of

the copolymer. The minimum Gibb's free energy for the copolymer domains were determined. The size of the micelle formed was expected to give the lowest free energy for the copolymer and therefore microphase separation was the most stable state for the A-B block copolymer. Complete phase separation is prevented by the chemical bonding of the two incompatible polymers, so they are unable to attain the stable state through macrophase separation as a simple blend of the homopolymers would be able to achieve.

LeGrand (81) developed a model based upon micelles to account for domain formation. The model is based upon the free energy changes which exist for a random mixture of block copolymers and that of a micelle or domain structure. The morphologies of the micelles were also discussed.

Krause (82,83) has taken a different approach by only studying the thermodynamic aspects of microphase separation without any consideration of the surfaces between the microphases. This model predicts that as the number of blocks of a given length increases in the copolymer, microphase separation becomes more difficult. It also states that the surface free energies at the polymer-polymer interface make phase separation much more difficult than would be expected for incompatible homopolymers. This is in agreement with the work of Meier (77). Both Krause and Meier have shown the importance of the Hildebrand solubility parameters and the

interaction parameter of the homopolymers when predicting microphase separation in the block copolymers.

Important studies have also been carried out into the more complex systems of copolymer-homopolymer blends. Meier (84) concluded that a block copolymer can solublise an equal volume of homopolymer, but this is highly dependant upon the relative molecular weights of the homopolymer and solublising segments of the copolymer. The two materials have to be of similar molecular weight, an observation which has been confirmed by a number of other workers (85-94). Meier (84) predicted that @ 5% of homopolymer A, molecular weight M_A will be solublised in a block coploymer containing A blocks of molecular weight M_A. This is not supported by the experimental data and further investigations have been carried out by Jiang et al (95-97) who have developed a theory based upon a gradual increase in block molecular weight throughout the coplymer to account for descrepancies. This is called the density gradient model.

Inoue et al (98) studied ternary blends of styrene-isoprene block copolymers with polystyrene and polyisoprene and also observed that the molecular weight of the homopolymer must be equal or less than that of the corresponding copolymer segment if the copolymer is to act as an emulsifier. If the homopolymer molecular weight is greater than that of the corresponding copolymer segment, then phase separation takes

place on a macroscopic scale and the copolymer no longer acts as an emulsifier.

Krause (99) investigated the effect the presence of one of the corresponding homopolymers in the copolymer had upon the microphase separation of the copolymer. The conclusions of this work are that the presence of homopolymer enhances the copolymer phase microphase separation, but only if the molecular weight of the homopolymer is comparable with the corresponding blocks of the copolymer.

The work which has been mentioned here is of obvious importance when considering the rubber toughening of polymers. It is important to note that the presence of homopolymer can enhance microphase separation and also that the correct choice of the molecular weight of the copolymer blocks is essential in forming domains. A microphase separated PES/elastomer block copolymer, dispersed throughout PES homopolymer satisfies many of the criteria for rubber toughening.

2.7 Morphologies of Block Copolymers.

Many of the workers who have studied microphase separation in block copolymers have also investigated the resulting morphologies of the copolymers. Inoue et al (80,98) described five different domain formations when studying styrene-isoprene A-B block copolymers. By changing the

proportion of styrene blocks to isoprene blocks in the copolymer, the following domain stuctures were seen:-

(i) A spheres in B matrix.

(ii) A rods in B matrix.

(iii) alternate lamellar or "sheet" arrangement.

(iv) B rods in A matrix.

(v) B spheres in A matrix.

This work has also shown the effect different solvents have upon the copolymer morphology. The composition of a 40/60 styrene-isoprene A-B block copolymer was kept constant and different solvents were used to cast films of the copolymer. The morphology of the copolymer changed as different solvents were employed, the size and shape of the domains changing as different solvents were used.
Methyl ethyl ketone, cyclohexane, carbon tetrachloride, n-hexane and n-isooctane formed polystyrene domains in a polyisoprene matrix, whereas toluene produced an alternately lamellar structure. Toluene is a good solvent for both segments of the copolymer. Of the other solvents, methyl ethyl ketone is a good solvent for polystyrene and a poor one for polyisoprene, the remaining solvents being just the opposite.

Leary and Williams (78,79) studied ABA triblock copolymers of polystyrene-butadiene-styrene and confirmed the formation of these five different morphologies. They

predicted these morphologies by studying the thermodynamics of the copolymer system. LeGrand (81) also predicted spheres, rods and lamellae morphologies for block copolymers by comparison with the micelle formation of soaps.

Saam and Fearon (100) studied polystyrene-polydimethylsiloxane A-B and ABA block copolymers. They concluded that the morphology of the copolymers was apparently influenced by the large difference in solubility parameters of the two homopolymers and the high interfacial surface free energy involved between the blocks. This work is also in agreement with Krause (83) and later Theodorou (101).

The basic shapes of spheres, rods and lamellae were observed in electron micrographs and these were dependant upon the solvent from which the films were cast. Films of A-B copolymer cast from cyclohexane, a preferential solvent for polydimethylsiloxane (PDMS), gave structures of polystyrene cells surrounded by PDMS. The same copolymer cast from styrene, a preferential solvent for the polystyrene segments gave the opposite structure. When the copolymer was cast from toluene, which solvates both blocks, the structure was a hybrid of both rods and spheres. Changing the block size caused inversion of the phases when one or the other of the components predominated, as seen by Inoue (80,98). The changes in morphology observed when the copolymers were prepared from a range of homopolymer blocks of different molecular weight, was thought to be due to film formation

under non-equilibrium conditions, as well as the high interfacial contact energy arising from the large difference in solubility parameters.

Saam and Fearon (100) also studied ABA triblock copolymers which showed far less distinct changes in morphology over broad molecular weight compositions in comparison with the AB copolymers. Using different preferential solvents gave better definitions of morphology changes for the triblock copolymers, but they were not as distinct as for the AB copolymers. This was attributed to a dominating positive entropy requirement for microphase separation arising from the larger number of blocks present in the ABA triblock copolymer system.

Using standard staining techniques, Matsuo et al (102) studied a series of styrene-butadiene ABA triblock copolymer films cast from toluene under the electron microscope. Unlike Saam and Fearon (100), Matsuo et al clearly identified a progressive change in morphology going from "spheres" through "rods" to "lamellae" as the rubber content of the copolymers was increased. From this work it was thought that such phase inversion occurs in every type of block copolymer.

2.8 Block and Graft Copolymers.

After discussing the requirements of interfacial agents and impact modifiers, we are able to understand more clearly

which are the most suitable structures for these purposes. In the previous discussion, more emphasis has been placed upon the use of block copolymers rather than graft copolymers and this can be explained by studying their suitability as impact modifiers.

Both graft and block copolymers resemble incompatible blends exhibiting two-phase morphology on a microscale rather than a macroscale. The intersegment link restricts the extent to which the phases can separate. The presence of long segments in block or graft copolymers presents the possibility of using these materials as interfacial agents or emulsifiers to reduce the incompatibility of homopolymer blends. Also by blending a graft or block copolymer with one of the homopolymers provides a means of achieving a fine dispersion of an incompatible polymer in the homopolymer matrix, a useful property which enables impact modification of polymers. These properties differentiate block and graft copolymers from random copolymers and physical blends.

In order to achieve the required properties of a microphase separated system, it is important to be able to exert precise structural control over the copolymers. In view of this, it is clear that block copolymers are superior to graft copolymers, because segment length, spacing, sequence and homopolymer contamination are more easily controlled for block copolymers. Graft copolymers are formed usually by free radical, anionic or cationic addition polymerisation in the

presence of a preformed functional backbone (4). Consequently the product is very difficult to characterise due to the problems of assaying:-

(i) the number of grafts per block.
(ii) the spacings between the grafted segments.
(iii) the average length of the grafts.

Difficulties are also encountered in determining the extent of contamination by homopolymeric products. The multifunctional backbone of graft copolymers and the unreliable nature with which these groups take part in the grafting reactions make the structural characterisation of these materials inaccurate.

Block copolymers are obtained with greater reliability and predictability because of the different synthetic techniques involved. The segment lengths of block copolymers are readily controlled by the selection or preparation of homopolymeric precursors with appropriate relative molecular mass. For block copolymers the spacing of the intersegment junctions is more clearly defined, as there is only one junction for an AB diblock copolymer and two for an ABA triblock copolymer. For $(AB)_n$ block copolymers, the distance between the intersegment links can be deduced from the relative molecular masses of the A and B homopolymer precursors.

This results in a much better control of important parameters such as:-

(i) sequence architecture.
(ii) segment length.
(iii) segment spacing.
(iv) polydispersity.
(v) contamination with homopolymer.
(vi) undesired copolymer architectures.

Although block copolymers are extremely difficult to synthesise, they give a higher degree of morphological control than graft copolymers, which in turn is reflected in superior physical properties. Consequently, block copolymers are preferred as impact modifiers.

2.9 Block Copolymer Architecture.

One of the important physical characteristics of block copolymers is their thermoplastic elastomeric behaviour. Block copolymers of this type display rubbery behaviour in the absence of chemical cross linking. This permits the processing of these materials by techniques applied to other thermoplastic polymers. This unique behaviour is achieved by forming a network structure by physical rather than chemical means and is influenced by the tightly controlled morphology of the copolymer.

Of the three different forms of block copolymer, AB, ABA and $(AB)_n$, only AB diblock copolymers are unable to form the required thermoplastic elastomeric networks required of an impact modifier. AB copolymers consist of one segment of "A" repeat units and one segment of "B" units joined by one intersegmental chemical bond. They are suitable as compatiblisers, acting as interfacial bridges, but are unable to form network structures since only one end of the rubber segment is chemically linked to the domain of the hard segment.

The key to forming a successful thermoplastic elastomer is the ability to develop a two phase physical network. Such a system requires small hard segments with a Tg above room temperature and soft block segments with a Tg below room temperature. In these systems, the hard blocks associate to form domains which act as reinforcing sites in the rubber, rather like cross links and as compatiblisers for the host matrix. Only copolymers containing two or more hard block segments per macromolecule are capable of producing this effect i.e. ABA or $(AB)_n$ block copolymers.

ABA triblock copolymers consist of a single segment of repeat unit "B" located between two segments of "A" repeat units. If the "B" segment is the soft rubbery phase, then thermoplastic elastomeric behaviour is observed. $(AB)_n$ multiblock copolymers consist of alternating "A" and "B" segments. It is important that the hard block volume fraction

is >20% to provide an adequate level of "crosslink" behaviour. If the volume fraction is too high, then the shape of the domains may change from being spherical to extended regions where the elastic recovery is restricted. Too little of the hard block and the network structure is lost, resulting in material which resembles weak uncured rubber, rather like A-B diblock copolymers.

Triblock and multiblock copolymers have an adverse effect upon the melt rheology of a blend, because of their ability to form network structures. Depending upon the specific chemical structure and block length, these networks can persist in the block copolymer melt, resulting in extraordinarily high melt viscosities. This is in contrast with AB diblock copolymers which do not form network structures and have much lower melt viscosities (103,104).

Thermoplastic elastomers based upon $(AB)_n$ multiblock copolymers rather than ABA triblock copolymers would be expected to display enhanced recovery properties due to the greater number of physical junctions per molecular chain. Similarly, it can be reasoned that the disruption due to degradation or network imperfections should be less extensive for multiblock copolymers than for triblock elastomers. Also, it is important to note that multiblock copolymers are more likely to have block molecular weights smaller than their characteristic entanglement molecular weights and this may be a factor influencing the melt rheology of the copolymer.

It has been observed that AB diblock copolymers exhibit a coarser particle morphology than the ABA triblock copolymers and by extrapolation, the finest particle morphology is expected from $(AB)_n$ multiblock copolymers. This fine particle morphology would be an obvious advantage as an impact modifier (4).

Block copolymers have been used to compatiblise homopolymers by an emulsifying effect and therefore by the virtue of their simple architecture, AB diblock copolymers should be the most suitable for this purpose. Impact modifiers however would be better suited by an $(AB)_n$ multiblock coplymer with a much finer particle morphology, substantial physical network and enhanced recovery properties.

2.10 Impact Modifiers.

It has already been mentioned that block copolymers have been used to improve the impact strength in blends with homopolymers. There are a number of examples in the literature of copolymers being used to improve the impact strength of polymers, in particular polystyrene homopolymer.

Childers et al (105) blended rubbery copolymers of styrene-butadiene with styrene homopolymer. The copolymers included both random and block copolymers containing different molecular weights and varying block lengths. When dicumylperoxide was added during the blending to crosslink the

rubber domains and to control the particle size, a great improvement in the impact strength was obtained. Blending polystyrene and polybutadiene without any copolymer present resulted in a two phase system with no compatibility between the phases. However, blending block copolymers containing 25% polystyrene in a 3:1 polystyrene homopolymer : copolymer ratio resulted in a pronounced increase in impact strength over a simple homopolymer blend of polystyrene and polybutadiene, as well as over a blend with a random copolymer.

Childers et al (105) also investigated the effect the polystyrene copolymer block length had upon the impact strength after blending with the homopolymer. When keeping the composition and molecular weight of the elastomer constant and varying the polystyrene block length in the copolymer, it was observed that the impact strength of the blend increased with increasing styrene block length. This would be expected as the hard block fraction is increased, so does the tensile strength. When the polystyrene block length was varied in the block copolymers between 8,000-36,000 relative molecular mass (RMM), with polystyrene content varying up to 25%, the blends reached an optimum impact strength at 23,000 RMM. This suggests that there is an optimum block size required for the effective toughening of the homopolymer and this is determined by the adhesion of the styrene blocks to the homopolymer matrix. The polystyrene chemically bonded to the rubbery polybutadiene domains act as anchors to the polystyrene matrix. The effectiveness of the copolymer is obviously

dependant upon the adhesion of the copolymer to the host matrix and is determined in this case by the molecular weight of the polystyrene block segments.

Further work with polystyrene by Durst et al (106) resulted in blends of polystyrene homopolymer with styrene-butadiene di or tri block copolymers prepared by mechanical mixing. The particle size of the rubbery domains was controlled by the shear exerted by the mixer. High shear mixing produced particle sizes <0.2μm which gave poor impact strength. A particle size of 1μm gave the optimum increase in impact strength, which is in agreement with the earlier discussion in section 2.3.

The styrene content of the copolymer needs to be 50% ± 10% in order to obtain the optimum impact strength. Lowering the styrene content reduces the impact strength and this can be attributed to the difficulty in maintaining adhesion between the low molecular weight blocks of polystyrene in the copolymer and the host matrix. Also, the particle size of the rubbery domains changes with the molecular weight decrease. Decreasing the molecular weight to below 150,000 RMM results in a small particle size which is unable to produce significant toughening, whereas 250,000 RMM is still able to produce domains of the required 1μm particle size. The block copolymers used by Durst et al (106) were not crosslinked unlike those of Childers et al (105), and so are more likely to result in low particle sizes under the high shear

mechanical blending, unless the copolymers have a high molecular mass and therefore higher tensile strength.

Later work by Fayt et al (74) on the tertiary blend of polystyrene and polyethylene with poly(hydrogenated butadiene-co-styrene) showed that the melt blending of the materials reduced the sensitivity of the homopolymers to phase separation when compared with solution blending. The diblock copolymers were used in small amounts, 1-2%, to stabilize the interface between the polystyrene and the rubbery phase. The AB diblock coplymers were found to be more effective than triblock, multiblock or star shaped polymers. This is in agreement with the discussion in section 2.9. This work also showed that the mechanical properties of the blends increases as the molecular weight of the diblock coplymer increases. However, this effect could also be produced by a copolymer with "tapered" polystyrene content i.e. the polystyrene content of the copolymer used decreases gradually below 50%. The work clearly emphasised the importance of molecular weight and particle size, as well as showing the importance of AB diblock copolymers in rubber toughening.

The work which is most relevant to this investigation has been carried out by Noshay, McGrath et al (4-18) in forming $(AB)_n$ block copolymers of "Udel" polysulphone:-

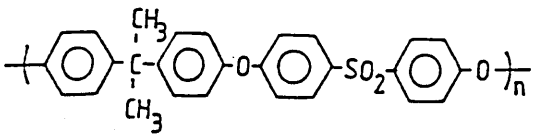

and polydimethylsiloxane (PDMS):-

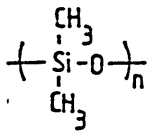

These copolymers were formed by the reaction of preformed blocks of hydroxy terminated polysulphone and bis(dimethylamino) terminated PDMS oligomers in solutions of THF or chlorobenzene (4):-

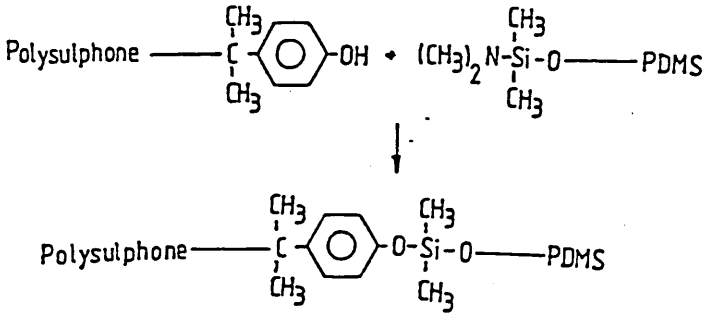

The resulting copolymers are linked via ≡Si-O-C≡ bonds at the intersegment junctions.

The block copolymer architecture is well controlled because the functional groups of the polysulphone and PDMS rubber will not self condense, so the resulting copolymer consists essentially of alternating segments identical to those of the oligomeric starting materials. The morphology of the copolymers formed could be controlled by varying the molecular weight of the oligomer blocks. At a constant polysulphone of Mn= 4,700, PDMS oligomers of Mn= 1,700 gave a single phase morphology as shown by the material displaying one Tg. Copolymers formed from PDMS oligomers with Mn> 5,000 produced a phase separated material displaying two Tg's. One

Tg at -123°C due to the PDMS phase and one at >160°C due to the polysulphone domains (4,6-8,15,16).

The extensive phase separation displayed by these block copolymers at such unusually low molecular weights was attributed to the extreme incompatibility of the homopolymers. The solubility parameters for polysulphone and PDMS are 21.7$(MJm^{-3})^{\frac{1}{2}}$ and 14.9$(MJm^{-3})^{\frac{1}{2}}$ respectively. As discussed in section 2.4, a difference of less than 1.0$(MJm^{-3})^{\frac{1}{2}}$ is sufficient to cause phase separation between two polymers.

The copolymers formed in this work displayed a very high degree of phase separation. When block molecular masses were Mn> 5,000, the materials were very difficult to melt process. Compression moulding gave poor quality films and extrusion produced a powdery extrudate. This behaviour was attributed to the extremely high melt viscosities of these materials, a property of block copolymers which was discussed in section 2.9. The high melt viscosities are caused by the network structure of the copolymers being maintained in the melt at 340°C (180°C above the Tg of the polysulphone phase). The polysulphone hard block segments act as a filler for the weaker siloxane segments, giving highly elastomeric properties comparable with crosslinked siloxane rubbers. This "crosslinked" structure is retained in the melt blends with polysulphone homopolymers (4,6,13-15). The crosslinked behaviour is enhanced by the polysulphone domains acting as anchor sites for the siloxane in the blends with polysulphone

homopolymer (5,6,8,9,13-15). Improved melt processing was observed in copolymers containing shorter polysulphone blocks, Mn=2,000. This was probably due to reduced chain entanglement. It was calculated that for a phase separated copolymer with good melt processability, the difference in solubility parameters should be $<1.0(MJm^{-3})^{\frac{1}{2}}$ (4,6,7).

The composition range of copolymers formed contained 10-79% PDMS and gave materials with properties ranging from hard, brittle materials to highly elastomeric gums (4,6,9,10,14,15). The molecular weights of the block segments were to be sufficiently high so as not to detract from the polysulphone properties e.g. Tg> 160°C which gives the high temperature strength, but low enough to enable melt processing of the material.

Blending as little as 5% by weight of a 50:50 copolymer containing polysulphone Mn=5,000/PDMS Mn=5,000 with polysulphone homopolymer produced the optimum toughening effect. The blending conditions produced good quality injection mouldings with a polysulphone/PDMS copolymer particle size of 0.5-8.0μm. The optimum particle size for increased toughening was found to be 0.5-3.0μm (4,6,8,13,14). This increased the notched Izod impact strength from 69.4 J/m for unmodified polysulphone to 1174 J/m with a 5%w/w copolymer blend (4,6,13-16). Equally as important is the observation that the high temperature properties of the polysulphone

homopolymer were not diminished significantly by blending with the copolymer.

This unique behaviour is thought to arise from two physical properties of the copolymer; incompatibility of polysulphone and PDMS and the melt rheology of the copolymer. The copolymers are at best only partially compatible with the polysulphone homopolymer due to the extreme incompatibility of polysulphone and PDMS. This promotes a good dispersion of the copolymer particles. The polysulphone segments of the copolymer still provide sufficient interfacial adhesion for the toughening processes to be effective. The rheological behaviour of the copolymer, which prevents it from being melt processed on its own by maintaining an extremely high melt viscosity, also prevents excessive breakdown of the copolymer particles during the high shear moulding processes.

More recently, "Victrex" polyethersulphone has been blended with polycarbonate and methacrylic esters to give increased impact strength, whilst maintaining good melt processing properties (107). "Udel" polysulphone has been blended with PDMS grafted with methylmethacrylate, acrylate, acrylonitrile and styrene to give an improved notched impact strength (108).

Block copolymers of "Victrex" polyethersulphone and PDMS have been synthesised by Morris (19). Blending up to 5% by weight of these copolymers with commercial grade "Victrex"

PES resulted in increasing the notched impact strength by over 100%. However, this work also suggested that the ≡Si-O-C≡ bonds linking the blocks of homopolymers are highly susceptible to hydrolysis and a more stable bond is required (20). The formation of a more stable block linkage for "Victrex" PES/PDMS block copolymers will be investigated in this study.

Chapter 3.

CHOICE OF SYNTHETIC ROUTES TO FORM PES IMPACT MODIFIERS.

3. CHOICE OF SYNTHETIC ROUTES TO FORM PES IMPACT MODIFIERS.

3.1 Selection of Copolymer Architecture.

From the examples given in the literature surveyed in section 2, a copolymer of a rubber and a material which is compatible with PES will adhere well to the PES homopolymer, providing polymers of suitable molecular weight are chosen. This is most easily achieved by using PES itself as one of the copolymer constituents.

All the copolymer architectures are capable of providing this adhesion, but a thermoplastic elastomer would be more suitable as an impact modifier. This reduces the choice of architecture to either ABA or $(AB)_n$ block copolymers. Both are capable of forming two phase networks with small hard block domains which serve as physical crosslinking or reinforcing sites. This dispenses with the need for chemically crosslinking the elastomeric segments of the copolymer and allows processing as a thermoplastic during blending with the PES homopolymer.

Copolymers exhibiting these characteristics have proved to be successful as impact modifiers for numerous polymer systems and have shown to be effective with polysulphone. The literature suggests that $(AB)_n$ block copolymers will have a number of advantages over the ABA structure, particularly enhanced recovery, better melt processing, less network disruption and a more finely dispersed domain morphology.

Consequently, the synthesis of $(AB)_n$ block copolymers for rubber toughening PES will be the aim of this investigation.

3.2 The Choice of Elastomer for Inclusion in the Copolymers.

The properties required of an elastomer suitable for copolymerisation with PES and then for possible use as an impact modifier of PES homopolymer severely restricts the choice available. "Victrex" PES finds commercial applications due to its high temperature stability and low flammability. The elastomer used for rubber toughening must not detract from these properties and must also be thermodynamically incompatible with PES.

Elastomers which can withstand the processing temperatures used with PES (320-390°C) are very limited. Fluorocarbon based elastomers would provide the high thermal stability, but would ruin the low smoke and toxic gas emission properties of PES as required for the aerospace industry (3). The work already carried out by Noshay et al (4-6,8,10) with polysulphone/PDMS block copolymers suggests that elastomers based upon the siloxane repeat unit:-

$$\left(\text{Si}[RR']\text{O}\right)_n$$

are stable under such high temperature processing conditions.

PDMS:-

$$\left(\text{Si}(CH_3)_2\text{-O}\right)_n$$

has high temperature thermal stability as reported in the literature (21-24,109) and also displays good low temperature

characteristics (Tg=-123˚C, Mpt=-53˚C) which satisfy the requirements of a Tg below room temperature. This is required to give elastomeric properties to the copolymer at low working temperatures.

These properties have enabled PDMS to be used successfully as an elastomer in copolymers giving outstanding strength and toughness. Copolymers with polystyrene (110-112), poly(bisphenol A carbonate) (113), polyester (114,115), polyamides (116-118), urea (119,120) and polyimides (121) have all been reported in the literature.

The simple linear PDMS was considered to be a suitable elastomer to be used in the copolymers with PES, not only for its high temperature properties, but also because of the large difference in solubility parameters between PDMS (14.9$[MJm^{-3}]^{\frac{1}{2}}$) and PES (25.2$[MJm^{-3}]^{\frac{1}{2}}$) which will ensure that there is microphase separation in the block copolymers.

3.3 Bond Stability in PES/PDMS Copolymers.

The work of Noshay et al to toughen "Udel" polysulphone was with polysulphone/PDMS block copolymers linked via ≡Si-O-C≡ bonds. Noshay et al have suggested that the copolymers displayed stable ≡Si-O-C≡ bonds at high temperatures, the copolymer showing thermogravimetric behaviour intermediate to that of the homopolymers. The onset of weight loss started at 400˚C. A cast film of the copolymer

placed in a circulating oven for 2 weeks at 170°C was unchanged in appearance and retained 90% of its reduced viscosity (RV).

It is also claimed that the ≡Si-O-C≡ bond is stable under hydrolytic conditions. A solution cast film retained 80% of its initial RV after exposure to boiling water for 8 weeks and after exposure to 10% aqueous sodium hydroxide at room temperature for 30 days, no loss in RV was observed (4-6,8,10-12,17).

This behaviour was attributed to four factors:-

(i) the extreme hydrophobic nature of the copolymers containing hydrocarbons and siloxanes repelling water.

(ii) the ≡Si-O-C≡ bonds sterically hindered by the polymer chains from hydrolytic attack.

(iii) the low number of ≡Si-O-C≡ bonds per copolymer chain reducing the possibility of hydrolytic attack.

(iv) the two phase morphology of the materials making attack by the hydrolysing molecules difficult.

The stability of the siloxane bonds has been studied extensively and it is accepted that the ≡Si-O-C≡ bond is less hydrolytically stable than ≡Si-C≡ bonds (21,24). The ≡Si-O-C≡

bond is chemically and technically simpler to form than the ≡Si-C≡ bond, but is undoubtedly less stable to hydrolysis in short molecules (122).

Although the ≡Si-O- bond has a higher ionic bond energy than the ≡Si-C≡ bond, the high electronegativity of the oxygen atom is accentuated in the case of heterosiloxane bonds e.g. ≡Si-O-C≡. The ≡Si-C≡ and ≡Si-O-C≡ bonds have similar stabilities towards nucleophilic attack, but the unequal bond polarity about the ≡Si-O-C≡ bond makes the silicon-oxygen bond highly sensitive to hydrolytic attack (25). The hydrolytic stability of these copolymers is of particular importance, because commercial grade PES retains moisture which will still be present during the blending process and could cause ≡Si-O-C≡ bond hydrolysis in the copolymers.

Whilst investigating copolymers of "Victrex" PES/PDMS linked via ≡Si-O-C≡ bonds, it was thought that the bonds may have been hydrolysed by the presence of moisture in deuterated dimethyl sulphoxide (d-DMSO) solvent at 80°C during nmr analysis, preventing the presence of ≡Si-O-C≡ bonds being established (26). Due to the increased hydrolytic stability of the ≡Si-C≡ bond over the ≡Si-O-C≡ bond, block copolymers linked directly through ≡Si-C≡ bonds will be studied in this investigation. Although "Udel" polysulphone/PDMS block copolymers have been synthesised containing ≡Si-C≡ bond links, no such work has been reported for "Victrex" PES.

There are two approaches to the preparation of block copolymers of PES/PDMS linked by ≡Si-C≡ bonds:-

(i) functionalise PES to react with a functional siloxane that will form an ≡Si-C≡ bond on copolymerisation.

(ii) functionalise a siloxane to give a material with a reactive end group already linked to the siloxane via an ≡Si-C≡ bond. The end group of the siloxane can then react to form a copolymer joined via a stable carbon bond to PES e.g. ≡C-O-C≡.

Four possible reactions were considered as part of this investigation.

3.4 Grignard Chemistry.

Silicon-carbon bonds are most frequently prepared by the use of Grignard chemistry. Either halosiloxanes or alkoxysiloxanes react with Grignard reagents to form silicon-carbon bonds (21,22,26,123).

$$\equiv SiCl + RMgX \rightarrow \equiv SiR + MgXCl$$

or

$$\equiv SiOR' + RMgX \rightarrow \equiv SiR + MgXOR'$$

This reaction scheme is particularly useful, as polyethersulphone is formed by a condensation reaction of 4,4'-sulphonyldiphenol (Bisphenol "S") and 4,4'-dichlorodiphenylsulphone (DClDPS).

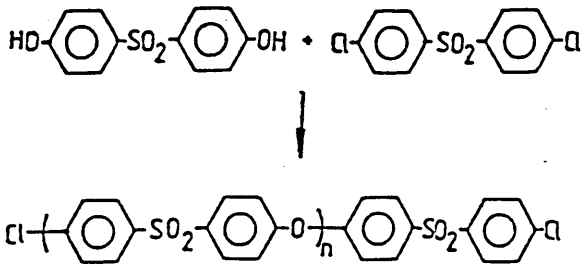

By using an excess of DClDPS, chloro ended PES can be formed and can be used in the formation of a Grignard reagent. The reaction with a halosiloxane would then form a copolymer linked through an ≡Si-C≡ bond.

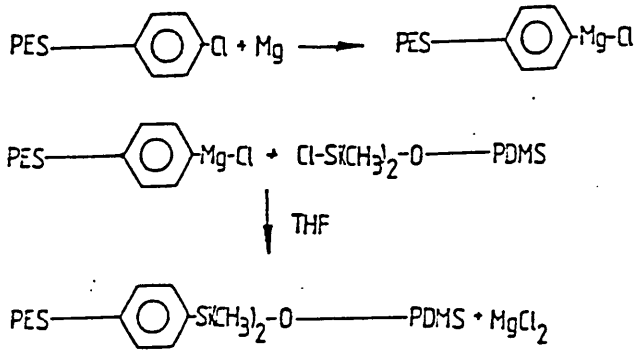

It has been suggested that the localised heat released during the formation of the Grignard reagent is sufficient to rupture ≡Si-O-Si≡ bonds. If the Grignard reagent is formed from the chloro ended PES chains rather than the halo PDMS, the heat generated will not effect the siloxane chains. There is however, a possibility of the siloxane chains being cleaved by the Grignard reagent (22).

3.5 Vinyl Addition Reactions.

Examination of the current literature shows that "Udel" polysulphone can be functionalised to give reactive end groups by an interfacial etherification, involving the use of tetrabutylammonium hydroxide (TBAH) as a Williamson phase transfer catalyst (ptc). The use of stoichiometric amounts of phase transfer catalyst leads to 100% conversion of the end groups at a very fast rate, by forming the onium bisphenolate from the sodium salt of hydroxy polysulphone (124-133). The sodium salt of the polymer precipitates immediately on formation and it is the function of the phase transfer catalyst to transfer the onium salt into the organic solvent in the form of an ion pair, where it then reacts with the functional molecules present. This reaction can be utilised to form vinyl functional PES.

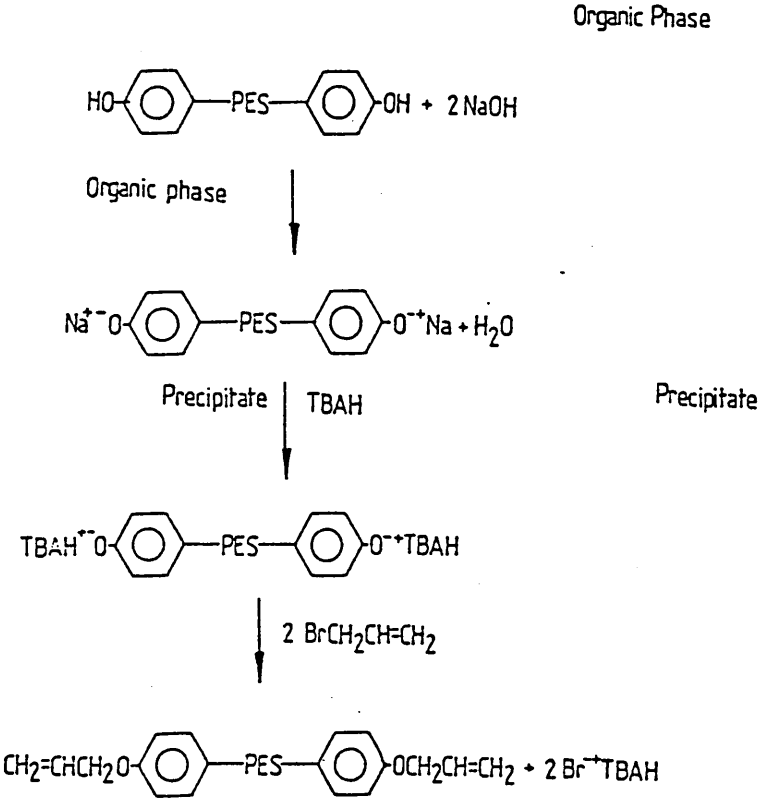

In non-polar solvents, the ion pairs are unsolvated and unshielded (except for the counter ion) and are therefore very reactive. An allyl ether group was chosen to functionalise PES as it is more reactive towards vinyl addition than a vinylbenzyl group.

By carefully choosing the end group, vinyl functionalised PES can be synthesised giving the opportunity for a vinyl addition reaction with hydride terminated PDMS to form ≡Si-C≡ bonds:-

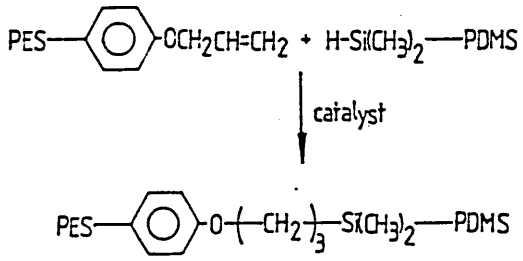

This reaction has been utilised by Percec et al (130-134) to synthesise $(AB)_n$ and ABA block copolymers of PDMS and "Udel" polysulphone. Percec et al achieved good phase separation with low block weight homopolymers, polysulphone Mn= 3,000 and PDMS Mn= 1,200-3,400. The copolymers displayed a polysulphone Tg @200°C and PDMS Tg @-120°C.

When homopolymers of high molecular weight were used to form the copolymer, the homopolymers formed an inhomogeneous reaction mixture in chlorobenzene, even at >100°C. This resulted in incomplete conversion to the block copolymer. This problem was not encountered when one of the homopolymers was of low molecular weight (Mn <1,000). To ensure a

homogeneous reaction mixture was maintained throughout the reaction, a homogeneous homopolymer solution was prepared with the minimum amount of solvent necessary to give homogeneity at the beginning of the copolymerisation. This does not favour the vinyl addition reaction, as concentrated solutions are required for high conversions of platinum catalysed hydrosilylation reactions. As the reaction progressed, the solvent was distilled off at a rate which maintained homogeneity and increased the solution concentration. As the copolymer is formed, it acts as an interfacial agent for the unreacted homopolymers, enabling less solvent to be required to maintain a homogeneous solution and so increase the chance of reaction taking place.

The conversion to copolymer was confirmed by a number of techniques. Proton nmr showed the disappearance of the ≡Si-H signal, movement upfield of the PDMS methyl signals and also the ≡Si-C≡ link was indicated by the appearance of the methylene proton signals formed by the hydrosilylation reaction. Gel permeation chromatography (gpc) and vapour phase osmosis (vpo) showed that the molecular weight of the product materials had increased. In the case of the triblock copolymers, this value was in agreement with the calculated values.

Thermal analysis data showed that the choice of the block lengths of the polysulphone and PDMS dictated the glass transitions of the ABA triblock copolymer as well as its

mechanical moduli. The increase in PDMS block length causes enhanced phase separation and the polysulphone segment Tg approaches that of polysulphone homopolymer. The loss modulus peak broadens with increases in PDMS block length, as both the storage and loss moduli decrease with the increase in PDMS block length.

The hydrosilylation reaction was carried out at 100-120°C to allow complete conversion of the vinyl groups. At lower temperatures, the conversion was reduced, possibly due to the increasing importance of the side reactions involving the ≡Si-H group or the vinyl groups. The longer the reaction time, the greater the possibility of the catalyst becoming deactivated.

The platinum catalysed reaction between the hydride terminated siloxanes and vinyl groups has been thoroughly investigated (21,21,123,135-140). These reactions have been used to form block copolymers of PDMS and polystyrene (141,142). Similarly catalysed vinyl addition reactions have been used extensively as a route to siloxanes functionalised through ≡Si-C≡ bonds (21,22,143-146). These reactions are all catalysed by platinum complexes such as Spier's catalyst; $H_2PtCl_6.6H_2O$ (hexachloroplatinic acid hexahydrate) (135,136).

The suggested reaction mechanism for this reaction is as follows (138):-

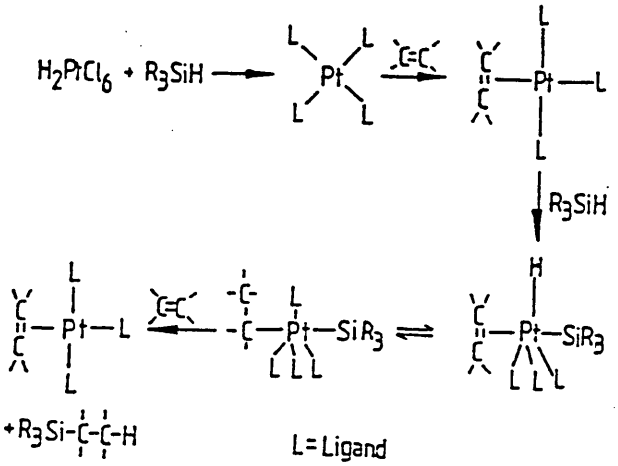

There are a number of side reactions possible when using platinum complex catalysts. The catalyst solution "ages" rapidly and requires fresh preparation under a nitrogen atmosphere (147). The ≡Si-H bond is sensitive to moisture in the presence of the catalyst and so must be kept in a dry medium under a dry nitrogen atmosphere (21,22,123,148-150).

$$\equiv Si\text{-}H + H_2O + Pt(IV) \rightarrow \equiv Si\text{-}OH + H_2\uparrow + Pt(II)$$

Other side reactions can take place, such as redistribution reactions to produce cyclic PDMS products (151) and vinyl hydrogen exchange ligands can be formed (152). Up to 20% of the silane end groups can be used up in isomeration reactions and so are removed from the vinyl addition reaction scheme (153,154).

One of the major side reactions associated with the "ageing" process of the catalyst is the reduction of the oxidation state of the platinum catalyst from IV to II (139,155). As the catalyst reacts with the alcoholic solvent

of the catalyst solution, it is reduced from Pt(IV) to Pt(II). The presence of Pt(II) can catalyse the reaction of the silicon hydride end groups to liberate hydrogen.

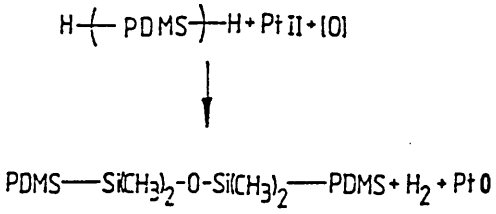

The reduced catalyst appears as fine grey or black solid platinum in the reaction solution. These side reactions can be minimised by the exclusion of air and moisture, as well as by the use of fresh catalyst solution. It is also reported that side reactions such as these proceed at a slower rate than vinyl addition and so should not generally interfere with the copolymerisation. Also the reactivity of Pt(II) and Pt(0) as catalysts is much less than that of Pt(IV) (131,132,139).

It can be seen from the literature that the vinyl addition of functionalised PES with hydride terminated PDMS is a useful synthetic route to providing PES/PDMS block copolymers linked via ≡Si-C≡ bonds.

3.6 Epoxidation Reactions.

As mentioned in section 3.5, vinyl addition reactions have been used to add functional groups to silanes. This can provide PDMS incorporating ≡Si-C≡ bonds as well as adding a specific functional group to PDMS which can then react with

PES to form a copolymer. An example of this is the vinyl addition of 1-allyloxy-2,3-epoxypropane (allyl glycidyl ether) to hydride terminated PDMS and the subsequent reaction of this with a dicarboxy polyester to form a block copolymer (156).

Copolymers have been prepared from epoxy functionalised PDMS formed in this way with "Udel" polysulphone (157). The PDMS is functionalised with allyl glycidyl ether as follows:-

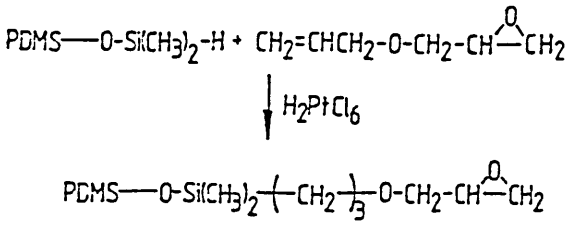

This creates the required ≡Si-C≡ bond as part of the PDMS chain, leaving the functionalised group to react with a suitable end group of polysulphone. If an excess of the hydroxy monomer is used in the formation of the polysulphone, then hydroxyl terminated polymer is produced. The hydroxyl groups are able to react with the epoxy functionalised PDMS (158-160).

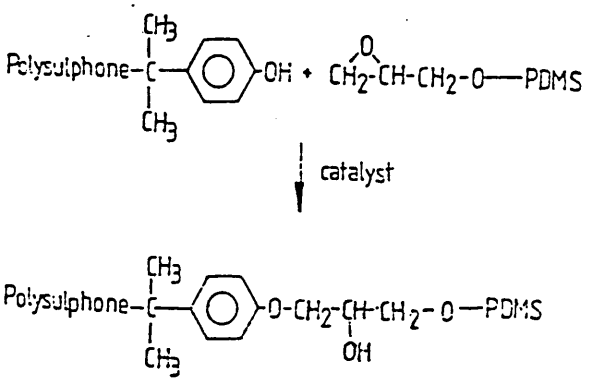

There are possible side reactions, including the reaction of epoxide groups with the pendant hydroxy group produced during the epoxidation reaction. This reaction depends very much

upon the temperature and the presence of any base (161). Madec et al have established that the side reactions make no significant contribution to the final product (156,162).

Gagnebien et al (162) initially investigated the reaction of the epoxide group with the phenolic group in model reactions between 1-allyloxy-2,3-epoxypropane (aep) and 4,4'-isopropylidenediphenol, the Bisphenol "A" monomer of "Udel" polysulphone.

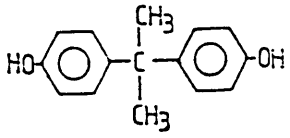

These reactions showed that the epoxidation can be carried out at moderate temperatures in the presence of a basic catalyst and that the two reactive end groups are stable. This work established that a quaternary ammonium catalyst was suitable for the epoxidation reaction. The initial study was carried out in the absence of solvent, which proved far more successful than a similar reaction as a solution in chlorobenzene. The solution reaction gave only a 10% conversion, whereas quantitative conversion was achieved without solvent.

The model reaction study showed that the more reactive epoxy groups were at the end of short alkyl chains, whereas epoxy groups attached to long alkyl chains, phenyl rings or short siloxane chains were less reactive towards phenol groups. The choice of catalyst used also influenced the extent to which side reactions took place. When the catalyst

was N,N'-dimethyldodecylamine (DMDA), the side reactions contributed to no more than 5% of the phenol group conversion. As the concentration of the catalyst increased, there was an increase in side reactions. A catalyst concentration of <5% was determined as the optimum in terms of reaction rate and low side reaction conversion. Infra-red and proton nmr were used to determine the extent of reaction by identifying the changes in signals due to the disappearance of the epoxide rings and the appearance of alcohol groups.

Amine catalysis of epoxidation reactions:-

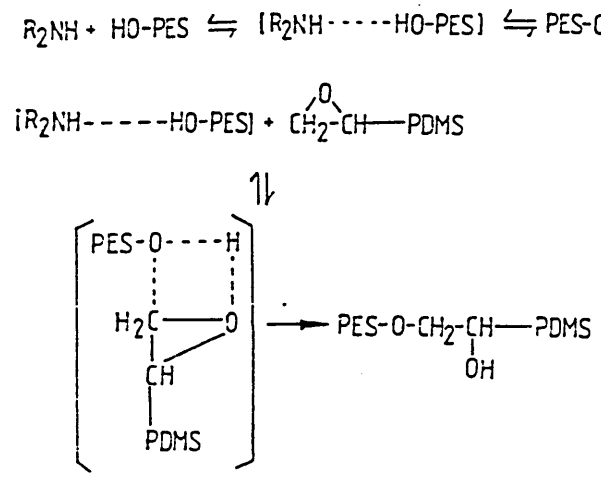

The reactions between polysulphone and epoxy functionalised PDMS posed additional problems (157). The first of these is that the reaction cannot be carried out at the moderate temperatures of molten polysulphone (@ 160°C) without a considerable increase in the contribution of the side reactions, so a solution reaction has to be used. The epoxy PDMS was added progressively to a solution of polysulphone. Initially the siloxane would demix, then after some time would react and form a homogeneous solution. As the

reaction progressed, the homogeneous solution was formed more easily as the copolymer acted as a compatiblising agent. The viscosity of the solution increased until stirring was impossible, so limiting the amount of chain extension of the copolymer. This problem of increasing reaction viscosity was improved by using a high shear mixer. The copolymers were characterised by proton nmr and gpc, which showed the increase in molecular mass of the product over that of the homopolymers.

Gagnebien et al (163) also studied the reaction of polysulphone with aep to form a polysulphone functionalised with vinyl groups. This material was then used in a vinyl addition reaction with disilane PDMS and chloroplatinic acid catalyst, in a similar reaction to those carried out by Percec. Again, the extent of the copolymerisation was limited due to the viscosity of the reaction solution.

From this work, it can be seen that functionalising PDMS through a vinyl addition reaction will form an ≡Si-C≡ bond, leaving the PDMS with epoxide end groups which can react with hydroxyl terminated "Victrex" polyethersulphone. This is another possible route for investigation in order to form PES/PDMS block copolymers.

3.7 Carboxy propyl PDMS/PES condensation.

Riffle et al (23) have formed polycarbonate/PDMS block copolymers by the catalysed condensation of the carboxy propyl terminated PDMS with 4,4'-isopropylidenediphenol (Bisphenol "A"):-

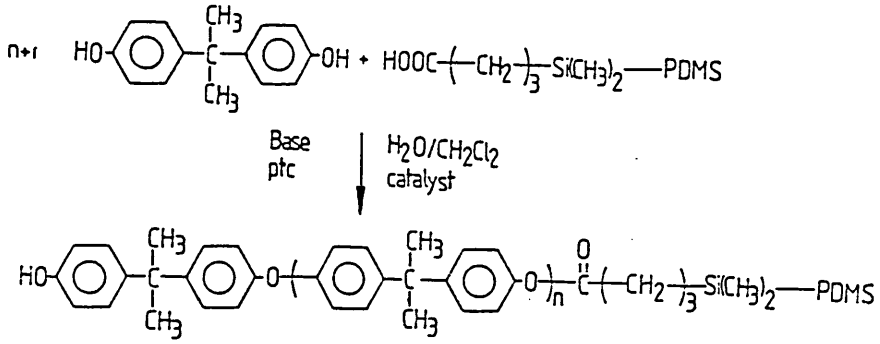

This report investigates the reaction between hydroxyl terminated "Victrex" PES and carboxy propyl terminated PDMS. The carboxy propyl PDMS already has preformed ≡Si-C≡ bonds and the copolymerisation will form stable ester linkages. PDMS is available containing the required functional groups.

The reaction will require the use of a condensation catalyst e.g. tin (II) 2-ethylhexanoate (stannous octoate) to complete the reaction (86,122,164,165).

3.8 Formation of Polydimethylsiloxanes.

Polydimethylsiloxanes are prepared by two main methods:-

(i) condensation of monomeric silanes.

(ii) ring opening polymerisation.

The condensation reaction involves the hydrolysis of labile groups to form silanols which readily condense to form a mixture of linear silanols and cyclic siloxanes (21,22,25).

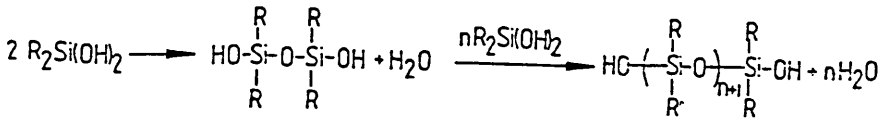

This method leads to materials with a broad relative molecular mass (RMM) distribution and a large percentage of oligomeric siloxanes and cyclic species.

Ring opening polymerisation of cyclic siloxanes can be either anionic or cationic. This may involve the use of a basic catalyst such as a siloxanolate (transient catalyst) (21,22,166-172), an acid (21,22,173,174) or an acid treated clay such as Fuller's earth (175).

The use of acid treated Fuller's earth clay as a cationic catalyst has been studied extensively. The clay is a montmorillonite with a SiO_2-Al_2O_3 surface. Acid treatment of the clay structurally modifies the surface so that it exhibits the properties of a solid acid. The acid treatment initially removes the calcium impurities and then attacks the octahedral sheet structure of the clay, removing aluminium, iron and manganese ions. The cationic sites are filled with H^+ ions and the surface area of the clay is increased (176-178)

The conversion of cyclosiloxanes into linear chains is an equilibrium process, whereby the ≡Si-O- linkages are

continuously broken and reformed until the system reaches an equilibrium condition at the thermodynamically most stable state (21,22). The principal cyclic siloxane used as the bulk starting material is octamethylcyclotetrasiloxane, the cyclic teramer (D_4)

The molecular mass of the linear PDMS is often controlled by a disiloxane, known as an endblocker. These materials control the molecular mass due to the fact that the silicon-oxygen bonds can exchange with and incorporate the growing siloxane chain (179). By contrast, the silicon-carbon bonds in these materials do not react, therefore at equilibrium most of the linear chains are incorporated between the two organosiloxy terminal groups, with some cyclic siloxanes formed as well. This permits the formation of functionalised linear PDMS, the molecular mass of which is controlled by the ratio of D_4:disiloxane.

n= 3 or 4

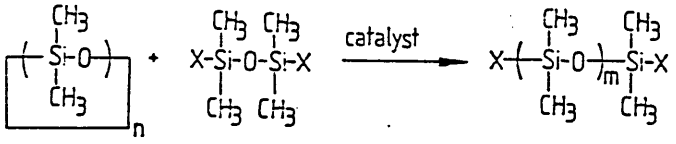

Since a variety of interactions take place, a quantitative conversion of the cyclic starting material to linear polymer is not achieved, since at thermodynamic equilibrium, the siloxane consists of a mixture of linear and cyclic species. The types of redistribution reactions thought to be occurring in these systems are shown below:-

$$-D_x- + D_4 \rightarrow -D_{(x+4)}-$$

$$-D_x- + MM \rightarrow MD_xM$$

$$MD_xM + MM \rightarrow MD_{(x-5)}M + MD_5M$$

$$MD_xM + MD_yM \rightarrow MD_{(x+w)}M + MD_{(y-w)}M$$

M= monofunctional siloxane unit 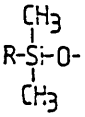

D= difunctional siloxane unit 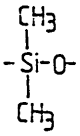

D_4= cyclic tetramer 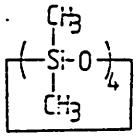

Both linear and cyclic products are formed from the equilibration reaction through the continual cleavage of the ≡Si-O-Si≡ bonds in the siloxane chains.

Alkali catalysed $HO^- + \equiv Si\text{-}O\text{-}Si\equiv \rightarrow \equiv SiOH + {}^-O\text{-}Si\equiv$ siloxanolate

$\equiv Si\text{-}O^- + \equiv Si^A\text{-}O\text{-}Si^B\equiv \rightarrow \equiv Si\text{-}O\text{-}Si^A\equiv + {}^-O\text{-}Si^B\equiv$ propagation

Acid catalysed $H^+ + \equiv Si^A\text{-}O\text{-}Si^B\equiv \rightarrow \equiv Si^A\text{-}OH^+\text{-}Si^B\equiv$

$\equiv Si^A\text{-}OH^+\text{-}Si^B\equiv + \equiv Si^C\text{-}O\text{-}Si^D\equiv \rightarrow \equiv Si^A\text{-}O\text{-}Si^C\equiv + \equiv Si^B\text{-}OH^+\text{-}Si^D\equiv$

This process leads to a random formation of siloxane chains producing a broad distribution of relative molecular mass siloxanes, containing both linear and cyclic species.

The amount of cyclic material formed can be influenced by the equilibration conditions employed. Jacobson and

Stockmeyer (180) described the theory of molecular mass distribution in linear/cyclic equilibrated polymer systems. This theory is based upon the assumption that the proportion of cyclic species present is related to the probability that the terminal atoms will interact to form a macrocyclic molecule. The probability will obviously be much greater if the equilibration is carried out as a dilute solution and much less for an equilibration of the neat siloxane. This prediction has been proved by Semlyen (174) who investigated the increase in cyclic species formed from equilibrations as the dilution was increased. For the bulk equilibration of dimethylsiloxanes, 15% cyclic material is produced, as shown by Semlyen (174) and Carmichael (181). The cyclic siloxane is more volatile than its corresponding linear siloxane consisting of the same number of skeletal bonds and so can be distilled from the equilibration mixture, leaving linear PDMS of high purity.

Butyllithium (BuLi) has been used extensively as an anionic polymerisation initiator for the cyclic trimer, hexamethyltricyclosiloxane (D_3). D_3 is polymerised more successfully with BuLi as it is more reactive due to its greater ring strain compared with D_4. This reaction gives linear PDMS with a relatively narrow RMM distribution. The reaction products can then be functionalised in situ with the appropriate chlorodimethylsiloxane, or can be used to initiate polymerisation with different monomeric species to form copolymers (182-194). These materials are monofunctional and

are ideal for the formation of AB or ABA block copolymers of well characterised PDMS.

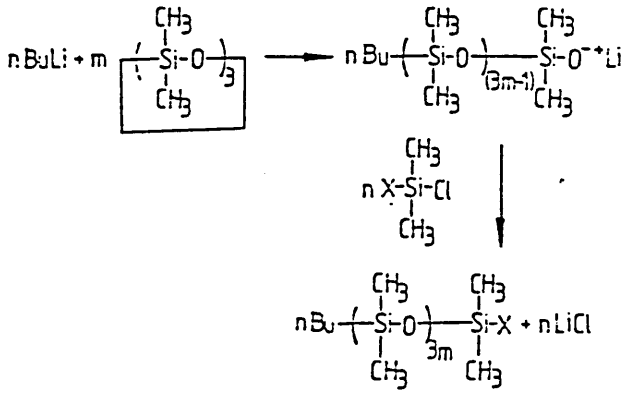

For this investigation, linear PDMS functionalised with hydride groups is required. From the literature, this would be most easily produced by the bulk equilibration of D_4 in the presence of 1,1,3,3-tetramethyldisiloxane to give hydride terminated PDMS of the required RMM. The catalyst most suited to this is acid activated Fuller's earth. This can be easily filtered out of the equilibration mixture prior to distilling off the cyclic siloxanes.

Potassium hydroxide has been used extensively to equilibrate the siloxanes, but if not successfully introduced to the reaction medium results in the formation of gels, as insufficient catalyst is present to continue the equilibration and crosslinking takes place. Liquid acid catalysts are difficult to remove from the reaction mixture after equilibration. This could cause PDMS chain scisson during the later uses of the PDMS.

4. EXPERIMENTAL WORK AND RESULTS.

The work presented here describes the synthesis and characterisation of precursors required to form PES/PDMS block copolymers via the following routes:-

(i) a Grignard reaction between chloro terminated PES and a halo siloxane.

(ii) a vinyl addition reaction between vinyl functionalised PES and a hydride terminated PDMS.

(iii) reaction between hydroxyl terminated PES and epoxy functionalised PDMS.

(iv) a condensation reaction between hydroxyl terminated PES and carboxypropyl functionalised PDMS.

To prepare these copolymers requires the synthesis, purification and characterisation of functionalised homopolymers including vinyl PES and epoxy PDMS before investigating the copolymerisation reactions. A number of model reactions were investigated to confirm the viability of these synthetic routes and copolymerisations. The copolymerisations were investigated as reactions in solution and as a melt.

4.1 Grignard reactions.

This initial work was to establish the formation of a Grignard reagent with an arylchlorosulphone compound. The

simplest and most suitable was dichlorodiphenylsulphone (DCDPS), one of the monomers used in the preparation of polyethersulphone. Grignard reagents have been prepared successfully from p-chlorostyrene (195,196) and it was hoped that DCDPS could be used in simple reactions to show that a silicon group would bond to DCDPS. Initially trimethylchlorosilane was chosen as the additive group:-

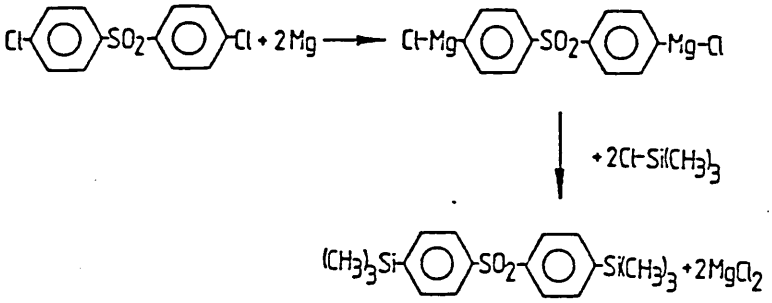

4.1.1 Dichlorodiphenylsulphone and trimethylchlorosilane.

The glassware and magnesium turnings were oven dried overnight at 110°C. 2.4g (0.1 moles) magnesium turnings were weighed into a 100ml 3-neck flask, flame dried under nitrogen. The flask was fitted with a condenser, thermometer, vented dropping funnel and nitrogen reservoir. The flask was purged from the nitrogen reservoir and stirred with a magnetic follower on a magnetic stirrer/hotplate, whilst heating to 35°C. 1.435g (0.05 moles) DCDPS were dissolved in 50mls THF freshly distilled over potassium. 25mls were introduced to the flask immediately along with two drops of 1,2-bromoethane. The remainder of the solution was added dropwise to the flask over 1 hour, whilst maintaining gentle reflux.

Inspite of refluxing for a further 2 hours, magnesium turnings still remained in the flask. 10.85g (0.1 moles) trimethylchlorosilane were added to the dropping funnel via a syringe and rubber septum under nitrogen to prevent hydrolysis of the silane. The silane was added dropwise over 30 minutes to the reaction mixture. The reaction mixture turned clear immediately upon the addition of the silane. After a further 15 minutes reflux, a violently exothermic reaction took place, during which the reaction mixture turned a vivid green colour and a distinctive sulphurous odour was emitted.

After 5 minutes uncontrolled boiling, the yellow coloured reaction returned to reflux. The mixture was cooled and poured over crushed ice. A yellow precipitate was collected and oven dried. The infra-red (ir) spectrum of the solid (Figure 1) was obtained as a KBr disc and was identical to that of DCDPS (Figure 2). The expected stretching frequencies at 1400, 1250, 850 and 725cm^{-1} of trimethylchlorosilane are absent from the ir spectrum of the product.

The violent reaction may have been due to a Grignard reagent being formed with the trimethylchlorosilane and possibly reacting with the sulphone group. The distinctive odour was that of a thiophenyl and a small signal at 2550cm^{-1} could be assigned to the presence of an S-H group, but this is far from conclusive.

This reaction was repeated using ether dried over sodium wire as the solvent and with a 1:1 mixture of THF and ether. Iodine was used to initiate the formation of the Grignard reagent. No other results were obtained however, except that on isolating the product with crushed ice caused a vigorous reaction, possibly from the chloromagnesiumtrimethylsilane and water.

4.1.2 3-Bromopropene and dichlorodiphenylsulphone.

A simpler Grignard compound, more easily prepared and characterised was thought more suitable for the initial investigation. A Grignard reagent prepared from 3-bromopropene (allyl bromide) and added to DCDPS would be more suitable to demonstrate the feasibility of the Grignard route.

The glassware and magnesium turnings were dried in an oven over night. A 250ml 3-neck flask was flame dried under nitrogen and 1.73g (0.072 moles) magnesium turnings and two iodine crystals were added to the flask. Ether (dried over sodium wire) was added to cover the magnesium. The flask was equipped with a condenser, thermometer, vented dropping funnel and a nitrogen reservoir. 8.71g (0.072 moles) 3-bromopropene were added dropwise to the ether, whilst stirring with a magnetic follower on a stirrer/hotplate. Gentle heating was applied and a sequence of colour changes were observed. The solution was iodine red initially and then went from yellow to grey and finally a cloudy white colour. After 5 minutes

heating, a sudden exothermic reaction took place during which the solution turned dark grey and most of the magnesium turnings were consumed.

10.19g (0.0035 moles) DCDPS were dissolved in a minimal amount of 1:1 sodium dried ether/THF (distilled over potassium) and introduced to the dropping funnel using a syringe and rubber septum. The solution was added dropwise over 30 minutes, during which the colour of the solution turned from grey to green and finally red. The solution was then refluxed for 2 hours, cooled and poured over crushed ice. A violent reaction took place on isolating the product, accompanied by a strong odour of thiophenyl. The yellow precipitate was colected and dried in an oven.

The infra-red spectrum of the solid was obtained in the form of a KBr disc (Figure 3) and is identical to that of the DCDPS starting material (Figure 2). The infra-red spectra of DCDPS (Figure 4) and the product (Figure 5) were recorded between 200-600cm^{-1}. This clearly shows no change in the ≡C-Cl stretch at 400-500cm^{-1}.

The product was dissolved in deuterated DMSO (d-DMSO) and the 60MHz ^{1}H nmr spectrum recorded (Figure 6). The aromatic para-substitution can clearly be seen from the DCDPS ring structure. The singlet is due to residual water in the product and the solvent. This signal can be removed from the spectrum by adding deuterated water to the ^{1}H nmr solution.

The distinctive splitting pattern of the allyl group (Figure 7) is absent from the product spectrum, confirming that the product is unreacted DCDPS.

The violent reaction between the product mixture and ice suggests that a Grignard has been formed but no reaction had taken place with DCDPS. The reaction was repeated but with reflux after the preparation of the Grignard prior to adding the DCDPS solution and also using THF as the solvent with no ether present. In both cases the results were the same as for the previous reaction, the Grignard failed to react with the DCDPS.

The failure to react a Grignard reagent with DCDPS curtailed any further investigations into this synthetic route to block copolymers. The evidence that a Grignard reagent was formed but failed to react with DCDPS and the inability of DCDPS to form a Grignard reagent gave little encouragement that the route would be successful. Also, the observation that sudden and violent exothermic reactions took place, generating sufficient heat to possibly break the sulphone linkage or at least discolour the product and boil the solvent encouraged the investigation of the other synthetic routes in the interests of safety.

4.2 Synthesis of hydroxyl terminated PES.

A number of synthetic routes to poly(arylene ether sulphones) have been described in the literature. These include:-

(i) the self condensation of dinuclear arylsulphonyl chlorides, catalysed by ferric chloride (197,198).

(ii) the condensation of arylsulphonyl chlorides with diphenylether, catalysed by ferric chloride (198,199).

(iii) the polycondensation of compounds containing halogenphenylsulphonyl and hydroxyphenyl groups in the presence of potassium fluoride (199,200).

(iv) the polycondensation of halogenophenylsulphonyl-phenoxides (200).

The route recommended by ICI plc and used here to prepare PES oligomers of differing molecular masses is given below (201):-

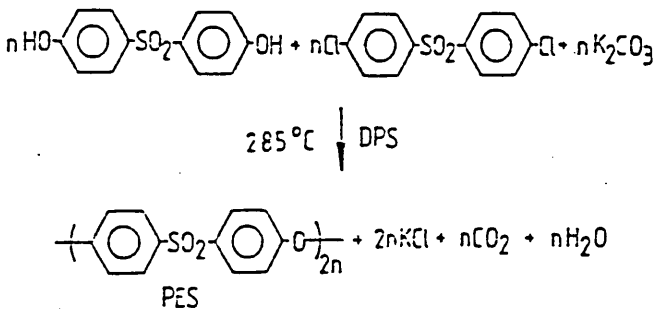

This involves the polycondensation of 4,4'-sulphonyldiphenol (Bisphenol"S") and 4,4'-dichlorodiphenylsulphone (DCDPS) in diphenylsulphone (DPS) solvent. Potassium carbonate is used as the base in a 4%

excess on the weight of the DCDPS monomer. 2% excess potassium carbonate is insufficient to ensure complete reaction and >4% excess leads to unwanted side reactions.

Potassium carbonate is the preferred base as it is more soluble in the DPS solvent and is more basic than sodium carbonate. It is also less destructive towards the ether linkages than potassium hydroxide. This is particularly important, as the ether link is activated by the electron withdrawing sulphone groups to such an extent that they would react just as readily as the chlorophenyl end groups (202,203).

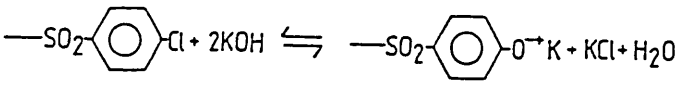

Base induced hydrolysis of the chlorophenyl end groups disturbs the stoichiometric balance of the reaction by using twice as much base to form a phenoxide ion as the reaction with the hydroxyphenyl would require, so reducing the molecular mass of the resulting polymer. Cleavage of the polymer chain at the ether linkages also reduces the molecular mass of the final polymer below that of the calculated value. Potassium hydroxide can also cause fission of the sulphone linkage:-

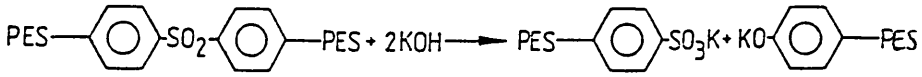

However, this is not usually extensive for para substituted monomers.

Potassium carbonate is sieved prior to the reaction and mixed thoroughly before heating to give a fine dispersion . This has a number of effects upon the polymer:-

(i) maximises the surface area of the potassium carbonate.

(ii) produces less gels as the potassium carbonate is less likely to agglomerate in the presence of water and float to the surface of the reaction mixture.

(iii) produces less foaming as carbon dioxide is released.

(iv) induces less side reactions, producing high molecular weight polymer.

(v) is easier to remove on purifying the copolymer, which gives a better colour to the product.

The high molecular weight material is produced by the reaction of water with the end groups -OH, $-SO_3K$, -OK and $-SO_3H$. This causes gels when the polymer is heated for moulding or extruding by the formation of high viscosity material in localised regions called "nibs".

At high reaction temperatures, chain exchange reactions take place:-

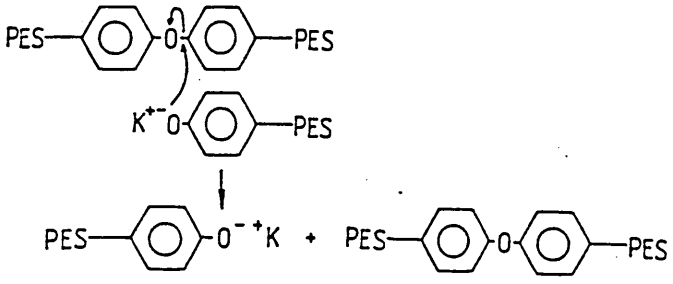

and

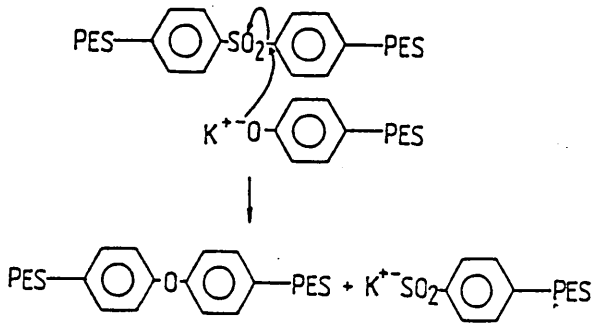

The polymerisation reaction is carried out over a controlled temperature gradient to prevent side reactions and to control the rate of polymerisation. The temperature profile gives the following reaction sequence (204):-

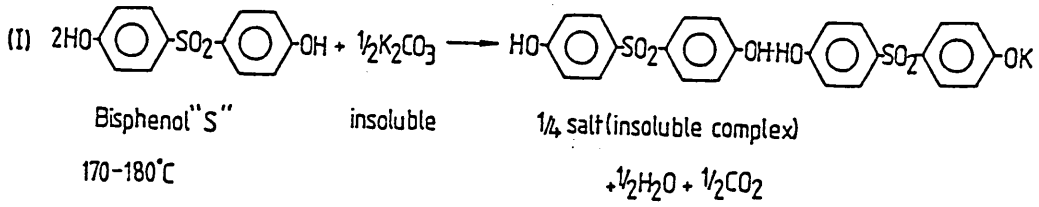

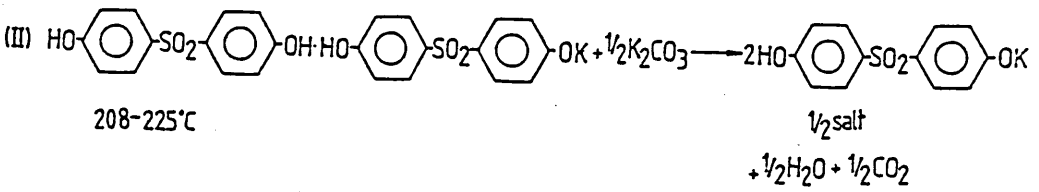

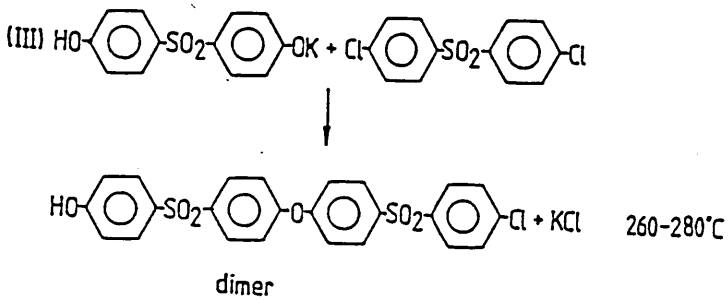

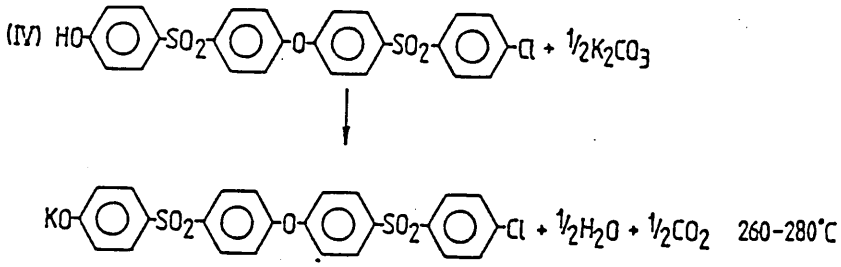

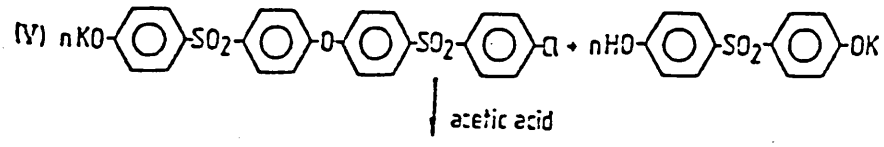

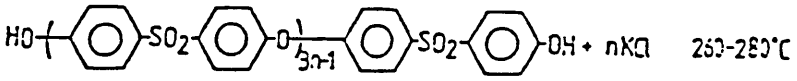

The heating rates are controlled to prevent the decomposition of the ¼ salt:-

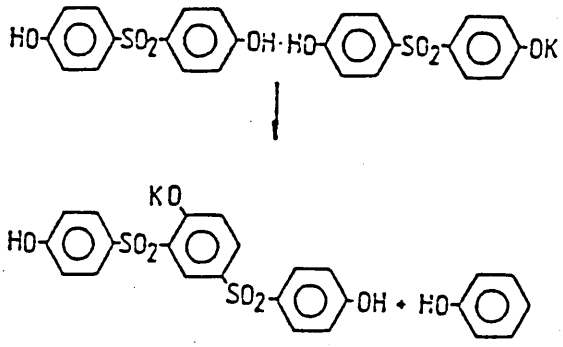

Also, the hydroxyl dimer must be formed before the potassium salt of the dimer, otherwise the resonance stability of the potassium salt would revent further reaction. The phenolic -OH group of the ½ salt is still able to activate the phenoxide ion through the sulphone bridges of the dimer.

In these reactions, Bisphenol"S" is used in excess to ensure that hydroxyl PES is produced. The molecular mass can be controlled by consideration of the following equations:-

$$Mn = 232.3 \times DP$$

and

$$DP = \frac{200}{\%xs} + 1$$

Mn= number average molecular mass of the product.

DP= degree of polymerisation.

%xs= mass percent excess of the controlling monomer i.e. Bisphenol"S" in the case of hydroxyl PES.

The amount of DPS required for the polymerisation was calculated to give 42.44% DPS by mass in the crude product. A 4% excess of potassium carbonate based upon the DCDPS was used. The excess potassium carbonate is based upon the DCDPS monomer rather than Bisphenol"S" to prevent the formation of an excess of bisphenate ions. This can lead to chain branching and chain scission at the sulphone group, producing $-SO_3K$ end groups. This causes micelles to form which show as a second peak in the gpc trace and gives misleading results when measuring the reduced visosity (RV) of solutions with a high micelle content. To produce copolymers from PES, the maximum number of hydroxyl end groups is required.

The PES oligomers were prepared at ICI plc, Wilton by the following method:-

Reagents.

Bisphenol"S" (Bis"S").

Dichlorodiphenylsulphone (DCDPS).

Diphenylsulphone (DPS).

Anhydrous potassium carbonate.

(The potassium carbonate was sieved to <300μm and then oven dried overnight prior to use).

Method.

For a 1 molar scale reaction based upon the weight of DCDPS, a 2 litre split flask was used. The reactants were weighed into the flask in the order listed previously. A stainless steel anchor stirrer was used to thoroughly mix the dry reactants before placing the flask in an oil bath. (Thorough mixing of the potassium carbonate is very important to prevent agglomeration of the base, which is insoluble in the solvent at the initial low temperature. The efficiency of the potassium carbonate dispersion critically affects the resulting RMM of the product.) The flask was then equipped with a thermocouple, nitrogen inlet and a short arm nitrogen bubbler with sufficient water to cover the nitrogen outlet. A low nitrogen pressure was applied and the oil bath heated to 180°C and maintained at this temperature for 2 hours. The flask contents were @170°C.

After 2 hours at 180°C, the contents of the flask were dissolved in the molten DPS except for a hard crust which formed on the surface of the reactants. This was broken up by stirring manually and dispersed in the liquid.

The reactants were stirred mechanically for 30 minutes at a very slow rate to prevent splashing on the side of the

flask. The oil bath temperature was increased to 220°C and maintained for 1 hour with an increased rate of stirring. The temperature was then increased to 275°C, maintained for 1¼ hours and finally increased to 280°C for 30 minutes or until a significant increase in viscosity was observed. Throughout the reaction, condensation was boiled off the flask walls using a hot-air gun, to prevent water running back into the reaction mixture. The final reaction temperature was maintained with the nitrogen bubbler removed. The reaction was stopped by pouring the molten product into 4 litres of cold water.

The crude product contained DPS and potassium salt impurities, both of which are removed by a continuous extraction process. The crude product was placed in a polythene bag and left in an insulated box cooled with "Drikold". The brittle product was then broken into small pieces and milled to a powder with a Christy and Norris laboratory mill. The powder was then slurried into a beaker containing 3½ litres methanol and left stirring at room temperature for 4 hours. The methanol was decanted off and the product slurried into a continuous extraction column. The product was extracted for 18 hours with each of the following solvents:-

(i) methanol/water 3.5:1

(ii) acetic acid/water 1:10

(iii) methanol

The acetic acid solution is used to replace any potassium phenoxide end groups with hydroxyl end groups. The product was then dried overnight under vacuum at 80°C.

4.3 Characterisation of hydroxyl PES oligomers.

The molecular structure of the PES oligomers was determined by infra-red (ir) and ^1H nuclear magnetic resonance spectroscopy (^1H nmr).

4.3.1 Infra-red.

The samples were prepared by casting a film of the product on a KBr disc from a solution of dichloromethane or directly from the solid as a KBr disc. An example of the resulting absorption spectrum is given in Figure 8. The specific bond stretching assigned to the absorption peaks is given in Table 1.

The main absorption peak of interest in this spectrum is that of the strong aryl ether stretch at 1250cm^{-1} due to the ether link formed between the monomers during polymerisation. This peak is absent from both the monomers and the DPS solvent (Figures 2,9,10). Also of note, is the relative intensity of the O-H stretch (3430cm^{-1}) to the aromatic C-H stretch (3090cm^{-1}) in the PES oligomer (Figure 8) and the monomer Bisphenol"S" (Figure 9). The O-H stretch of the monomer is

of far greater intensity than the C-H stretch absorption, but in the PES oligomers, they are much more equal in intensity.

Infra-red spectroscopy was used by ICI, Wilton to determine if the oligomers contained a significant number of chloro end groups, if any were present. No absorption was detected at 400-500cm^{-1} due to aromatic C-Cl stretch, confirming that the PES oligomers were hydroxyl ended. Residual DPS in the product is identified by the presence of an absorption signal at 1180cm^{-1}, appearing as a shoulder on the PES absorption peak at 1125cm^{-1}. None were detected in the PES oligomers.

4.3.2 ^1H nmr.

^1H nuclear magnetic resonance spectroscopy (^1H nmr) provides further evidence of the structure and purity of the PES oligomers. Figure 11 shows the ^1H nmr spectrum of hydroxyl terminated PES as a solution in deuterated dimethyl sulphoxide (d-DMSO) from an 80MHz Brüker instrument. At 2.5ppm is a peak due to an impurity in the Bisphenol"S" monomer (Figure 12). At 7-8ppm is the typical A-B quartet splitting pattern of a para-substituted aromatic ring, as expected from the repeat unit of PES:-

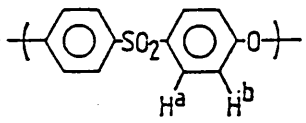

The aromatic rings consist of two adjacent non-equivalent proton pairs. Each pair forms one peak, split by the adjacent non-equivalent proton. Diphenylsulphone present as an

impurity would introduce smaller peaks in between this main splitting pattern. ^1H nmr is also used to check for the presence of monomers and DPS solvent in PES samples. Figure 13 shows the nmr splitting pattern of DPS.

The choice of an appropriate solvent is important to obtain all the information from an nmr spectrum. Figure 14 shows the ^1H nmr spectrum of PES when deuterated chloroform ($CDCl_3$) is used as the solvent. The peak at 1.5ppm is due to water present in the sample and the peak at 3.5ppm is due to the impurity in the Bisphenol"S" monomer. The intense peak at 7.2ppm is due to residual protons in the deuterated solvent. The splitting pattern of the aromatic protons at 7-8ppm is strongly distorted when compared with the spectrum made with d-DMSO as the solvent (Figure 11). This is due to the PES being sparingly soluble in $CDCl_3$ and leaving undissolved material in the solution. The resolution of the spectrum is reduced and a poor signal collected.

Figure 15 shows the ^1H nmr spectrum of a PES solution in d-DMSO solvent collected from a 200MHz Brüker nmr instrument. The AB splitting pattern is the main feature, but three other groups can be seen. The doublet labelled 1 is due to the signal of the aromatic protons adjacent to the hydroxyl end groups:-

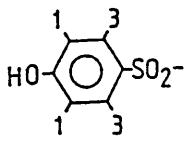

2 is due to the signal of the aromatic protons adjacent to the chloro end groups:- 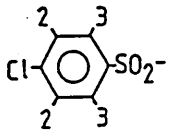

The doublets labelled 3 are due to the protons adjacent to the sulphone groups.An enlarged spectrum (Figure 16) shows this more clearly.

Investigation of this area of the PES spectrum shows how the end groups can be quantitatively identified. Figure 17 shows the ^1H nmr spectrum of a hydroxyl PES sample with integration lines. Integration of the aromatic protons adjacent to the hydroxyl groups and integration of the signal from the PES repeat unit protons allows the calculation of the polymer RMM. This PES sample shows that only hydroxyl end groups are present.

4.4 Relative Molecular Mass (RMM).

The RMM of the PES oligomers can be determined by end group analysis as described in section 4.3.2. Other methods were employed to confirm these results.

4.4.1 Gel Permeation Chromatography (gpc).

The PES oligomers were examined by gpc at ICI, Wilton under the following conditions:-

Column: 4x4ft, packed with silica, pore size 30-30,000 $x10^{-10}$m.

Solvent: dimethylformamide (DMF).

Temperature: 40°C.

Run time: 2½ hours.

Flow rate: 0.5 ml/minute.

Calibration: Polystyrene standards.

The main information to be gained from gpc concerns the "high molecular size" (HMS) material which appears upon the gpc trace as the smaller of the two peaks in the bimodal distribution. The HMS material are micelles formed by the aggregation of highly polar end groups, -OH, OK, $-SO_3H$. For hydroxyl PES, this would be expected to be more significant than for chloro ended PES. Also, the higher the RMM of the polymer, the higher the level of HMS expected.

Figure 18 shows the bimodal distribution of a PES oligomer prepared in the laboratory and Figure 19 the distribution for a commercial sample of hydroxyl ended PES 5003P. The amount of HMS material is significantly greater in the commercial material.

Generally, the amount of HMS material is low for the oligomers prepared in the laboratory, as accurate temperature control and water removal are more easily obtained. A summary of the RMM analyses for the PES oligomers prepared, along with a commercial sample of hydroxyl PES are given in Table 2. The

RMM values determined by gpc are calculated by computer from the polystyrene calibration curve, disregarding the contribution of the HMS peak.

4.4.2 Solution Viscometry.

The number average molecular weight (Mn) of the PES oligomers was determined by using a viscometric method developed by ICI plc.

0.25g dry polymer were weighed into a clean dry 25ml volumetric flask. The flask was half filled with DMF and was shaken mechanically until all the polymer had dissolved. The solution was then made up to the mark with DMF to give a 1% w/v PES solution.

A clean, dry grade "A" capillary U-tube viscometer was placed in a thermostat bath at 25°C. The viscometer was filled with DMF via a sintered funnel and allowed to equilibrate. The excess DMF was removed with a syringe, leaving the reservoir filled to the etched minimum mark. The DMF was drawn into the bulb and the time taken for the DMF to flow between the two timing marks was recorded. This was repeated until two consecutive readings ± 0.1 seconds were made. The viscometer was then washed out with DMF and polymer solution before similarly measuring the flow time of the polymer solution. The reduced viscosity (RV) of the polymer

and Mn was calculated for a 1% solution of PES using the following equations:-

$$RV = \frac{\textit{average flow time of the solution (seconds)}}{\textit{average flow time of the solvent (seconds)}} - 1$$

$$DP = 292 \times RV^{1.508}$$

$$Mn = 232.3 \times DP$$

The results of the analysis are given in Table 2. PES samples 12-14 were unable to be characterised by reduced viscosity, because the flow time of the 1% w/v solution was within 10 seconds of the flow time of the solvent.

4.5 Synthesis of vinyl Polyethersulphone (v-PES).

With reference to the work of Percec et al (129,133), the following method was devised for the preparation of PES functionalised with vinyl groups.

10g hydroxyl PES (RMM=4,370 by gpc, 2.3×10^{-3} moles, 4.6×10^{-3} moles OH groups) were dissolved in 400mls dichloromethane (distilled over phosphorous pentoxide and stored over 4A molecular sieve) under reflux in a 500ml 3-neck round bottomed flask. The flask was equipped with a reflux condenser, nitrogen reservoir, pressure equalising dropping funnel and was stirred by a magnetic follower on a stirrer/hotplate.

The solution was allowed to cool with stirring and 1.75g (5.15×10^{-3} moles) tetrabutylammonium hydrogen sulphate (TBAH) were added. 2g (1.65×10^{-2} moles) allyl bromide were added dropwise and the solution was stirred for 10 minutes. 10mls (0.125 moles) 12.5M aqueous sodium hydroxide solution were added dropwise. The sodium salt of PES precipitated immediately. The solution was then refluxed for 20 hours during which, the precipitate disappeared.

The reaction was cooled and precipitated in methanol. The crude product was filtered off and solvent extracted with methanol for 24 hours to remove any excess allyl bromide. The product was then oven dried at 80°C.

4.6 Characterisation of v-PES.

The molecular structure of the functionalised PES was determined by infra-red and ^1H nuclear magnetic resonance spectroscopy.

4.6.1 Infra-red.

The sample was prepared by casting a film of the product onto a KBr disc from a solution in dichloromethane. An example of the resulting spectrum is given in Figure 20.

The main area of interest is in the region $3430cm^{-1}$. The OH stretch seen in the hydroxyl PES starting material

(Figure 8) is completely absent, suggesting that the reaction has taken place.

4.6.2 ^{1}H nmr.

The purified product after functionalising PES with vinyl groups was fully soluble in both $CDCl_3$ and d-DMSO, suggesting that modification of the highly polar hydroxyl end groups had taken place. Hydroxyl PES was not sufficiently soluble in $CDCl_3$ to give a clearly resolved spectrum (Figure 14).

Figure 21 shows the ^{1}H nmr spectrum of v-PES taken as a solution in $CDCl_3$ with a Brüker 80MHz instrument. The large singlet at 0.1ppm is due to the internal standard, tetramethylsilane (TMS). The doublet at 4.5ppm (H^a), the triplet at 5-5.5ppm (H^b) and the multiplet at 5.7-6.2ppm (H^c) are typical of the allylbromide protons.

$$\overset{a}{Br\text{-}CH_2}\text{-}\overset{b}{CH}=\overset{c}{CH_2}$$

This spectrum does not change after reprecipitation and further soxhlet extraction. The spectrum is also unchanged when obtained from d-DMSO solution. From the integration of the aromatic and the vinyl protons and the known RMM of the original hydroxyl PES starting material, the extent of the reaction can be calculated. Typically this was >95%.

Closer examination of the v-PES product by 200MHz ^{1}H nmr shows the peaks due to the aromatic allyl and the aromatic hydroxyl splitting. Figure 22 shows the ^{1}H nmr of a vinyl PES product in d-DMSO solution:

(i) doublet A is due to ^{13}C satellites.

(ii) doublet B is due to chloro ended PES. 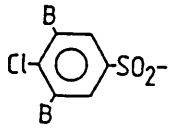

(iii) doublet C is due to hydroxyl ended PES. 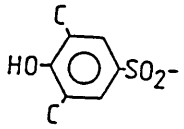

(iv) doublet D is due to vinyl ended PES. 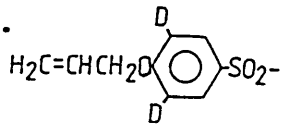

From this sample it can be seen that the hydroxyl and vinyl PES end groups are present in equal proportions, along with a small amount of chloro ended PES.

Figure 23 shows the ^{1}H nmr spectrum of a v-PES sample after 95% conversion of the hydroxyl groups to vinyl end groups. The signal due to the aromatic hydroxyl splitting is only just detected in comparison with the prominent signal from the aromatic allyl protons, confirming the almost quantitative conversion of the end groups.

4.7 Synthesis of polydimethylsiloxanes (PDMS).

Two approaches were used in the formation of functionalised PDMS oligomers:

i) 1,1,3,3-tetramethyldisiloxane and D_4 were equilibrated with acid activated Fuller's earth to produce hydride functionalised PDMS. This material can then be used in

catalysed vinyl addition reactions with v-PES to form block copolymers linked via ≡Si-C≡ bonds.

The hydride PDMS can also be functionalised with epoxy groups through a vinyl addition reaction. This incorporates ≡Si-C≡ bonds in the PDMS and provides functional groups which can react with hydroxyl PES to form copolymers.

ii) 1,1,3,3-tetramethyldisiloxane was functionalised with epoxy groups through a vinyl addition reaction. The disiloxane was then equilibrated with D_4 using a siloxaolate catalyst to produce epoxy functionalised PDMS incorporating ≡Si-C≡ bonds. This can react with hydroxyl PES to form copolymers linked via ≡Si-C≡ bonds.

The siloxanolate catalyst was prepared by the reaction between D_4 and the tetramethylammonium hydroxide.

Reagents.

D_4.

The D_4 was supplied by Dow Corming. 95% D_4, with D_3 and D_5 as the impurities, as determined by gas liquid chromatography (glc). The following glc method was developed to determine the purity of D_4:

Column:	3% OV1 on Chromasorb WHP, 6ft x ⅛"
Initial oven temperature:	60°C.
Final oven temperature:	300°C (held for 20 minutes).

Heating rate:	15°C/minute.
Injection temperature:	250°C.
Detector temperature:	250°C.
Attenuation:	256.
Chart speed:	10mm/minute.
Carrier gas flow rate:	20ml/minute.
Sample:	0.2μl (100% sample). Syringe cleaned with ether.

Figure 24 shows the glc chromatogram of the D_4, with the peaks due to ether, D_3, D_4 and D_5.

Fuller's earth

The Fuller's earth was supplied by BDH and activated by stirring in concentrated sulphuric acid overnight. The Fuller's earth was filtered off in a sintered crucible and washed with water until the filtrate was collected at pH7. The Fuller's earth was then kept in an oven at 100°C.

Siloxanolate catalyst.

The siloxanolate catalyst was prepared by the reaction between D_4 and tetramethylammonium hydroxide in a 4:1 mole ratio (169). The tetramethylammonium hydroxide pentahydrate was supplied by Aldrich.

20g (0.068 moles) D_4 and 3.2g (0.017 moles) tetramethylammonium hydroxide pentahydrate were weighed into a 100ml 3-neck flask, equipped with a condenser, nitrogen

inlet and thermometer. The reactants were stirred with a magnetic follower on a stirrer/hotplate for 48 hours at 60°C with a strong nitrogen flow to remove moisture. A cloudy viscous liquid was formed, which set to a white solid on standing.

1,1,3,3-tetramethyldisiloxane.

The disiloxane was used as supplied by Fluka.

Mixed PDMS cyclics.

A sample of mixed cyclic PDMS were obtained from S.Cockett (Sheffield Polytechnic). This was used as a reference for glc and gpc analysis to determine the purity of the linear PDMS oligomers after distillation to remove cyclic PDMS impurities.

The sample was prepared by the equilibration of D_4 with finely ground potassium hydroxide in a dilute toluene solution.

4.7.1 Fuller's earth equilibration.

The ratio of D_4 to disiloxane end-blocker used to form linear PDMS of RMM @5000 was determined empirically.

50g (0.16 moles) D_4, 0.275g (0.5% on total weight of reactants) acid activated Fuller's earth (175) and 1.95g (0.015 moles) disiloxane were weighed into a 100ml 3-neck

round bottomed flask, equipped with a condenser, nitrogen reservoir and thermometer. The reaction mixture was stirred with a magnetic follower in an oil bath for 72 hours at 80°C. The reaction product was filtered through glass wool (to remove the Fuller's earth) into a Vigreux Claisen flask and was distilled under 0.03mm Hg pressure at 150°C for 6 hours to remove the cyclic siloxanes.

4.7.1.1 Infra-red.

The infra-red spectrum of the purified PDMS was obtained as a thin film of the liquid between potassium bromide plates.

Figure 25 shows the infra-red spectrum of a linear hydride terminated siloxane (RMM=4,370). The specific bond stretching assigned to the absorption peaks is given in Table 3. The main peaks of interest are the Si-H stretch at 2120cm^{-1} and the Si-O-Si stretch at 1090 and 1020cm^{-1}.

The Si-H stretch is quite distinct and will disappear on the completion of a vinyl addition reaction. The disappearance of this absorption and the decrease in the size of this signal when compared with the adjacent C-H signal (2960cm^{-1}) are very useful in determining the extent of a vinyl addition reaction. PDMS oligomers of lower RMM show a more pronounced absorption signal in this region, as shown in Figure 26 (PDMS RMM @700).

The twin absorptions at 1090 and 1020cm^{-1} due to Si-O-Si stretch are characteristic of linear PDMS. Cyclic PDMS oligomers only display a single absorption in this region, as shown in Figure 27, the infra-red spectrum of the D_4 starting material. Only a single absorption at 1070cm^{-1} due to the Si-O-Si stretch is displayed.

The infra-red spectrum of the distillate is shown in Figure 28. The Si-O-Si stretch at 1070cm^{-1} is only a singlet, indicating cyclic PDMS and there is no absorption due to the Si-H stretch at @ 2100cm^{-1}. The spectrum is identical to that of the cyclic starting material shown in Figure 27.

4.7.1.2 ^{1}H nmr.

The ^{1}H nmr spectrum of the distilled linear siloxane was obtained as a solution in $CDCl_3$, using a Brüker 80MHz instrument (Figure 29).

The main signal at 0.08ppm is due to the siloxane chain methyl protons. The two singlets at 0.15ppm and 0.2ppm are due to methyl protons adjacent to the end group displaying a different chemical shift. The multiplet at 4.7ppm is due to the ≡Si-H protons. This is shown more clearly in the enlarged section of the spectrum.

The enlarged ^{1}H nmr signal for the silicon-hydride protons enables the integration to provide a more accurate

result when it is used to calculate the RMM of the PDMS. The ratio of the silicon hydride protons to the siloxane chain methyl protons provides a simple method for calculating the RMM of the polymer. As the RMM of the PDMS increases, the signals of the methyl protons and the silicon hydride protons appear as singlets.

4.7.1.3 Gpc.

A more accurate method for determining the RMM of the linear PDMS is gpc. A number of mono dispersed linear trimethyl terminated PDMS polymers were supplied by Dr K Dodgson (Sheffield Polytechnic) which enabled accurate calibration of the gpc instrument to be made. The samples of low polydispersity (<1.1) were passed through an Applied Chromatography Systems dual piston pump gpc instrument under the following conditions:-

Columns:	1xBondagel E500 and 1xPorasil 60Å in series.
Solvent:	Toluene.
Flow rate:	1ml/minute.
Samples:	1 drop of sample from a Pasteur pipette per 1ml toluene solvent, filtered three times through a 0.45μm nylon 66 membrane. Samples made up in glass vials with polypropylene lids to prevent the leaching of any plasticisers into the sample. 1 drop of D_4 added as an internal standard.

Temperature: Ambient.

Detector: Waters R401 refractometer.

Attenuation: x16.

Chart speed: 6cm/minute.

The mono dispersed PDMS samples (Mn=770-12,300) were prepared in micro filtered toluene with 1 drop of D_4 added to the solution as an internal standard. From the gpc traces, the retention index of each of the samples was calculated.

$$\textit{Sample retention index} = \frac{\textit{Retention volume of sample}}{\textit{Retention volume of } D_4}$$

Plotting ln Mn versus retention index for the calibration standards produces a linear relationship over the RMM examined here (Figure 30). A typical gpc chromatogram is shown in Figure 31.

Gpc separates species of different volumetric size. The cyclic and linear PDMS species take up different conformations in solution and so are clearly separated by gpc (Figure 31) as shown by Clarson and Semlyen (109). Figure 32 shows the gpc chromatogram of the mixed cyclic oligomers. Only one peak is observed with the same retention volume as D_4, so the identification of cyclic impurities in samples of distilled linear PDMS can easily be made.

In calibrating Mn for the linear PDMS samples by gpc, the following method was used. Samples of D_4 only were run through the gpc instrument until concurrent values for the retention volume were obtained. The sample of linear PDMS with no internal standard was run next, followed by another sample of D_4. If the retention volume of the D_4 samples bracketting the unknown linear sample had changed, then the average of the two values was taken when calculating the smple retention index. The Mn of the sample was then determined from the calibration graph (Figure 30). The presence of any residual cyclic material can easily be identified as a second peak with the same retention volume as D_4.

A comparison of the RMM values of hydride PDMS determined by ^1H nmr and gpc are given in Table 4.

4.7.1.4 Glc.

The glc method described in section 4.7 was used to identify the rings in the "mixed cyclics" equilibration mixture. This is shown in Figure 33 and is comparable with the work of Clarson (109). Under the same glc conditions a sample of distilled hydride PDMS, shown to be free of cyclic material by gpc was analysed by glc (Figure 34). This shows only small traces of cyclic material remaining after distillation. The hydride PDMS sample was diluted with toluene to the same concentration as the "mixed cyclics" equilibration sample. Figure 35 shows the glc chromatogram

of the distillate, indicating the presence of mainly the lower cyclic species.

4.7.2 Siloxanolate equilibration.

10g (0.034 moles) D_4, 0.4g (0.0011 moles) diepoxydisiloxane (as prepared in section 4.7.3.2) and 0.058g (0.55% on total weight of reactants) siloxanolate catalyst (169) were weighed into a 50ml round bottomed flask, equipped with a condenser and nitrogen reservoir. The contents of the flask were stirred with a magnetic follower for 48 hours in an oil bath maintained at 80°C. At this temperature, the siloxanolate catalyst dissolved in the cyclic siloxane. The temperature of the reaction mixture was then raised to 150°C and maintained for 3 hours to decompose the catalyst and hence stop the reaction. The product was then distilled under vacuum for 3 hours at 150°C, 0.01mm Hg pressure.

4.7.2.1 ^{1}H nmr.

Figure 36 shows the ^{1}H nmr spectrum of the diepoxysiloxane functionalised starting material as a solution in $CDCl_3$, using an 80MHz Brüker instrument. This spectrum will be discussed in more detail in section 4.5.3.4. Figure 37 shows the ^{1}H nmr spectrum of the epoxy functionalised PDMS product. The peak splitting and integration of the allyl epoxy propyl groups are identical to that of the disiloxane material (Figure 36), indicating that the equilibration in the

presence of the anionic catalyst has not disturbed the epoxide rings.

4.7.2.2 Gpc.

The distilled product was analysed by gpc under the same conditions as described in section 4.7.1.3. Figure 38 shows an example of the gpc chromatogram obtained from a purified siloxanolate/diepoxydisiloxane equilibration reaction. The peak of the linear material is broad and has a long tail of low molecular weight material. This is much broader and less symmetrical than the peak obtained from the Fuller's earth catalysed equilibrations (Figure 32), but does show that linear, functionalised PDMS has been formed. There is also a small peak indicating residual cyclic or low RMM material in the sample.

4.7.2.3 Glc.

The distilled product was analysed by glc under the same conditions used in section 4.7.1.4. Figure 39 shows the chromatogram for a sample of the diepoxydisiloxane (0.5μl injection of 50% diepoxydisiloxane in ether). Figure 40 shows the chromatogram of the distillate (0.5μl injection of 50% linear PDMS in ether). The linear PDMS shows little cyclic contamination other than from unreacted D_4 and diepoxysiloxane.

4.7.3 Allyl glycidyl ether/hydride PDMS vinyl addition.

The initial investigations into the vinyl addition reactions with hydride PDMS using chloroplatinic acid catalyst (hydrogen hexachloroplatinate IV hydrate) followed the work of Gagnebien et al (157). Allyl glycidyl ether was used to functionalise 1,1,3,3-tetramethyldisiloxane, the product being used in siloxanolate/D_4 equilibrations (section 4.7.2). From the information gained in these reactions, suitable conditions were developed to functionalise hydride terminated PDMS with allyl glycidyl ether.

4.7.3.1 Preparation of the platinum catalyst solution.

The chloroplatinic acid catalyst is easily reduced in moist air and was stored as the solid in a sealed container inside a sealed flask, covered with aluminium foil, purged with nitrogen in a refrigerator. Solutions of the catalyst were prepared in a glove box under nitrogen using vessels covered with aluminium foil to prevent reduction of the catalyst.

In the glove box, the solid catalyst was transferred to a pre-weighed sample vial. The sample vial was then re-weighed. The catalyst was dissolved in either 1-butanol or THF (freshly distilled over potassium) and transferred to a graduated flask. The solution was made up to the mark with washings from the sample vial. The distinctive orange-yellow

colour of the catalyst solution was seen if the catalyst was not fully dissolved initially. The graduated flask was then stoppered, sealed with "Nescofilm" and then covered with aluminium foil before storing in the refrigerator. The catalyst solution was discarded after 5 days storage.

4.7.3.2 Allyl glycidyl ether/1,1,3,3-tetramethyldisiloxane.

The initial reactions following the literature (157) involved adding the disiloxane to a mixture of allyl glycidyl ether and catalyst solution at 50°C. The catalyst required was 0.1% by weight based upon the reacting species in a 1% solution. This produced a highly exothermic reaction which caused boiling of the allyl glycidyl ether and the 1-butanol.

Further examination of the literature detailing vinyl addition reactions suggest that lower levels of catalyst would be more appropriate (135). The following method was developed for the vinyl addition of the disiloxane with allyl glycidyl ether. This provided a less vigorous reaction and caused less discolouration of the product due to thermal degradation of the catalyst.

11g (0.095 moles) allyl glycidyl ether were weighed into a 50ml 3-necked round bottomed flask covered with aluminium foil. The flask was placed in a glove box under nitrogen and 0.7mls (4.1×10^{-8} moles) chloroplatinic acid catalyst (6.1×10^{-3}g in 200mls 1-butanol) were added to the flask. The vessel was

stoppered, removed from the glove box and equipped with a thermometer, vented dropping funnel, condenser and a nitrogen reservoir. The flask was then purged with nitrogen and was stirred in an oil bath with a magnetic follower.

5g (0.0373 moles) 1,1,3,3-tetramethyldisiloxane were added dropwise at room temperature. The temperature was then increased to 50˚C and maintained for 1 hour. A sample was taken at this stage for infra-red analysis (Figure 41). The reaction was heated to 150˚C and re-sampled for infra-red analysis (Figure 42), which showed that the reaction was completed. Reactions with high catalyst concentrations did not require heating above 50˚C.

The crude product was cooled and transferred to a Vigreux-Claisen flask for vacuum distillation at 100˚C, 0.6mm Hg pressure over 2 hours. The distilled product was a colourless liquid and was analysed by infra-red and ^{1}H nmr spectroscopy.

4.7.3.3 Infra-red.

Figure 43 shows the infra-red absorption spectrum of allyl glycidyl ether made as a liquid film between KBr plates. The main absorption peaks of note are the C=C out of plane stretch at 1420cm^{-1} and 1640cm^{-1}, as well as the C-H stretch of the epoxide ring at 1250cm^{-1} and 3040cm^{-1}.

Figure 44 shows the infra-red absorption spectrum of 1,1,3,3-tetramethyldisiloxane made as a liquid film between KBr plates. The main peaks are the Si-H stretch at 2130cm^{-1} and the aliphatic C-H stretch at 2960cm^{-1}. Note the relative intensities of these absorptions in comparison with those in Figure 41, the partially reacted product. The remainder of this spectrum consists of the Si-CH_3 stretch at 1255cm^{-1} and 880cm^{-1}, Si-O-Si stretch at 1065cm^{-1} and the Si-H stretch at 910cm^{-1}.

Figure 41, the infra-red absorption spectrum of the reaction mixture after one hour at 50°C shows all the main features of the two starting materials, in particular the Si-H stretch at 2120cm^{-1} and the C=C stretch at 1645cm^{-1}. Both these peaks appear to be lower in intensity than in the starting materials, indicating that some reaction has taken place.

Figure 42, the infra-red absorption spectrum of the reaction mixture after heating to 150°C shows a complete absence of the Si-H stretch at @ 2120cm^{-1}, but there is a peak at 1665cm^{-1} due to the C=C stretch of allyl glycidyl ether. Excess allyl glycidyl ether was used in the reaction.

Figure 45 shows the infra-red absorption spectrum of the purified product made as a liquid film between KBr plates. The absorption peak due to the C=C stretch seen in Figure 42

is absent (1665cm^{-1}) and the main features of the product can be identified:-

i) Si-O-Si stretch 1060cm^{-1}.

ii) Si-CH_3 stretch 1260, 845 and 800cm^{-1}.

iii) epoxide C-H stretch 3040cm^{-1}.

iv) aliphatic C-H stretch 3090-2850cm^{-1}.

This suggests that both the reaction and purification stages have been successful. Figure 46 shows the infra-red absorption spectrum of the distillate taken from the reaction product, made as a liquid film between KBr plates. The spectrum is identical to that of allyl glycidyl ether (Figure 43), confirming that the distillation has removed the excess starting material.

4.7.3.4 ^{1}H nmr.

The ^{1}H nmr spectrum of allyl glycidyl ether was obtained as a solution in $CDCl_3$ using a Brüker 80MHz instrument (Figure 47). The following structural assignments can be given to the spectrum:-

a) 2.0 - 2.4ppm 

b) 2.5 - 2.9ppm 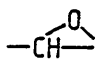

c) 3.0 - 3.4ppm 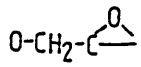

d) 3.5 - 3.9ppm $-CH_2-O-$

e) 4.9 - 5.5ppm $CH_2=$

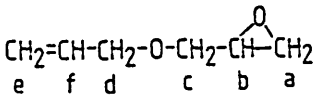

f) 5.6 - 6.3ppm =CH-

Figure 48 shows the ^1H nmr spectrum of 1,1,3,3-tetramethyldisiloxane as a solution in $CDCl_3$. The position of the silicon hydride proton signal is clearly seen at 4.25 - 4.5ppm.

The ^1H nmr spectrum of the diepoxydisiloxane is shown in Figure 36. The most important feature of this spectrum is the complete absence of proton signals in the region 4-6ppm. For the starting materials, this is where the silicon hydride protons (4.25-4.5ppm, Figure 48) and the allyl glycidyl ether vinyl groups (4.9-6.3ppm, Figure 47) appear. The following structural assignments can be given to the spectrum:-

a) 2.8 - 3.7ppm 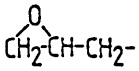

b) 2.2 - 2.6ppm $-O-CH_2-$

c) 1.2 - 1.6ppm $-CH_2-$

d) 0.1 - 0.5ppm $-CH_2-Si$

e) -0.2ppm $Si-CH_3$

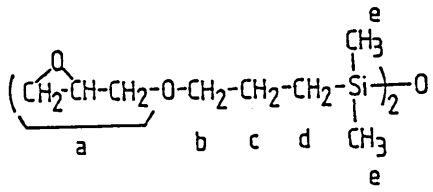

The assignment of the proton signals from the three methylene groups is that the protons of the methylene group furthest removed from the silicon atom will give a signal furthest up field and the protons of the nearest methylene group give a signal nearest to that of the $Si-CH_3$ protons.

The integration of the spectrum corresponds to the assignments given and confirms the successful completion of the vinyl addition reaction.

4.7.3.5 Allyl glycidyl ether/hydride PDMS.

The following method is a general example of the conditions used to prepare epoxy PDMS.

10g (1.72×10^{-3} moles, RMM @5,821) hydride PDMS and 4g (3.51×10^{-2} moles, large excess to reduce the possibility of side reactions of the silane) allyl glycidyl ether were weighed into a 50ml round bottomed 3-neck flask, covered with aluminium foil. The flask was equipped with a condenser, thermometer, nitrogen reservoir and was stirred with a magnetic follower in an oil bath. @ 10mls 40-60 petroleum ether were added to reduce the viscosity of the solution and 10mls (9.59×10^{-3}g catalyst in 100mls THF distilled over potassium, 0.1% on the weight of silane) chloroplatinic acid catalyst. The flask was purged with nitrogen and stirred for 3 days at 150°C. The extent of the reaction was monitored by the disappearance of the silicon hydride absorption signal in the infra-red spectrum.

After the reaction was completed, the crude product was washed with water to remove the catalyst and extracted with chloroform. The organic layer was then dried over anhydrous magnesium sulphate and filtered through glass wool into a

Vigreux-Claisen flask for vacuum distillation at 150°C for 4 hours. The usual yield of the colourless product was 60-70%, the majority being lost through filtering off the magnesium sulphate.

4.7.3.6 Infra-red.

Figure 49 shows the infra-red absorption spectrum of epoxy functionalised PDMS obtained as a liquid film between KBr plates. This spectrum is almost identical to that of hydride functionalised PDMS (Figure 25) except for the absence of the Si-H stretch at 2120cm^{-1}, indicating full reaction of the Si-H groups.

4.7.3.7 ^1H nmr.

The ^1H nmr spectrum of the product was obtained as a solution in $CDCl_3$ using a Brüker 80MHz instrument (Figure 50). the main feature of this spectrum is the absence of any signal in the region 4-6ppm, where the Si-H protons (Figure 29) and the vinyl protons of allyl glycidyl ether (Figure 47) appear, confirming the complete reaction of the Si-H groups and removal of the excess allyl glycidyl ether. The ^1H nmr spectrum is identical to that of the vinyl addition product of allyl glydicyl ether and 1,1,3,3-tetramethyldisiloxane (Figure 36) and has the same structural assignation:-

a) 3.8 - 2.9ppm 

b) 2.85 - 2.4ppm 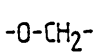

c) 1.85 - 1.35ppm 

d) 0.7 - 0.2ppm 

e) 0.1 - 0ppm 

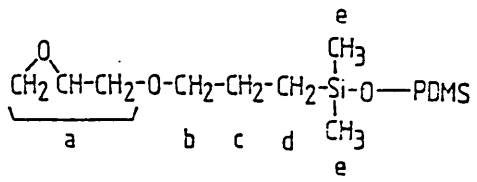

If allyl glycidyl ether still remains in the product after distillation, the vinyl groups are easily detected by ^{1}H nmr, as shown in Figure 51. The signal due to the vinyl protons is seen at 6.3-5.0ppm and is easily recognised when compared with the ^{1}H nmr spectrum of allyl glycidyl ether (Figure 47). The allyl glycidyl ether can be removed by further vacuum distillation.

Integration of the epoxide group and the siloxane repeat unit signals gives information of the extent of the reaction. The RMM of the hydride PDMS starting material is already known from ^{1}H nmr and gpc analysis (sections 4.7.1.2 and 4.7.1.3). From the relative integration of the epoxide group and siloxane repeat unit, the RMM of the epoxy functionalised PDMS can be calculated. This should correspond to the value found previously for the hydride starting material.

This method of synthesising epoxide functionalised PDMS was preferred over the siloxanolate equilibration reaction with the diepoxydisiloxane terminating group (section 4.7.2), as it provides more reliable methods to determine the RMM of the polymer. The packing of the gpc columns used for PDMS

analysis (section 4.7.1.3) is highly sensitive to strongly polar functional groups, resulting in bonding of the sample to the column packing. The gpc calibration has been carried out with trimethyl ended siloxanes and the gpc distribution results depend upon the molecular volume of the polymer, therefore the calibration is only valid for polymers taking up similar molecular conformations. Clearly the hydride terminated PDMS oligomers will adopt molecular conformations similar to the calibration standards, whereas the PDMS oligomers which have been prepared by equilibration in the presence of the endblocking diepoxydisiloxane will not. The gpc calibration will therefore be more valid for the hydride PDMS oligomers.

The RMM of the hydride PDMS oligomers may be more easily calculated from their ^1H nmr spectrum, as the spectrum is much simpler to interpret from the integration of the peaks than that of the epoxide PDMS oligomers. The methylene proton signals of the epoxide functionalised PDMS are partially overlapped by the much more intense signal of the silicon-methyl protons, making the integration less accurate. The silicon hydride proton signal is sufficiently removed from the silicon-methyl signal for there to be no interference between the two (Figure 29).

The epoxide functionalised PDMS used in the following copolymer experiments was prepared by equilibration of D_4 with acid activated Fuller's earth catalyst in the presence of

1,1,3,3-tetramethyldisiloxane. This gave hydride PDMS of a narrower RMM distribution (Figure 31) than the equilibration of D_4 in the presence of diepoxydisiloxane endblocker (Figure 38). The hydride terminated PDMS was then functionalised with epoxide groups by a platinum catalysed vinyl addition reaction with allyl glycidyl ether as described in section 4.7.3.6.

4.8 Choice of solvent for the copolymer synthesis.

The importance of microphase separation for a rubber toughening copolymer product has been explained in detail in section 2. This is achieved by forming a copolymer between two highly incompatible homopolymers. The cause of the incompatibility is the large difference in solubility parameters. The solubility parameters for PES and PDMS are 25.2 $(MJm^{-3})^{\frac{1}{2}}$ and 14.9 $(MJm^{-3})^{\frac{1}{2}}$ respectively indicating gross incompatibility of the two homopolymers.

This incompatibility is beneficial in creating the required microphase separation in the copolymers, but raises the problem of selecting a solvent capable of producing a homogeneous solution of the reactants. Such a large difference in solubility parameters often results in the solvent preferentially dissolving one of the homopolymers and produces a physical blend rather than a copolymeric product. After considering the literature values (28,205) for solubility parameters of solvents, a wide range were used in attempts to

form copolymers by the epoxidation route described in section 4.9.2.

Of the more promising solvents used, dimethyl formamide (δ=24.8[MJm^{-3}]$^{\frac{1}{2}}$), N-methyl pyrrolidone (δ=23.1[MJm^{-3}]$^{\frac{1}{2}}$) and dimethyl sulphoxide (δ=24.6[MJm^{-3}]$^{\frac{1}{2}}$) preferentially dissolved PES, giving cloudy solutions or more obvious phase separation when the PDMS was added. Noshay et al in copolymerising Udel polysuphone (δ=21.7[MJm^{-3}]$^{\frac{1}{2}}$) used chlorobenzene (δ=19.4[MJm^{-3}]$^{\frac{1}{2}}$) as the solvent, but this was found to be ineffective in dissolving polyethersulphone.

Tetrahydrofuran (δ=18.6[MJm^{-3}]$^{\frac{1}{2}}$) and dichloromethane (δ=19.8[MJm^{-3}]$^{\frac{1}{2}}$) both seemed to produce a homogeneous solution of the reactants, but no reaction was detected. This could have been due to the low boiling point of the solvents, 67°C and 40°C respectively. In the case of vinyl addition reactions, a temperature of @ 100°C is required for the reaction of polysulphone/PDMS polymers (132). The epoxidation reaction involves hydroxyl terminated PES which easily hydrogen bonds with polar solvents such as tetrahydrofuran (THF) or dichloromethane. Such strong solvation of the hydroxyl group inhibits copolymerisation of PES. This is supported by Noshay et al (8) who found that the reaction of hydroxyl terminated polysulphone with dimethylamino terminated PDMS proceeded at a much slower rate in THF than in chlorobenzene. It was suggested that the hydrogen bonding of the THF with the polysulphone hydroxyl group reduced the

availability of the hydroxyl group for hydrogen bonding with the silylamine end groups as the initial part of the copolymerisation reaction. Chlorobenzene is a poor hydrogen bonding solvent and is therefore unlikely to prevent reaction by solvation in this way and an increased rate of reaction was observed. Similarly, a reaction between hydroxyl PES and epoxy functionalised PDMS would be adversely affected by a strong hydrogen bonding solvent.

Morris (19) used 1,2-dichlorobenzene (δ=20.5[MJm^{-3}]$^{\frac{1}{2}}$) as the solvent whilst copolymerising hydroxyl PES with dimethylamino terminated PDMS, but large quantities of the solvent were required to successfully dissolve the PES. It was thought that such dilution would be acceptable for the reaction with the labile dimethylamino PDMS, but the catalysed vinyl addition and epoxidation reactions require concentrated solutions to successfully form high molecular weight copolymers (133,141,142,156,157,163).

Two other solvents were considered for the copolymerisation reactions. 2-methoxyethyl ether (diglyme) gave a homogeneous solution in the temperature range 30-70°C. The upper solubility limit of PES in diglyme was only 70°C, above this, PES began to precipitate. Reactions were carried out at 60°C, but were unsuccessful. The low temperature and the strong hydrogen bonding of the solvent would explain this.

The most promising of the solvents investigated was 1,1,2,2-tetrachloroethane (δ=19.8[MJm^{-3}]$^{\frac{1}{2}}$). This solvent has a suitably high boiling point (147°C) and does not strongly hydrogen bond. A number of epoxidation and vinyl addition reactions were attempted in this solvent with only limited success. Chlorinated solvents such as chloroform and dichloromethane show a degree of hydrogen bonding with PES as reported by Swinyard and Barrie (206). This is of a similar level of solvation as shown by 1,1,2,2-tetrachloroethane (TCE) and may be sufficient to prevent the reaction of hydroxyl PES.

Problems obtaining a homogeneous solution of PDMS in TCE have been encountered previously (26). In trying to obtain a calibration curve of PDMS standards for the ^{1}H nmr analysis of PDMS in blends, a number of PDMS samples of known molecular weight were dissolved in TCE. The spectra and integration curves were obtained by ^{1}H nmr spectroscopy. The ^{1}H nmr analysis of blends containing known levels of PDMS, on reference to the calibration curve, gave results much lower than the known levels of PDMS present. The reason for this was found to be a concentrated layer of siloxane in the solvent around the wall of the glass nmr tube when the blends were dissolved. The solution was clear and apparently homogeneous, but the level of siloxane was depleted in the bulk of this solution due to the "deposits" on the wall of the tube.

This may have occurred in the reactions described here, is spite of the vigorous stirring employed and would obviously reduce the possibility of copolymerisation if there was little PDMS remaining in the bulk solution.

The silicon hydride bond can be highly solvated by polar solvents such as dioxane, as described by Qui and Hu (207). This may be part of the reason why only limited reaction was observed in the solution experiments and suggests that melt reactions may be more favourable.

4.9 Epoxidation reactions*.

The initial experiment to investigate the epoxidation reaction between hydroxyl PES and epoxy functionalised PDMS followed the example of Gagnebien et al (162). They used the polysulphone monomer 4,4'-isopropylidenediphenol and allyl glcyidyl ether in a model reaction to show that the reaction between the hydroxyl groups and the epoxide rings takes place. The PES monomer 4,4'-sulphonyldiphenol (Bisphenol"S") was used in the model reaction described here, to represent the hydroxyl terminated PES.

*The term epoxidation as used throughout this thesis refers to a reaction resulting in the opening of an epoxide ring.

4.9.1 Bisphenol"S" and allyl glycidyl ether.

The Bisphenol"S" was dried at 100°C in a vacuum oven overnight before use, as the presence of water may prevent reaction of the hydrophobic reactants (208).

5g (0.02 moles) Bisphenol"S" and 4.56g (0.04 moles) allyl glycidyl ether were weighed into a 50ml 3-neck flask equipped with a condenser, nitrogen reservoir and rubber septum. The flask was stirred by a magnetic follower in an oil bath placed on a stirrer hotplate. The oil bath was heated to 100°C and 0.16g (7.6×10^{-4} moles) 1-dimethylaminododecane (N,N'-dimethyldodecylamine) were injected into the solution. The contents of the flask were stirred for 3½ hours, after which a pale yellow solid product was obtained.

On initially mixing the two reactants together, a white paste was formed. The oil bath was heated to 100°C and a homogenous solution was formed as the Bisphenol"S" dissolved in the allyl glycidyl ether.

4.9.1.1 ^{1}H nmr.

The ^{1}H nmr spectrum of the reaction product was obtained as a solution in $CDCl_3$ using a Brüker 80MHz instrument (Figure 52).

Comparison of the spectrum with the one obtained from allyl glycidyl ether (Figure 47) clearly shows that the reaction product does not have the proton signals of the allyl glycidyl ether epoxide ring (2.2-3.0ppm). The para substituted benzene ring of Bisphenol"S" (Figure 12) is shown at 6.6-7.8ppm. At 4.9-6.0ppm are the two groups assigned to the vinyl protons of the allyl glycidyl ether vinyl group seen in Figure 47. The signal at 0.8-1.3ppm is due to the presence of the catalyst dimethylaminododecane (DMDA).

The remainder of the spectrum is due to the proton signals of the reacted epoxide ring and can be assigned as follows:-

a) 4.1ppm 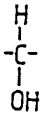

b) 4.0ppm 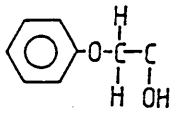

c) 3.6ppm 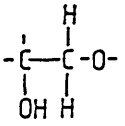

d) 3.5ppm 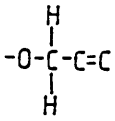

e) 2.9ppm 

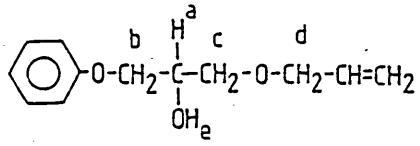

The distinct difference in spectra of the allyl glycidyl ether epoxide ring and the reaction product confirms that the reaction between Bisphenol"S" and the allyl glycidyl ether

epoxide ring takes place. The integration of the spectrum corresponds to that expected of the reaction product.

The success of this reaction is helped largely by Bisphenol"S" dissolving in the allyl glycidyl ether at 80°C. This not only provides a homogeneous solution, but without the need of a solvent, gives the maximum concentration of end groups. The use of small reactive molecules also increases the possibility of a reaction taking place. Gagnebien et al (162) found that the same reaction carried out in chlorobenzene solvent attained only 10% reaction in 3 hours, whereas the reaction without solvent attained quantitative conversion over this time. The functionalised oligomers needed to produce copolymers reduce the concentration of end groups due to the higher RMM and require a solvent present to form a homogeneous solution, as increasing the RMM of the reactants reduces the compatibility. Both these points make a reaction much more difficult.

The success of this model reaction suggests that a reaction of the functionalised oligomers in the melt may be successful in forming copolymers by increasing the concentration of end groups and removing the possibility of end group solvation slowing down the reaction.

4.9.2 Hydroxyl PES/epoxy functionalised PDMS in solution.

The following method is the general procedure followed in preparing copolymers from hydroxyl PES and epoxy functionalised PDMS in different solvents.

1g (RMM=4,370, $3.3x10^{-4}$ moles) vacuum oven dried hydroxyl PES and a minimal amount of solvent were weighed into a 50ml 3-neck flask equipped with a condenser, nitrogen reservoir and pressure equalising dropping funnel. The flask was purged with nitrogen and stirred with a magnetic follower in an oil bath on a stirrer/hotplate. The oil bath was heated to 140°C and left stirring until the PES had dissolved.

0.6g(RMM=2,600, $2.3x10^{-4}$ moles) epoxy PDMS and the catalyst DMDA were weighed into the dropping funnel. The weight of catalyst was <5% on the weight of PES. The PES was added dropwise to the solution. Depending upon the solvent used, the solution became cloudy or remained clear. After the PDMS had been added, the solution was left stirring for 18 - 24 hours, after which it was cooled and the product precipitated from methanol.

The solvent and methanol were decanted off and the solid product was collected and placed in a pre-weighed soxhlet thimble. The product was then soxhlet extracted with toluene over 72 hours to remove any unreacted PDMS from the product and then vacuum oven dried before re-weighing the thimble.

Toluene was chosen as the soxhlet extraction solvent as it is an excellent solvent for PDMS and does not dissolve PES. A blend of PDMS and PES was prepared using the same method as described above, but no DMDA catalyst added. This product was then soxhlet extracted with toluene and analysed to see if any PDMS remained in the blend after extraction. The absence of PDMS would show this to be a suitable method for removing any unreacted PDMS homopolymer from the copolymerised product. Any PDMS found in a reaction product after extraction with toluene could only be in the form of a copolymer. No solvent could be found for PES only with a low enough boiling point that could be used for this purpose without degrading the soxhlet thimbles, therefore the products obtained after soxhlet extraction with toluene were analysed by ir and nmr spectroscopy for the presence of PDMS.

4.9.2.1 Infra-red.

The infra-red spectra of the soxhlet extracted reaction products were obtained as cast films from dichloromethane, dried onto KBr plates. Figure 53 shows a typical example obtained from a reaction carried out in TCE. The product obtained was a brittle solid and the infra-red spectrum is identical to that of PES (Figure 8).

A physical blend was prepared of PES containing 30%w/w PDMS and the infra-red spectrum obtained as a cast film (Figure 54). This spectrum shows the PDMS C-H stretch at

2960cm^{-1}, the Si-O-Si stretch in the region 1000-1100cm^{-1}, Si-C stretch at 800cm^{-1} and the shoulder at 1260cm^{-1} is due to the Si-CH_3 stretch.

^{1}H nmr is much more sensitive to low levels of PDMS as would be expected (section 4.9.2.2) and was used to select one of the copolymer samples with a higher PDMS content for more detailed infra-red analysis. A film of the copolymer was cast from TCE and the ir spectrum obtained using a Nicolet FT-IR spectrometer was stored on a Mattson-Cygnus data handling system (Figure 55).

The spectrum of the hydroxyl ended PDMS used in the copolymerisation was then stored in the data base (Figure 56). This spectrum was then subtracted from that of the copolymer and the resultant spectrum is shown in Figure 57. This spectrum shows a number of peaks, in particular 1260cm^{-1} (Si-CH_3 stretch), 1015 and 1100cm^{-1} (Si-O-Si stretch) and 800cm^{-1} (Si-C stretch). However, had the copolymerisation proceeded to a significant extent, these peaks would have been visible in the spectrum of the product itself.

4.9.2.2 ^{1}H nmr.

The spectrum of the "blend product" after soxhlet extraction with toluene was obtained using an 80MHz Brüker instrument. The solvent used was $CDCl_3$. This is a good solvent for PDMS and should any remain in the brittle solid

product it will be easily dissolved and the signal of the Si-CH_3 protons will be obviously identifiable. As $CDCl_3$ is not a good solvent for PES, the para-substituted benzene ring splitting pattern from PES is badly resolved (as shown in Figure 14). A badly resolved spectrum can be caused by undissolved solids in the deuterated nmr solvent.

Figure 58 shows the spectrum obtained from the blend product after soxhlet extraction. There is no signal at 0ppm showing the complete absence of siloxane methyl protons and confirming that soxhlet extraction with toluene successfully removes PDMS homopolymer from PES. The para-substituted benzene ring splitting pattern at 7-8ppm is badly resolved and partially masked by two other peaks. These peaks are due to residual protons in the deuterated solvent and due to protons from toluene remaining in the extracted product. The methyl protons of toluene give the signal at 2.3ppm.

The two commonly used solvents for preparing sample solutions for nmr analysis are $CDCl_3$ and d-DMSO. Each solvent preferentially dissolves one of the homopolymers used in these copolymerisations. Initially, the ^1H nmr analysis is required to indicate the presence of any PDMS that many be present as a copolymer, so $CDCl_3$ was the solvent used in the initial ^1H nmr investigations.

The spectrum of the copolymer sample with the highest PDMS content is shown in Figure 59. The small, distorted

para-substituted benzene ring signal of PES is at 7-8ppm, along with the toluene benzene ring signal and residual protons of the deuterated solvent. The methyl protons of toluene give the signal at 2.3ppm. The signal at 1.5ppm may be due to an impurity or water contained in the PES (cf. Figure 15). The signal at 0.05ppm is due to the methyl protons of PDMS. The integration of the PES (benzene) signal to the PDMS (methyl) signal shows that 96% of the PDMS in the reaction is still present in the copolymer sample. The calculation is based upon the integration of the para-substituted benzene ring and the known RMM of the PES to give the integral height per proton. From this, the RMM of the PDMS can be calculated from the PDMS methyl proton signal and is compared with the known value. Basing the calculation upon the PDMS methyl proton signal gives the same results. Only a simple method is needed to show which samples are comparitively PDMS rich. No other information could be gained from the spectrum. A signal due to PES-O-CH_2- methylene protons would be expected at @ 4.0ppm, but the 80MHz instrument is not sensitive enough to detect a signal there. Weighing the soxhlet thimble before and after extraction gave unreliable results due to the retention of toluene in the samples.

A sample of the same product was analysed using a 270MHz ^1H nmr instrument, this time in d-DMSO solvent (Figure 60). From this spectrum, the para-substituted splitting pattern of the PES benzene rings is clearly defined, but the signal due to PDMS methyl protons is hardly evident. There is no signal

due to PES-O-CH_2- methylene protons formed if copolymerisation had taken place. Had there been copolymer present, some of the PDMS would have been drawn into the d-DMSO solution by the more soluble PES blocks, then the methylene signal of the linking group would have been detected. It is possible that if a small amount of PDMS had undergone copolymerisation to form PDMS rich chains (e.g. A-B-A type copolymers) with only a small amount of chain extension, then this material may be only soluble in $CDCl_3$, in effect removing PES from d-DMSO solutions. The brittle nature of the product however, suggests only a small smount of PDMS may be present. The difference made by using solvents which are preferential to one or the other of the homopolymers is clearly evident. As toluene is used as the extracting solvent, unreacted PES homopolymer is always likely to be present and give a signal in either of the solvents.

A number of experiments were carried out using the different solvents already mentioned, as well as varying the level of amine catalyst between 1-5%, however, no more than 20% of the expected level of PDMS was detected in $CDCl_3$ solvent by ^1H nmr. Boron trifluoride was used as the initiator instead of the alkylamine, but no PDMS was detected after extraction. In view of this, the three samples which ^1H nmr analysis suggested contain PDMS >50% of the expected value were soxhlet extracted a second time and analysed by ^1H nmr. The amount of PDMS determined was within 5% of the original value. The three samples were all brittle, powdery

materials with PDMS levels of 22% (67% of theory), 25% (74% of theory) and 30% (96% of theory) were all produced by copolymerisation in TCE by the methold described in section 4.9.2.

An increase in RMM in the product would confirm the formation of a copolymer, but the samples undoubtedly contain unreacted PES. Gpc would be suitable for this analysis, but the presence of hydroxyl groups in the samples, either from the copolymer linking group or unreacted PES would result in the samples binding on the column packing as explained in section 4.7.3.8. and so was not attempted.

4.9.2.3 Differential Scanning Calorimetry (dsc).

All the dsc measurements made for this report were carried out using a Mettler TA 3000 series thermal analyser system, consisting of a Mettler DSC 30 differential scanning calorimeter and a Mettler TC 10 TA microprocessor. Aluminium sample pans were used, one with 10-20mg sample and an empty pan as the reference. In all cases, the heating rate was 10°K/minute and the measurements taken were on the second heating cycle, the first heating cycle was used to soften the solid samples and obtain good thermal contact with the sample pans. The thermal changes over the temperature range were recorded by the microprocessor.

Figure 61 shows the dsc thermogram of the hydroxyl PES used in the copolymer reactions. The only feature of this is the glass transition (Tg) of PES. Figure 62 shows the construction calculated by the microprocessor to determine the sample Tg. Three values of the Tg are calculated, the second being defined as the temperature at which an extrapolation of the base line prior to any specific heat capacity change intercepts the tangent to the curve at the point where half the specific heat change has occurred. The results reported here will quote this value as the Tg of the sample. The Tg of the hydroxyl PES was 189.4°C, compared with the literature value of 232°C (28) for high RMM commercial grade PES.

Figure 63 shows the dsc thermogram of the epoxy functionalised PDMS. This shows only a Tg for the PDMS. For PDMS with RMM >2000, melting endotherms and a crystallization exotherm are observed (209). These observations are all for PDMS samples with trimethyl end groups, rather than the epoxy propyl groups involved here. Polar end groups are reported in the literature to increase the Tg of PDMS due to the restrictions in the chain preventing the crystallization of PDMS (110).

The Tg of this epoxy PDMS sample is -116.5°C. The literature value (209) of the Tg for a trimethyl terminated PDMS sample of similar RMM is -126.5°C, higher values of Tg for functionalised PDMS oligomers have been reported (110).

Figure 64 shows the dsc thermogram of the epoxy copolymer sample (30% PDMS by ^1H nmr analysis) after the first heating cycle. This shows a Tg endotherm in the region where the PES Tg is expected and another endotherm at -50°C. If a copolymer has been formed and phase separation takes place, then a Tg for each of the homopolymer phases would be observed. If the copolymer forms one phase, one Tg is observed at a value intermediate between those of the two homopolymers (210). The RMM of the PDMS used in the copolymerisation is too low for phase separation to take place and any copolymer formed would display a single Tg. As only a maximum of 30% PDMS would be incorporated in this material, the copolymer Tg would be nearer to the value displayed by PES. Therefore, the endotherm at -50°C is unlikely to be due to the presence of any copolymer. Unreacted PES in the sample would produce the Tg at @ 190°C.

A simple blend of 30%w/w epoxy PDMS (RMM=2,600) and hydroxyl PES (RMM=4,370) was prepared and then examined by dsc. The thermogram obtained (Figure 65) shows a small Tg at -118.4°C and one at 191°C due to the PDMS and PES respectively as would be expected from the two phase separated polymers.

4.10 Vinyl addition reactions in solution.

From the solution reactions of epoxy PDMS and hydroxyl PES, TCE was chosen as the solvent for the vinyl addition reactions. A number of experiments were carried out varying

the amount of solvent present and using catalyst solutions of different concentrations, made up in different solvents. Although different concentrations of catalyst were used in the reactions, no trend was apparent in the results. The main factors influencing the reaction seemed to be the ability to maintain an inert atmosphere and reaction was aided by the use of a freshly prepared catalyst solution. The following method is a general outline of the procedure followed in preparing copolymers in TCE solution from vinyl PES and hydride PDMS through a vinyl addition reaction.

1g (RMM=4,450, 2.25×10^{-4} moles) vacuum oven dried vinyl PES and a minimum amount of TCE (6-10 mls) were weighed into a 50ml 3-neck flask, equipped with a condenser, nitrogen reservoir, septum and pressure equalising dropping funnel. The flask was wrapped in aluminium foil to exclude light. The flask was purged with nitrogen and stirred with a magnetic follower in an oil bath on a stirrer/hotplate. The oil bath was heated to 140°C and left stirring until the PES had dissolved.

0.1575g (RMM=700, 2.25×10^{-4} moles) hydride PDMS was weighed into the dropping funnel. 1ml catalyst solution (0.0443g chloroplatinic acid in THF freshly distilled over potassium) was injected into the flask. The siloxane was added dropwise to the solution over 2-3 hours. After the siloxane was added, the solution was left stirring over 18-24 hours, cooled and filtered through glass wool into methanol

to precipitate the product and remove the solid platinum metal. The solvent and methanol were decanted off and the solid product collected for soxhlet extraction with toluene over 72 hours to remove unreacted PDMS and vacuum oven dried to remove the toluene.

4.10.1 Infra-red.

The infra-red spectra of the soxhlet extracted products showed no obvious bond stretching due to PDMS presence, as was seen with the products of the epoxide copolymerisation reaction (section 4.9.2.1). ^1H nmr proved to be more sensitive in detecting low levels of PDMS and a copolymer sample which showed a comparatively high PDMS level (11%) was examined by the FT-IR technique described in section 4.9.2.1.

A film of the copolymer was cast from TCE and the ir spectrum using a Nicolet FT-IR spectrometer was stored in a Mattson-Cygnus data handling system (Figure 66). This spectrum is almost identical to the spectrum obtained from the sample of pure vinyl PES used in the copolymerisation (Figure 67). The v-PES spectrum was subtracted from that of the copolymer and the resultant spectrum is shown in Figure 68. This spectrum shows a number of peaks, including 2970cm^{-1} (C-H aliphatic stretch), 1245cm^{-1} (Si-CH_3 stretch), 1105 and 1025cm^{-1} (Si-O-Si stretch) and 805cm^{-1} (Si-C stretch). This spectrum is easily recognisable as that of a siloxane, more so than the one obtained from the epoxidation copolymer

(Figure 57), however, had the vinyl addition proceeded to a significant extent, these peaks would have been visible in the spectrum of the product itself.

4.10.2 ^{1}H nmr.

The spectrum of the copolymer sample with the highest PDMS content is shown in Figure 69 (PES RMM=4,450, PDMS RMM=700). The spectrum was obtained using an 80MHz instrument with $CDCl_3$ solvent. The para-substituted benzene ring signal of PES is at 7-8ppm along with the residual protons of the solvent and toluene. The signal at 2.35ppm is due to the methyl protons of toluene. The two singlets at 1.2-1.6ppm are due to an impurity in the PES and water. Between 4.5-5.5ppm there are signals due to a very small number of unreacted PES vinyl groups. The PDMS methyl proton signal is at 0.1ppm.

The integration of the PES to the PDMS signal shows that 78% of the PDMS from the reaction is still present after soxhlet extraction. As explained in section 4.9.2.2 this is only a simple comparative test for the copolymer samples which contain unreacted PES homopolymer. This sample was analysed by a 270MHz instrument using d-DMSO as the solvent (Figure 70). From this spectrum, it can be seen that the v-PES has undergone some hydrolysis of the functional vinyl groups back to hydroxyl PES. The doublets at the side of the para-substituted benzene rings of PES (7-8ppm) are of about equal intensity and suggest approximately an equal number of

remaining vinyl and hydroxyl end groups. The proton signals for the unreacted vinyl end groups are between 4.4-5.9ppm (c.f. Figure 21). Unlike the epoxy reaction products described in section 4.9.2.2 (Figure 60) a strong signal for PDMS is shown even in the unfavourable solvent d-DMSO. This strongly suggests that some copolymer is present. The small signal at 4.05ppm is in the expected area of a proton signal from a methylene group (a) adjacent to PES, had vinyl addition taken place.

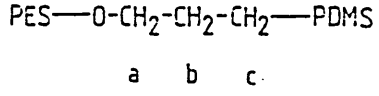

The signals of methylene groups b and c would be expected in the region 0-2ppm. Numerous small signals can be seen in this area of the spectrum, but no firm assignment can be made. The small signal at 4.05ppm is insufficient to account for such a strong PDMS signal. Possibly a small amount of copolymer present may be sufficient to bind unreacted PDMS homopolymer in the PES homopolymer matrix and then stabilise the PDMS in the d-DMSO solvent, giving a larger PDMS signal than was expected. No silicon hydride signal is seen at 5ppm but these end groups may be consumed by side reactions. However, the presence of PDMS in the d-DMSO suggests that some degree of copolymerisation has taken place.

A second copolymer sample prepared by the same method, in TCE and then soxhlet extracted with toluene was of particular interest (PES RMM=4,450, PDMS RMM=4,370). This sample had rubbery, elastomeric recovery properties on

applying stress to the solid. The ^1H nmr spectrum obtained in $CDCl_3$ solvent using an 80MHz nmr instrument is shown in Figure 71. A number of interesting observations can be made about this spectrum. A strong para-substituted benzene ring splitting pattern is seen and a surprisingly small PDMS methyl proton singlet by comparison. The integration of the two shows only 20% of the PDMS used in the reaction still present in the ^1H nmr sample. Also, the spectrum is not very well resolved, but in particular, the normally sharp PDMS methyl proton signal is very broad, suggesting that the sample is not entirely soluble in the solvent. This may be due to a reduction in solubility in the copolymer due to adjacent PES blocks. At 1ppm and 1.4ppm are two small signals which may be due to the protons of the methylene groups formed as a result of vinyl addition.

A sample of the same product was analysed by a 270MHz ^1H nmr instrument in d-DMSO solvent (Figure 72). From the spectrum, the para-substituted benzene ring splitting pattern (7-8ppm) of PES shows that only a very few hydroxyl end groups remain in the sample. The smaller doublet at 7ppm is due to the hydroxyl end groups and the larger doublet at 7.2ppm is due to the functionalised end groups. The unreacted allyl proton signals are between 4.7-6ppm. A small PDMS signal is at 0ppm and there is no silicon hydride signal, expected at 5ppm.

The main peaks of interest are the triplets at 4.05ppm and 1.0ppm, as well as the multiplet at 1.7ppm. These small signals are ones expected for the copolymer linking group after a successful vinyl addition reaction. These are only small signals and so only a small amount of copolymer has been formed. However, the presence of PDMS bonded to PES has had a distinct effect upon the physical properties of the PES, imparting elasticity to the product.

4.10.3 Dsc.

Figure 73 shows the dsc thermogram of the vinyl functionalised PES used in the vinyl addition reactions. The Tg of the material is at 195.75°C. Figure 74 shows the dsc thermogram of the hydride PDMS (RMM=700) used in the copolymerisation giving 78% reaction. The Tg of this sample is -136.4°C and shows an exothermic peak at -100.5°C and an endothermic peak at -68.8°C. The exothermic peak corresponds to the crystallisation exotherm and the endotherm to the melting endotherm of a low RMM PDMS. The measured Tg is comparable with the values reported by Clarson et al (209) for low RMM PDMS samples.

Figure 75 shows the dsc thermogram of the copolymerisation product showing 78% reaction by ^{1}H nmr. The high temperature Tg at 192.6°C is due to the v-PES (Figure 73) as would by expected if PDMS had been copolymerised with PES and is partially soluble in the unreacted PES homopolymer.

There is an endothermic peak at @ -50°C which is in the region of the PDMS melting endotherm. At @ -120°C there is a very small endotherm which is too small to be identified as a glass transition endotherm.

Figure 76 shows the dsc thermogram of the hydride PDMS (RMM=4,370) used in the vinyl addition reaction which gave an elastomeric product and also showed probable copolymer links by ^1H nmr. The PDMS has a Tg endotherm at -123.8°C which is in agreement with the literature value (209), as are the values obtained for the cold crystallization exotherm -87°C and the two crystalline melting endotherms at -45.8°C and -29.1°C.

Figure 77 shows the dsc thermogram of the copolymer reaction product. There is a large, distinct endotherm at @ -40°C which can be attributed to a PDMS crystalline melting endotherm. There is a peak at @ 190°C which is due to the v-PES glass transition. The Tg endotherm was calculated at 181.7°C, a reduction in 14°C over the starting material (Figure 73).

The dsc thermogram does not show a Tg for any PDMS present. If PDMS is present and incorporated into a copolymer network, a cold crystallization exotherm would not be expected, because incorporation in a copolymer chain will reduce the chain mobility and freedom to form crystalline regions, particularly at the high cooling rate employed during

the cooling cycle. The absence of a PDMS Tg can be explained if the PDMS is present as a copolymer which is partially soluble in the PES phase. As unreacted v-PES is present, the PDMS is unable to locate itself at the edge of the sample, as expected for a phase separated copolymer (96,98,105,113,211,212). In this case, the Tg of PDMS would not be detected or would be greatly reduced (19 ,213). This theory is supported by the reduction in the v-PES Tg suggesting partially soluble PDMS is present.

4.10.4 Gpc.

Gpc would be an ideal method for determining the presence of block copolymers in the two samples investigated by ir, ^{1}H nmr and dsc. Any increase in RMM of the product would be due to copolymer formation and would be seen as a peak separated from the unreacted v-PES. The conditions described in section 4.7.1.3 were used, with dichloromethane as the eluent and solvent for the samples.

Several samples of v-PES were put through the column, but only a very slight detector response was seen, even for saturated solutions of v-PES. The refractive index response was also the opposite to the one observed for PDMS. This was verified by measuring the refractive indeces of the two homopolymers.

A blend of v-PES and PDMS was made and put through the column, but only a peak corresponding to PDMS was detected. As the v-PES may be bound to the column packing, no further development of this method was attempted in order to preserve the column.

4.11 Chloroplatinic acid solutions containing silanes.

After the experiments in which chloroplatinic acid has been used in solution to catalyse vinyl addition reactions, fine black solid particles were found in the reaction flask, or a grey colour was seen in the solution. This is evidence of the reduction of the platinum from oxidation state IV to platinum metal. Although platinum in the oxidation state IV will catalyse vinyl addition reactions, it is easily reduced to platinum II in the presence of air, moisture and alcoholic solvents (139,155). Platinum II catalyses the reaction of silicon hydride end groups to form a siloxane link and liberates hydrogen (see section 3.5). This reaction reduces the catalyst to platinum metal.

As the catalyst solutions "age", the pale yellow colour of the solution becomes more intense. The comparative Pt II content of the solutions was estimated by adding one drop of catalyst solution to 1,1,3,3-tetramethyldisiloxane and recording the time taken for the appearance of the first bubbles of hydrogen. Catalyst solutions stored for over 2 days were appreciably quicker in producing hydrogen than

freshly prepared catalyst solutions. This test was used as an indication of the amount of Pt II in the catalyst solution. The catalyst solutions used for copolymer reactions were freshly prepared immediately prior to beginning the experiment.

It was also observed that the solvent used to prepare the catalyst solution contributed to the rate at which hydrogen was liberated on addition to disiloxane. This is probably due to the amount of moisture retained in the solvent. THF freshly distilled over sodium and butanol stored over molecular sieve both gave more stable solutions than a solution of chloroplatinic acid in TCE. In order to see if TCE inhibited vinyl addition by reduction of the catalyst, a reaction to functionalise hydride PDMS with allyl glycidyl ether by the method given in section 4.7.3.6 was carried out in TCE instead of petroleum ether. There was no difference in the product when analysed by ^1H nmr, nor a reduction in the yield.

To test the thermal stability of the catalyst, a commercial sample of non-functional, trimethyl ended PDMS (Dow Corning DC200/200) was heated under nitrogen overnight at 120°C in TCE with catalyst solution at the same concentration as used in the copolymerisation reactions. In less than 1 hour, black platinum metal was seen in the reaction flask. The amount of moisture present in the solvent is sufficient to reduce the catalyst in reactions competing with vinyl

addition. However, as shown by the successful vinyl addition to functionalise PDMS in TCE, the side reactions which consume the catalyst do not interfere with the overall product yield and proceed at a slower reaction rate than vinyl addition.

4.12 Carboxy propyl PDMS and hydroxyl PES in TCE solution.

A condensation reaction between carboxy propyl functionalised PDMS and hydroxyl PES as a solution in TCE was attempted in the presence of stannous octoate (stannous 2-ethyl hexanoate) catalyst.

10g PES (RMM=4,370, 2.29×10^{-3} moles) were dissolved in 30mls TCE at 120°C under nitrogen and 2.06g (RMM=900, 2.29×10^{-3} moles) carboxy propyl PDMS (supplied by Goldschmidt) were added. Two phases separated out and a homogeneous solution could not be formed. The mixture was cooled and the two layers allowed to separate. A further 40mls TCE were added, at which point a homogeneous solution was formed. The solution was then reheated. At 80°C, phase separation took place again, but on cooling, a homogeneous solution reformed. However, on cleaning the reaction flask, a coating of PDMS was left on the vessel surface. Due to the problems of forming a homogeneous solution at a high temperature, no reaction could be carried out in solution.

It is possible that at low temperatures, the low RMM carboxy propyl PDMS forms a dimer making it more soluble at

such temperatures. As the temperature is increased, the dimer breaks up leaving the highly polar PDMS insoluble in TCE. A second possibility is that the highly polar carboxyl end groups are solvated by TCE and form a homogeneous solution at room temperature. On heating, the solvation cloud is dispersed and the PDMS phase separates.

Further investigation of the solubility of PES and PDMS in TCE was carried out. A solution of hydroxyl PES and hydride terminated PDMS (RMM=700) was prepared at similar concentrations as detailed above. On cooling the solution, the PES precipitated out of solution, which suggests that the most insoluble component of the mixture comes out of solution on cooling.

In view of these observations, the only possible way of investigating the condensation reaction between hydroxyl PES and carboxyl PDMS seems to be as a melt reaction. This would provide the maximum concentration of reactive end groups and also remove any problems caused by the presence of solvents.

4.13 Melt reactions.

The successful melt reaction of Bisphenol"S" and allyl glycidyl ether as well as the problems encountered in obtaining a homogeneous solution of the homopolymers, particularly with carboxy propyl PDMS suggested that reactions in the melt would be more successful than the solution

reactions. A number of reactions were carried out to pursue the three copolymer routes investigated here.

Considering the Tg of the low RMM PES samples synthesised for this investigation (@ 190°C), all the reactions were carried out at 250°C. This temperature was sufficiently high to soften the PES enough to enable mixing without degradation of the PDMS. PDMS begins to show signs of degradation at 350°C in an inert atmosphere (109). Nitrogen was blown over the cavity entrance to introduce a nitrogen atmosphere in the mixer. The mixer used was a Brabender Plasticorder cavity and twin screw mixer, with the cavity holding @ 30g of material. A PTFE gasket was made to fit between the flange of the backplate and the mixing block to prevent the liquid PDMS from leaking from the mixer. The PES used in the reactions was oven dried at 150°C overnight before use. Prior to adding to the mixer, the solid PES and liquid PDMS were mixed by hand to form a paste.

After the reaction, the product was removed from the mixer whilst at reaction temperature and allowed to cool. The solid product was then milled in a Glen Creston laboratory mill. The powdered product was then continuously extracted with toluene for 18 hours and dried overnight in a vacuum oven at 110°C.

4.13.1 Melt reaction of epoxy PDMS/hydroxyl PES.

The catalyst used in the initial model reaction (section 4.9.1), dimethyldodecylamine (DMDA) boiled out of the Brabender mixer at 250°C and so was not suitable for use at this temperature. The amine chosen to replace it was diaminodiphenylsulphone (DDS), which is used as a linking agent in the preparation of epoxides reinforced with hydroxyl PES. As an aromatic sulphone, it is compatible with PES and is stable at high temperatures.

Three reactions were carried out using the following method:-

The reactants were mixed by hand and the resulting paste added to the Brabender at 250°C. Nitrogen was blown over the mouth of the mixer and the twin screws rotated at 100-140rpm. The speed was maintained as high as possible without splashing PDMS out of the cavity. The individual details of the reactions are given below:-

EB1. No catalyst used.

EB2. DDS catalyst used. 1:1 ratio with PES and PDMS.

EB3. As for EB2. Product soxhlet extracted with toluene and then TCE.

During the reactions, some white vapour was given off due to degradation and redistribution reactions of the PDMS. The nitrogen flow cooled the surface of the PES melt causing it

to solidify if not controlled carefully. Initially on mixing in the Brabender, the PDMS was squeezed out of the mixture and remained on the surface of the PES as a separate liquid phase, irrespective of the rotation speed of the Brabender mixing screws. After the reactions, a rubbery gel was found around the mouth of the Brabender mixing cavity. This was taken to be crosslinked PDMS gel.

Both reactions which involved the use of DDS as a catalyst produced a product which was dark yellow in colour. The reaction without catalyst produced a dark brown solid, which was only slightly coloured after toluene extraction. After soxhlet extraction, reactions EB1 and EB2 were both light brown brittle powders, whereas EB3 had produced an elastomeric rubbery material.

4.13.1.1 ^{1}H nmr.

The ^{1}H nmr spectra of the reaction products were made using an 80MHz nmr instrument. Spectra were obtained in both d-DMSO and $CDCl_3$ solvents. The following table shows the relative amounts of PDMS remaining after extraction with toluene, as calculated from the integration of the PES and PDMS proton signals.

	$CDCl_3$	d-DMSO
EB1	17.5%	0.9%
EB2	46%	2.2%
EB3 after toluene extraction	55%	0%
EB3 after TCE extraction	133%	135%

From the results the significant effect the solvent and amount of free PES have upon the ^1H nmr spectra of the products can be seen. This is particularly noticeable for the two extractions of EB3. After soxhlet extraction with TCE, only a very small amount of product remained in the soxhlet thimble. As both PES and PDMS can be dissolved in TCE no residue at all was expected to remain in the thimble. This suggests that the remaining material is of a very high RMM, or that the sample is crosslinked, the latter being more likely. However, the sample does contain PES, as shown by the ^1H nmr spectrum (Figure 78).

This spectrum is typical of the ones obtained for these products. The aromatic ring protons of PES and toluene are at 7-8ppm, the TCE protons are at 5.95ppm. The two singlets at 1.6ppm and 1.2ppm are due to toluene and water. The singlet at 0.5ppm is due to the PDMS present.

The removal of all the unreacted PES and PDMS by extraction with TCE has left only a small amount of PES in the residue, consequently, the calculation of the amount of remaining PDMS in comparison to the PES gives a figure >100%.

It is important to note that the result is reproducable in both $CDCl_3$ and d-DMSO, a solvent which is not very good for dissolving PDMS. This suggests that greater compatibility of PDMS with d-DMSO has been achieved in this product, most likely by the formation of a copolymer. The absence of PDMS from the spectrum of the same material in d-DMSO after toluene extraction only is more difficult to explain. The amount of unreacted PES present should enable more PDMS present as a copolymer to be detected in this solvent. This suggests that a blend has been formed rather than a copolymer, aided by the presence of a small amount of copolymer to dissolve PDMS in d-DMSO.

EB1 and EB2 show only small amounts of PDMS present, EB2 being more successful due to the choice of catalyst used in this reaction. The presence of PDMS in EB1 can be due to two possibilities:

i) PDMS is present as a copolymer formed by epoxidation due to thermal opening of the epoxide ring.
ii) PDMS has formed some crosslinked gel which cannot be fully leached out of the product, due to its crosslinked nature.

The second explanation is the most probable after observing gel form on the Brabender mixing cavity wall.

4.13.1.2 Dsc.

The extracted products were examined by dsc under the conditions described in section 4.9.2.3. The results for the three reactions are summarised below.

EB1

Figure 79 shows the dsc thermogram of the toluene extracted product. The most obvious feature of this is the high temperature glass transition due to the PES phase. The Tg is 184.07°C, a reduction of 5.4°C from that of the starting material (Figure 62). This suggests that PDMS is present as either a copolymer, or is soluble in the PES phase. The latter is unlikely due to the large differences in solubility parameters, even with the low RMM homopolymers used here. No glass transition due to PDMS can be observed. This has already been explained as PDMS trapped in the PES matrix is unable to display its glass transition. The other main features are the exotherms at @ -45°C and -80°C and the endotherm at @ -50°C. These could correspond to the cold crystallisation exotherms and crystalline melting endotherm of PDMS.

EB2

The dsc thermogram of the toluene extracted product is very similar to that of EB1 (Figure 79), but the glass transition of the PES is at an even lower temperature, 167.2°C. Such a large reduction in Tg suggests that the PDMS

is present as a copolymer. The other peaks are exotherms at @ -45°C and -80°C and an endotherm at @ -50°C. Again, these could be the cold crystallisation exotherms and the crystalline melting endotherm of PDMS.

EB3

The dsc thermograms for the reaction product after toluene and TCE extraction were identical. Figure 80 shows the dsc thermogram of the product after TCE extraction, showing two distinct glass transitions. The high temperature Tg at 205.2°C is due to PES and the low temperature Tg at -117.9°C is due to PDMS. This does suggest that a phase separated copolymer has been formed as the glass transitions of both PES and PDMS are clearly detected and the material does display rubber like elasticity.

The PES used in experiment EB3 was from a different batch of material than was used in experiments EB1 and EB2. EB1 and EB2 involved the reaction of hydroxyl PES with RMM=4,370, Tg=189.4°C (Figure 62). The PES used in EB3 had a Tg=203.7°C (Figure 81). However, the RMM of the polymer as determined by ^{1}H nmr was 3,709 (Table 2). Obviously this raises questions about the accuracy of the RMM determination.

The three low RMM hydroxyl PES samples 12, 13 and 14 (Table 2) used throughout this report were analysed by ^{1}Hnmr at ICI, Wilton and the glass transitions measured by dsc at Sheffield Polytechnic. The following results were obtained.

Polymer	RMM (1st analysis)	RMM (2nd analysis)	Tg(°C)
12	5,881	2,765	189.4
13	3,709	3,493	203.7
14	2,112	2,591	180.9

The RMM figures obtained on the second analysis correspond much better to the glass transition temperatures determined by dsc. Unfortunately, the second analysis was not completed until after the practical work for this investigation was completed. Obviously this seriously effects the stoichiometry of the homopolymer ratios used in the reactions and the possibilty of obtaining high levels of chain extension when forming copolymers is drastically reduced.

4.13.2 Melt reactions of v-PES/hydride PDMS.

Three experiments were carried out with v-PES and hydride PDMS using different forms of catalyst. Two were carried out using chloroplatinic acid catalyst added as the solid and as a solution in THF. Due to the difficulties of applying an inert atmosphere there is only a slight possibility of preventing rapid reduction of the catalyst.

The third reaction involved the use of cumene hydroperoxide as a radical catalyst. Radicals can be formed not only from the vinyl groups of PES, but also by proton abstraction of the PDMS. This would help form segmented and graft copolymers by the uncontrolled placing of the polymer

chains. The lack of an adequate nitrogen blanket would reduce the possibility of reaction.

The general conditions for these melt reactions are the same as given in section 4.13. The individual conditions are given below:-

VB1

Chloroplatinic acid catalyst:- 5mls of a solution containing 0.0613g catalyst in 25mls THF were added to the PES/PDMS paste immediately before adding to the Brabender mixer. The low viscosity of the reaction mixture only allowed the mixing screws to rotate at 60rpm without splashing PDMS out of the mixing cavity. The reaction product was removed after 30 minutes. After soxhlet extraction with toluene a brittle light brown powder was left.

VB2

0.0530g chloroplatinic acid catalyst was added to the reaction mixture whilst mixing at 140rpm. The reaction product was removed after 30 minutes, consisting of molten PES and some residual liquid PDMS. After toluene extraction of the solid, a brittle dark brown powder was left.

VB3

0.07g cumene hydroperoxide were added to themixing cavity whilst mixing the reactants at 140rpm. The reaction product was removed after 30 minutes and consisted of molten PES with

some residual liquid PDMS. Some clear solid gel remained on the cavity walls, this was taken to be crosslinked PDMS. After toluene extraction of the solid, a brittle light brown powder was left.

4.13.2.1 ^{1}H nmr.

The ^{1}H nmr spectra of the reaction samples were made using an 80MHz instrument. Spectra were obtained in both $CDCl_3$ and d-DMSO solvents. The following table shows the relative amounts of PDMS remaining after extraction with toluene, as calculated from the integration of the PES and PDMS proton signals.

	$CDCl_3$	d-DMSO
VB1	9.25%	0.0%
VB2	5.2%	3.4%
VB3	2.5%	0.2%

The particularly low levels of PDMS, especially in d-DMSO solvent shows that very little PDMS remains in the extracted samples, or is probably in the form of a blend as in the case of VB1. A sample of VB3 in d-DMSO solvent was investigated using a 400MHz instrument. This shows far more detail than the spectra obtained using the 80MHz instrument and some interesting observations can be made from this spectrum (Figure 82).

The para-substituted aromatic ring of PES is shown strongly at 7-8ppm. At 3.4-6.0ppm are the signals of unreacted vinyl groups. However, in comparison with the vinyl PES starting material (Figure 21) the vinyl group signals are shifted upfield, suggesting that the vinyl groups have been cleaved from the PES chains. The pronounced singlet at 5.1ppm is due to the unreacted silicon hydride protons. This suggests that the PDMS present is a blend or that a copolymer link has been formed along the PDMS polymer chain. The spectra of VB1 and VB2 do not show any signal due to side reactions involving the platinum catalyst. The broad peak at @ 3.2ppm is due to water in the solvent and the two signals at 2.4 and 2.65ppm are due to the residual protons in the deuterated solvent and an impurity in the PES. The PDMS protons are at 0.5ppm. Two doublets are at 1.55 and 2.0ppm which are in the area in which the methylene proton signals of the vinyl addition product would be, but had methylene groups been formed, the signals would be in the form of triplets and a quintet. These two signals may be related to the cleaved vinyl groups.

4.13.2.2 Dsc.

The extracted products were examined by dsc under the conditions described in section 4.9.2.3. The results for the three reactions are summarised below.

VB1

Figure 83 shows the dsc thermogram of the toluene extracted product. The high temperature glass transition at @ 200°C corresponds to the starting material, v-PES (Tg=195.9°C, Figure 73). There is a broad endotherm at @ 70°C and at @ -20°C. There is a sharp endotherm at @ -50°C and an exotherm at @ -85°C. Both of these could be due to the crystalline melting and cold crystalline thermal changes of PDMS. The endotherm at -117.4°C may be interpreted as that of a glass transition for PDMS.

VB2

Figure 84 shows the thermogram of the toluene extracted product. The high temperature glass transition displayed at @ 210°C corresponds to the v-PES homopolymer. There are two small exotherms at @ -50°C and -60°C, but there is no obvious glass transition attributable to PDMS.

VB3

Figure 85 shows the thermogram of the toluene extracted product. The high temperature glass transition due to PES is at 190.6°C and corresponds to the v-PES homopolymer starting material (Tg=195.7°C). The thermogram also displays endotherms at -29.6°C and at -76.2°C and an exotherm at -43.3°C, which could be due to the cold crystallisation exotherm and crystalline melting endotherm of PDMS. There is no obvious glass transition attributable to PDMS.

4.13.3 Melt reactions of hydroxyl PES/carboxy propyl PDMS.

Two commercial samples of carboxy propyl PDMS were obtained with nominal RMM of 1,000 and 2,000. These samples were analysed by ^1H nmr spectroscopy but not by gpc, as the highly polar nature of the end groups would cause the samples to bind to the column packing (section 4.7.1.3).

The ^1H nmr spectra of the two samples showed an unexpected peak present. Figure 86 shows the spectrum of the carboxy propyl PDMS, RMM=2,000. The spectra of both samples show similar features. The PDMS methyl signal is at 0ppm, the three methylene proton signals are at 0.3-0.6ppm, 1.4-1.8ppm and 3.8-4.2ppm. The hydroxyl protons of the carboxylic acid groups are at @ 10.5ppm. The signal at 7.15ppm is due to the residual protons in the deuterated solvent. This leaves the unexplained signal at 2.6ppm. The most likely explanation for this peak is that the methyl ester of the carboxylic acid has been formed during synthesis and this peak corresponds to the methyl proton signal. The functionalised PDMS has been formed by vinyl addition of vinyl acetic acid, the carboxylic acid group having been protected to prevent side reactions with the catalyst and PDMS chain. This is achieved by forming the trimethyl silyl ester of the acid and after vinyl addition, removing the protecting group by refluxing with an alcohol. Under these conditions an ester can be formed from the alcohol. Alternatively, the methyl ester was formed as the

protecting group and has not been quantitatively removed after functionalising the PDMS.

The ^{13}C spectrum of the lower RMM sample is given in Figure 87. From this spectrum, two almost equivalent signals are given at 178ppm and 172ppm. The signal at 178ppm corresponds to the carbon atom of a carboxylic acid and the signal at 172ppm, the carbon atom of the methyl ester. These appear to be present in roughly equal amounts.

Integration of the two proton spectra gives RMM values of 900 and 2,500 for the two samples. Obviously the presence of the ester invalidates this calculation, but the presence of the ester was not fully determined until after the experimental work was completed. Figure 88 shows the infra-red spectrum of a carboxy propyl PDMS sample, which clearly shows two stretching absorbance peaks at @ 1700cm^{-1} and @ 1800cm^{-1}, which suggests the presence of two different carbonyl species.

A number of melt reactions were carried out using hydroxyl PES and the commercial carboxy propyl PDMS. The PES and PDMS were mixed together along with 2000ppm stannous octoate catalyst. Although the esterification of carboxyl groups is an equilibrium reaction aided by the use of an acid catalyst, at such high temperatures any acid present would cause redistribution of the PDMS chains. At a reaction temperature of @ 250°C, water will be easily removed from the

mixing cavity, forcing the equilibrium towards esterification, aided by the condensation catalyst.

The individual details of the reactions are given below.

CB1

PES RMM=4,370, PDMS RMM=900, 2,000ppm catalyst were mixed at 250°C, 160rpm for 2¼ hours. After toluene extraction, a light brown elastomer remained. After further extraction with TCE no product remained in the extraction thimble, which is expected as both homopolymers are soluble in TCE. The toluene extracted product was moulded into 500μm plaques, but they were too brittle to be used for DMTA analysis.

CB2

PES RMM=2,112, PDMS RMM=900 and 2,000ppm catalyst were mixed at 250°C, 140rpm for 2¼ hours. Initially the PDMS squeezed out of the reaction mixture and began to boil out of the cavity. After toluene extraction, a brittle, brown powder remained.

CB3

PES RMM=4,370, PDMS RMM=900 and 2,000ppm catalyst plus a further 2000ppm catalyst added after 1 hour at 250°C, mixing at 160rpm. The product was removed after 2¼ hours reaction time. The product after toluene extraction was mainly a brittle, brown powder, but a small amount of elastomeric material was present.

CB4

PES RMM=35,739, PDMS RMM=2,500 and 2,000ppm catalyst were mixed at 320°C, 160rpm for @ 40 minutes, after which, discolouration due to the onset of degradation was apparent. After toluene extraction, a light brown, brittle powder remained. By using higher RMM polymers, it was hoped that the higher temperature employed may promote reaction.

CB5

PES RMM=22,124, PDMS RMM=2,500 and 2,000ppm catalyst were mixed at 300°C, 160rpm for 30 minutes. After toluene extraction a brittle, brown powder remained.

CB6

PES RMM=2,112, PDMS RMM=900 and 4,000ppm catalyst were mixed at 250°C, 130rpm for 2 hours. The product after extraction with toluene was a dark brown brittle powder. By using the lowest RMM polymers available, it was hoped that the increased compatibility of the homopolymers would increase the chances of reaction taking place.

4.13.3.1 ^{1}H nmr.

The ^{1}H nmr spectra of the reaction products were made using an 80MHz instrument. Spectra were obtained in both $CDCl_3$ and d-DMSO solvents. In $CDCl_3$, the spectra were very badly resolved, but much better resolution was obtained in d-DMSO, suggesting the product properties are dependant upon the

PES present. The following table shows the relative amounts of PDMS remaining after extraction with toluene. The results are based upon the integration of the PES and PDMS proton signals.

	$CDCl_3$	d-DMSO
CB1	21.4%	2.1%
CB2	46.7%	1.5%
CB3	13.0%	0.0%
CB4	>100.0%	3.1%
CB5	50.0%	20.0%
CB6	>100.0%	14.7%

The spectra are all similar, except for the differing PDMS proton signals. No structural information could be obtained about the products from the spectra. All the spectra showed a complete absence of a carboxylic acid proton signal.

Considering the elastomeric nature of the products obtained, from CB1 in particular, low levels of PDMS were detected, with the exception of CB6. If a significant amount of PDMS was present, a much tougher moulding would have been obtained with the product of CB1.

4.13.3.2 Dsc.

The extracted products were examined by dsc under the conditions described in section 4.9.2.3. The results are summarised below.

The dsc thermogram of carboxy propyl PDMS (RMM=900) is shown in Figure 89, displaying a glass transition of -85.6°C. The dsc thermogram of carboxy propyl PDMS (RMM=2,500) is similar to that of the carboxy propyl PDMS (RMM=900) shown in Figure 89, but has a glass transition of -113.4°C. As the chain length of the PDMS increases, the glass transition is lowered, as the effect of the large and highly polar end groups is less influencial upon the thermal behaviour of the polymer.

CB1

Figure 90 shows the dsc thermogram of the toluene extracted product. This shows a high glass transition at 193.4°C corresponding to the PES (189.4°C, Figure 62). There is a large exotherm at -43.9°C. Surprisingly, there is no thermal indication of PDMS present in spite of the highly rubbery physical nature of the product.

CB2

The dsc thermogram for this product is very similar to the CB1 product thermogram (Figure 89). There is a PES glass

transition at 190.5°C and a large exotherm at -45.2°C. At @ -100°C there is a small thermal transition, which may be a glass transition, but it is too small to interpret. The glass transition of the PES starting material was 180.9°C.

CB3

The thermogram of this product shows all the same features as the thermogram of product CB1 (Figure 90). There is a PES glass transition at 182.1°C, which is 7°C lower than that of the PES homopolymer, 189.4°C (Figure 62). There is an exotherm at -44.0°C and a small thermal transition at 5°C which may be a Tg. There is no other evidence of PDMS present.

CB4

The dsc thermogram of the toluene extracted product shows the features of the previous reaction products, PES glass transition at 228.7°C and an exotherm at -45°C. The Tg of the PES homopolymer was 231.6°C, so a slight reduction in the high temperature glass transition is seen. There is no other evidence of PDMS present.

CB5

Figure 91 shows the dsc thermogram of the toluene extracted product. There is a PES glass transition at 229.8°C and an exotherm at -44.7°C. There is also an unidentified thermal transition at @ 10°C. The Tg of the PES homopolymer was 232.0°C, so a small reduction in Tg is seen here. The two

PES homopolymers used in reactions CB4 and CB5 display glass transitions at values comparable with the literature value for commercial grade PES (28).

CB6

Figure 92 shows the dsc thermogram of the toluene extracted product. There is a PES glass transition at 184.2°C, whereas the Tg of the homopolymer is 180.4°C. There is also a second Tg, which is quite broad at -100°C. If this second glass transition is attributed to PDMS, then it has been reduced from a value of -85.6°C (Figure 89). This could be due to the reaction of the carboxylic acid groups to form a copolymer and therefore without the polar end groups affecting the Tg, it would be expected to move nearer to the Tg of the non-functionalised PDMS at @ -123°C. However, such a low RMM PDMS would be expected to form a single phase product with PES. The lowering of the glass transition temperature indicates that some form of chain extension has taken place.

4.13.4 PDMS/PES blends.

In order to investigate the effects of maintaining PDMS at such high temperatures for so long, a series of reactions were carried out with PDMS and PES functionalised with end groups not expected to take part in chemical reactions.

Two reactions were carried out in the Brabender mixer with hydroxyl PES and PDMS with unreactive end groups towards the PES.

BN1

15.1g PES (RMM=3,709) and 12.6g hydride terminated PDMS were mixed together and added to the mixing cavity at 250°C. The product was removed after mixing for 2½ hours. The product was a white elastomeric material, which was soxhlet extracted with toluene over 48 hours. The sample was then extracted with TCE. The elastomeric product resembled a cross linked PDMS gel.

BN2

15.1g hydroxyl PES (RMM=3,709) and 12.0g trimethyl ended PDMS (Dow Corning DC200/200) were mixed together and added to the mixing cavity at 250°C. The product was removed after mixing for 2½ hours. The product was a brittle solid which was milled before extracting with toluene over 48 hours.

4.13.4.1 ^{1}H nmr.

The ^{1}H nmr spectra of the products after toluene extraction were made using an 80MHz instrument. Spectra were made in both $CDCl_3$ and d-DMSO solvents.

BN1

In both solvents, signals for the PDMS protons and para-substituted aromatic rings of PES were seen for the sample after TCE extraction. In $CDCl_3$, the PES signal is badly resolved and in d-DMSO the PDMS proton signal is reduced and broadened as would be expected (Figure 93).

BN2

Similar results were obtained as for reaction BN1, with the exception of only a very small signal for the PDMS protons in d-DMSO (Figure 94) compared with the spectrum obtained in $CDCl_3$ (Figure 95).

The results are interesting in that PDMS is retained in the product after toluene extraction, particularly for reaction BN2, where the PDMS has no reactive functional groups. The physical nature of the product from reaction BN1 suggests that the PDMS has crosslinked by a free radical route involving proton abstraction. This is quite probable for hydride terminated PDMS and is confirmed by the observations made whilst carrying out other melt reactions described here.

4.13.4.2 Dsc

The extracted products were examined by dsc, under the conditions described in section 4.9.2.3.

BN1

Figure 96 shows the dsc thermogram of the product after toluene extraction. There is a glass transition due to PES at 205.7°C, which is comparable with the starting material, (203.7°C, Figure 81). There is an endotherm at -46°C and a low temperature glass transition at -112.6°C. The thermogram of the PDMS homopolymer used in the experiment is shown in Figure 97. This displays a glass transition at -124.3°C as well as a cold crystallisation exotherm and crystalline melting endotherms.

There has been no decrease in PES Tg expected for a copolymeric product, but an increase in the PDMS glass transition suggests that some crosslinking has taken place. This could also be due to a reaction of the hydride end groups in the presence of any moisture to undergo chain extension.

$$\equiv Si\text{-}H + H\text{-}Si\equiv \xrightarrow{H_2O} \equiv Si\text{-}O\text{-}Si\equiv + 2H_2$$

Figure 98 shows the dsc thermogram of the product after extraction with TCE. There is no glass transition due to PES, but a PDMS glass transition is at -108.2°C. This suggests that the PES seen in the ^1H nmr spectra is trapped within the PDMS matrix and is unable to display a glass transition (as shown in Figure 96 by the PES homopolymer) which was later removed on extraction with TCE. An endotherm is seen at -40.6°C.

BN2

Figure 99 shows the dsc thermogram of the product after toluene extraction. There is a glass transition at 202.8°C which compares with the starting material, 203.7°C (Figure 81). There are two small endotherms at @ -40°C and @ -50°C, but no other indication of PDMS present.

The results of BN1 show that the PDMS is able to crosslink, (most likely by proton abstraction) under the conditions employed when carrying out the reactions in the Brabender mixer. This would account for PDMS being found in the reaction products after soxhlet extraction, as crosslinked PDMS would not be extracted from the reaction product. The residual PDMS found in experiment BN2 suggests that either soxhlet extraction of the milled product is not an efficient method of removing PDMS from a blend with PES, or that a low level of crosslinking has taken place at high temperature, as shown in reaction BN1.

4.14 Model reactions of PES and PDMS.

The work so far has shown indications of reaction to form small amounts of copolymer, contaminated by PES homopolymer. Further work was needed to clarify the validity of the three reaction routes investigated here, using short chain molecules representative of the homopolymers used to form the copolymers.

4.14.1 Epoxidation reactions.

The reaction of Bisphenol"S" and allyl glycidyl ether has already been described in section 4.9.1. Two other reactions were carried out to confirm this as a route to form copolymers.

E1

Bisphenol"S" was oven dried overnight at 120°C. A sample of hydride terminated PDMS (RMM=2,200) was functionalised through a vinyl addition reaction with allyl glycidyl ether, for use in this reaction.

0.5g (0.002 moles) Bisphenol"S" and 4.86g (0.002 moles) epoxy PDMS were dissolved in 2mls cyclohexanone in a 50ml 3-necked flask, equipped with a reflux condenser, nitrogen reservoir and septum. The flask was stirred by a magnetic follower and the contents heated to 140°C under nitrogen by an oil bath on a stirrer/hotplate. 0.02g DMDA catalyst were injected into the flask and the solution stirred for 20 hours. After the reaction, the cyclohexanone was removed on a rotary evaporator, leaving a clear, yellow, viscous liquid.

E2

Hydroxyl PES (RMM=4,370) was oven dried overnight at 120°C. 1.0g PES (2.3×10^{-4} moles) and a 0.6g (0.0053 moles) allyl glycidyl ether were weighed into a 50ml 3-neck flask equipped with a reflux condenser, nitrogen reservoir and

septum. The flask was stirred by a magnetic follower and the contents heated to 140°C under nitrogen by an oil bath on a stirrer/hotplate. 0.01g DMDA was injected into the flask and left stirring for 6 hours. The excess allyl glycidyl ether was then distilled off under vacuum, leaving a cloudy, viscous liquid.

4.14.1.1 ^{1}H nmr.

The reaction products described above and a sample of the product from the reaction of Bisphenol"S" and allyl glycidyl ether described in section 4.9.1 were analysed by ^{1}H nmr spectroscopy, using a 400MHz instrument.

E1

Figure 100 shows the ^{1}H nmr spectrum of the reaction product made as a solution in d-DMSO. Between 6.7-7.8ppm are the proton signals of the para-substituted aromatic rings. The para-substituted splitting pattern shows that there are more than one species of end group adjacent to the aromatic rings, not all are soluble as shown by the broad signals at 6.7-7.5ppm. The PDMS proton signal is at 0.0ppm and residual cyclohexanone accounts for the multiple signal at 1.6-2.4ppm. The signals at 0.3 and 0.4ppm are due to the alkyl chain of the DMDA.

The assignment of the ^{1}H nmr spectrum of allyl glycidyl ether (Figure 47) is given in section 4.7.3.4. The proton

signals of the epoxide ring structure are between 2.2-3.0ppm. From the spectrum of the E1 reaction product it can be seen that very few epoxide rings are intact. The proton signal for the opened epoxide ring accounts for the signals at 3.3-4.3ppm. These proton signals have been shifted downfield, suggesting that they are linked closely to the aromatic rings.

One further piece of information which also suggests that a successful reaction has taken place between the epoxy PDMS and Bisphenol"S" is that the opened epoxide ring signal is separated into two main groups. Had a hydroxyl group formed from an open epoxide ring reacted to ring open another epoxide ring, then a signal would be expected at 3.8ppm, there is none detected.

In order to obtain more information from the para-substitution splitting pattern of the aromatic rings, a sample of the product was dissolved in $CDCl_3$. The insoluble material was filtered off, dried and dissolved in d-DMSO. The spectrum obtained form the d-DMSO solution is shown in Figure 101. The proton signal of the PDMS is strong at 0ppm. The signals adjacent to it at 0.5-1.6ppm are due to methylene protons formed by vinyl addition of the allyl glycidyl ether to the hydride PDMS. Between 2.0-3.0ppm there is only a very small signal due to the intact epoxide rings, more clearly visible now the cyclohexanone has been transferred into the $CDCl_3$ layer. The opened epoxide ring signals are at 3.3-4.2ppm.

Most of the information can be found from the para-substitution splitting at 7-8ppm. The residual Bisphenol"S" proton signal accounts for the two strong signals at 7.0 and 7.8ppm. The smaller splitting pattern at 7.2 and 7.9ppm is due to the aromatic ring material which has reacted with the epoxide rings. This clearly shows the two different aromatic ring species present in the reaction product, corresponding to unreacted Bisphenol"S" and the material which has reacted with the epoxide rings.

E2

Figure 102 shows the ^{1}H nmr spectrum of the reaction product of hydroxyl PES with excess allyl glycidyl ether, as a solution in d-DMSO. By comparison with the spectrum of allyl glycidyl ether (Figure 47), it can be seen that the vinyl proton signal of allyl glycidyl ether is intact at 5-6ppm. The methylene protons of the allyl groups are at 3-4ppm, but the proton signal from the epoxide ring expected at 2-3ppm is absent, suggesting that reaction has taken place and the excess allyl glycidyl ether has been successfully removed.

The para-substitution splitting pattern of the aromatic rings is very complex at 7-8ppm. Obviously more than one substitution product is present i.e. hydroxyl PES as well as the reaction products with one or two allyl glycidyl ether molecules.

From this it can be seen that the epoxide ring has reacted with the hydroxyl PES. Reaction is undoubtedly hindered by the reactants not forming a homogeneous mixture, but still supports the use of melt reactions reported earlier.

The reaction product of Bisphenol"S" and allyl glycidyl ether described in section 4.9.1 was also analysed as a solution in d-DMSO using a 400MHz nmr instrument. The spectrum shown in Figure 103 was obtained.

The assignment of the spectrum obtained previously as a solution in $CDCl_3$ using an 80MHz instrument (Figure 52) is descibed in section 4.9.1.1. The more detailed spectrum confirms the earlier interpretation:- intact vinyl groups at 5-6ppm and ring opened epoxide signals at 3-4ppm, but also provides further information about the para-substituted aromatic ring structures.

The signals of the substituted rings are at 6.7-7.75ppm and consist of four different pairs of para-substituted aromatic ring signals, each with different intensities and positions. These correspond to the signal of Bisphenol"S", the signal of the disubstituted material and the two signals of the mono substituted product where only one hydroxyl group remains, the second having reacted with allyl glycidyl ether.

The two signals of equal intensity correspond to the signals of the mono substituted product (seen clearly at 7.55-

7.65ppm), the very small signal (seen at 7.45ppm) is due to the residual Bisphenol"S" and the strongest signals are due to the disubstituted material. This clearly shows that the Bisphenol"S" hydroxyl groups react with the epoxide ring of allyl glycidyl ether and that reaction was halted by the high viscosity of the reaction product.

4.14.2 Vinyl addition reactions.

The model compound used in these exploratory reactions was Bisphenol"S" functionalised with allyl bromide to give an aromatic vinyl sulphone compound representative of vinyl PES.

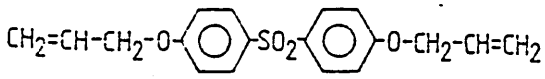

The model reactions were carried out both in solution and as melt reactions.

4.14.2.1 Preparation of vinyl Bisphenol"S".

The following method was developed to produce a v-Bisphenol"S".

10g (0.04 moles) Bisphenol"S", 3g (0.088 moles) tetrabutylammonium hydrogen sulphate and 10g (0.083 moles) allyl bromide were dissolved in 350mls cyclohexanone at 60°C in a 500ml 3-necked flask equipped with a reflux condenser and dropping funnel. The flask was stirred with a magnetic follower and the flask heated in an oil bath on a

stirrer/hotplate. When the Bisphenol"S" had dissolved, 17.5mls 12.5M sodium hydroxide solution were added dropwise and the sodium salt of Bisphenol"S" precipitated. The reaction was stirred for 20 hours at 60°C, during which a clear solution was formed.

The product was precipitated from ice-cold methanol:water (1:5). The product was filtered off and soxhlet extracted with hexane and then oven dried at 110°C.

4.14.2.1.1 ^{1}H nmr.

The ^{1}H nmr spectrum of the product was obtained from a solution in $CDCl_3$, using an 80MHz instrument (Figure 104). The spectrum is similar to that obtained for vinyl PES (Figure 21) described in section 4.6.2. The para-substituted aromatic ring splitting signal is at 6.8-8.0ppm. The multiplet at 5.7-6.2ppm (H^a), triplet at 5.1-5.4ppm (H^b) and the doublet at 4.45ppm (H^c) are typical of the allyl bromide protons.

$$Br\text{-}\overset{c}{C}H_2\text{-}\overset{a}{C}H=\overset{b}{C}H_2$$

The singlet at 7.2ppm is due to residual protons in the deuterated solvent. The integration of the spectrum corresponds to the required product. ^{1}H nmr anaylsis of the product dried without solvent extraction showed the integration for the correct product, i.e. none of the excess allyl bromide remained, but was contaminated with

cyclohexanone and water. These were removed by soxhlet extraction.

4.14.2.1.2 Dsc.

The product was examined by dsc under the conditions described in section 4.9.2.3. The thermogram obtained is shown in Figure 105, displaying a melting point for the product of 142.5°C. This is a reduction in melting point of 110°C over Bisphenol"S", which melts at 250.3°C (Figure 106). This confirms that a significant change in end groups has taken place and by functionalising the Bisphenol"S", the large contribution to the melting point of hydrogen bonding through the hydroxyl end groups is lost. The product was also soluble in a number of solvents that would not dissolve Bisphenol"S", as the solvation of the vinyl end groups was easier with non-polar solvents.

4.14.2.2 Vinyl addition reactions in solution.

Two vinyl additions were carried out in TCE solution with vinyl Bisphenol"S" and either 1,1,3,3-tetramethyldisiloxane or low RMM hydride PDMS (RMM=700). 1,1,3,3-tetramethyldisiloxane has a boiling point of 70°C, so the reaction was carried out at 60°C over a longer period of time, but there is still a possibility that the siloxane will reflux or boil away therefore upsetting the stoichiometry of the reaction.

VS1

0.5g (0.0015 moles) vinyl Bisphenol"S" and 2mls TCE were added to a 50mls 3-neck flask covered in aluminium foil, equipped with a reflux condenser, rubber septum and nitrogen reservoir. The flask was stirred with a magnetic follower and heated to 60°C in an oil bath on a stirrer/hotplate. When the vinyl Bisphenol"S" had dissolved, 1ml catalyst solution (0.0182g chloroplatinic acid in 25mls THF) and 0.2083g (0.0016 moles) 1,1,3,3-tetramethyldisiloxane were injected into the flask and the solution stirred at 60°C for 20 hours. After the reaction, solid black platinum was left in the solution.

VS2

0.5g (0.0015 moles) vinyl Bisphenol"S" and 2mls TCE were added to a 50ml 3-neck flask covered in aluminium foil, equipped with a reflux condenser, septum and nitrogen reservoir. The flask was stirred with a magnetic follower and heated to 120°C in an oil bath on a stirrer/hotplate. When the vinyl Bisphenol"S" had dissolved, 1ml catalyst solution (0.0231g chloroplatinic acid in 25mls THF) and 1.06g (0.0015 moles) hydride PDMS (RMM=700) were injected into the flask and the solution stirred at 120°C for 18 hours. The product was free of solid platinum on cooling.

4.14.2.2.1 ^{1}H nmr.

The ^{1}H nmr spectra of the reaction products were made in $CDCl_3$ solvent using a 400MHz instrument.

VS1

Figure 107 shows the ^1H nmr spectrum of the vinyl addition reaction product of vinyl Bisphenol"S" and 1,1,3,3-tetramethyldisiloxane. The intense peak at 5.9ppm is due to the TCE solvent and the peaks at 3.65 and 1.75ppm are due to the THF used in the catalyst solution. The PDMS methyl proton signal is at 0ppm and the proton signals of residual vinyl groups are seen at 4.45ppm and 5.15-5.4ppm (cf. Figure 104). The para-substituted aromatic ring signal is between 6.8-7.8ppm. Two distinctly different aromatic substitution signals are seen, the larger one is due to unreacted vinyl Bisphenol"S" and the smaller one to the vinyl addition product. No signal due to silicon hydride protons is detected at 4.5ppm (Figure 108). There are two small signals at 3.95ppm and at 0.95ppm which are due to methylene protons from the linking group formed by a successful vinyl addition reaction. These correspond to the similar peaks seen in the solution vinyl addition reactions detailed in section 4.10 (Figure 72).

The relative intensities of the methylene proton signals and the signals of the residual vinyl groups show that the vinyl addition reaction was only partially successful. The reaction does however confirm the interpretation of the reaction described in section 4.10. The lack of reaction can be explained by the low reaction temperature employed due to the low boiling point of the disiloxane. Loss of the

disiloxane through boiling also contributed to the low level of reaction.

VS2

Figure 109 shows the ^{1}H nmr spectrum of the vinyl addition reaction product of vinyl Bisphenol"S" and hydride PDMS (RMM=700). The interpretation of the spectrum is the same as for VS1 but with two notable exceptions. The para-substituted aromatic ring splitting pattern at 6.7-7.8ppm again shows too different species, but the relative intensities this time are more equal. The proton signal of the residual vinyl groups at 4.5ppm and 5.2-5.4ppm are smaller than the signals of the methylene linking group at 3.9, 0.9 and possibly 0.5-0.6ppm. These two points suggest reaction to a far greater extent than in VS1, possibly as far as to produce a low RMM "copolymer".

4.14.2.3 Vinyl addition melt reactions.

The low melting point of vinyl functionalised Bisphenol"S" (section 4.14.2.1) makes if quite suitable for investigating the vinyl addition reaction as a melt.

0.5g (0.0015 moles) vinyl Bisphenol"S" were weighed into a 50ml 3-neck flask covered with aluminium foil, equipped with a condenser, nitrogen reservoir and a septum. The flask was stirred with a magnetic follower and heated in an oil bath to 160°C on a stirrer/hotplate. When the vinyl Bisphenol"S" was

fully molten, 1.06g (0.0015 moles) hydride PDMS (RMM=700) and 1ml catalyst solution (0.0182g chloroplatinic acid in 25mls THF) were injected into the flask. The reaction was stirred at 160°C for 20 hours, during which, a clear, brown elastomeric product was formed.

4.14.2.3.1 ^{1}H nmr.

Figure 110 shows the ^{1}H nmr spectrum of the product made in $CDCl_3$ solvent, using a 400MHz instrument. This spectrum has very few peaks and is quite easy to interpret. The para-substituted aromatic ring splitting signal is at 6.8-7.8ppm. There is only one signal here, indicating only one product is present. There is no signal at all for residual vinyl groups at 4.5ppm and 5.2-5.4ppm, nor a silicon hydride proton signal at 4.5ppm. The large signal at -0.2-0.25ppm is due to the siloxane methyl protons.

In the spectra of reactions VS1 and VS2 (Figures 107 and 109) the proton signals due to the catalyst solvent THF are at 1.75 and 3.65ppm. In the spectrum of the melt reaction product (Figure 110) no signals are seen due to THF, which has boiled off during the reaction. The strong triplet at 3.85ppm is due to a methylene group of the propyl link formed through the successful vinyl addition reaction. The peak at 0.85ppm is also due to this linking group, which leaves one more signal due to the propyl linking group to be identified. The signal seen at 1.75ppm would have been masked by the THF

signal in the previous spectra examined (Figures 72, 107, 109) and would not have been visible. It is a quintet, so would correspond to the middle methylene group of the propyl link and is situated between the two other methylene triplets. The triplets correspond to the methylene groups closest to either the aromatic ring, in which case it is the signal furthest downfield or nearest the PDMS chain, in which case it would be closest to the siloxane methyl signals at 0ppm. This suggests that the multiplet at 0.55ppm is not due to the vinyl addition methylene group but may be due to a by product of the reaction with the catalyst.

The main features of the spectrum are the single aromatic para-substitution splitting pattern indicating a high polymer, the absence of residual vinyl groups and three clear signals of the linking group formed through a successful vinyl addition reaction. The reaction product was clear, indicating no contamination with unreacted starting material and displayed the physical characteristics of a crosslinked rubber, but was easily soluble in solvents favoured by PDMS. The success of this reaction was helped by the ease with which the two reactants could be mixed. Although incompatible as a melt, the two reactants were low viscosity liquids and so could be stirred rapidly to achieve interfacial mixing which could not be attained during the melt reactions of PES in the Brabender mixer due to the high viscosity of the PES.

The nitrogen atmosphere could be maintained for a long period of time and so help preserve the life of the catalyst, this was not achieved in the Brabender mixer. The success of this model reaction suggests that melt reactions involving vinyl PES could be viable if the life of the catalyst could be preserved and the mixing level increased.

4.14.2.3.2 Dsc.

The reaction product was examined by dsc under the conditions described in section 4.9.2.3. Figure 111 shows the thermogram of the product. The main features of this are a glass transition at -44.6°C and the complete absence of the vinyl Bisphenol"S" melting endotherm at 142.5°C. The dsc thermogram of the siloxane homopolymer is shown in Figure 74 and displays a glass transition at -136.4°C, as well as a crystalline melting endotherm at -68.9°C.

The large increase in the siloxane Tg to a value between that of a siloxane and the melting point of vinyl Bisphenol"S" as well as the absence of the vinyl Bisphenol"S" melting endotherm and no crystalline endotherm confirm that a successful vinyl addition has taken place. Incorporation of inflexible Bisphenol"S" units into the high polymer chain would reduce the ability of the product to form crystallites.

4.14.3 Hydroxyl PES/carboxy propyl PDMS condensation reaction.

5g (0.02 moles) Bisphenol"S" were placed in a reaction tube and fitted into a vapour bath filled with triethylene glycol (b.pt.=285°C). The vapour bath was heated on an isomantle and the reaction tube was stirred mechanically with an anchor stirrer through a stirrer gland in the reaction tube head. The tube was kept under a flow of nitrogen and the outlet of the tube connected to a condenser and vented receiver flask.

On heating the reaction tube, the temperature of the contents was maintained at 273°C, as determined using a thermocouple probe. The melting point of Bisphenol"S" is 250.3°C, as determined by dsc (Figure 106). When the Bisphenol"S" was completely molten, the stirrer was started and 18g (0.02 moles) carboxy propyl PDMS (RMM=900) and 0.01g stannous octoate catalyst were added to the reaction tube. The reaction was stirred for 2¼ hours, after which a highly viscous, clear brown product remained in the tube.

4.14.3.1 ^{1}H nmr.

Figure 112 shows the ^{1}H nmr spectrum of the product made in $CDCl_3$ solvent, using a 400MHz instrument. This spectrum consists of the proton signals due to the PDMS chains (as shown in Figure 86) and the para-substituted aromatic ring splitting signal.

The signals of the PDMS chains are between -0.2-4ppm and have not changed from the starting material (Figure 86) and would not be expected to after the condensation reaction. No signal was detected due to carboxylic acid hydroxyl protons, suggesting that the condensation reaction of the acid groups had taken place.

The para-substitution signal of the aromatic rings is very complicated (6.7-7.9ppm). This suggests that a number of different substitution species are present and that the reaction has formed a number of different low RMM polymer chains. Due to the possible contamination of the PDMS starting material with the methyl ester (section 4.13.3), the stoichometry of the reaction is changed dramatically and so the reaction would be unable to produce high polymer. However, the ^{1}H nmr spectrum suggests that reaction has taken place, by the number of different aromatic species other than Bisphenol"S" present.

4.14.3.2 Dsc.

The reaction product was examined by dsc under the conditions described in section 4.9.2.3. Figure 113 shows the thermogram of the reaction product. There is a small glass transition at about -85°C which is due to unreacted PDMS methyl ester contaminant. The dsc thermogram of carboxy propyl PDMS homopolymer is given in Figure 89. The polymer used in this experiment has a glass transition at -85.6°C.

There is a second glass transition at -37.6°C due to the reaction product. This glass transition has greatly increased from the value obtained for the PDMS starting material and suggests that the condensation reaction has been successful. This is confirmed by the absence of a melting endotherm for Bisphenol"S" at 250.3°C.

4.14.4 Chain extension of carboxy propyl PDMS.

In order to investigate the effects of maintaining carboxy propyl PDMS at >250°C for 2 hours, an experiment was carried out under vacuum to see if any physical changes occurred.

18g (0.02 moles) carboxy propyl PDMS (RMM=900) and 0.01g stannous octoate were mixed mechanically in a reaction tube heated by a vapour bath containing triethylene glycol (b.pt.=285°C). The reaction tube was evacuated to 1.0mm Hg pressure and left stirring for 1½ hours at 273°C. On cooling, a brown viscous liquid was obtained.

4.14.4.1 Dsc.

The reaction product was examined by dsc under the conditions described in section 4.9.2.3. Figure 114 shows the thermogram of the product. The two features of this are the glass transition at -120.7°C and the endotherm at -48.0°C. The glass transition of the starting material is only -85.7°C

and has no other thermal transitions. The sample of carboxy propyl PDMS with RMM=2,500 had a glass transition at -113°C. The endotherm at -48°C is due to crystalline melting.

The conditions employed were severe enough for chain extension to take place and produce a siloxane polymer of higher RMM than the starting material. This reaction shows that the movement of the glass transition in the reaction product of carboxy propyl PDMS and Bisphenol"S" (section 4.14.3) was due to a reaction rather than an increase in the RMM of the PDMS chains. Other reasons for decrease in Tg, could be due to the loss of the highly polar end groups or chain scission.

5. CONCLUSIONS.

The polycondensation reaction of 4,4'-dichlorodiphenyl sulphone with excess Bisphenol"S" in diphenylsulphone solvent has proved to be a simple and effective method for the preparation of hydroxyl ended poly(ethersulphone) oligomers. Continuous extraction of the crude product successfully removes the solvent and by products leaving a reasonably pure product.

Infra-red and proton nuclear magnetic resonance spectroscopy (^{1}H nmr) verified the structure of the PES oligomers and showed that the material contained no detectable chloro end groups. Gel permeation chromotography (gpc) showed small amounts of high molecular size material or crosslinked polymer present in the samples. The relative molecular mass (RMM) determinations for the low RMM oligomers determined by ^{1}H nmr spectroscopy contradicted the trend in the glass transition temperatures found by differential scanning calorimetry (dsc). The RMM values were re-evaluated towards the end of the project and values more consistent with the glass transition temperatures were obtained. This however lead to stoichiometric imbalances in the reactions forming copolymers, so conversion to high copolymer was not possible, as there was always an excess of PES present.

The RMM vlaues of the PES oligomers were mostly lower than expected when compared with the calculated values. This

was attributed to the accurate temperature control throughout the reactions and the ease with which water was removed from the reaction vessel, so preventing loss of Bisphenol"S" monomer through side reactions with water. This resulted in more hydroxyl monomer being present than was expected. The oligomers with the lowest RMM values were higher than the calculated values, but using such large excesses of Bisphenol"S", side reactions of the monomer could not be avoided.

The conversion of the hydroxyl PES oligomers to vinyl functionalised material was completed quantitatively. The functionalised materials were characterised by infra-red and proton nuclear magnetic resonance spectroscopy confirming the end group conversions at >95%.

The functionalisation of Bisphenol"S" with vinyl end groups was also quantitative, as shown by ^{1}H nmr spectroscopy. Differential scanning calorimetry showed the product had a melting point 110°C lower than Bisphenol"S". This is a consequence of removing the hydrogen bonding by converting the hydroxyl groups to less polar vinyl groups. The extreme change in physical nature of the product was shown by the different solubility characteristics of the vinyl functionalised material.

Two methods of forming poly(dimethylsiloxanes) were investigated; equilibration of the cyclic siloxane tetramer

with acid activated clay being chosen as the most suitable. This method provided material with a narrow RMM distribution and the RMM could be calculated by gpc and then confirmed from the ^{1}H nmr spectrum. The hydride terminated material could be functionalised to give epoxy end groups and introduced the required silicon-carbon bonds through a vinyl addition reaction. This reaction was highly successful and showed no signs of side reactions when the products were examined by ^{1}H nmr spectroscopy. The ^{1}H nmr spectrum integration was used to determine the extent of reaction. The only problems encountered with the method used were the losses of product after drying with anhydrous magnesium sulphate. The reaction also provided useful practical information about vinyl addition reactions and the use of chloroplatinic acid catalysis for the copolymerisation reactions carried out.

The initial experiments carried out involving Grignard reagents were very disappointing. It was not possible to form a Grignard reagent from dichlorodiphenylsulphone (DCDPS). When a Grignard reagent was prepared in the presence of DCDPS the extremely violent exotherm observed was sufficient to suggest the cleavage of the sulphone bond. The resulting solutions still contained unreacted Grignard on isolation in ice/water. The literature suggests that Grignard reagents cleave siloxane bonds, particularly at the high temperatures achieved after the exotherm in forming the Grignard reagent was experienced (22). From these experiments it was quite

clear that other reaction schemes were more suitable for forming the required block copolymers.

In order to pursue the formation of PES/PDMS block copolymers by the synthetic routes chosen, a suitable solvent system was required. The large difference in solubility parameters between PES and PDMS ($\Delta=10.3[MJm^{-3}]^{\frac{1}{2}}$) inhibits the formation of a homogeneous solution. The most promising solvent tried was 1,1,2,2-tetrachloroethane, which appeared to dissolve both PES and PDMS oligomers, but there was evidence to suggest that a siloxane rich layer was formed on the side of the reaction vessel.

Other solvents tried were unable to dissolve both of the oligomers. In some cases this may have been due to the water content of the solvent or the PES oligomers, which can be quite high and is critical to the dissolution of the oligomers. 1,2-dichlorobenzene was used by Morris (19) as the solvent to form PES/PDMS copolymers via the reaction of hydroxyl PES and dimethylamino PDMS. The dilution required to dissolve both PES and PDMS oligomers in 1,2-dichlorobenzene was sufficient to suggest that reaction between less reactive oligomers would be unreasonable. The reaction between the labile dimethylamino PDMS and hydroxyl PES produces silicon-oxygen-carbon bonds, whereas the aims of this project were to prepare block copolymers linked by silicon-carbon bonds.

Two of the routes investigated here have also been investigated in the formation of polysulphone/PDMS block copolymers, both of which require high concentrations of the reactive oligomers. Polysulphone is formed by the condensation of DCDPS and Bisphenol"A". The propylidene group of Bisphenol"A" increases the reactivity of this material by over seven hundred times that of Bisphenol"S" (202), consequently reactions in dilute solutions would further reduce the reaction rates of PES.

The problems of finding a suitable solvent for PES and PDMS oligomers are emphasised by noting the effects the highly polar end groups of hydroxyl PES and carboxy propyl PDMS have upon solubility. No solvent could be found that would form a homogeneous solution of the two oligomers at high temperatures. This was attributed to the formation of PDMS dimers at room temperature enabling dissolution, which were broken up on heating and caused phase separation. Hydroxyl PES also forms dimers in solution which makes the solution properties of PES more difficult to control (214).

Solution reactions were carried out to prepare block copolymers by the reaction of hydroxyl PES and epoxy propyl PDMS followed by selective solvation with toluene to remove any unreacted PDMS homopolymer. Copolymers such as these formed from low RMM precursors will be soluble in solvents preferential to one of the homopolymer blocks if the copolymer is rich in one of the precursors i.e. an ABA copolymer

structure with PDMS A blocks would be soluble in toluene (215). The reaction products were characterised by differential scanning calorimetry, infra-red and ^1H nmr spectroscopy. ^1H nmr was used primarily to determine the level of siloxane remaining after selective extraction from the integrals of the PES aromatic ring signal and PDMS methyl proton signal. This method is only accurate if all the sample is soluble and no copolymer has been removed during selective solvation and has been used successfully with polystyrene/PDMS copolymers (142). The samples analysed here are contaminated with unreacted PES, which is not soluble in solvents suitable for PDMS dissolution, hence only qualitative information can be gained from these spectra. Dsc showed very little evidence of copolymer formation from these solution reactions.

The solution reactions of vinyl functionalised PES and hydride terminated PDMS catalysed by chloroplatinic acid showed better results. The successful reactions are easier to characterise by ^1H nmr spectroscopy, as a propyl group is formed as the block link and is easily identified. Further evidence to support this was that strong signals of PDMS methyl protons were seen in solutions of the product in d-DMSO, a good solvent for PES but not for PDMS. This suggests that PES bonded to PDMS is bringing the siloxane into solution. Although dsc did not show any thermal transitions due to PDMS, the glass transition of PES was reduced by 14°C. The physical characterisitics of the product were different from those of the starting materials. PES is a powder and the

low RMM PDMS samples are low viscosity liquids. The successful reactions, although not displaying thermal characteristics of PDMS or high levels of PDMS in the ^{1}H nmr spectrum, gave products which were elastomeric solids. This is expected for block copolymers containing hard and soft block segments, as they behave as crosslinked rubbers displaying good recovery properties. The results seen here suggest that a small inclusion of rubber into the PES chains has a strong influence on the physical characteristics of the product. The most successful reactions were carried out using very low RMM PDMS oligomers. As the chain length of the PDMS oligomers decreases, they became more miscible with PES and also the reactivity of the silane end group is increased (216).

The problems associated with using an air sensitive catalyst such a chloroplatinic acid are accentuated when the reactive species involved are highly incompatible. The use of dried solvents, fresh catalyst solutions and the exclusion of air and moisture help the reaction, but the longer the reaction time required, the more depleted the catalyst becomes through degradation and side reactions. The incompatible reactants make this aspect of the reaction very important. Consequently, vinyl addition reactions are described in the literature, but in practice are very difficult to control due to the sensitivity of the catalyst to oxygen (217).

Carrying out the copolymerisations as a melt is an excellent way of increasing the end group concentration, whilst removing problems associated with solvation by the solvent. As PES is an amorphous thermoplastic, the viscosity of the "melt" above the glass transition temperature is still very high, making efficient mixing very difficult (6). Due to the high incompatibility of the PES and PDMS, stirring has to be extremely vigorous for there to be any mixing and hence reaction take place (218). The temperatures involved are also detrimental to the PDMS, causing degradation and free radical crosslinking (112).

The reactions between the epoxy propyl PDMS and hydroxyl PES produced a number of interesting results. Throughout these reactions, crosslinked PDMS was found in varying amounts in the mixer, which accounts for the small amount of siloxane in the products after selective extraction when no amine catalyst was present. Again, a large signal for PDMS methyl protons was observed, both in d-DMSO and $CDCl_3$ solvents, when characterised by ^1H nmr spectroscopy. The sample showed both glass transitions for PES and PDMS when analysed by dsc, suggesting the formation of a phase separated copolymer. A residue was left after extraction with 1,1,2,2-tetrachloroethane, which suggests crosslinking had taken place, so a mixture of copolymer and crosslinked PDMS or PES trapped in the PDMS gel was present. The detection of a PES glass transition suggests that the PES is evenly distributed throughout the sample, rather than as one domain in the gel

in which case the PES glass transition would not be detected. Other samples prepared by this route displayed PES glass transitions at reduced temperatures, which suggest the formation of copolymers.

The investigation of vinyl addition reactions in the melt were always likely to be less successful than in solution, because the Brabender mixer could not be kept under a nitrogen atmosphere as effectively as the reaction flasks used for solution reactions. Consequently, the reaction products obtained using chloroplatinic acid catalyst showed only small amounts of siloxane present when characterised by ^1H nmr spectroscopy and no PDMS thermal transitions by dsc. The reaction involving a free radical catalyst also required an inert atmosphere, but the vinyl addition reaction is less reactive towards free radicals than it is towards platinum catalysed vinyl addition (22 ,123). No inclusion of PDMS was observed in this reaction, suggesting that the lack of an inert atmosphere rapidly quenched the radicals being formed.

The reaction between carboxy propyl PDMS and hydroxyl PES in the presence of stannous octoate catalyst also provided an elastomeric product, but surprisingly no PDMS glass transition was detected by dsc. Other reaction products were more brittle in their physical characteristics, but showed significant quantities of siloxane present when characterised by ^1H nmr spectroscopy and even PES glass transitions at reduced temperatures, which suggest the formation of a

copolymer. The catalyst (stannous octoate) is also deactivated in the presence of radicals, water and oxygen as it is hydrolysed to form the oxide. Stannous octoate is then less effective when used in the open cavity of the Brabender mixer (165). The presence of the methyl ester of the carboxy propyl PDMS was not determined until the reactions had all been carried out. This obviously introduces stoichiometric imbalance to these reactions, reducing the possibility of obtaining high levels of copolymerisation.

The melt blending of PES and PDMS with non-reactive end groups produced a highly elastomeric product which consisted of a crosslinked siloxane and PES. Whether the PES was trapped within the siloxane network or was chemically bonded to the PDMS could not be determined, but this confirmed the observations earlier of gel being formed in the Brabender mixer.

The model reactions carried out as part of the project confirmed that all the reactions pursued were suitable for producing the silicon-carbon links required of the copolymers.

The reaction between Bisphenol"S" and allyl glycidyl ether showed clearly that the epoxidation reaction would link hydroxyl PES and epoxy functionalised PDMS. The reaction almost reached completion, but some mono substituted material remained, as the extent of the reaction is controlled in the latter stages by the viscosity of the product. The reaction

between PES low polymer (RMM=4,370) and allyl glycidyl ether suggested that inspite of the gross incompatibility of the materials, reaction could take place. Similarly, reaction takes place between the epoxy PDMS (RMM=2,200) and Bisphenol"S". The reaction was shown to be possible between low RMM polymer and small reactive molecules. When polymers of high incompatibility and with low concentrations of end groups were used, the extent of reaction was understandibly reduced.

The vinyl addition reactions in solution between v-Bisphenol"S" and low RMM PDMS showed that the vinyl addition reaction can take place in solution, but the reaction was even more successful in the melt. The product of the melt reaction clearly produced a high polymer. ^{1}H nmr spectroscopy showed only one set of signals due to the substituted aromatic ring, which is from the vinyl Bisphenol"S" fully reacting with the PDMS. Strong signals due to the propyl link formed through the vinyl addition reaction were seen. Dsc showed that the product had a single glass transition 91°C above that of the PDMS starting material and no melting endotherm from vinyl Bisphenol"S", indicating complete reaction inspite of the high viscosity reached. The extent of this reaction compared with the solution reaction shows that a melt reaction could be possible if sufficient mixing and an inert atmosphere could be maintained. It also shows that the presence of a solvent does impede the vinyl addition reaction.

The melt reaction between Bisphenol"S" and carboxy propyl PDMS gave a product which showed no Bisphenol"S" melting endotherm and a glass transition 48°C above that of the siloxane starting material. This clearly shows that the reaction is suitable for the formation of the required copolymers. The glass transition corresponding to unreacted PDMS shows that the methyl ester of carboxy propyl PDMS does not take part in the reaction with the hydroxyl groups.

5.1 Suggestions for future work.

The work carried out for this project provides important information on which to base further work. Three viable synthetic routes to prepare PES/PDMS block copolymers linked via silicon-carbon bonds have been investigated. A more complete investigation of the melt reactions is required under inert conditions using high shear mixing. The chloroplatinic acid catalyst used in this investigation is not sufficiently stable for use at high temperatures, but recent work using ultrasound to catalyse vinyl addition reactions has proved successful and would aid mixing of the polymers (219,220).

Using phenylmethyl siloxanes would increase the high temperature stability of the rubber phase in melt reactions and would be slightly more miscible with PES than PDMS by virtue of having a higher solubility parameter ($18.3[MJm^{-3}]^{\frac{1}{2}}$). This could be important in finding a solvent to form a

homogeneous reaction mixture and to develop the solution reactions.

The products of the model reactions, v-Bisphenol"S" with hydride PDMS and Bisphenol"S" with carboxy propyl PDMS may be useful materials acting as compatiblisers for reactions involving high RMM polymers. Adding a small percentage of the product to a reaction between functionalised PES and PDMS homopolymers may provide sufficient compatibility to enable extensive copolymerisation to take place. Also, those materials may act as compatiblisers for blending low levels of PDMS with PES. Simple blends of 3%w/w PDMS homopolymer with commercial grade PES show increased levels of toughening in sharp notched impact tests (19). Compatible additives such as these may improve this performance even further. The additives themselves are not of sufficiently high RMM to provide toughening alone.

A further synthetic route to investigate would be PDMS grafts onto the PES chains using butyllithium to abstract protons from the PES aromatic rings (221). Addition of the cyclic siloxane trimer (D_3) could then be polymerised anionically from the anionic site left by proton abstraction or a suitably functionalised PDMS oligomer linked to the PES chains at this point.

The literature shows that migration of the PDMS copolymers when blended to tougher homopolymers is a source

of reduced impact strength and toughness due to delamination occurring. If the PDMS could be crosslinked during the preparation of the copolymer or during the blending with the homopolymer, migration to the surface of the moulding would be reduced. The high temperature reactions investigated in this report have shown that crosslinking does occur and can be advantageous in toughening applications. There is obviously reason to investigate this further by introducing reagents which will promote crosslinking. This work could be linked with the proton abstraction properties of butyllithium to grow siloxane chains from the PES backbone.

These are just a few of the ideas which could be pursued in order to provide toughening additives for PES.

REFERENCES

1 RB Rigby, Proc Electron/Electric (Insul.Conf.) 15th Proc. Electron/Electric (Insul.Conf.), 126, 1981.

2 VJ Leslie, JB Rose, GO Rudkin and J Feltzin in "New Industrial Polymers", ACS Symp. Ser. 4, ACS, 1974.

3 AA Collyer, DW Clegg et al, IX International Congress on Rheology, Acapulco October 8-13 1984, **Vol 3**, 543, 1985.

4 A Noshay, JE McGrath in "Block Copolymers", Academic Press, 1977.

5 A Noshay, M Matzner and CN Merriam, Polym. Prepr., Am. Chem. Soc. Div. Polym. Chem., **12(1)**, 247, 1971.

6 A Noshay, M Matzner and CN Merriam, J. Polym. Sci: Pt A-1, **9(11)**, 3147, 1971.

7 M Matzner, A Noshay and JE McGrath, Polym. Prepr., Am. Chem. Soc. Div. Polym. Chem., **14(1)**, 68, 1973.

8 A Noshay, M Matzner and TC Williams, Ind. Eng. Chem. Prod. Res. Devel., **12(4)**, 268, 1973.

9 LM Robeson, A Noshay, M Matzner and CN Merriam, Angew. Makromol. Chem., **29/30**, 47, 1973.

10 M Matzner, A Noshay, LM Robeson, CN Merriam et al, Appl. Polym. Symp., **22**, 143, 1974.

11 M Matzner, A Noshay, DL Schober and JE McGrath, Ind. Chim. Belge., **38**, 1104, 1974.

12 A Noshay and M Matzner, Angew, Makromol. Chem., **37**, 215, 1974.

13 A Noshay, M Matzner, BP Barth and RK Walton, Am. Chem. Soc. Div. Org. Coat. Plast. Chem. Prepr., **34/2**, 217, 1974.

14 A Noshay, M Matzner, BP Barth and RK Walton in "Toughness and Brittleness of Plastics", Eds RD Deanin and AM Crugnola, Adv. Chem. Series 154, ACS, 1974.

15 A Noshay, M Matzner and LM Robeson, J. Polym. Sci: Polym. Symp., **60**, 87, 1977.

16 DC Webster, JL Hedrick, JE McGrath, Procs. Natl., S.A.M.P.E. Symp. Exhib. 1085, 29(Technol Vectors), 1984.

17 D Tygai, JL Hedrick, DC Webster, JE McGrath and GL Wilkes, Polymer, **29**, 833, 1988.

18 NM Patel, DW Dwight, JL Hedrick, DC Webster and JE McGrath, Macromolecules, 21, 2689, 1988.

19 M Morris, PhD Thesis, Sheffield City Polytechnic, 1988.

20 D Parker, ICI plc., Private Communication.

21 W Noll, "Chemistry and Technology of Siloxanes", Academic Press, 1968.

22 C Eaborn, "Organosilicon Compounds", Butterworths, 1960.

23 JS Riffle, RG Freelin, AK Banthia and JE McGrath, J. Macromol. Sci: Chem. Edn., A15(5), 967, 1981.

24 MG Voronkov, VP Mileskevich and YA Yuzhelevski, "The Siloxane Bond", Plenum Press, 1978.

25 EG Rochow, "An Introduction to the Chemistry of the Silicones", Wiley, 1951.

26 A Bunn, ICI plc, Private Communication.

27 Kirk-Othmer, "Encyclopoedia of Chemical Technology", Vol 18, 3rd Edition, Wiley, 1982.

28 JA Brydson, "Plastics Materials", 4th Edition, Butterworth Scientific, 1982.

29 PM Hergenrother, J. Polym. Sci: Polym. Chem. Edn., 20, 3131, 1982.

30 JB Rose, Polymer, 15, 456, 1974.

31 WF Hale, AG Farnham, RN Johnson and RA Clendenning, J. Polym. Sci: Pt A-1, 5, 2399, 1967.

32 E Macho, JM Alberdi, A Alegria and J Colmenero, Makromol. Chem., Macromol. Symp., 20/21, 451, 1988.

33 TA Vigilis, Polymer, 29, 327, 1988.

34 "Victrex PES High Temperature Engineering Thermolplastic", ICI Advanced Materials, 1985.

35 RY Ting, J. Mater. Sci., 16, 3059, 1981.

36 CB Bucknall, "Toughened Plastics", Applied Science, London, 1977.

37 EH Merz, GC Claver and M Baer, J. Polym. Sci., 22, 325, 1956.

38 CB Bucknall and RR Smith, Polymer, 6, 437, 1965.

39 CB Bucknall in "Polymer Blends", Vol 2, Eds DR Paul and S Newman, Academic Press, 1978.

40 M Matsuo, Polymer, 7, 421, 1966.

41 S Newman in "Polymer Blends", Vol 2, Eds DR Paul and S Newman, Academic Press, 1978.

42 S Newman and S Strella, J. App. Polym. Sci., 9, 2297, 1965.

43 CB Bucknall, CJ Page and VO Young in "Toughness and Brittleness of Plastics", Eds RD Deanin and AM Crugnola, Adv. Chem. Ser. 154, ACS, 1976.

44 RP Kambour, D Faulkner, EE Kampf et al in "Toughness and Brittleness of Plastics", Eds RD Deanin and AM Crugnola, Adv. Chem. Ser. 154, ACS, 1976.

45 AJ Kinloch and RJ Young, "Fracture Behaviour of Polymers", Applied Science Publishers, 1983.

46 PJ Hine, RA Duckett and IM Ward, Polymer, 22(2), 1745, 1981.

47 RP Petrich, Polym. Eng. Sci., 13, 248, 1973.

48 RP Kambour, J. Polym. Sci: Pt A., 2, 4168, 1964.

49 CB Bucknall, Brit. Plast., 11, 118, 1967.

50 TL Smith, J. Polym. Sci: Polym. Phys. Edn., 12, 1825, 1974.

51 RP Kambour, J. Polym. Sci: Macromol. Revs., 7, 1, 1973.

52 M Matsuo and S Sagaye, Polym. Prepr., 11(2), 384, 1970.

53 FC Stehling, T Huff et al. J. Appl. Polym. Sci., 26, 2693, 1981.

54 G Cigna, P Lomellini and M Meriott. J. App. Polym. Sci., 37, 1527, 1989.

55 S Wu, Polymer, 26, 1855, 1985.

56 M Matsuo, TT Wang and TK Kwei, J. Polym. Sci: Pt A-2, 10, 1085, 1972.

57 NM Bikales, "Mechanical Properties of Polymers", Wiley-Interscience, 1971.

58 B Baum, WH Holley, H Stisskin et al in "Toughness and Brittleness of Plastics", Eds RD Deanin and AM Crugnola, Adv. Chem. Ser. 154, ACS, 1976.

59 CB Bucknall, Makromol. Chem. Macromol. Symp., **20/21**, 425, 1988.

60 PJ Flory, "Principles of Polymer Chemistry", Cornell University Press, 1953.

61 RP Sheldon, "Composite Polymeric Materials", Applied Science, 1982.

62 JH Hildebrand, J. Am. Chem. Soc., **51**, 66, 1929.

63 S Krause, J. Macromol. Sci. Rev. Macromol. Chem., **C7(2)**, 251, 1972.

64 E Helfand and Y Tagami, J. Polym. Sci., **9B**, 741, 1971.

65 R Porter and J Johnson, Chem. Rev., **66**, 1, 1966.

66 DR Paul in "Polymer Blends", Vol 2, Eds DR Paul and S Newman, Academic Press, 1978.

67 D Heikens, N Hoen, W Barensten et al, J. Polym. Sci: Polym. Symp., **62**, 309, 1978.

68 NG Gaylord in "Copolymers, Polyblends and Composites", Ed NJ Platzner, Adv. Chem. Ser. 142, ACS, 1975.

69 HW Kammer and J Piglowski in "Polymer Blends", Vol 2, Eds M Kryszewski, A Galeski and E Martuscelli, Plenum Press, 1984.

70 G Maglio and R Palumabo in "Polymer Blends", Vol 2, Eds M Kryszewski, A Galeski and E Martuscelli, Plenum Press, 1984.

71 DR Paul and JW Barlow, J. Macromol. Sci. Rev. Macromol. Chem., **C18(1)**, 109. 1980.

72 G Reiss and Y Jolivet in "Copolymers, Polyblends and Composites", Ed NJ Platzner, Adv. Chem. Ser. 142, ACS, 1975.

73 R Fayt, R Jerome and PH Teyssie, J. Polym Sci: Polym. Letts. Edn., **19**, 79, 1981.

74 R Fayt, R Jerome and PH Teyssie, J. Polym. Sci: Pt B, Polym. Phys., **27**, 775, 1989.

75 G Krause in "Polymer Blends", Vol 2, Eds DR Paul and S Newman, Academic Press, 1978.

76 AA Collyer and DW Clegg, High Perf. Plasts., **2(10)**, 6, 1985.

77 DJ Meier, J. Polym. Sci: Pt C, **26**, 81, 1969.

78 DF Leary and MC Williams, J. Polym. Sci: Polym. Phys. Edn., **11**, 345, 1973.

79 DF Leary and MC Williams, J. Polym. Sci: Polym. Phys. Edn., **12**, 265, 1974.

80 T Inoue, T Soen, T Hashimoto, H Kawai, J. Polym. Sci: Pt A-2, **7**, 1283, 1969.

81 DG LeGrand, Polym. Prepr., **11(2)**, 434, 1970.

82 S Krause, J. Polym. Sci: Pt A-2, **7**, 249, 1969.

83 S Krause, Macromol, **3(1)**, 84, 1970.

84 DJ Meier, Polym. Prepr., **18**, 340, 1977.

85 JC Saam and FWG Fearon, Polym. Prepr., **11(2)**, 455, 1970.

86 MR Munch and AP Gast, Macromol., **21**, 1360, 1988.

87 MR Munch and AP Gast, Macromol., **21**, 1372, 1988.

88 MO de la Cruz and IC Sanchez, Macromol., **19**, 2501, 1986.

89 J Kohler, G Reiss and A Bandert, Env. Polym. J., **4**, 173, 1968.

90 X Quan, I Gancraz et al, Macromol., **20**, 1431, 1987.

91 B Wang and S Krause, J. Polym. Sci: Pt B, Polym. Phys., **26**, 2237, 1988.

92 LZ Rogovina, AY Chalykh et al, Polym. Sci. USSR, **21**, 431, 1979.

93 PJ Flory, Macromol., **11(6)**, 1141, 1978.

94 N Alberola, J. Appl. Polym. Sci., **36**, 787, 1988.

95 M Jiang, X Huang, T Yu, Polymer, **24**, 1259, 1983.

96 M Jiang, X Huang, T Yu, Polymer, **27**, 1689, 1986.

97 H Xie, Y Liu, M Jiang et al, Polymer, **27**, 1928, 1986.

98 T Inoue, T Soen et al, Macromol., **3(1)**, 87, 1970.

99 S Krause, Polym. Prepr., **11(2)**, 568, 1970.

100 JC Saam and FWG Fearon, Ind. Eng. Chem. Prod. Res. Dev., **10(1)**, 10, 1971.

101 DN Theodorou, Macromol., **21**, 1422, 1988.

102 M Matsuo, S Sagae and H Asai, Polymer, **10**, 79, 1969.

103 LA Utracki and MR Kamal, Polym. Eng. and Sci., **22(2)**, 96, 1982.

104 LA Utracki, Polym. Eng. Sci., **23(11)**, 602, 1983.

105 CW Childers, G Kraus, JT Gruver and E Clark in "Colloidal and Morphological Behaviour of Block and Graft Copolymers", Ed GE Molau, Plenum Press, 1971.

106 RR Durst, RM Griffith, AJ Urbanic and WH Van Essen, in "Toughness and Brittleness of Plastics", Eds RD Deanin and AM Crugnola, Adv. Chem. Ser. 154, ACS, 1976.

107 T Ueki, M Yoshimura, K Kanezaki, T Sato, Jpn. Patent 01,256,569.

108 T Eckel, D Wittmann, KH Ott, K Fuhr, Eur. Patent 338,361.

109 SJ Clarson and JA Semlyen, Polymer, **27**, 91, 1986.

110 JC Saam, AH Ward and FWG Fearon, Am. Chem. Soc. Polym. Prepr. Div. Polym. Chem., **13**, 524, 1972.

111 JG Zilliox, JEL Roovers and S Bywater, Macromolecules, **8(5)**, 573, 1975.

112 D Feng, GL Wilkes and JV Crivello, Polymer, **30**, 1800, 1989.

113 HA Vaughn, J. Polym. Sci: Pt B, **7**, 569, 1969.

114 JJ O'Malley and WJ Stauffer, Polym. Eng., **17(8)**, 510, 1977.

115 PJA Brandt, CLS Elsbernd, N Patel, G York and JE McGrath, Polymer, **31**, 180, 1990.

116 M Kajiyama, Y Nishikata, M Kakimoto and Y Imai, Polym. J., **18(10)**, 735, 1986.

117 M Kakimoto, M Kajiyama and Y Imai, Polym. J, **18(12)**, 935, 1986.

118 M Kajiyama, M Kakimoto and Y Imai, Macromolecules, **22(11)**, 4143, 1989.

119 I Yilgor, AK Sha'aban, WP Steckle jr, D Tygai, GL Wilkes and JE McGrath, Polymer, **25**, 1800, 1984.

120 D Tygai, I Yilgor, JE McGrath and GL Wilkes, Polymer, **25**, 1807, 1984.

121 CA Arnold, JD Summers, YP Chen, RH Bott, D Chen and JE McGrath, Polymer, **30**, 986, 1989.

122 DC Allport and WH Janes, "Block Copolymers", Applied Science, 1973.

123 RJH Voorhoeve, "Organohalosilanes - Precursors to Silicones", Elsevier, 1967.

124 V Percec, PL Rinaldi and BC Auman, Polym. Bull., **10**, 215, 1983.

125 V Percec, PL Rinaldi and BC Auman, Polym. Bull., **10**, 391, 1983.

126 V Percec and BC Auman, Makromol. Chem., **185**, 617, 1984.

127 V Percec and BC Auman, Makromol. Chem., **185**, 1867, 1984.

128 V Percec and BC Auman, Makromol. Chem., **185**, 2319, 1984.

129 V Percec and BC Auman in "Reactive Oligomers", Eds FW Harris and HJ Spinelli, ACS Symp. Ser. 282, ACS, 1985.

130 J Wu, BC Auman, HA Schneider, H Cantow and V Percec, Mackromol. Chem. Rapid Comm., **7(5)**, 303, 1986.

131 BC Auman and V Percec, Polym. Prepr., **27(1)**, 320, 1986.

132 BC Auman, V Percec, HA Schneider, W Jishan and H Cantow, Polymer, **28**, 119, 1987.

133 BC Auman, V Percec, HA Schneider and H Cantow, Polymer, **28**, 1407, 1987.

134 Y Nagase, A Naruse and K Matsui, Polymer, **30**, 1931, 1989.

135 JL Speir, R Zimmerman and J Webster, J. Am. Chem. Soc., **78**, 2278, 1956.

136 JL Speir, JA Webster and GH Barne, J. Am. Chem. Soc., **79**, 974, 1957.

137 EP Plueddemann and G Fanger, J. Am. Chem. Soc., **81**, 2632, 1959.

138 CS Cundy, BM Kingston and MF Lappert, Adv. Orgmet. Chem., **11**, 253, 1973.

139 GW Gray, D Lacey, G Nester and MS White, Macromol. Chem. Rapid Comm., **7**, 71, 1986.

140 B Marciniec in "Organosilicon and Bio-organosilicon Chemistry", Ed H Sakurai, J Wiley, 1985.

141 P Chaumont, G Beinert, J Herz and P Rempp, Eur. Polym. J., **15**, 459, 1979.

142 P Chaumont, G Beinert, J Herz and P Rempp, Polymer, **22**, 663, 1981.

143 BA Ashby, J. Chem. and Eng. Data., **18**, 238, 1973.

144 EM Valles and CM Macosko, Macromolecules, **12(3)**, 521, 1979.

145 X He, J Herz and JM Guenet, Macromolecules, **20(8)**, 2003, 1987.

146 H Qiu and Z Du, J. Polym. Sci: Pt A, Polym. Chem., **27**, 2861, 1989.

147 VB Puhknarevich et al, Zh. Obsh. Kim., **43**, 2691, 1973.

148 J Lipowitz and SA Bowman, J. Org. Chem., **38(1)**, 162, 1973.

149 CW Macosko and GS Benjamin, P. and A. Chem., **53**, 1505, 1981.

150 CW Macosko and JC Saam, Polym. Prepr., **26(2)**, 48, 1985.

151 WA Gustavson, PS Epstein and MD Curtis, J. Orgmet. Chem., **238**, 87, 1982.

152 CG Pitt and KR Skellern, J. Orgmet. Chem., **7**, 525, 1967.

153 G Torres, PJ Madec and E Marechal, Makromol. Chem: Macro. Chem. Phys., **190(1)**, 203, 1989.

154 Y Kuwae and N Kushibiki, J. Polym. Sci: Pt A, Polym. Chem., **27**, 3969, 1989.

155 IS Alchrem, NM Chistovalova and ME Vol'pin, Russ. Chem. Rev., **52**, 542, 1983.

156 PJ Madec and E Marechal, J. Appl. Polym. Sci: Polym. Chem. Edn., **16**, 3165, 1978.

157 D Gagnebien, PJ Madec and E Marechal, Eur. Polym. J., **21(3)**, 289, 1985.

158 I Skeist, "Epoxy Resins", Reinhold Books, 1968.

159 WG Potter, "Epoxide Resins", Iliffe Books, 1970.

160 CA May and Y Tanaka, "Epoxy Resins", Marcel Dekker Inc., 1973.

161 L Schecter and J Wynstra, Ind. and Eng. Chem., **48(1)**, 86, 1956.

162 D Gagnebien, PJ Madec and E Marechal, Eur. Polym. J., **21(3)**, 273, 1985.

163 D Gagnebien, PJ Madec and E Marechal, Eur. Polym. J., 21(3), 301, 1985.

164 K Gebreyes and HL Frisch, J. Polym. Sci: Pt A, Polym. Chem., 26, 3391, 1988.

165 XW He, JM Widaier, JE Herz and GC Meyer, Polymer, 30, 364, 1989.

166 PM Sormani, RJ Minton and JE McGrath in "Ring Opening Polymerisation", Ed JE McGrath, ACS Symp. Ser. 286, ACS, 1985.

167 PM Sormani, RJ Minton, I Yilgor, PJA Brandt, J Riffle, C Tran and JE McGrath, Polym. Prepr., 25(1), 227, 1984.

168 PM Sormani and JE McGrath, Polym, Prepr., 26(1), 258, 1985.

169 JS Riffle, I Yilgor, C Tran, GL Wilkes, JE McGrath and AK Banthia in "Epoxy Resin Chemistry", Vol 2, ACS Symp. Sers. 221, ACS, 1983.

170 I Yilgor and JE McGrath, Polym. Prepr., 26(1), 57, 1985.

171 CA Veith and RE Cohen, J. Polym. Sci: Pt A, Polym. Chem., 27, 1241, 1989.

172 I Yiligor, JS Riffle and JE McGrath in "Reactive Oligomers", Eds FW Harris and HJ Spinelli, ACS Symp. Ser. 282, ACS, 1985.

173 JB Carmichael and J Heffel, J. Phys. Chem., 69(7), 2218, 1965.

174 JA Semlyen in "Advances in Polymer Science", Vol 21, Springer-Verlag, 1976.

175 JV Crivello, DA Conlon and JL Lee, J. Polym. Sci: Pt A, Polym. Chem., 24, 1197, 1986.

176 I Novak and M Gregor, Proc. Int. Clay. Conf., Tokyo, 851, 1969.

177 DA Morgan, DB Shaw, MJ Sidebottom et al, J. Am. Oil. Chem. Soc., 62(2), 292, 1985.

178 "Acid Treatment of English Montmorillite", MH Yates, Laporte Earths plc.

179 JE McGrath, JS Riffle, AK Banthia et al in "Initiation of Polymerisation", Ed JE McGrath, ACS Symp. Ser. 212, ACS, 1983.

180 H Jacobson and WH Stockmayer, J. Phys. Chem., **18**, 1600, 1950.

181 JB Carmichael, J. Macromol. Chem., **1(2)**, 207, 1966.

182 CL Lee, CL Frye and OK Johannson, Polym. Prepr., **10**, 1361, 1969.

183 JC Saam, DJ Gordon and S Lindsey, Macromolecules, **3(1)**, 1, 1970.

184 EE Bostick in "Block Copolymers", Ed W Aggarwal, Plenum, 1970.

185 CL Frye, RM Salinger, FWG Fearon et al, J. Org. Chem., 35, 1308, 1970.

186 WA Fessler and PC Juliano, Polym. Prepr., **12(2)**, 150, 1971.

187 JC Saam, AH Ward and FWG Fearon, Polym. Prepr., **13**, 524, 1972.

188 HJ Holle and BR Lehnen, Eur. Polym. J., **11**, 663, 1975.

189 Y Kawakami, Y Miki, T Tsuda et al, Polym. J., **14(11)**, 913, 1982.

190 GC Cameron and MS Chisholm, Polymer, **26**, 437, 1985.

191 Y Kawakami and Y Yamashita in "Ring Opening Polymerisation", Ed JE McGrath, ACS Symp. Ser. 286, ACS, 1985.

192 S Boileau in "Ring Opening Polymerisation", Ed JE McGrath, ACS Symp. Ser. 286, ACS, 1985.

193 JE McGrath in "Ring Opening Polymerisation", Ed JE McGrath, ACS Symp. Ser. 286, ACS, 1985.

194 T Suzuki, Polymer, **30**, 333, 1989.

195 JR Leebrick and HE Ramsden, J. Org. Chem., **23**, 935, 1958.

196 AE Sinear, J Wirth and RG Neville, J. Org. Chem., **60**, 807, 1960.

197 MEA Cudby, RG Feasby, BE Jennings, MEB Jones and JB Rose, Polymer, **6**, 589, 1965.

198 MEB Jones, GB Patent No. 1,016,245 (1965).

199 JB Rose, Chimia, **28(9)**, 561, 1974.

200 TE Attwood, DA Barr, T King, AB Newton and JB Rose, Polymer, **18**, 359, 1977.

201 B Spence, ICI plc, Private Communication.

202 AB Newton and JB Rose, Polymer, **13**, 465, 1972.

203 JB Rose, Polymer, 15, 456, 1974.

204 R Cooper, ICI plc, Private Communication.

205 J Brandup and GM Immergut, "Polymer Handbook", Vol 4, Wiley, 1975.

206 BT Swinyard and JA Barrie, Brit. Polym. J., **20**, 317, 1988.

207 H Qiu and Z Du, J. Polym. Sci: Pt A, Polym. Chem., **27**, 2849, 1989.

208 PJ Madec and E Marechal, J. Polym. Sci. Polym. Chem. Edn., **16**, 3157, 1978.

209 SJ Clarson, K Dodgson and JA Semlyen, Polymer, **26**, 930, 1985.

210 SW Shalaby and HE Bair in "Thermal Characterisation of Polymeric Materials", Ed EA Turi, Academic Press, 1981.

211 JE McGrath, DW Dwight, JS Riffle et al, Polym. Prepr., **20(2)**, 528, 1979.

212 DW Dwight, JE McGrath, AR Beck and JS Riffle, Polym. Prepr., **20(1)**, 702, 1979.

213 GC Corfield, GW Wheatley and DG Parker, J. Polym. Sci: Pt A, Polym. Chem., **28**, 2821, 1990.

214 JE McGrath, TC Ward, E Sachori and AJ Wnuk, Polym. Eng. and Sci., **17(18)**, 647, 1977.

215 AA Collyer, DW Clegg, M Morris, DG Parker, GW Wheatley and GC Corfield, J. Polym. Sci., **29(2)**, 193, 1991.

216 J Chrusciel and Z Lasocki, Pol. J. Chem., **52**, 121, 1988.

217 L Lestel, H Cheradame and S Boileau, Polymer, **31**, 1154, 1990.

218 HA Nguyen and E Marechal, JMS - Rev. Macromol. Chem. Phys., **C28(2)**, 187, 1988.

219 RS Davidson, AM Patel, A Safdar and D Thornwaite, Tet. Letts., **24(52)**, 5907, 1983.

220 RF Abdulla, Aldrichimia Acta, **21(2)**, 31, 1988.

221 Y Nagase, A Naruse and K Matsui, Polymer, **30**, 1931, 1989.

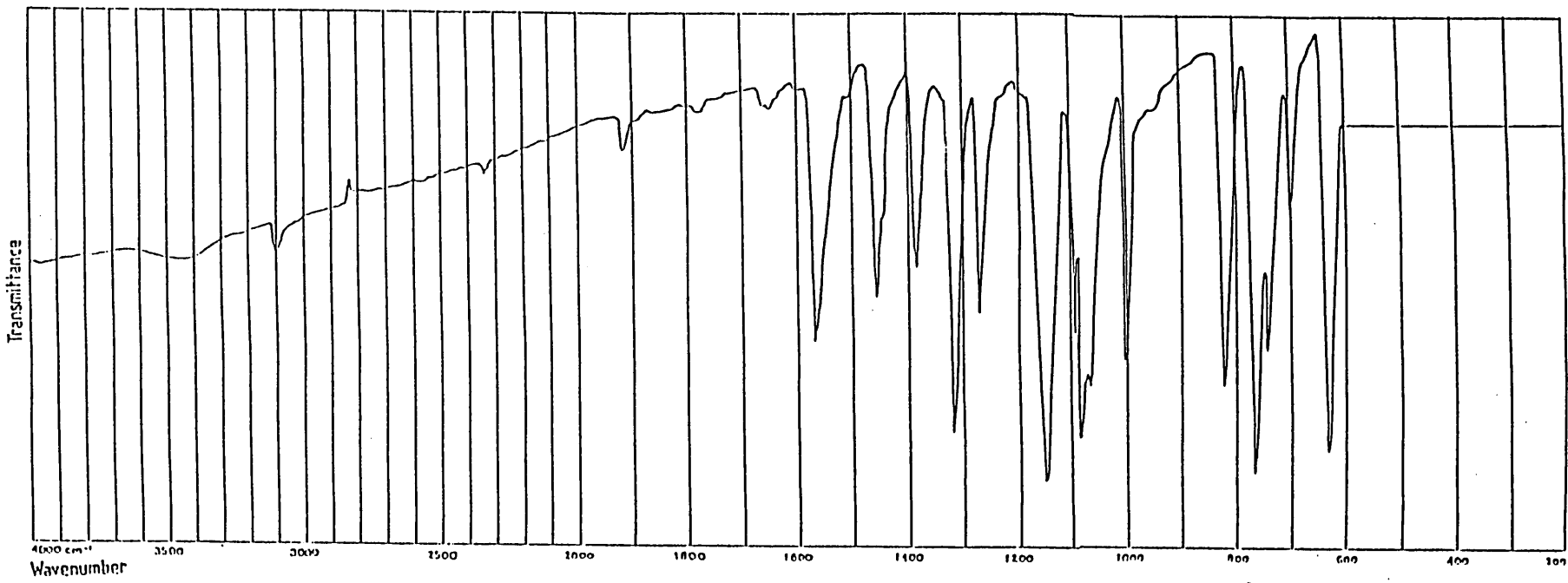

Figure 1: Infra-red spectrum of the Grignard reaction product between trimethylchlorosilane and DCDPS.

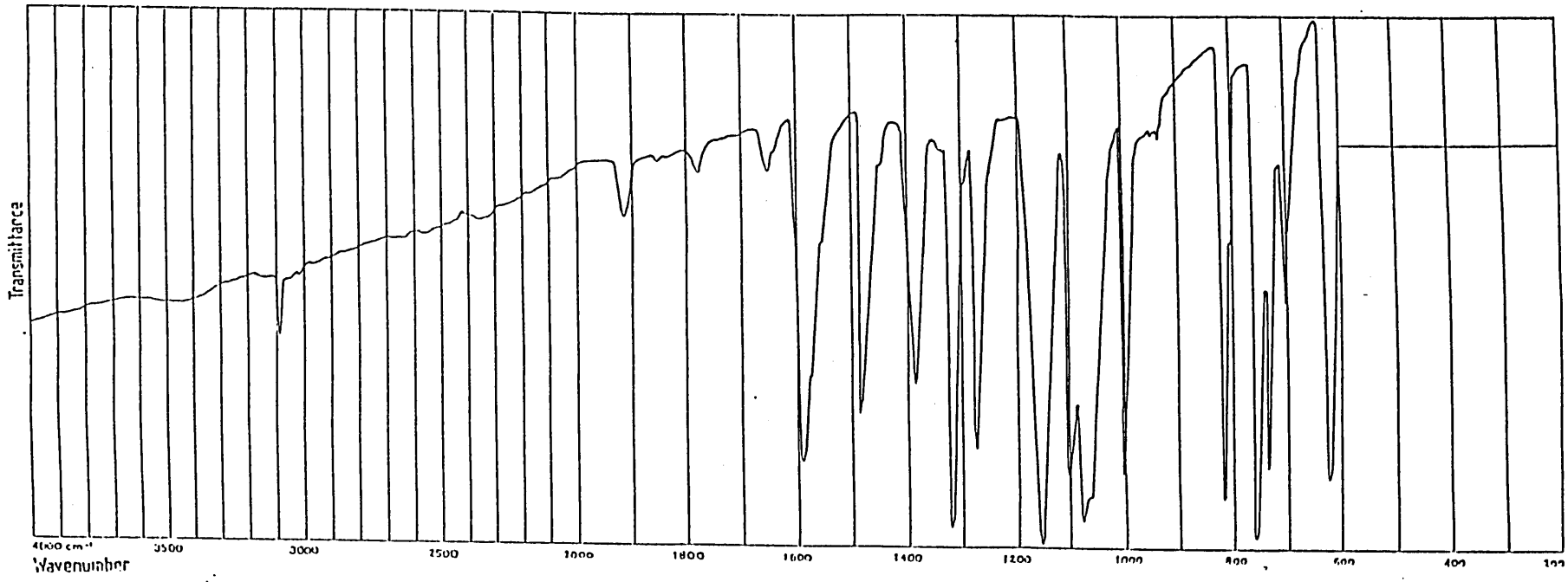

Figure 2: Infra-red spectrum of dichlorodiphenylsulphone (DCDPS).

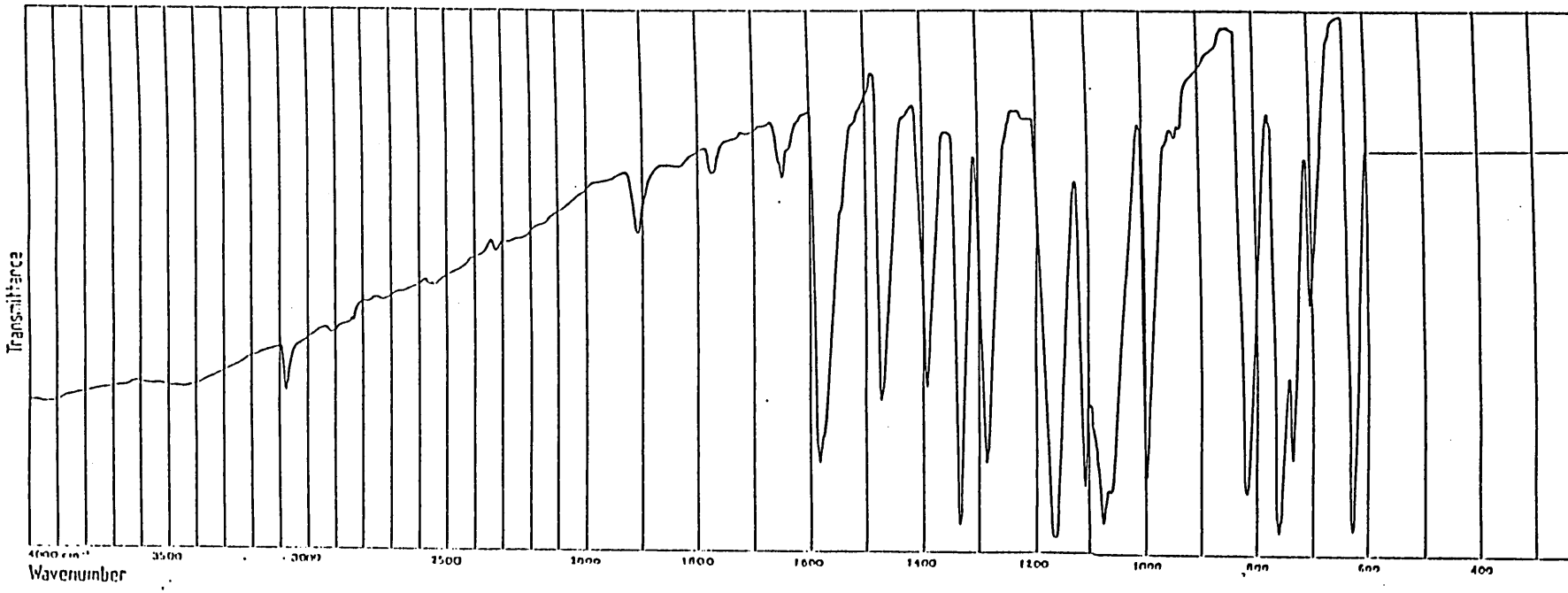

Figure 3: Infra-red spectrum of the Grignard reaction product between allyl bromide and DCDP

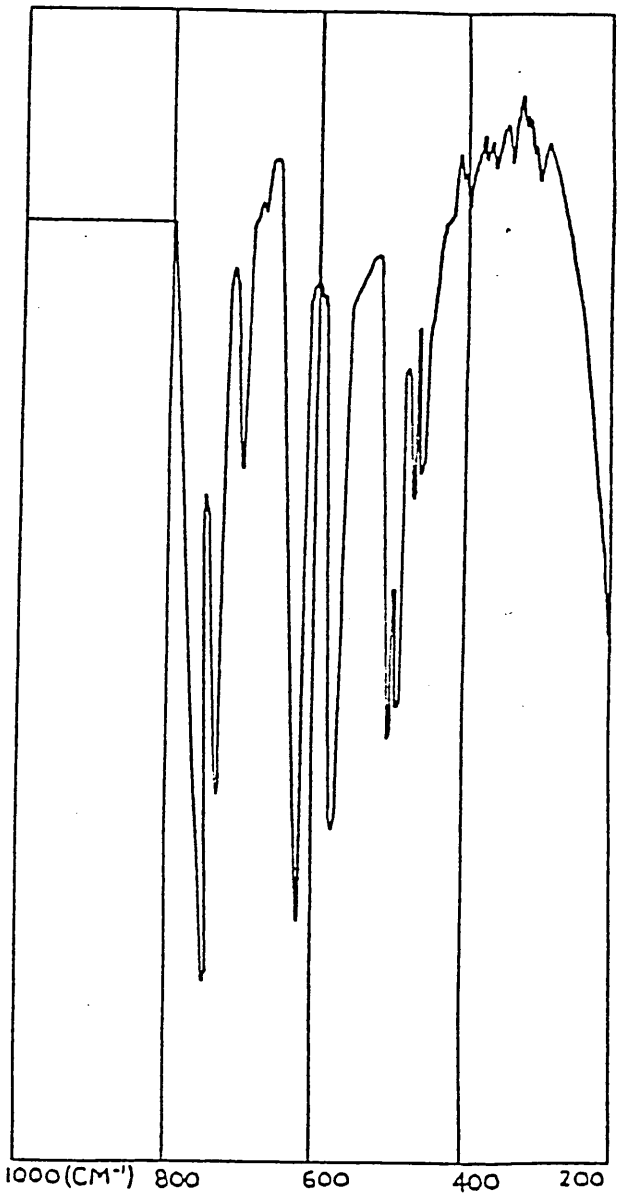

Figure 4: Infa-red spectrum of dichlorodiphenylsulphone (DCDPS) 200-600cm^{-1}.

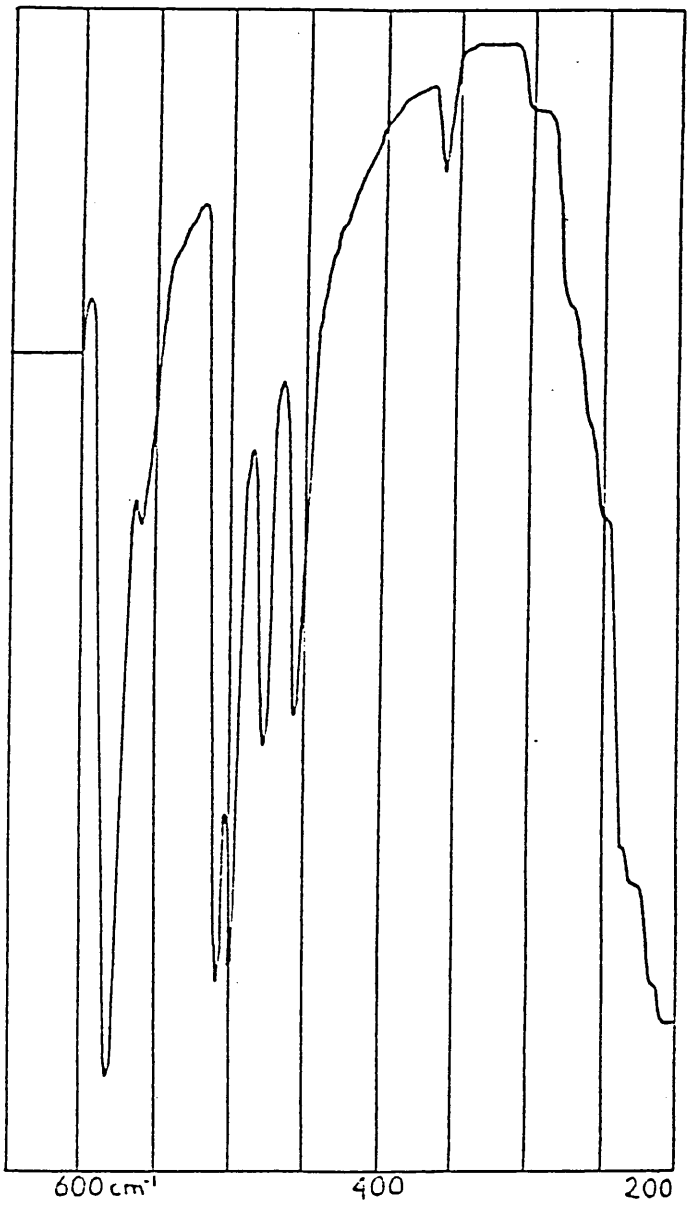

Figure 5: Infra-red spectrum of the Grignard reaction product between allyl bromide and DCDPS (200-600cm^{-1}).

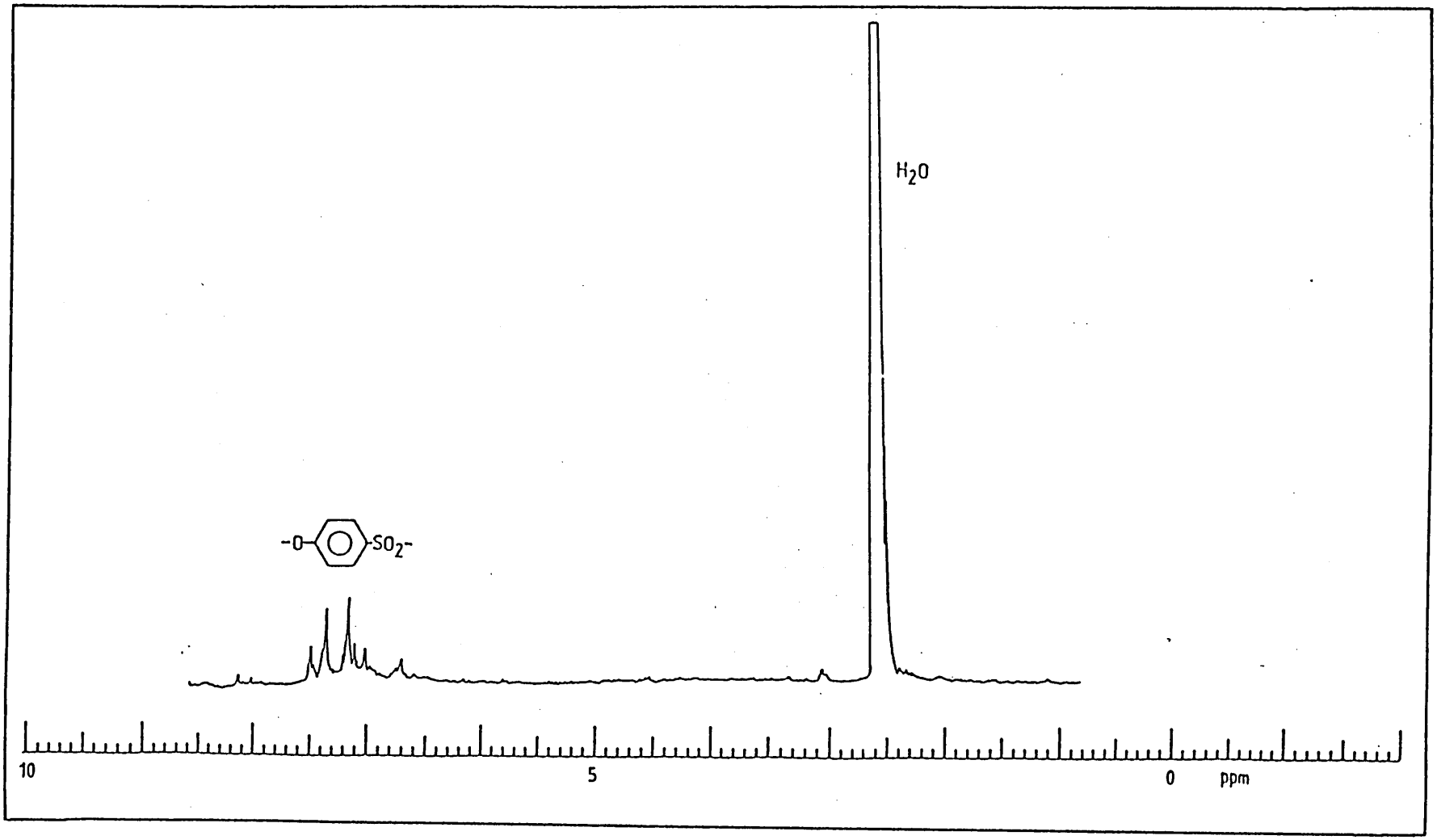

Figure 6: 80MHz ^1H nmr spectrum of the Grignard reaction product between allyl bromide and DCDPS (d-DMSO solvent).

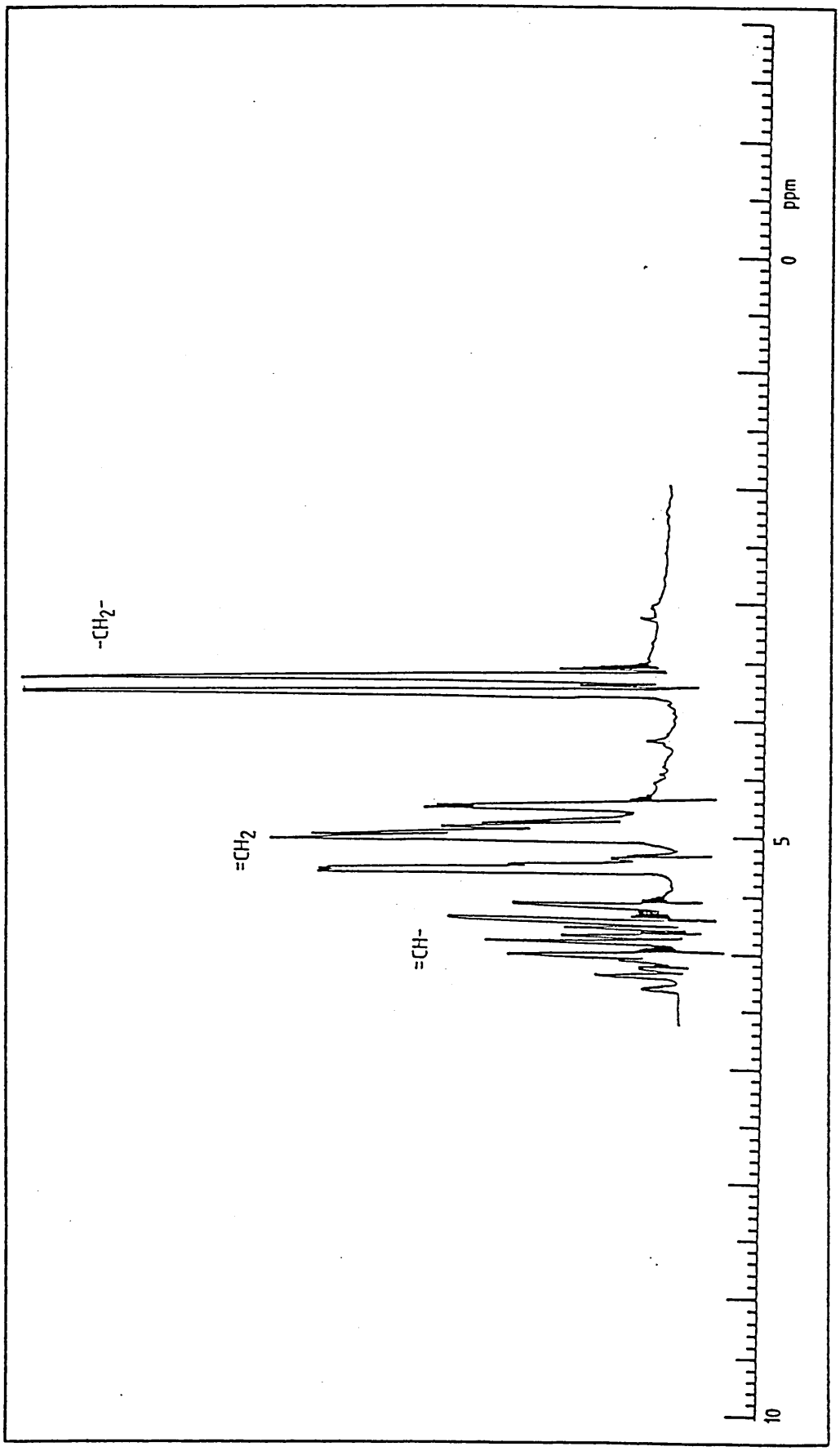

Figure 7: 80MHz ^1H nmr spectrum of allyl bromide ($CDCl_3$ solvent).

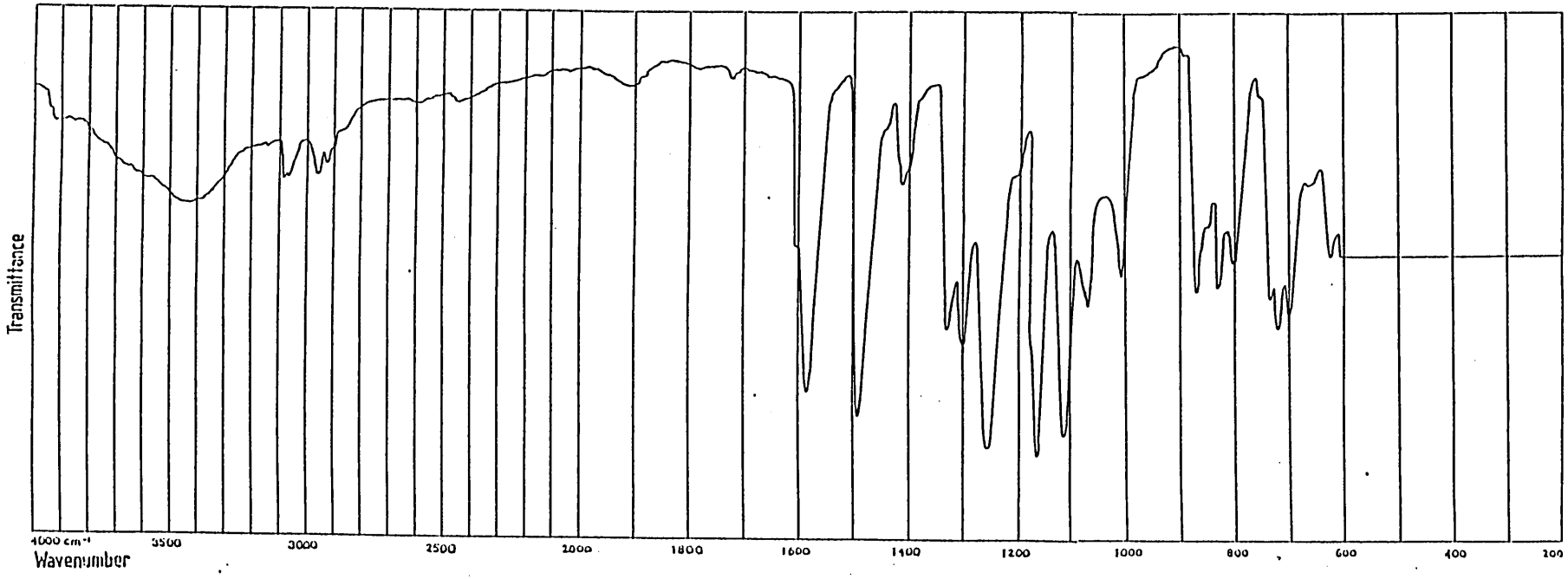

Figure 8: Infra-red spectrum of hydroxyl polyethersulphone (PES) prepared as a KBr disc.

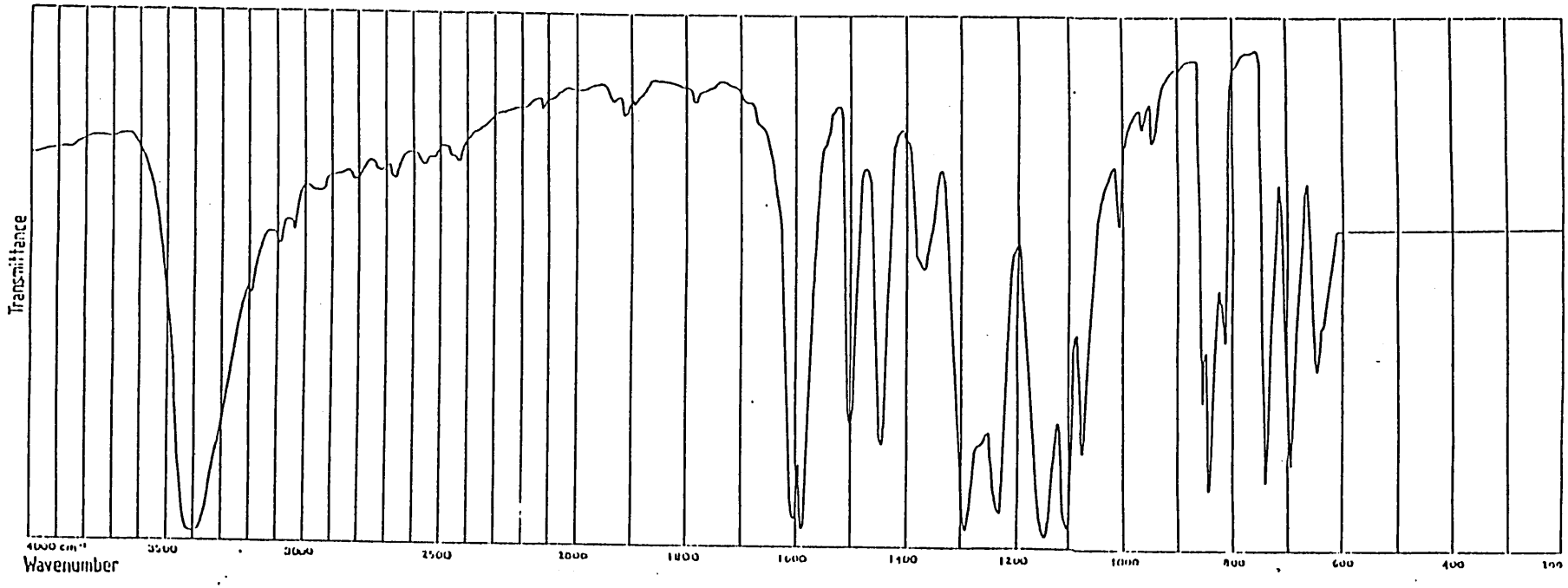

Figure 9: Infra-red spectrum of Bisphenol"S" prepared as a KBr disc.

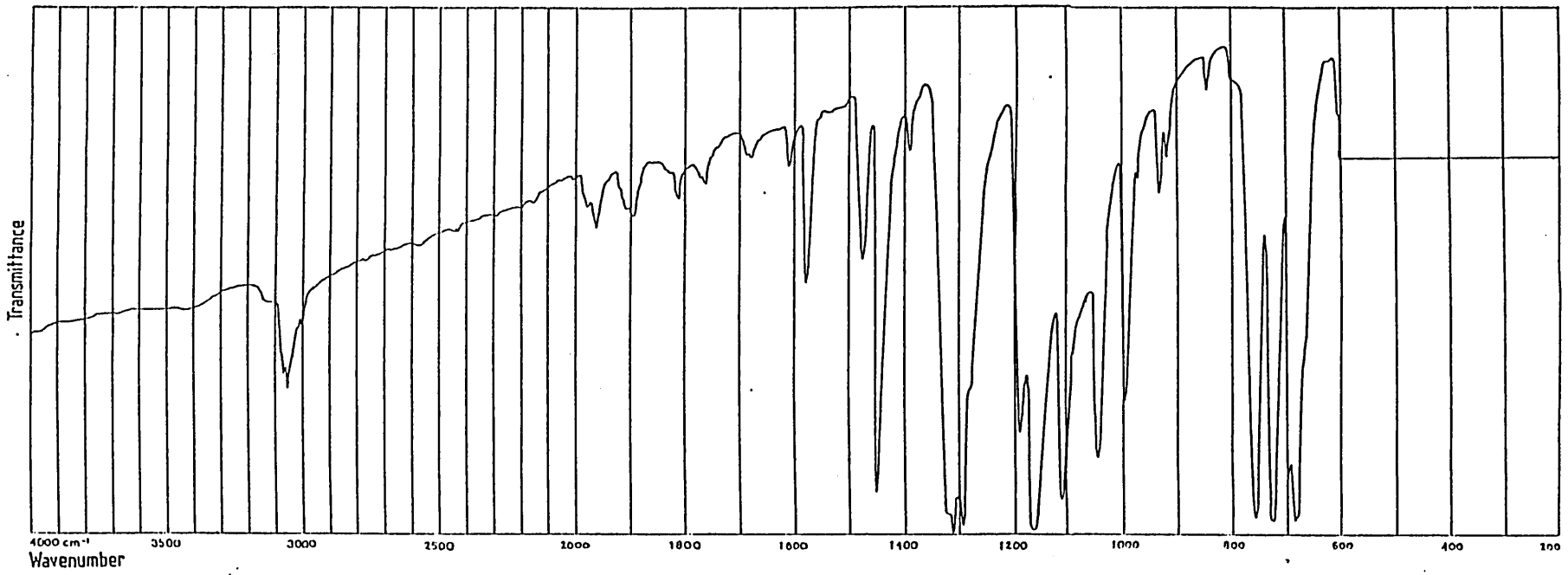

Figure 10: Infra-red spectrum of diphenylsulphone (DPS) prepared as a KBr disc.

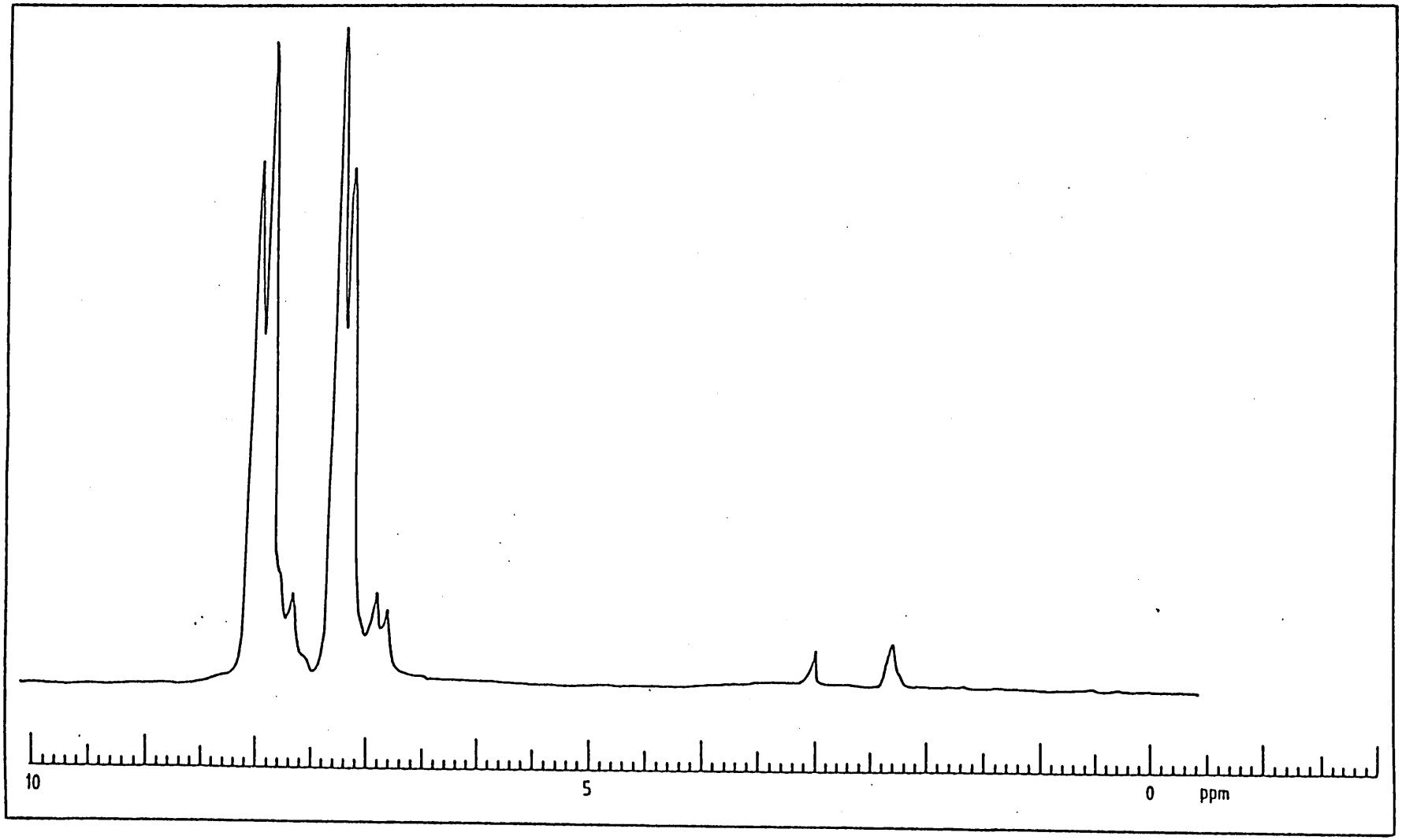

Figure 11: 80MHz ^1H nmr spectrum of hydroxyl PES (d-DMSO solvent).

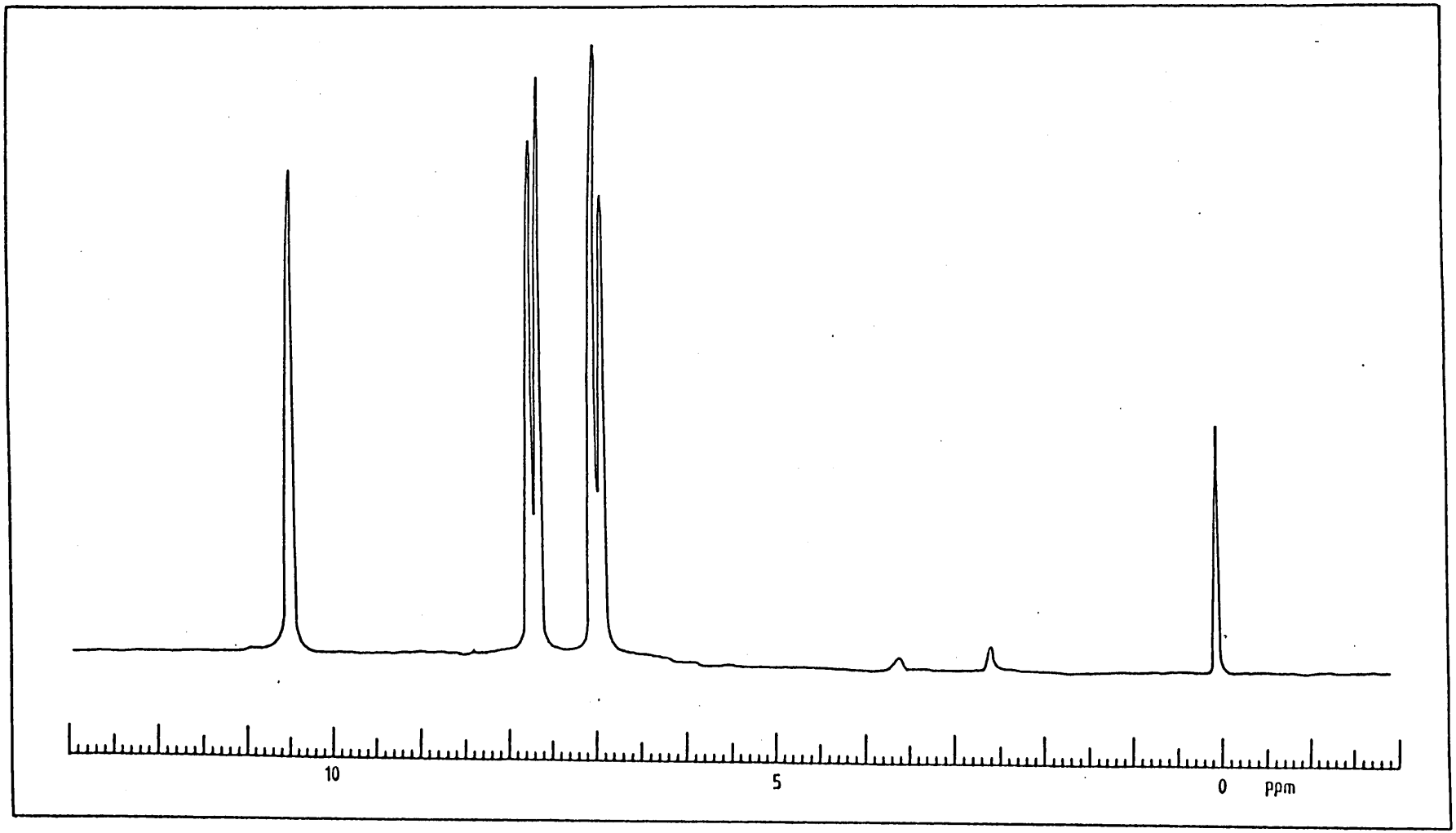

Figure 12: 80MHz ^1H nmr spectrum of Bisphenol"S" (d-DMSO solvent).

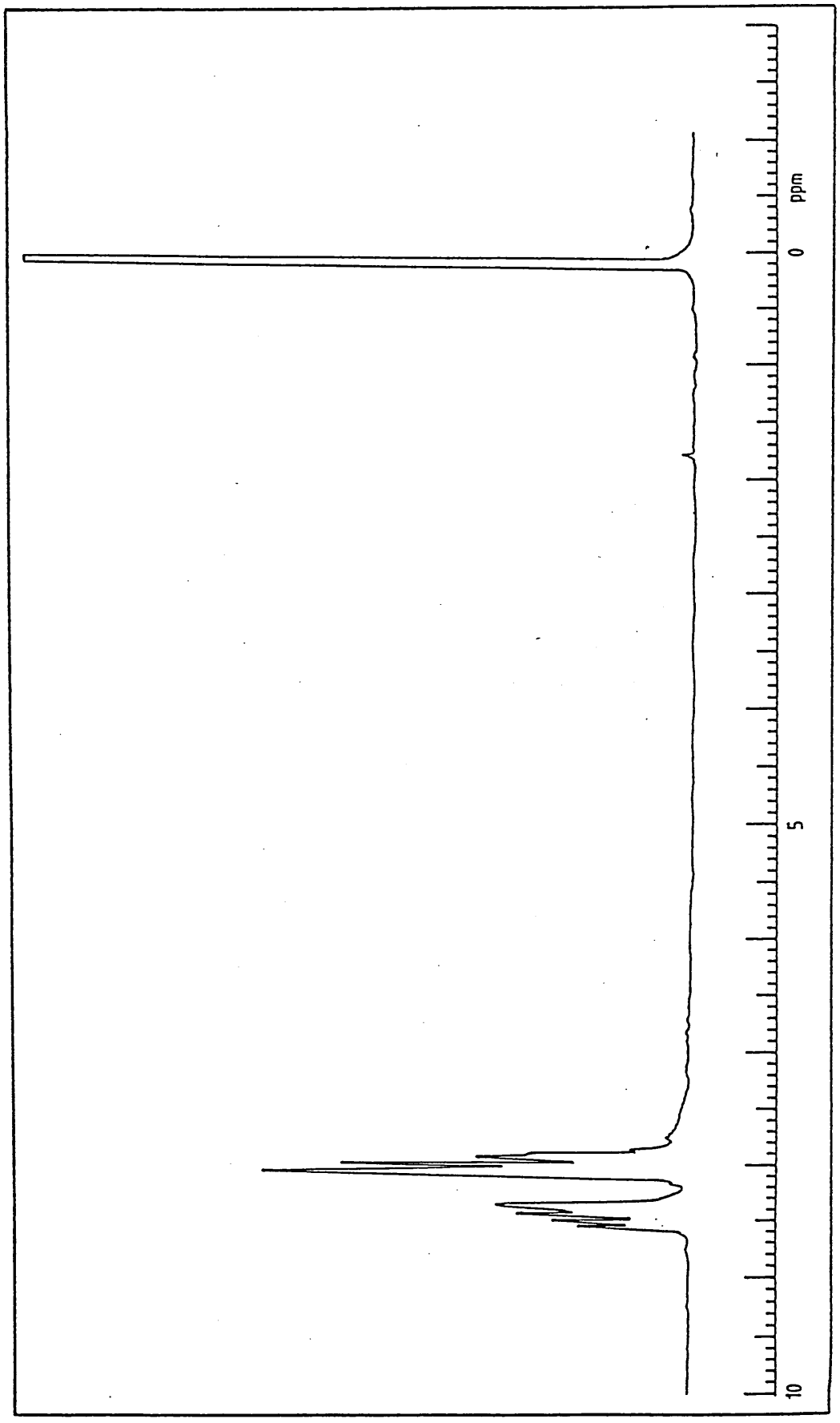

Figure 13: 80MHz ^1H nmr spectrum of diphenylsulphone (DPS) in d-DMSO solvent.

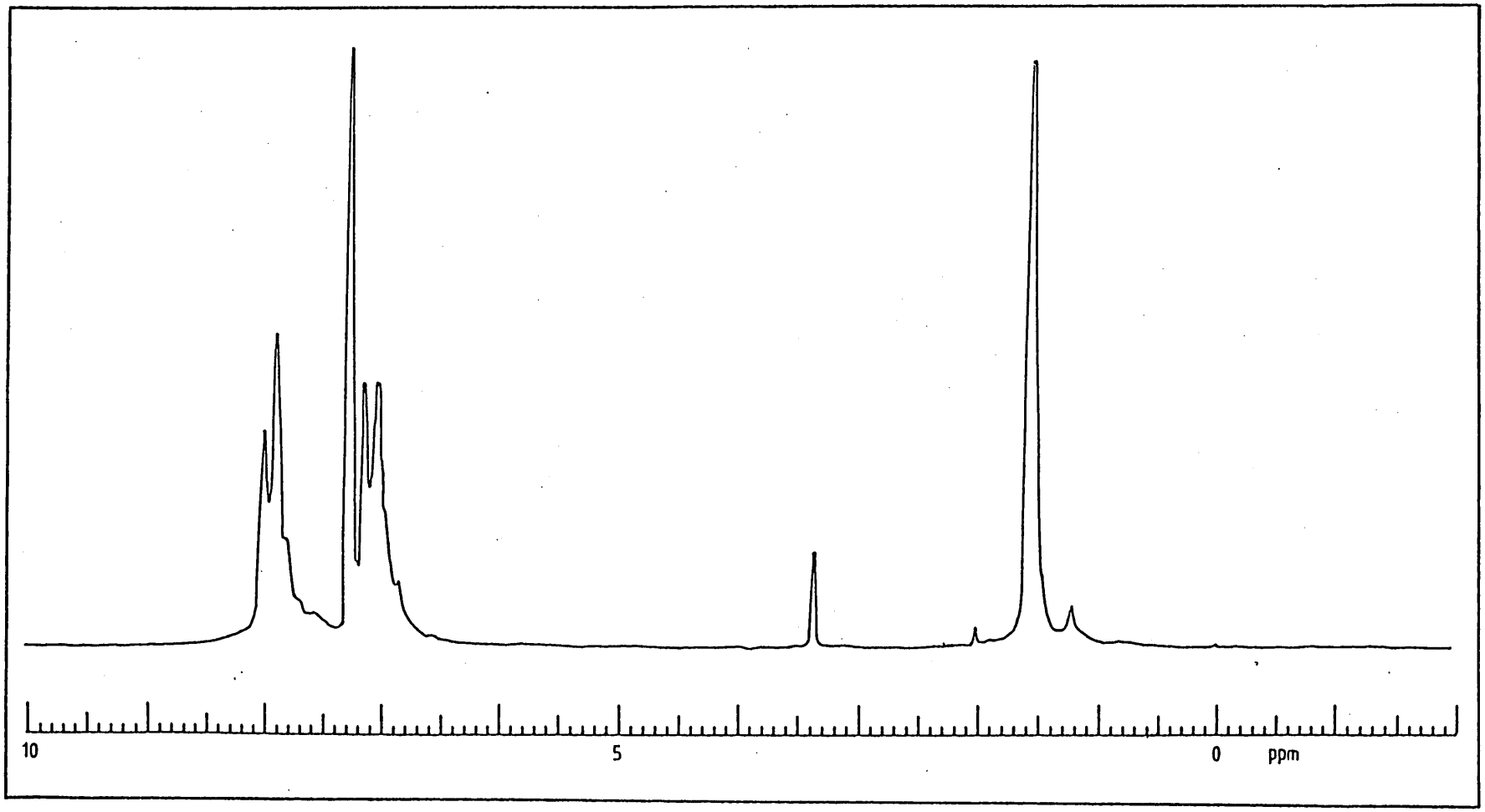

Figure 14: 80MHz ^{1}H nmr spectrum of hydroxyl PES in $CDCl_3$ solvent.

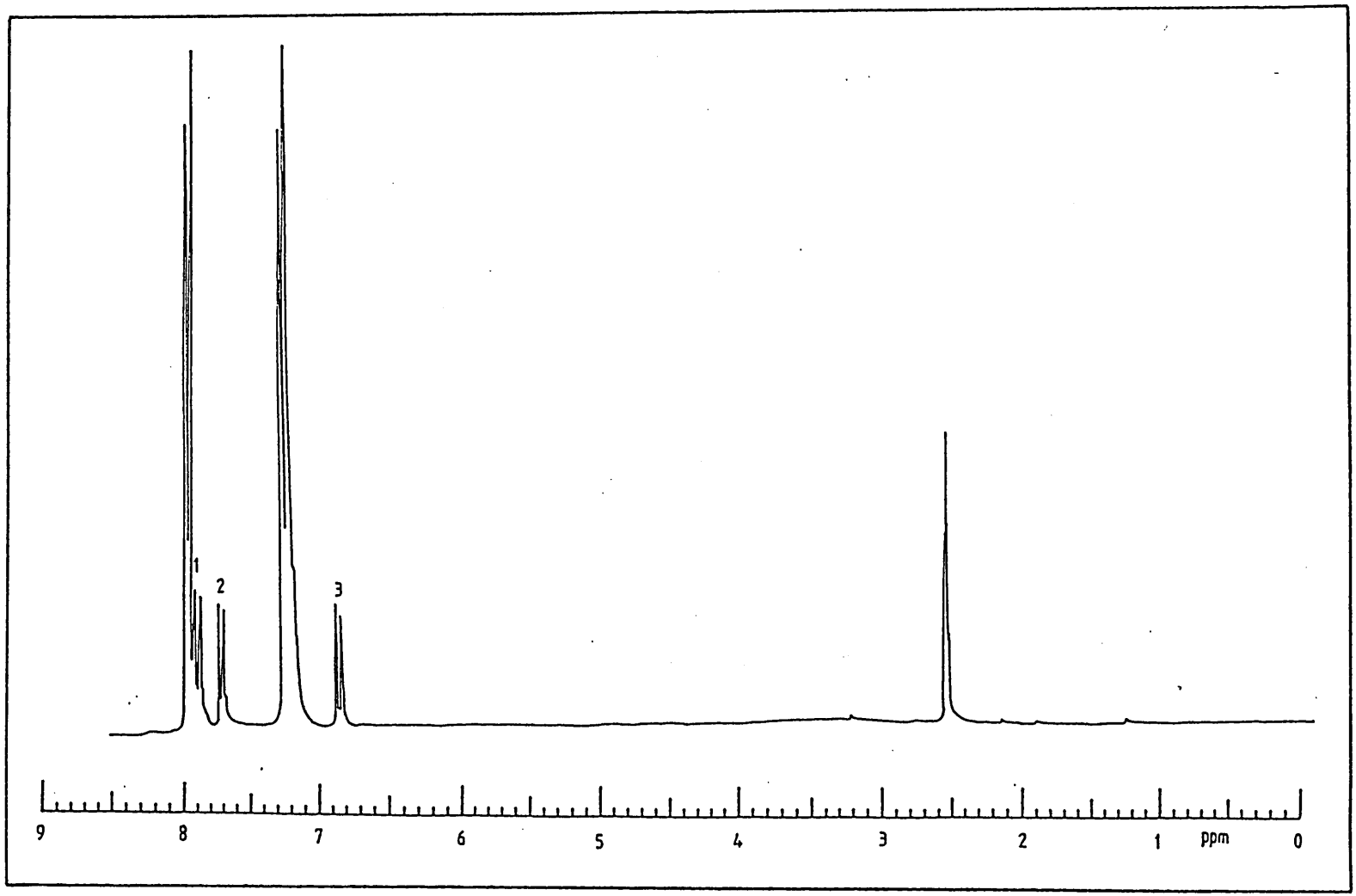

Figure 15: 270MHz ^{1}H nmr spectrum of hydroxyl PES (d-DMSO solvent).

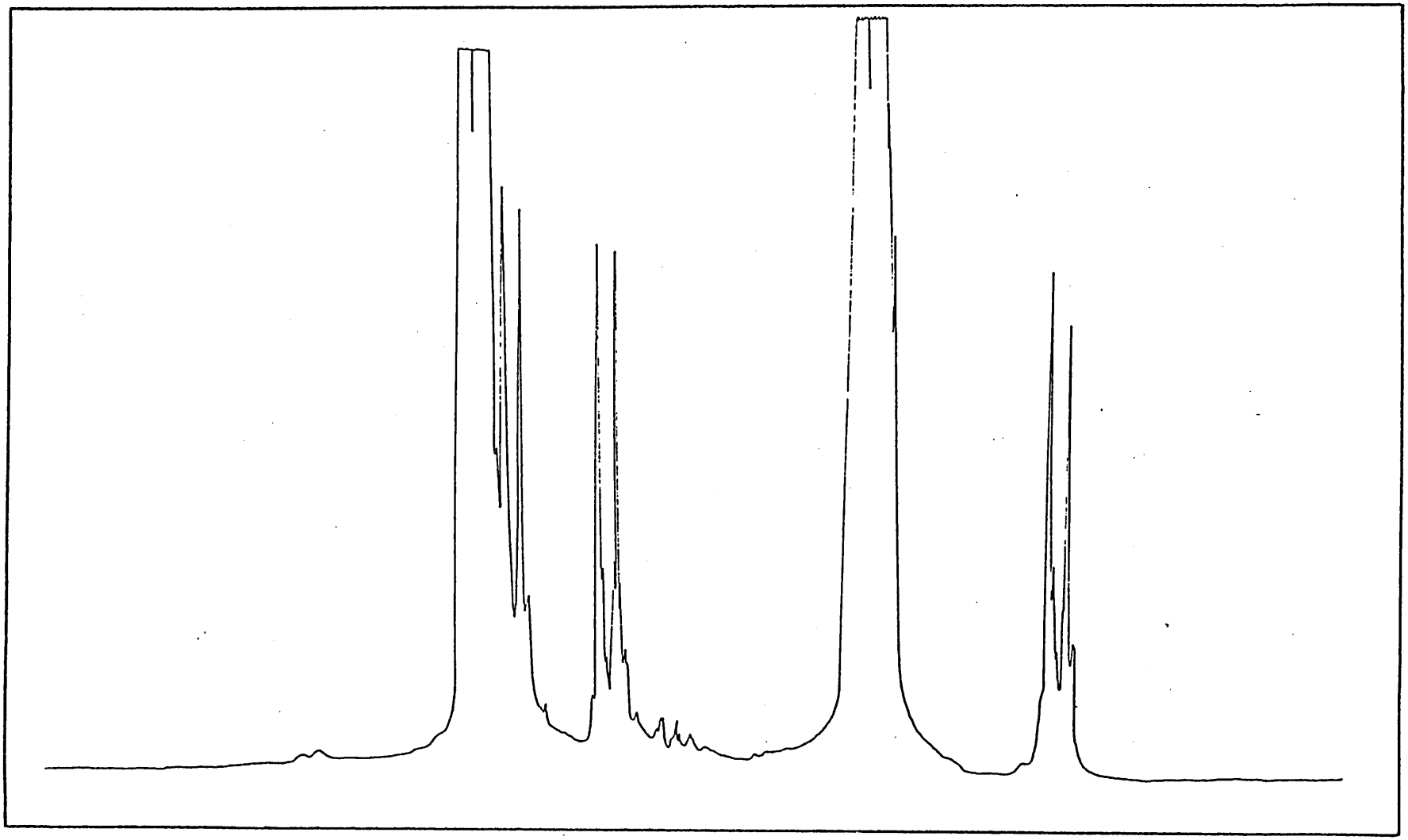

Figure 16: 270MHz ^{1}H nmr spectrum showing the aromatic proton splitting of hydroxyl PES.

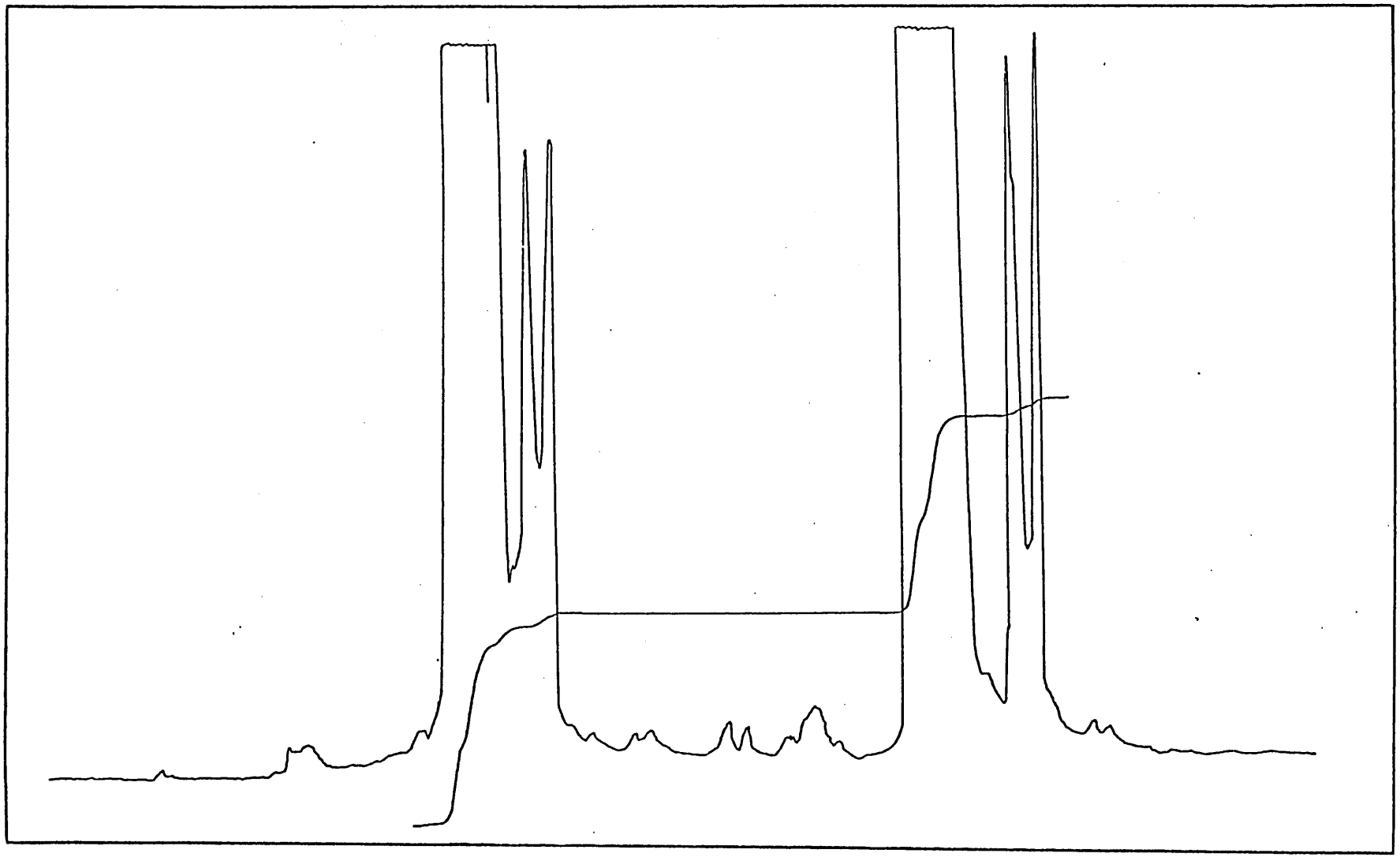

Figure 17: 270MHz ^1H nmr spectrum of hydroxyl PES displaying the integration of the end group and aromatic protons.

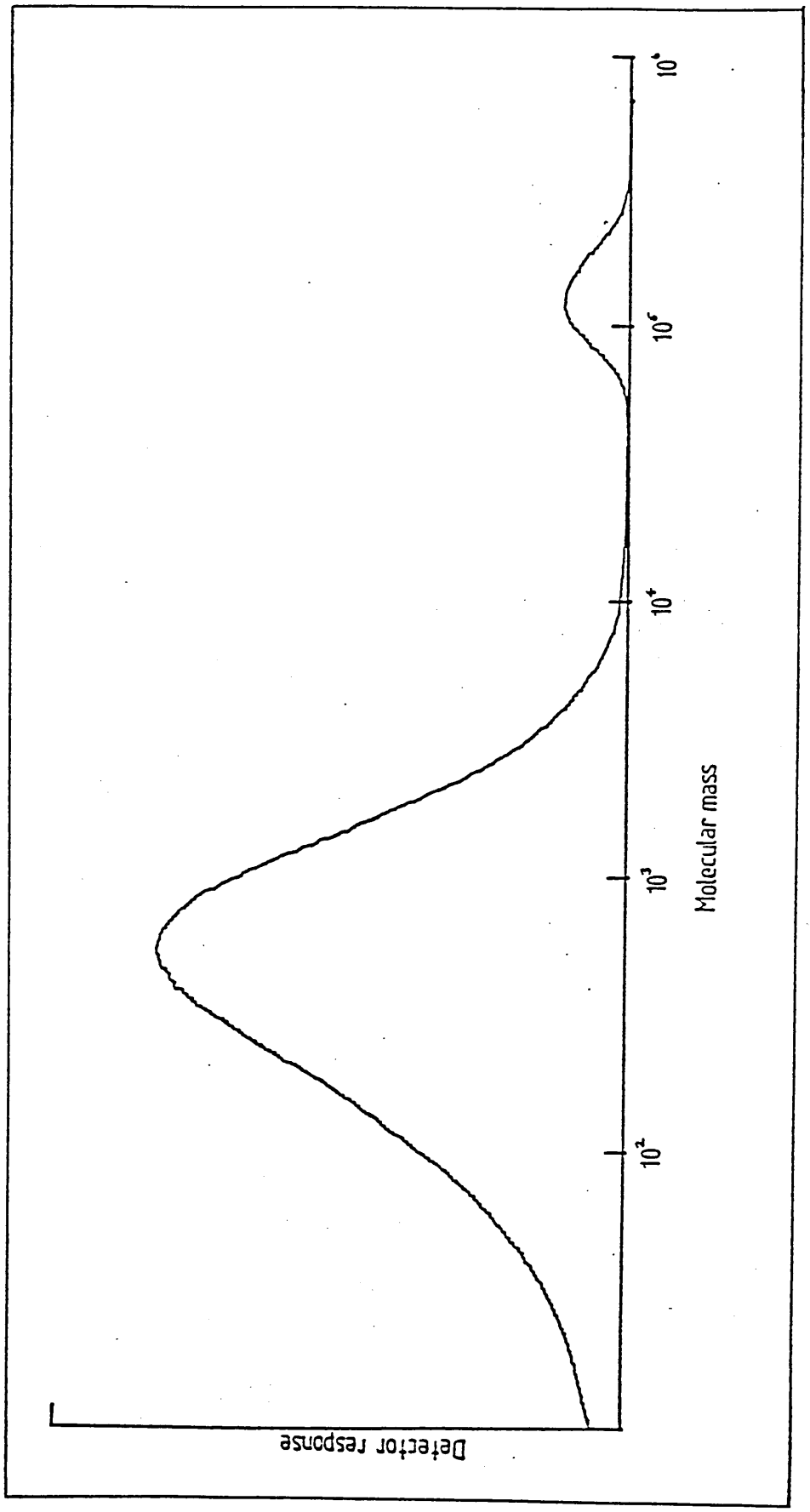

Figure 18: Gpc trace of hydroxy PES prepared in the laboratory.

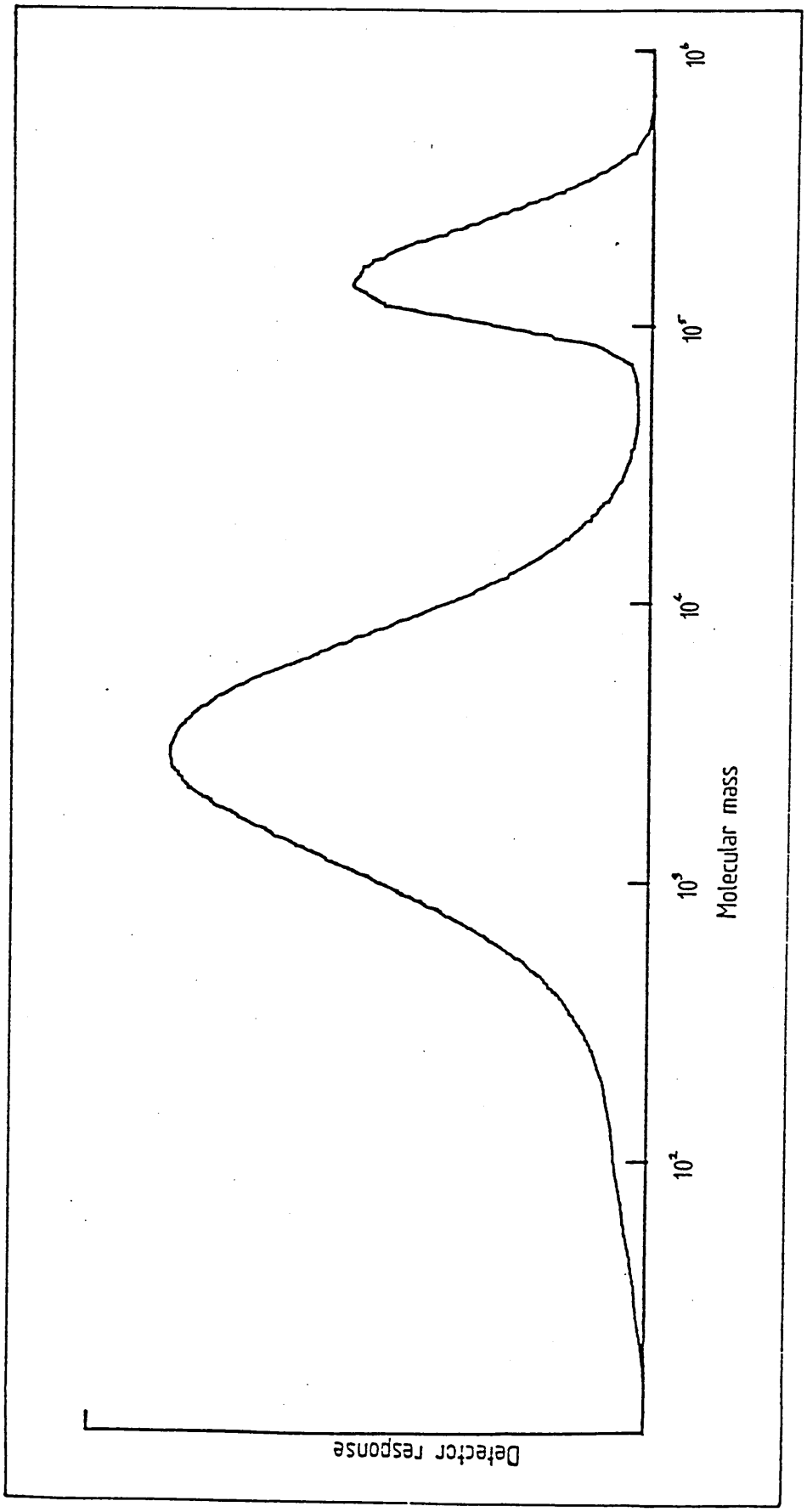

Figure 19: Gpc trace of commercial hydroxyl PES (5003P).

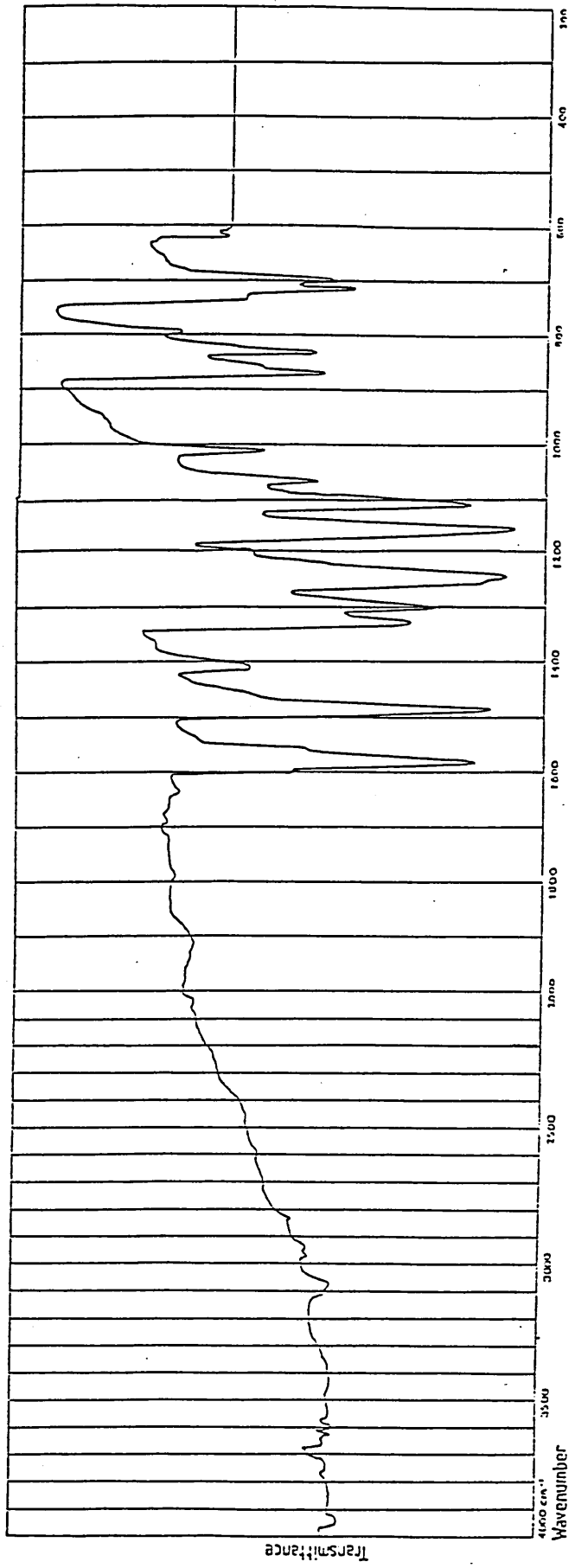

Figure 20: Infra-red spectrum of vinyl PES (v-PES).

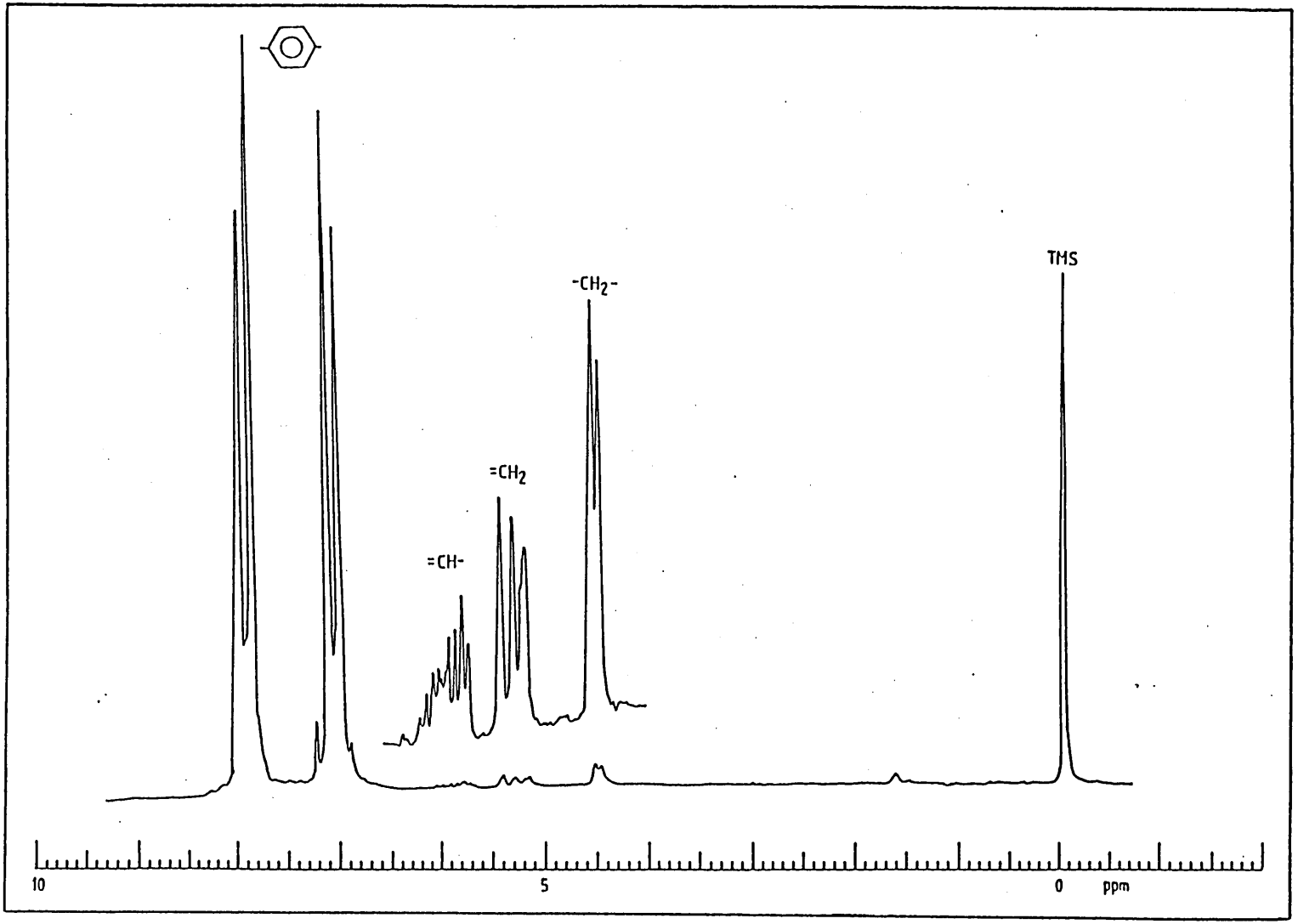

Figure 21: 80MHz ^1H nmr spectrum of v-PES ($CDCl_3$ solvent).

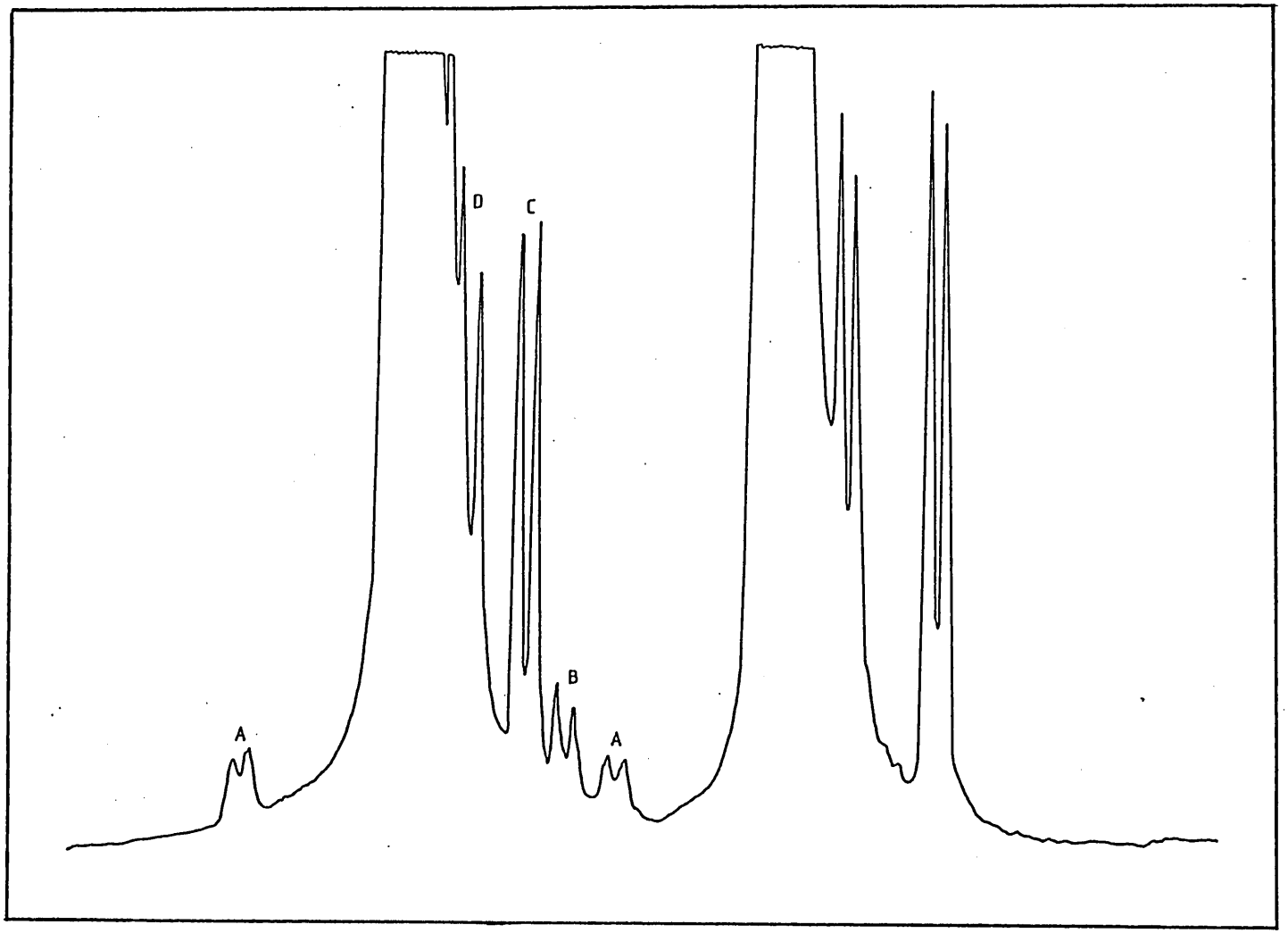

Figure 22: 270MHz ^1H nmr spectrum of v-PES/OH PES (showing the aromatic proton splitting).

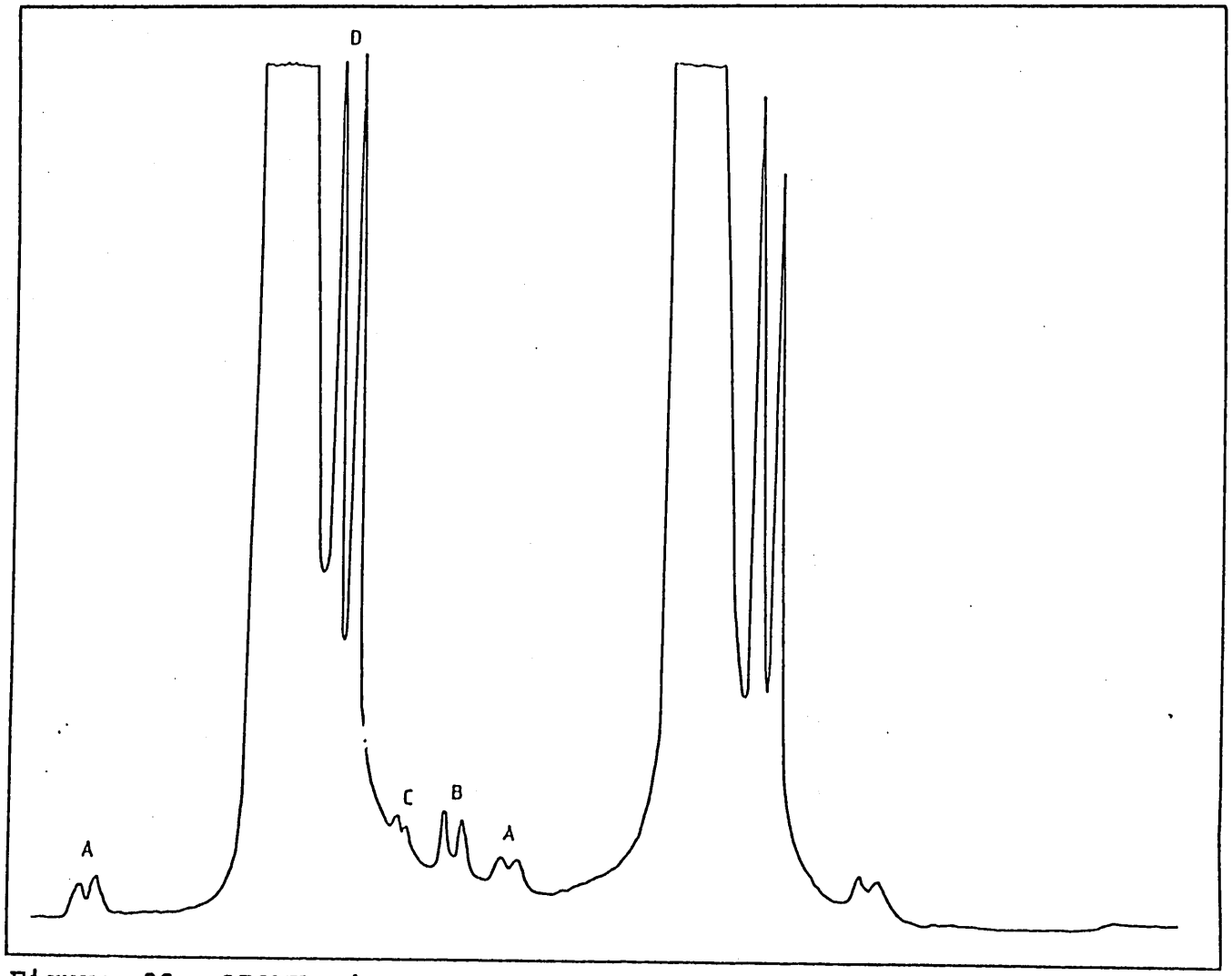

Figure 23: 270MHz ^1H nmr spectrum showing the aromatic proton splitting of v-PES (>95% conversion).

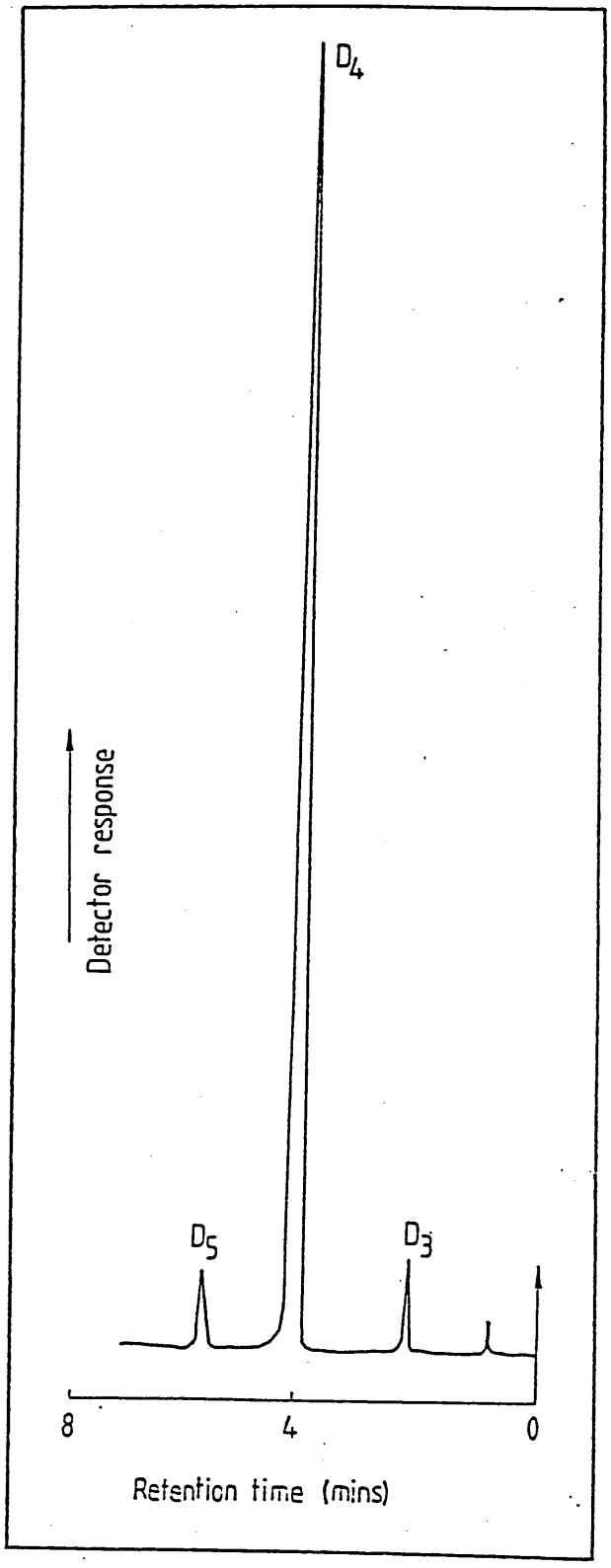

Figure 24: Glc trace of D_4.

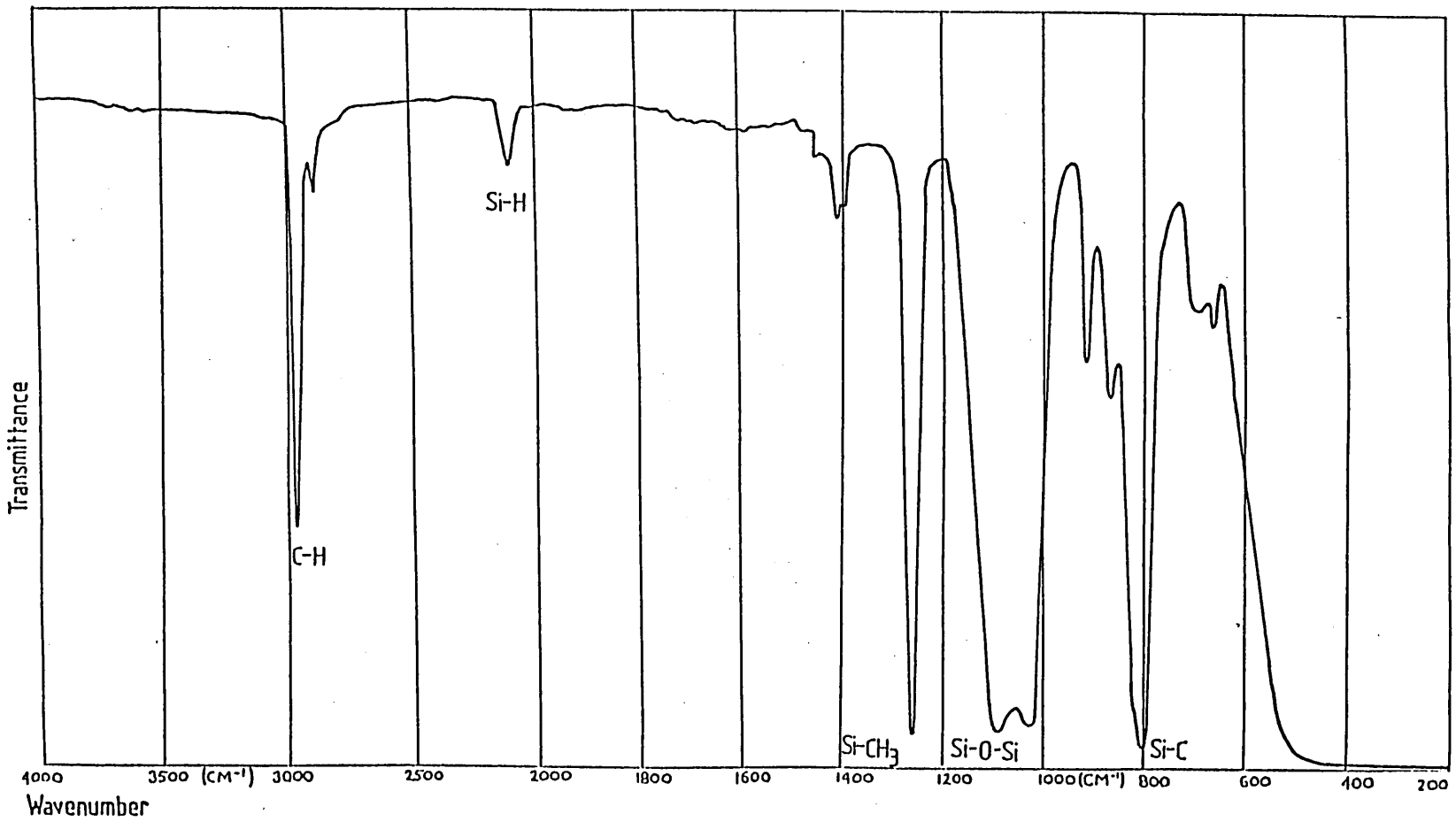

Figure 25: Infra-red spectrum of hydride PDMS (RMM=4,370).

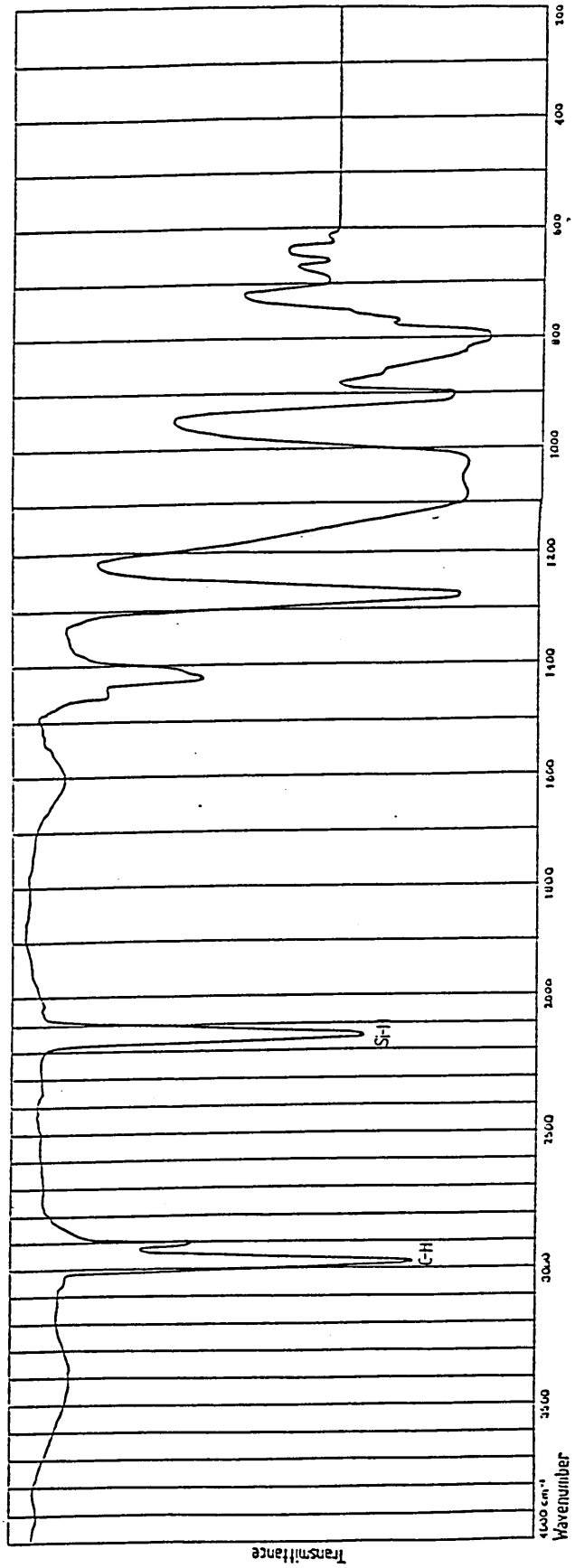

Figure 26: Infra-red spectrum of hydride PDMS (RMM @700).

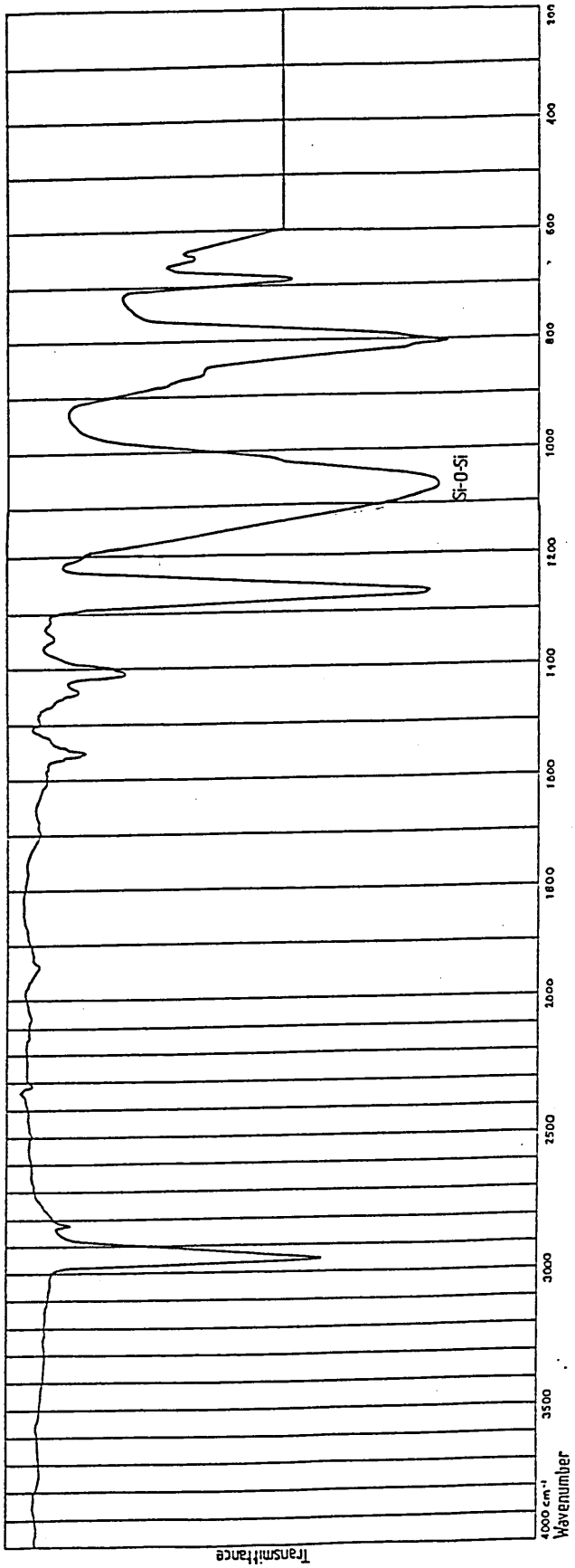

Figure 27: Infra-red spectrum of D_4.

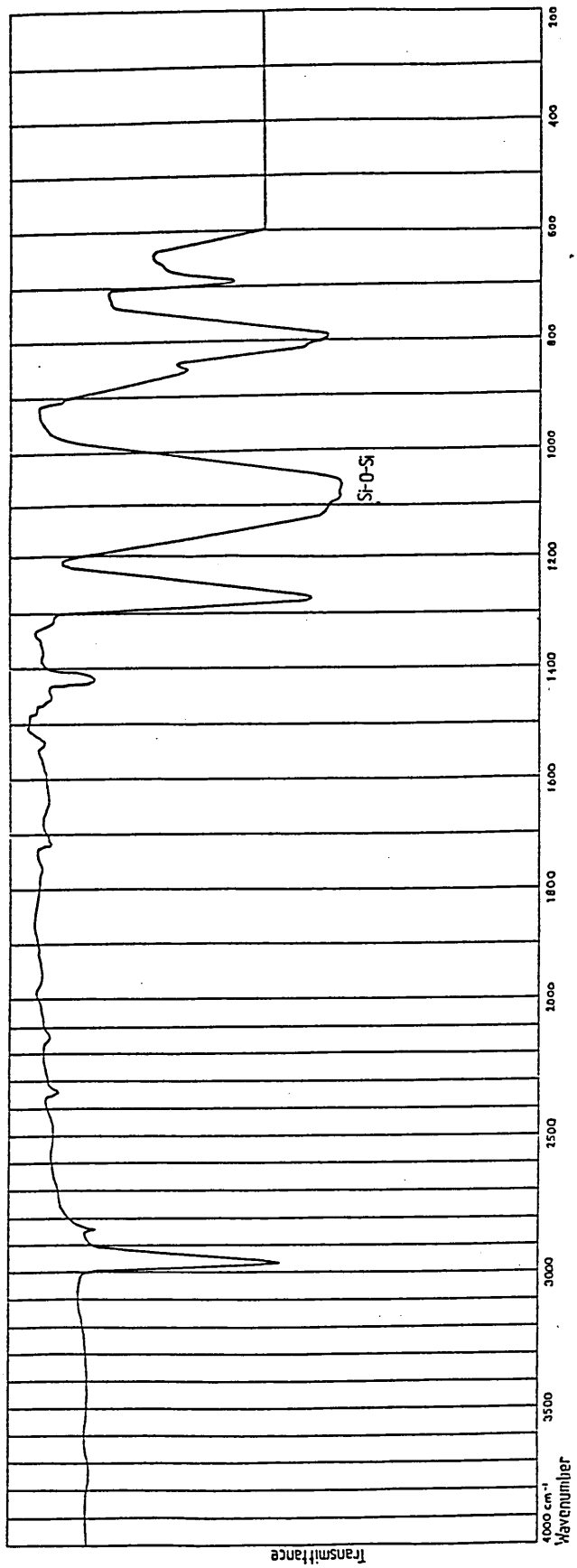

Figure 28: Infra-red spectrum of the hydride PDMS equilibration product distillate.

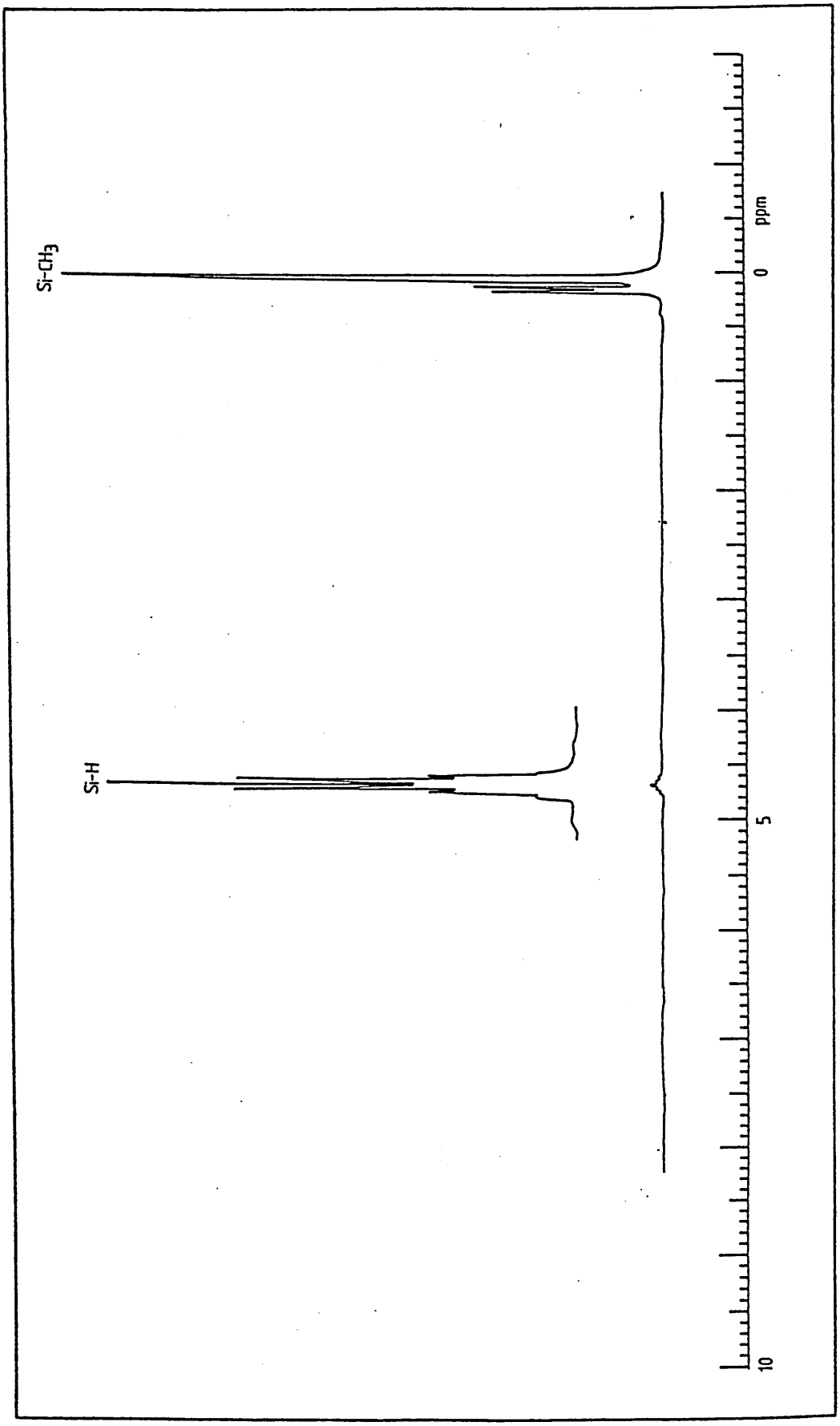

Figure 29: 80MHz ^1H nmr spectrum of the hydride PDMS product.

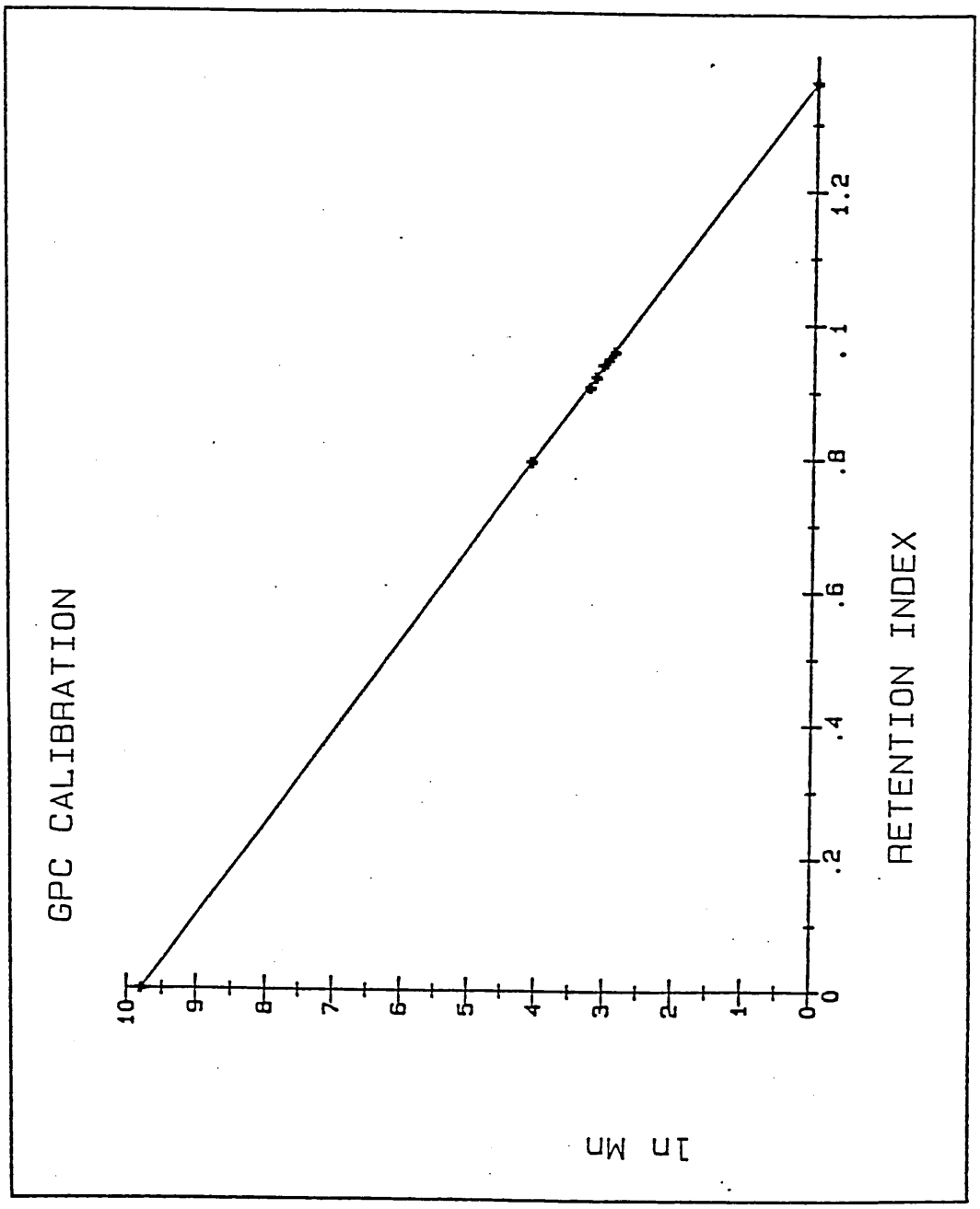

Figure 30: Plot of ln Mn versus gpc retention index for the PDMS standards.

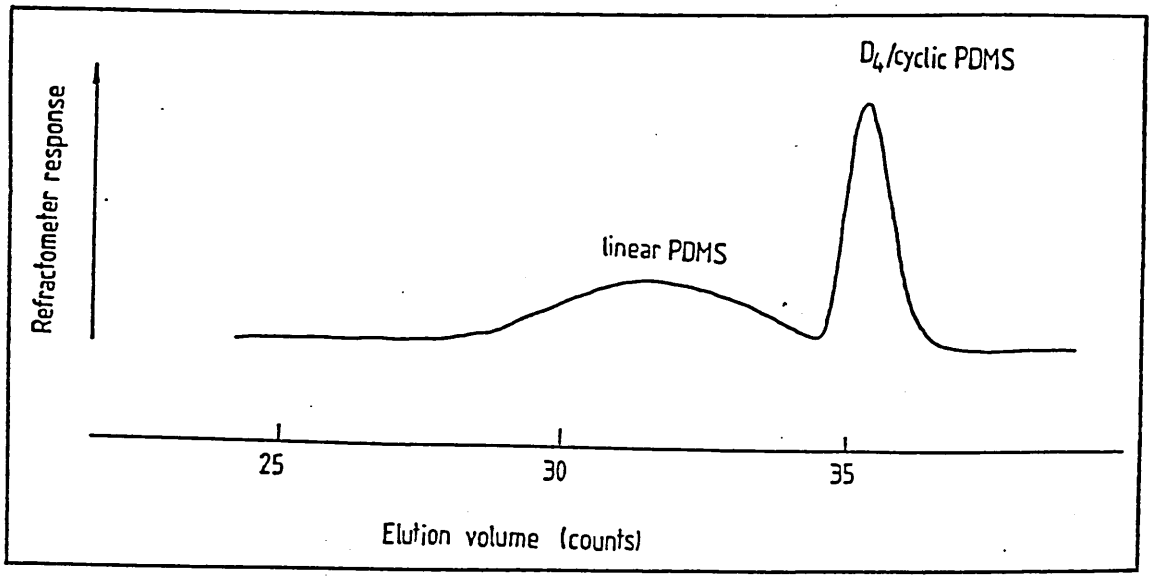

Figure 31: A typical gpc trace showing a mixture of linear and cyclic PDMS oligomers.

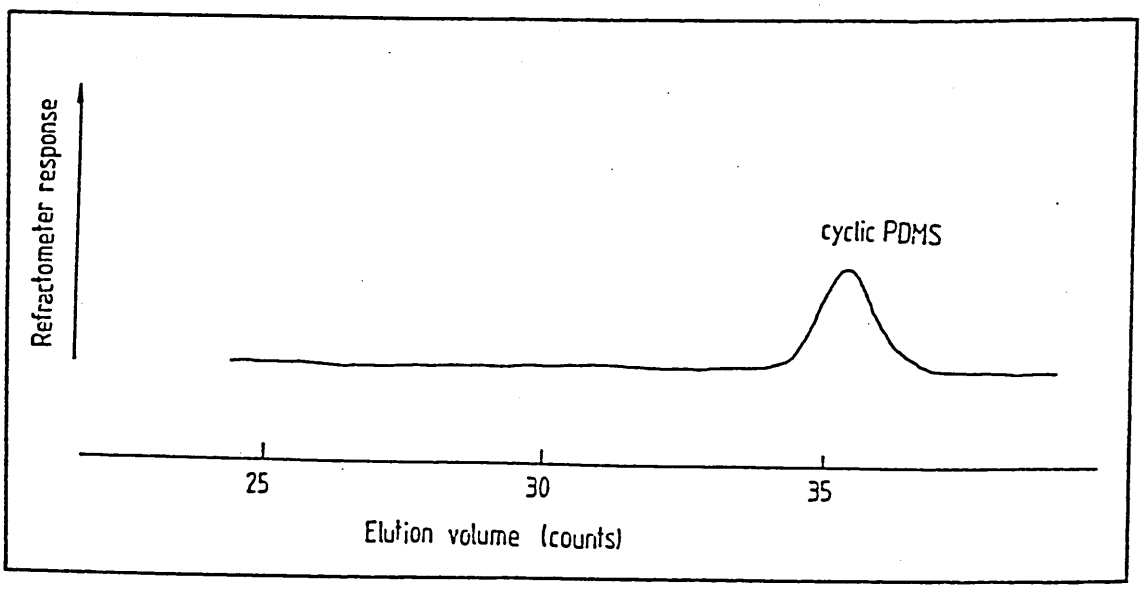

Figure 32: Gpc trace of mixed cyclic PDMS oligomers.

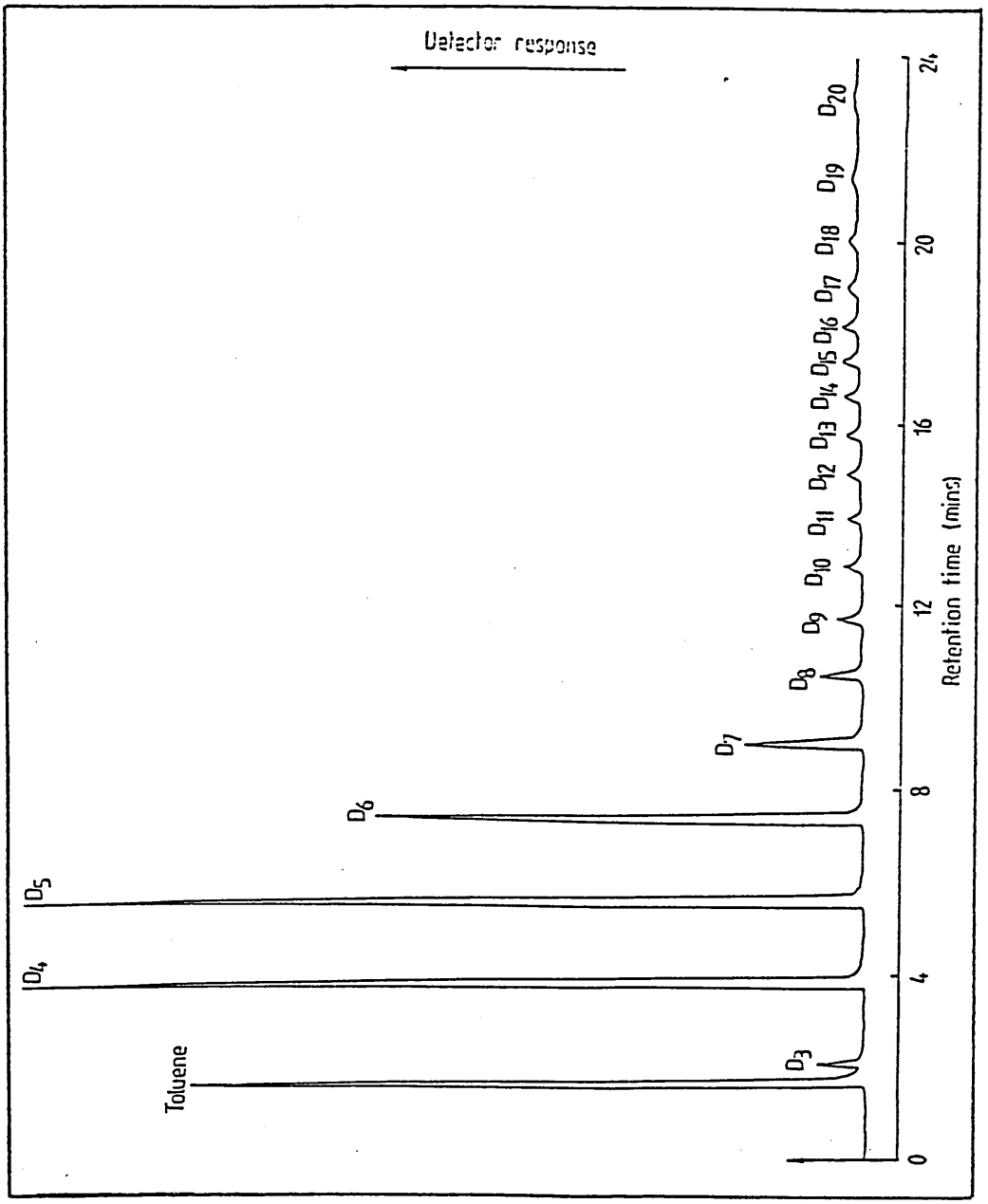

Figure 33: Glc trace of mixed cyclic PDMS oligomers.

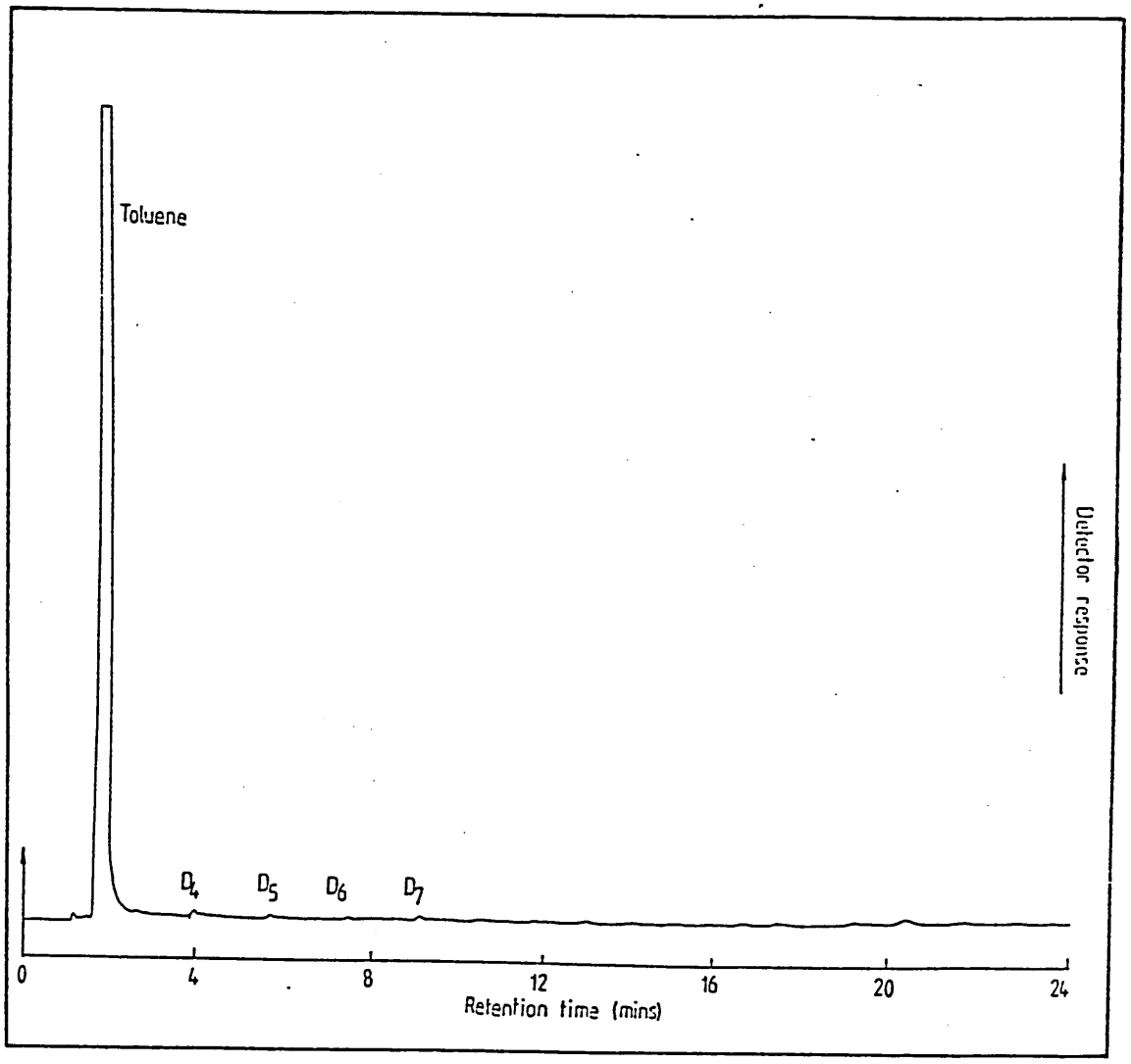

Figure 34: Glc trace of the hydride PDMS product.

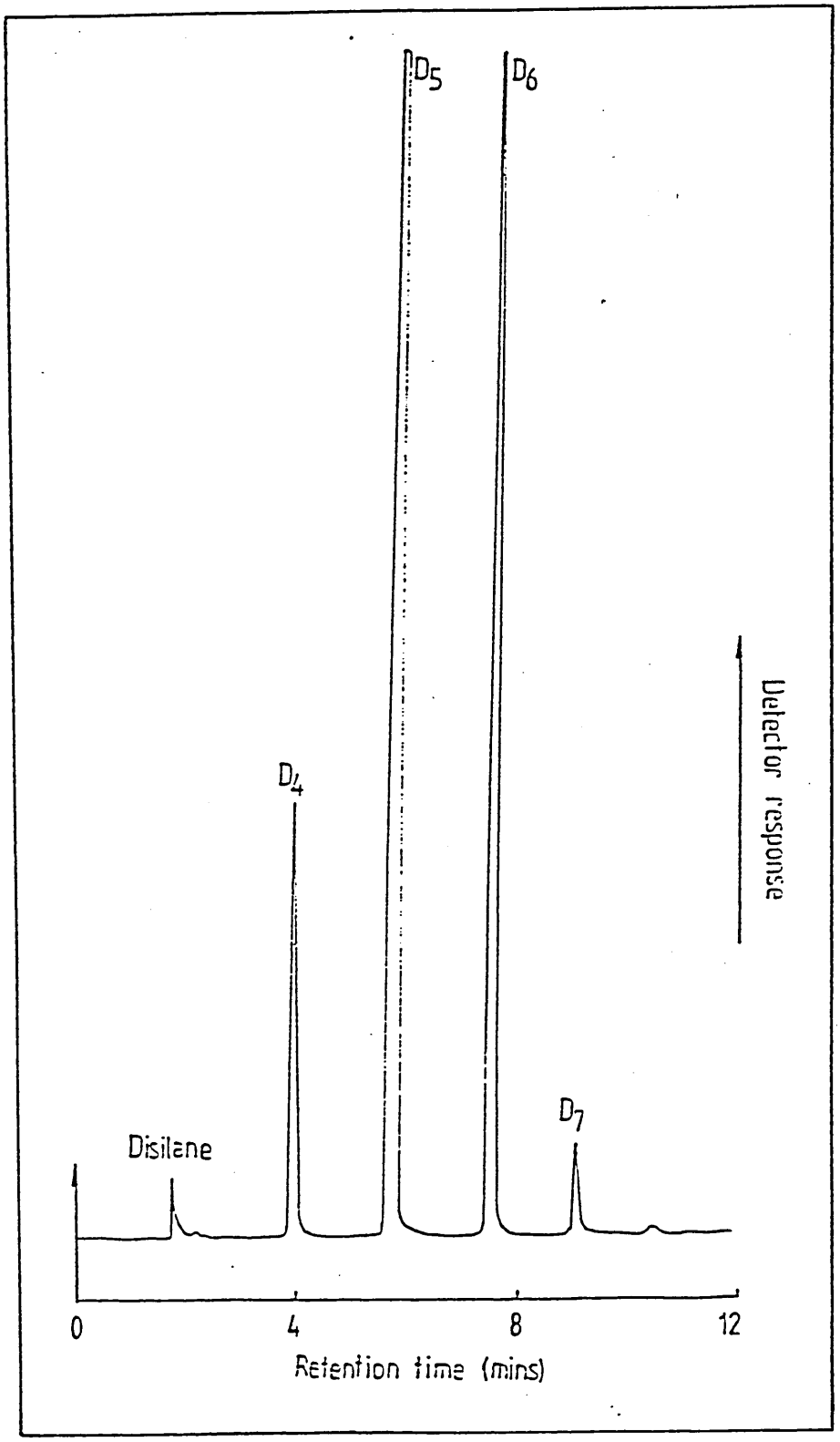

Figure 35: Glc trace of the hydride PDMS equilibration product distillate.

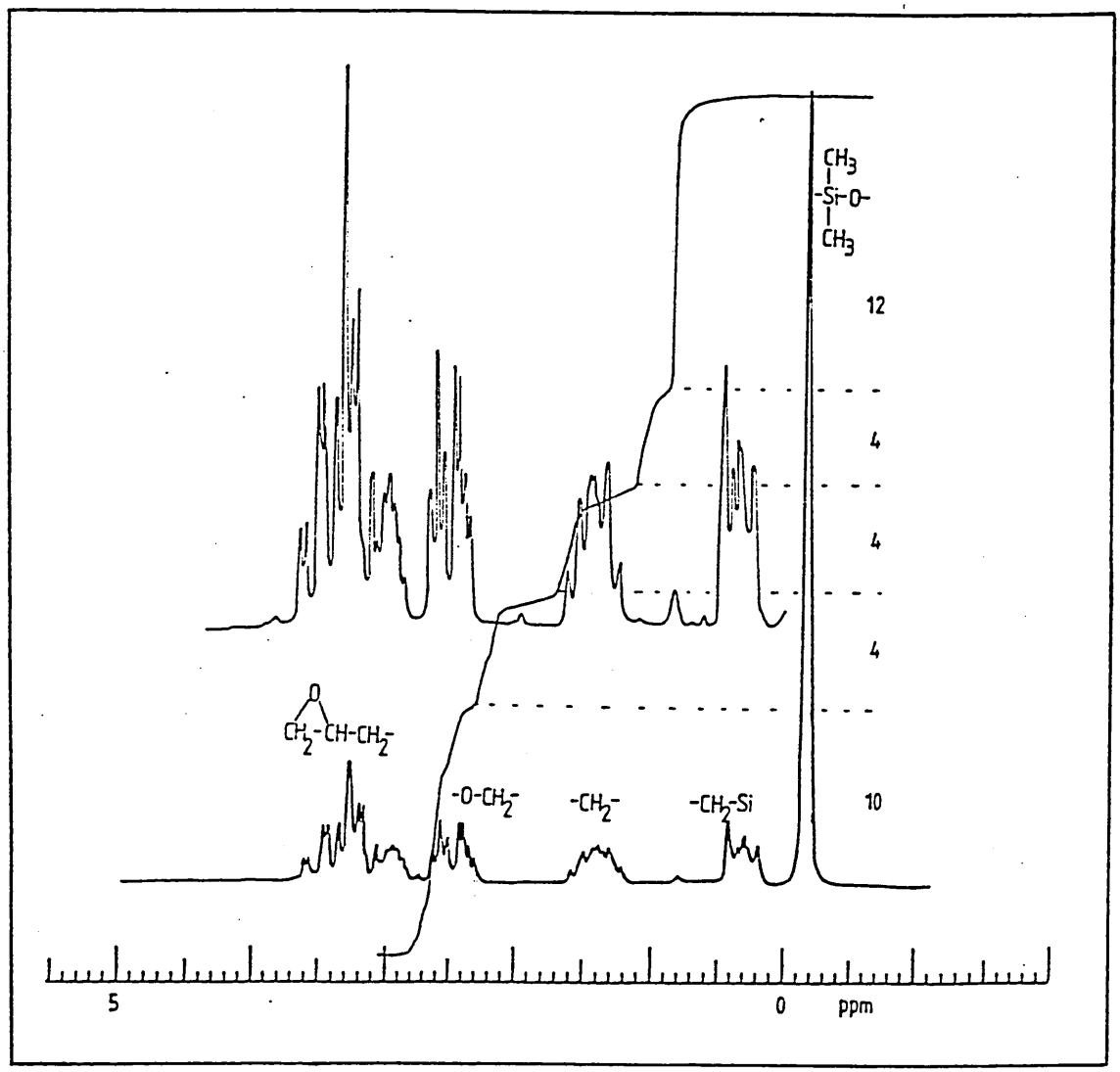

Figure 36: 80MHz ^1H nmr spectrum of diepoxydisiloxane in $CDCl_3$ solvent.

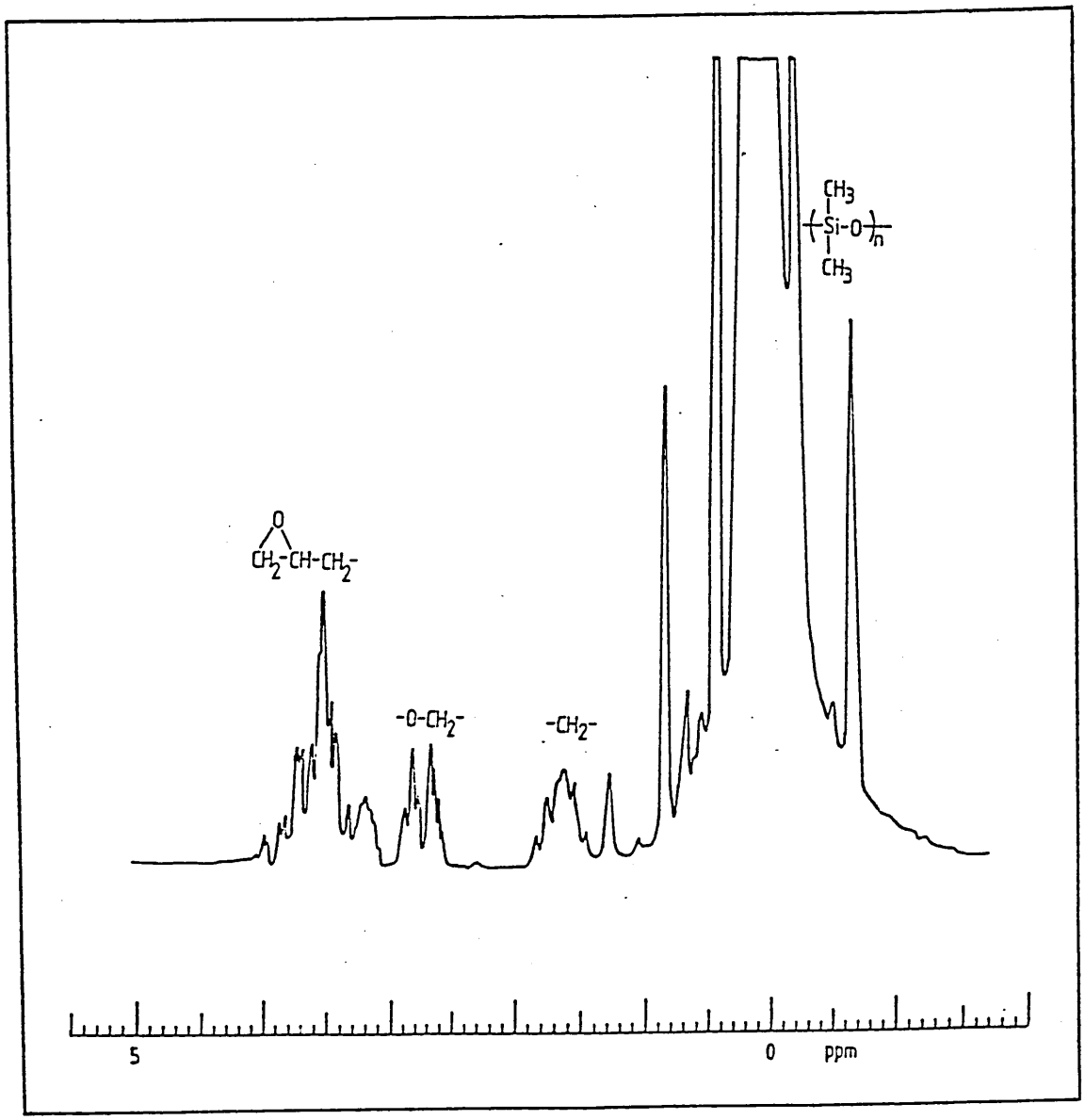

Figure 37: 80MHz ^1H nmr spectrum of epoxy functionalised PDMS in $CDCl_3$ solvent.

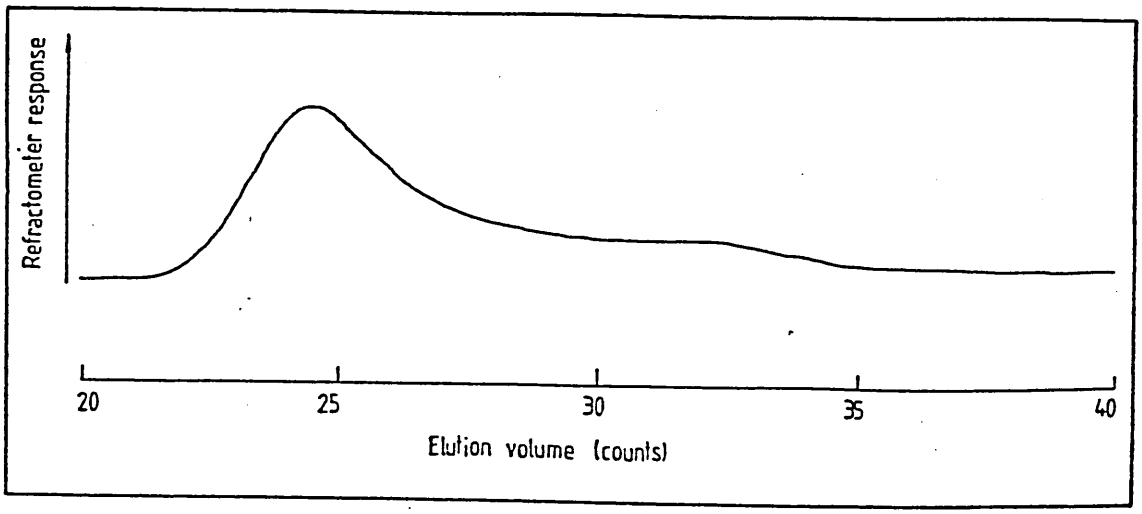

Figure 38: Gpc trace of epoxy PDMS product prepared by equilibration with siloxanolate catalyst.

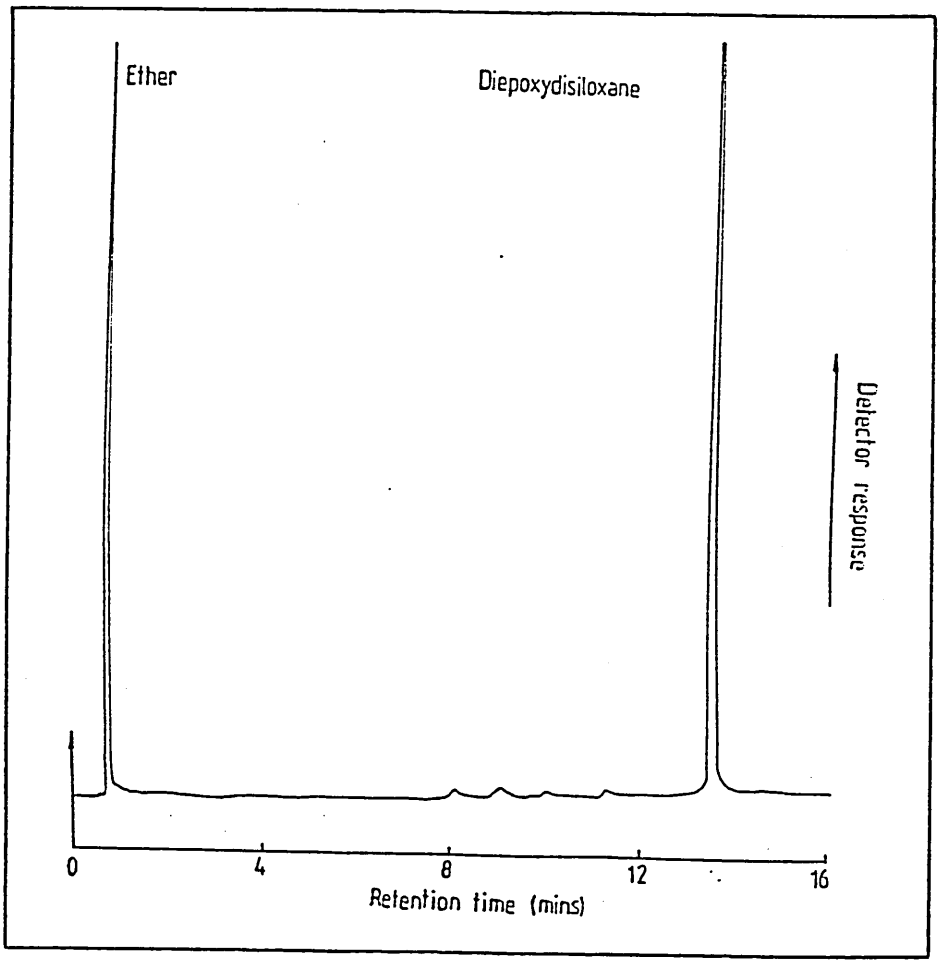

Figure 39: Glc trace of diepoxydisiloxane.

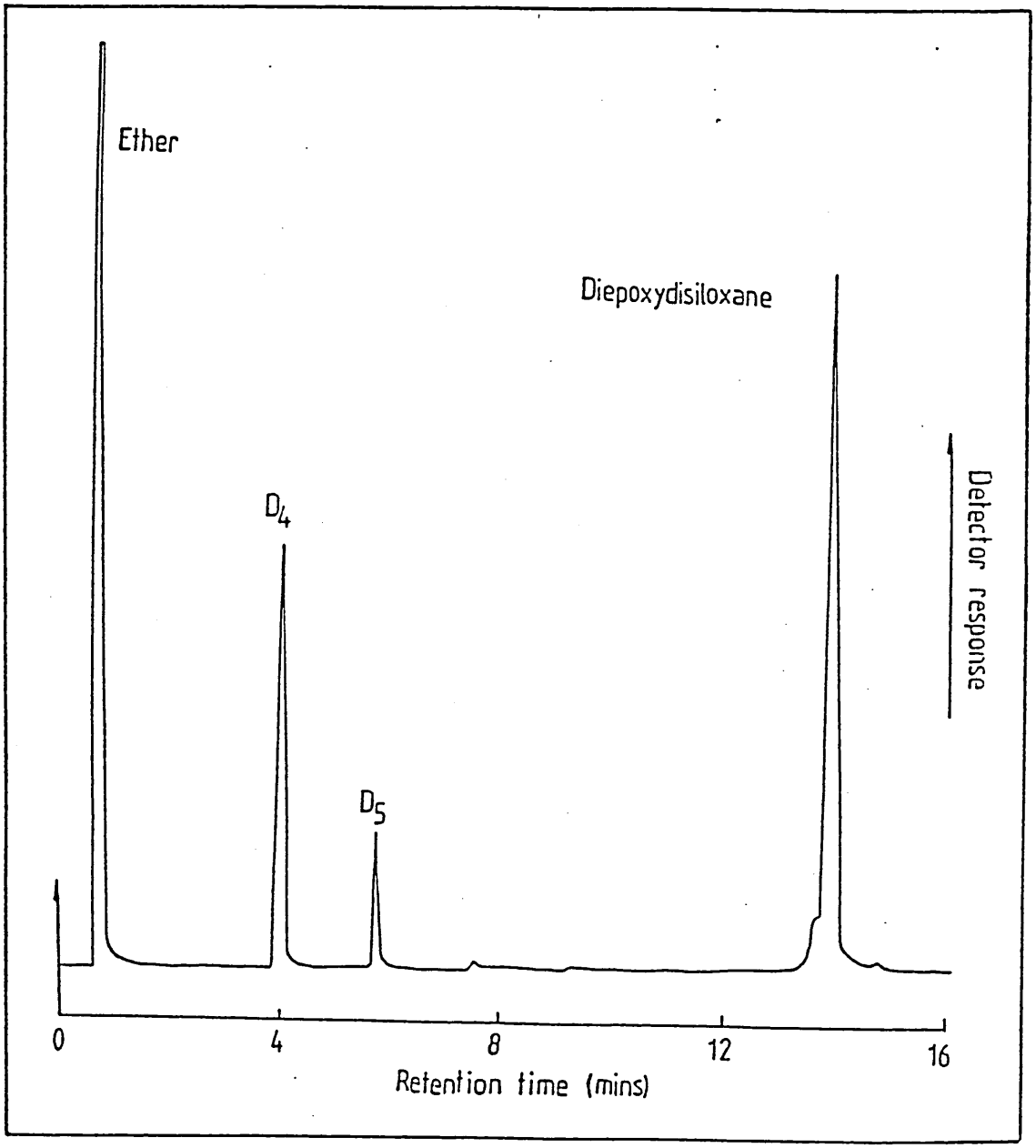

Figure 40: Glc trace of diepoxydisiloxane distillate.

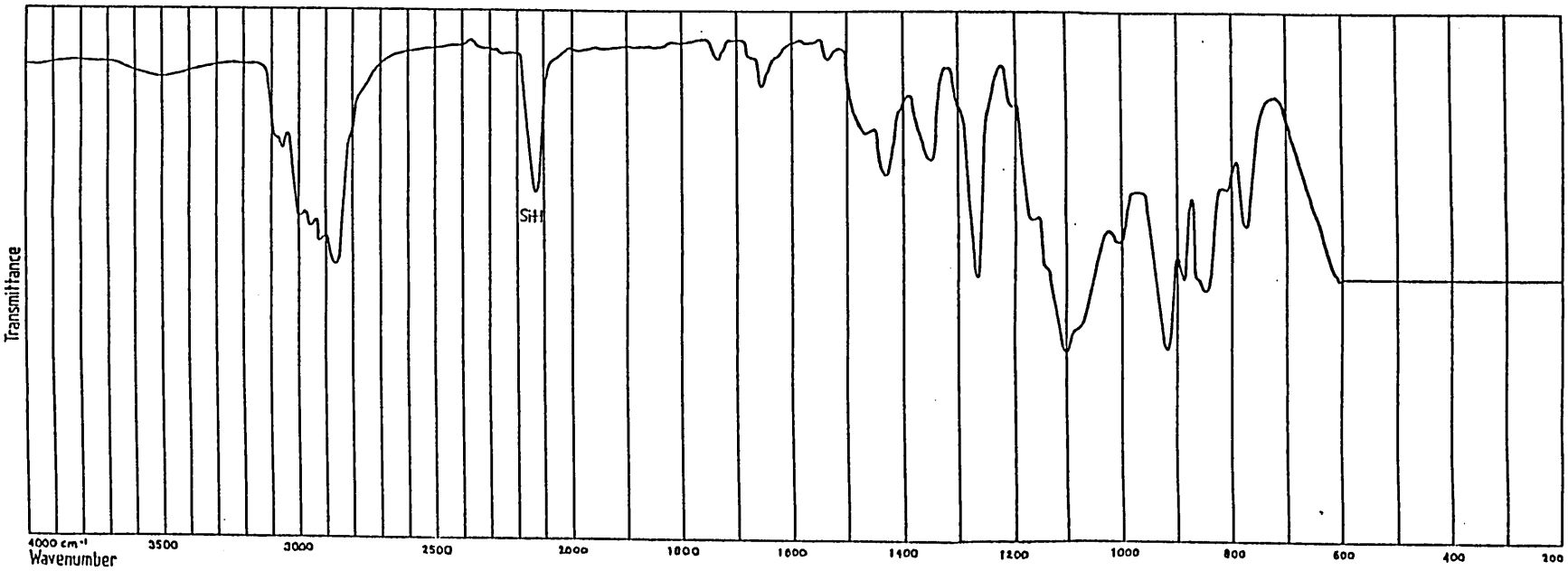

Figure 41: Infra-red spectrum showing the partial vinyl addition reaction between allyl glycidyl ether and 1,1,3,3-tetramethyldisiloxane.

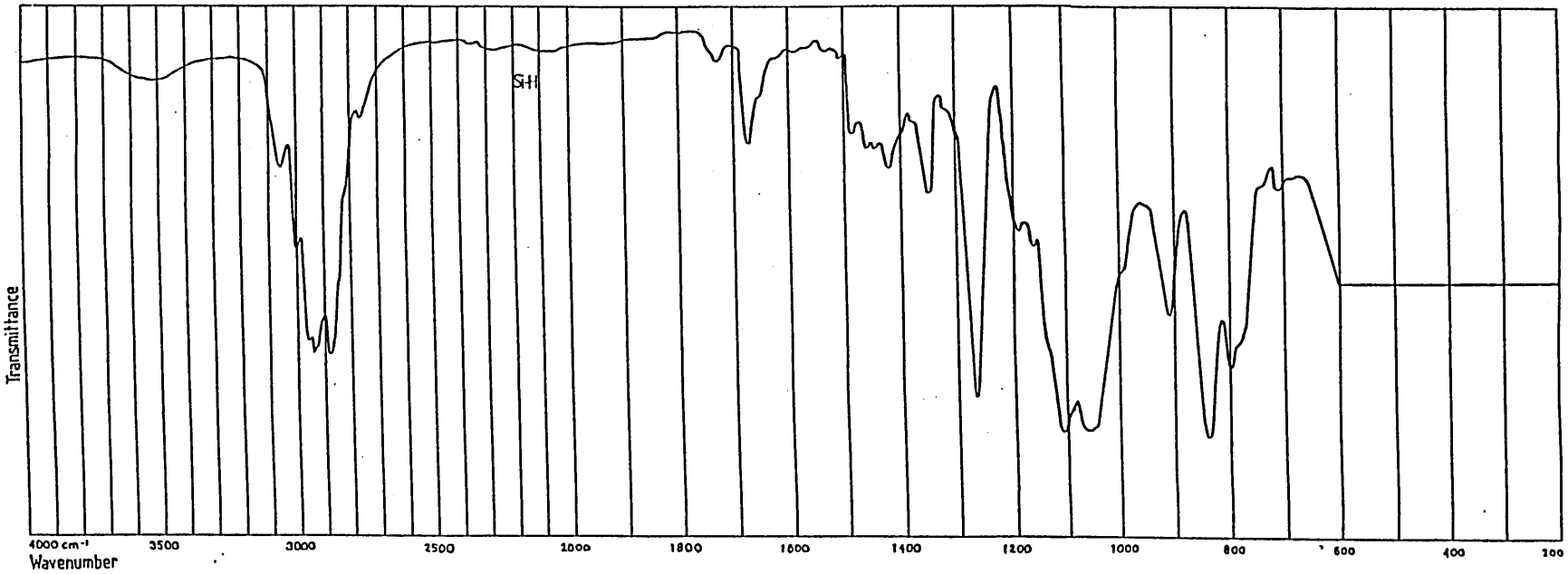

Figure 42: Infra-red spectrum showing the completed vinyl addition reaction between allyl glycidyl ether and 1,1,3,3-tetramethyldisiloxane.

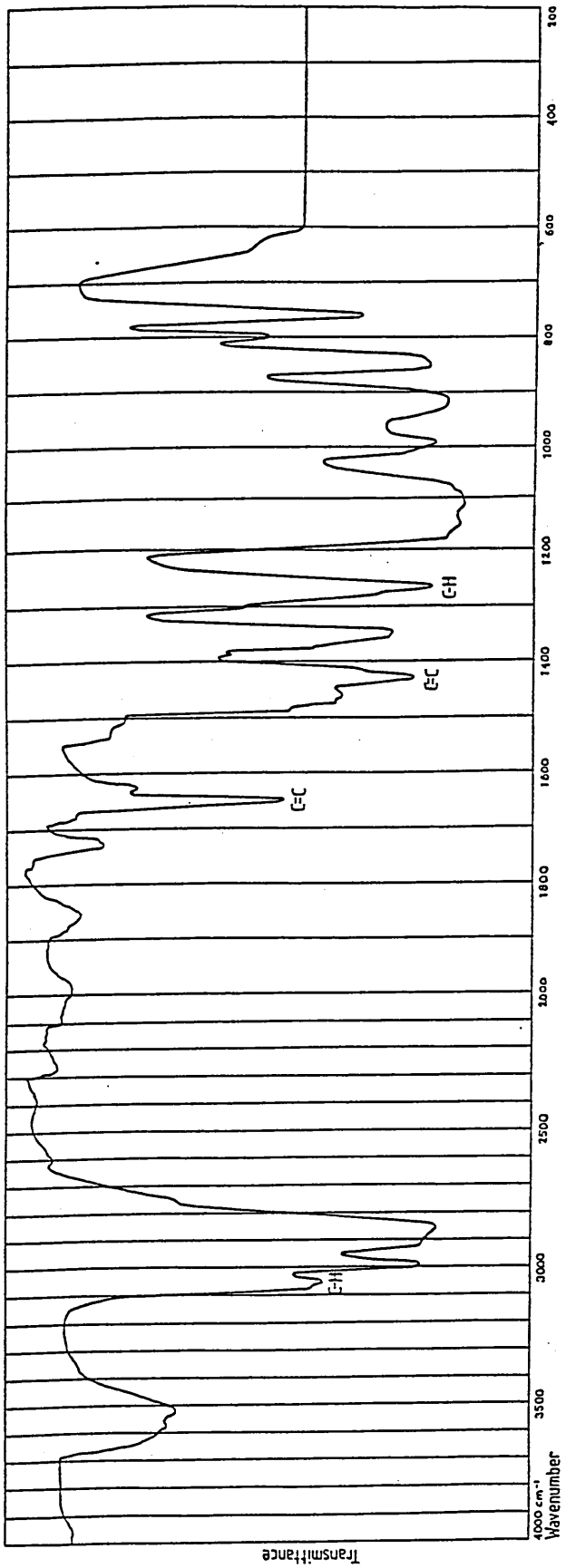

Figure 43: Infra-red spectrum of allyl glycidyl ether.

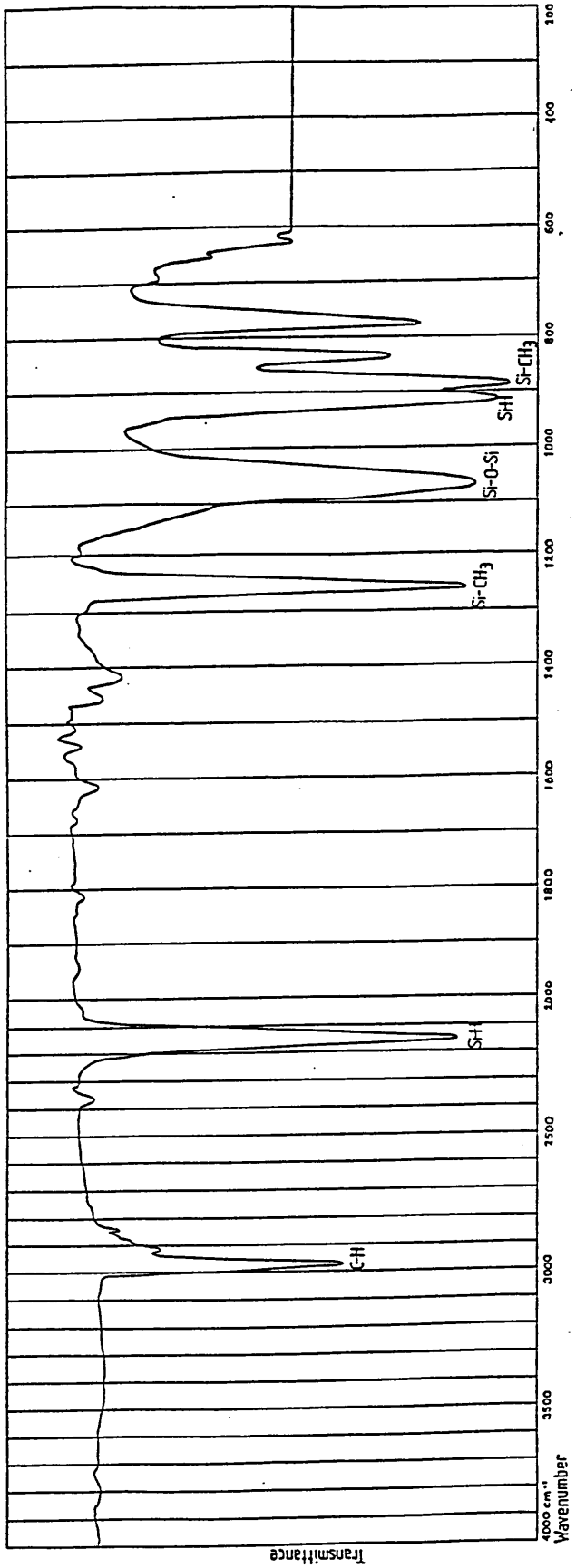

Figure 44: Infra-red spectrum of 1,1,3,3-tetramethyldisiloxane.

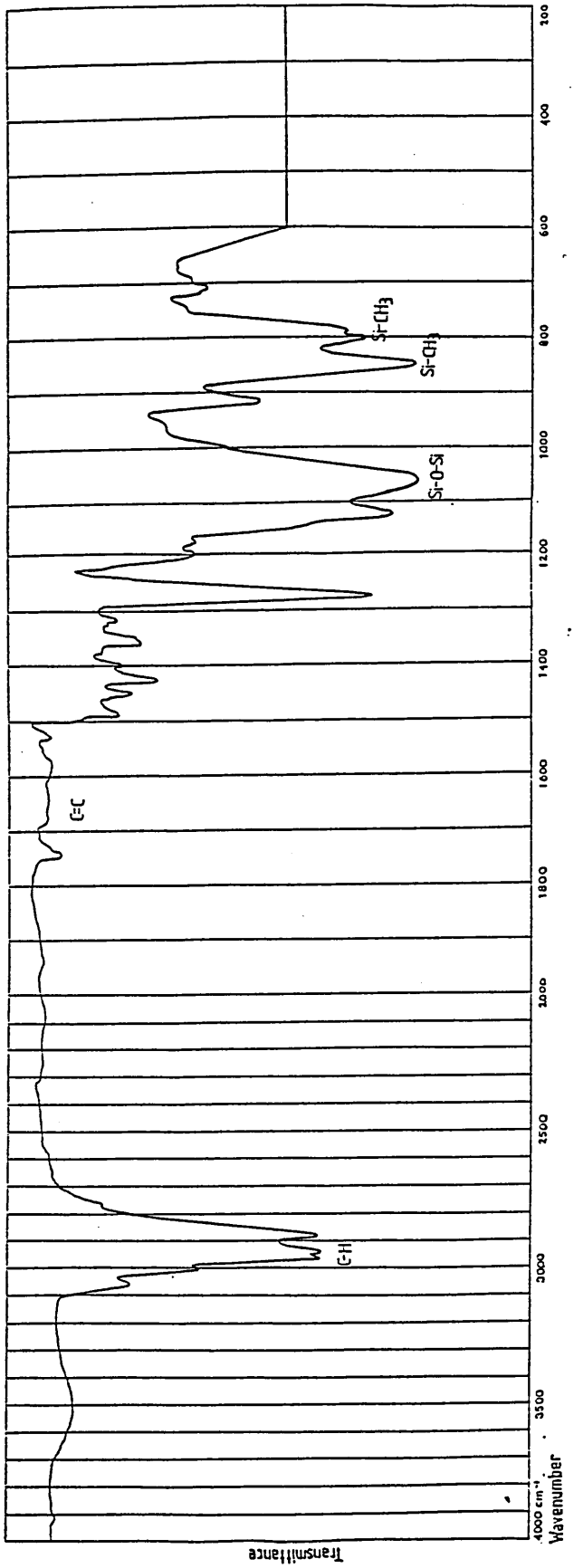

Figure 45: Infra-red spectrum of purified epoxy disiloxane.

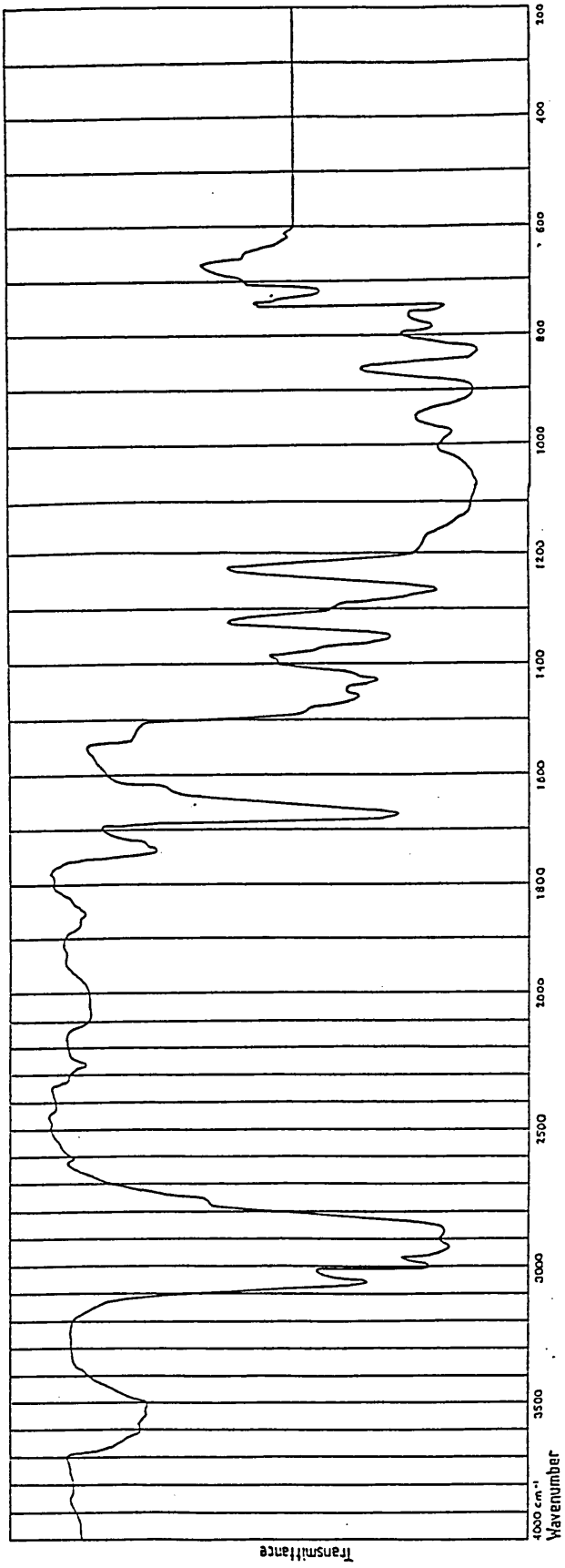

Figure 46: Infra-red spectrum of the epoxy disiloxane distillate.

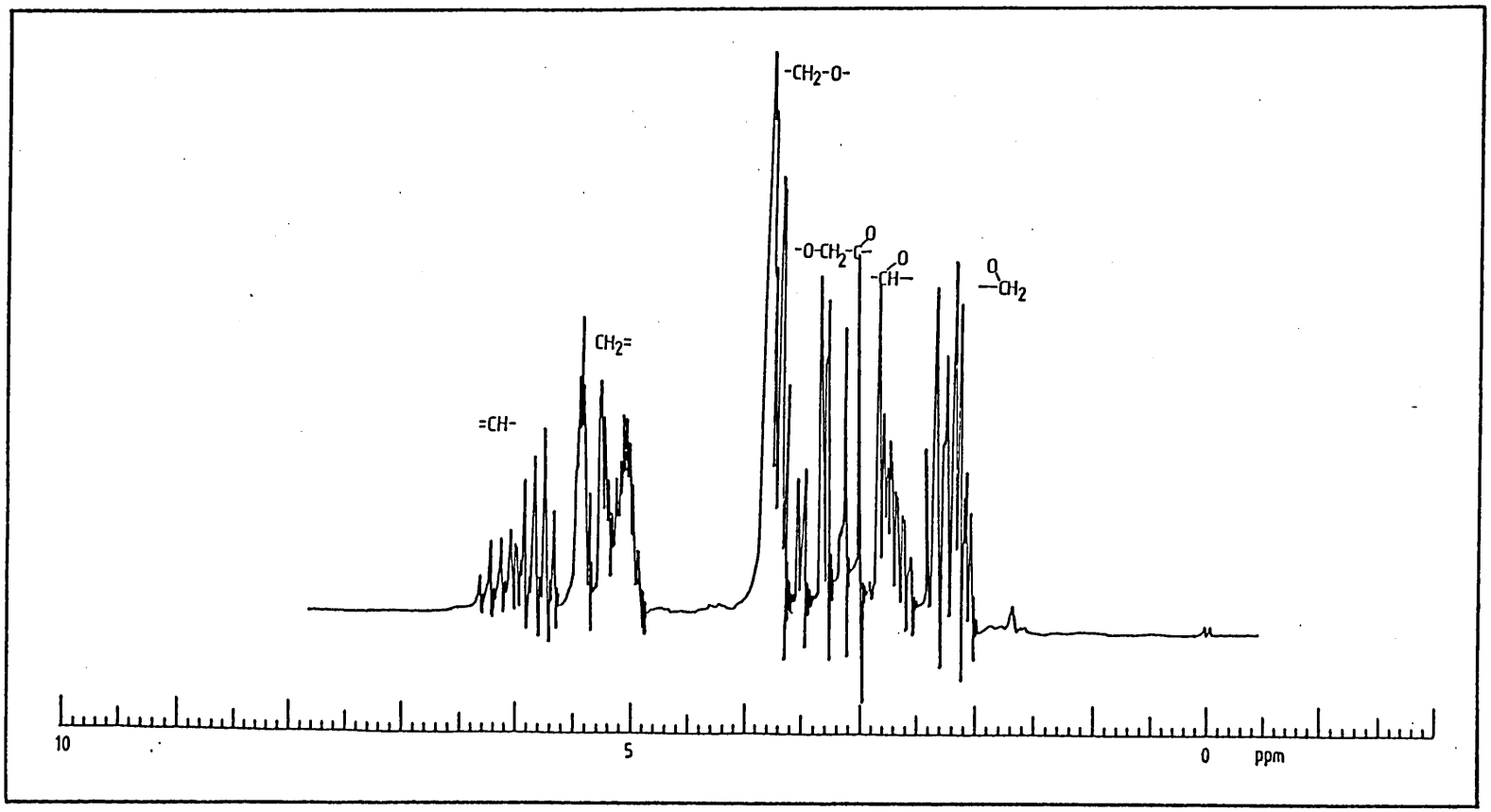

Figure 47: 80MHz ^1H nmr spectrum of allyl glycidyl ether ($CDCl_3$ solvent).

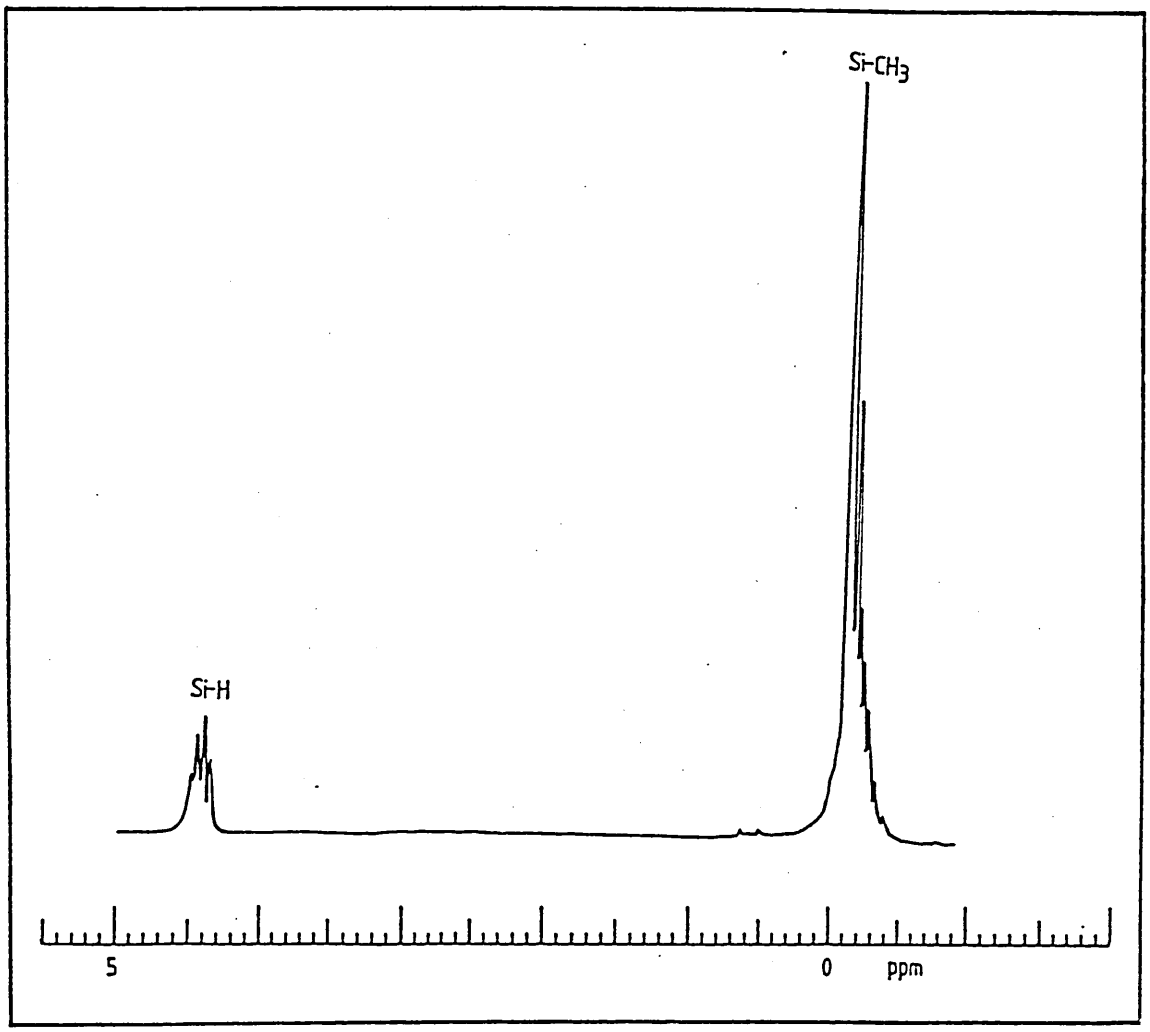

Figure 48: 80MHz ^1H nmr spectrum of 1,1,3,3-tetramethyldisiloxane ($CDCl_3$ solvent).

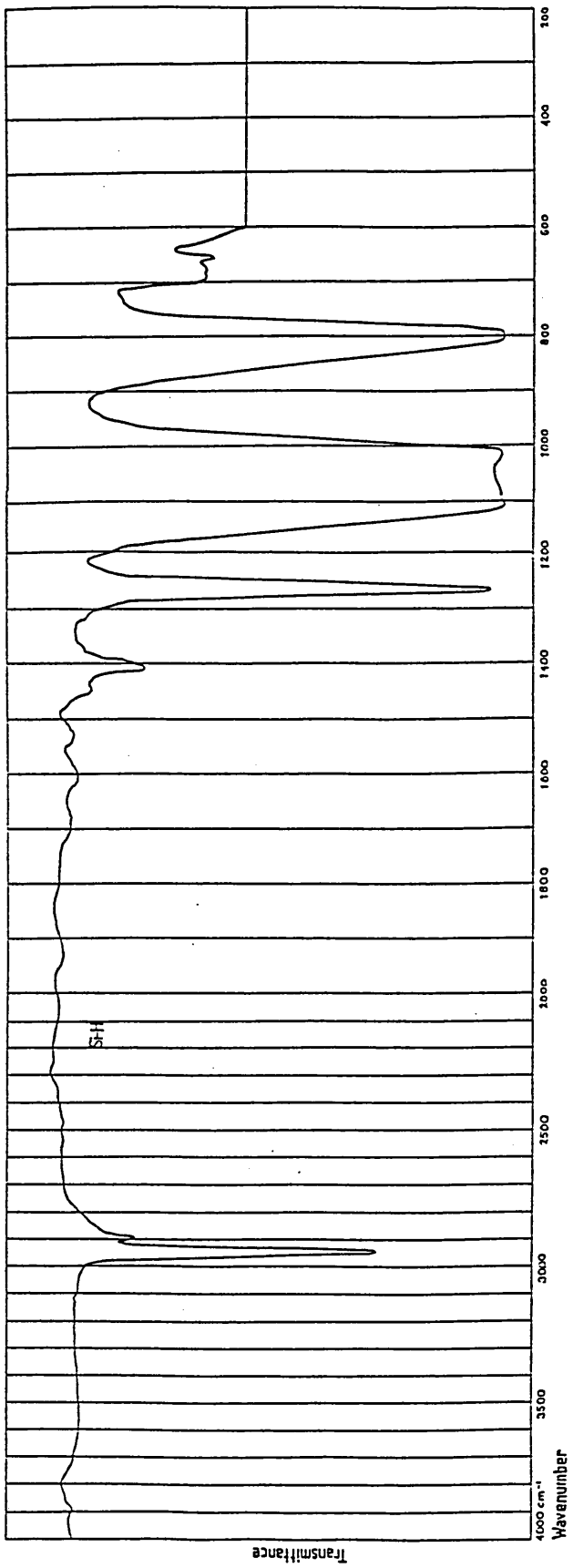

Figure 49: Infra-red spectrum of epoxy PDMS.

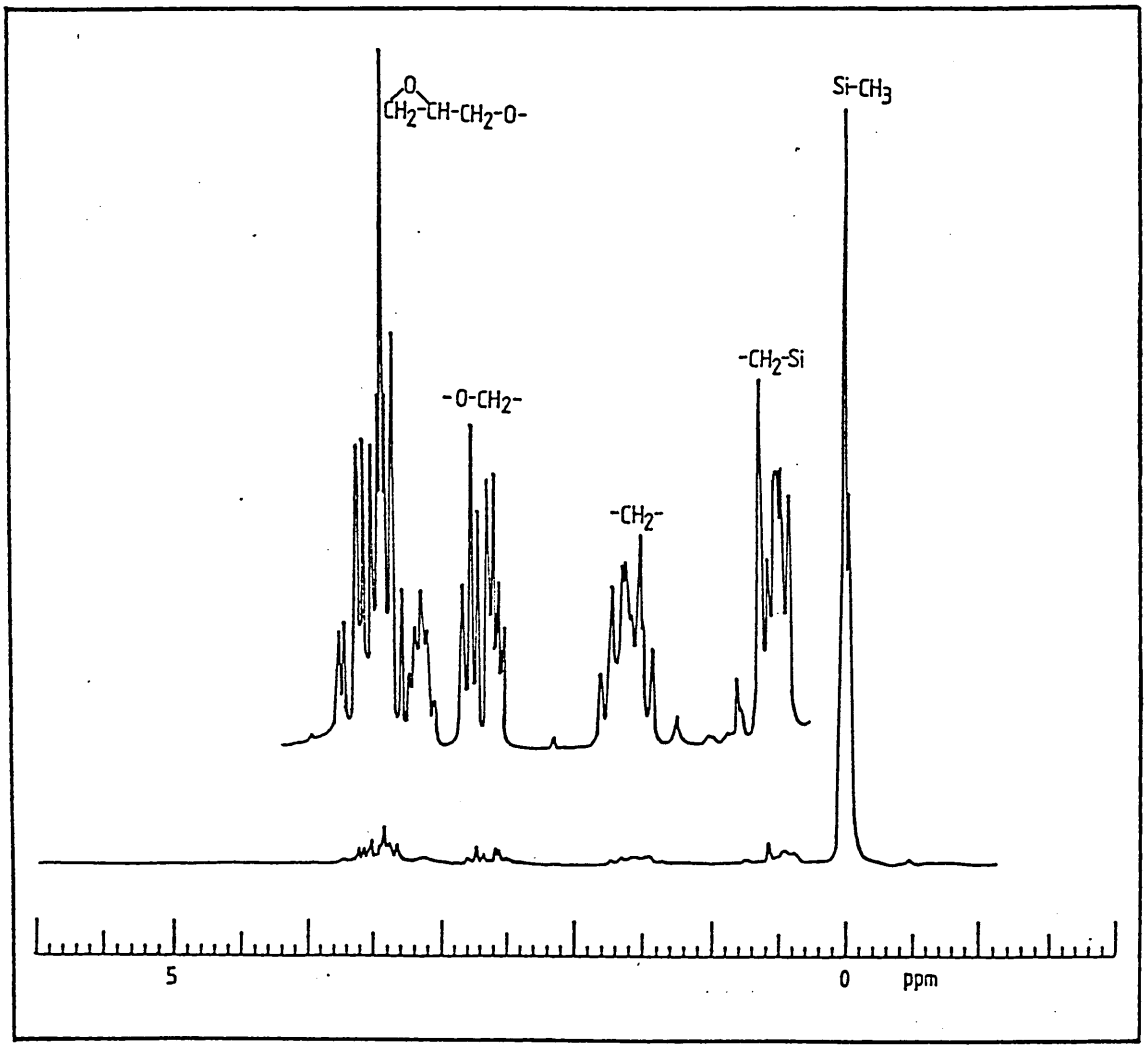

Figure 50: 80MHz ^1H nmr spectrum of epoxy PDMS ($CDCl_3$ solvent).

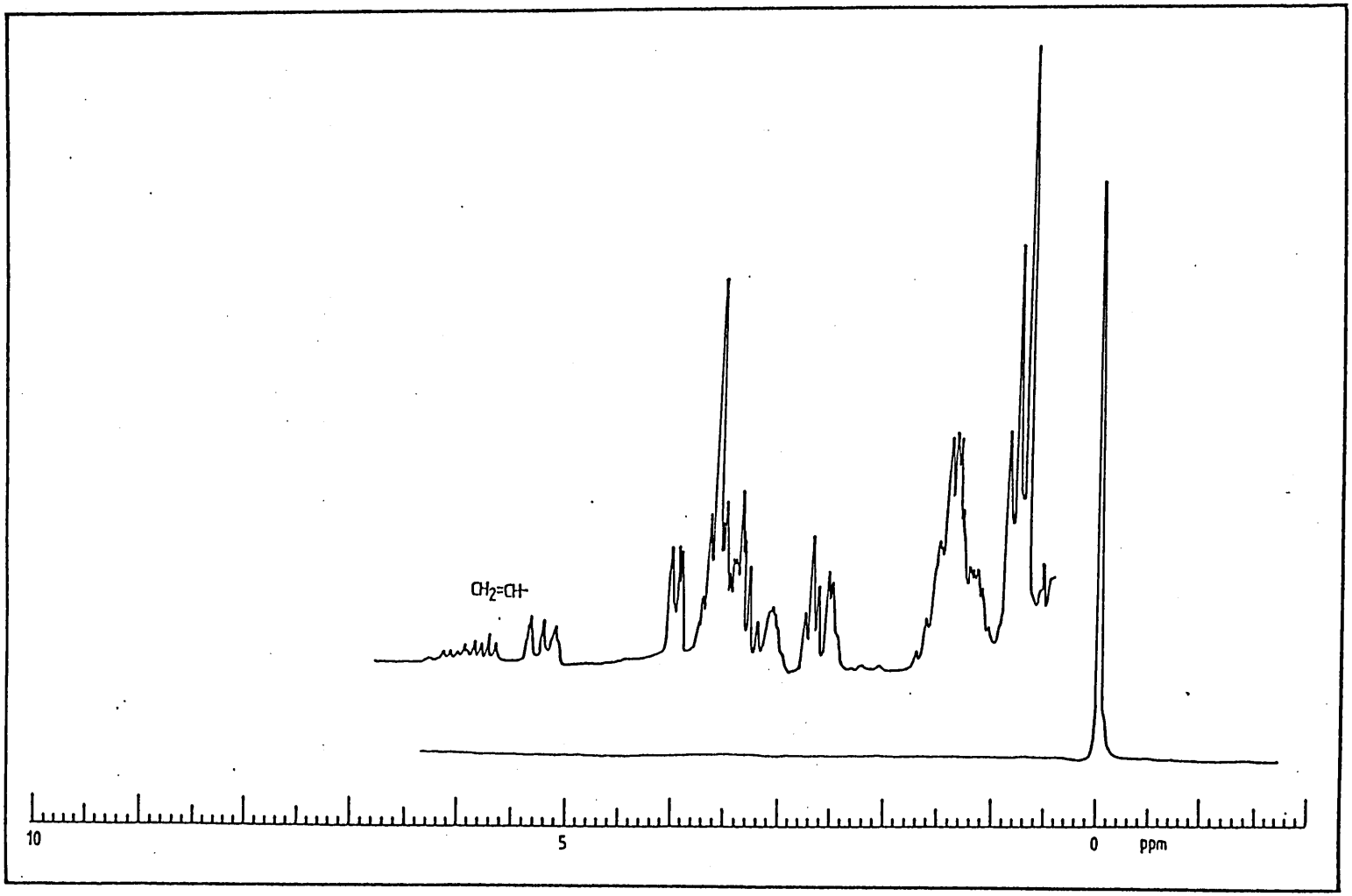

Figure 51: 80MHz ^{1}H nmr spectrum of epoxy PDMS contaminated with allyl glycidyl ether.

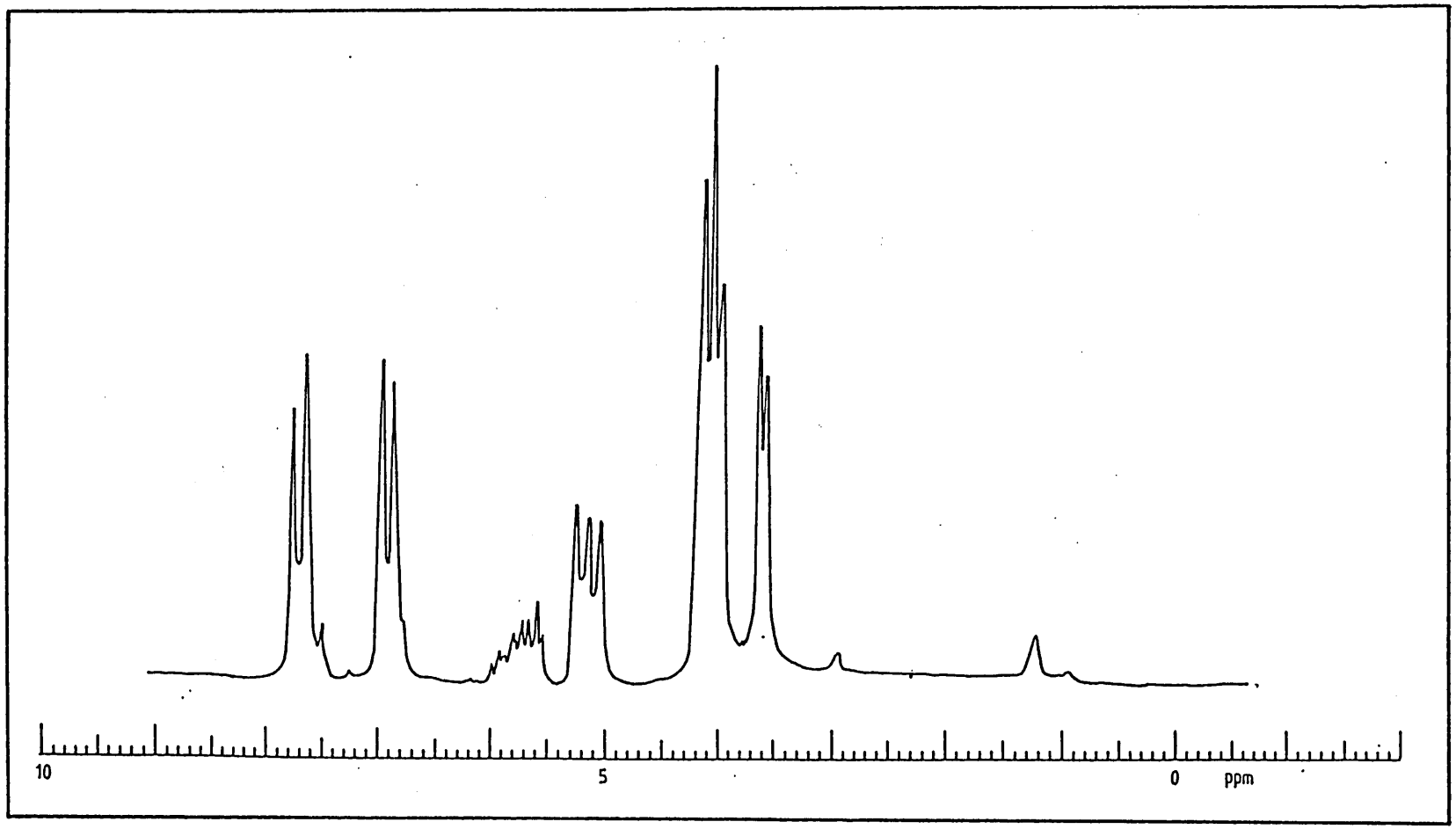

Figure 52: 80MHz ^1H nmr spectrum of the reaction product of allyl glycidyl ether and Bisphenol"S".

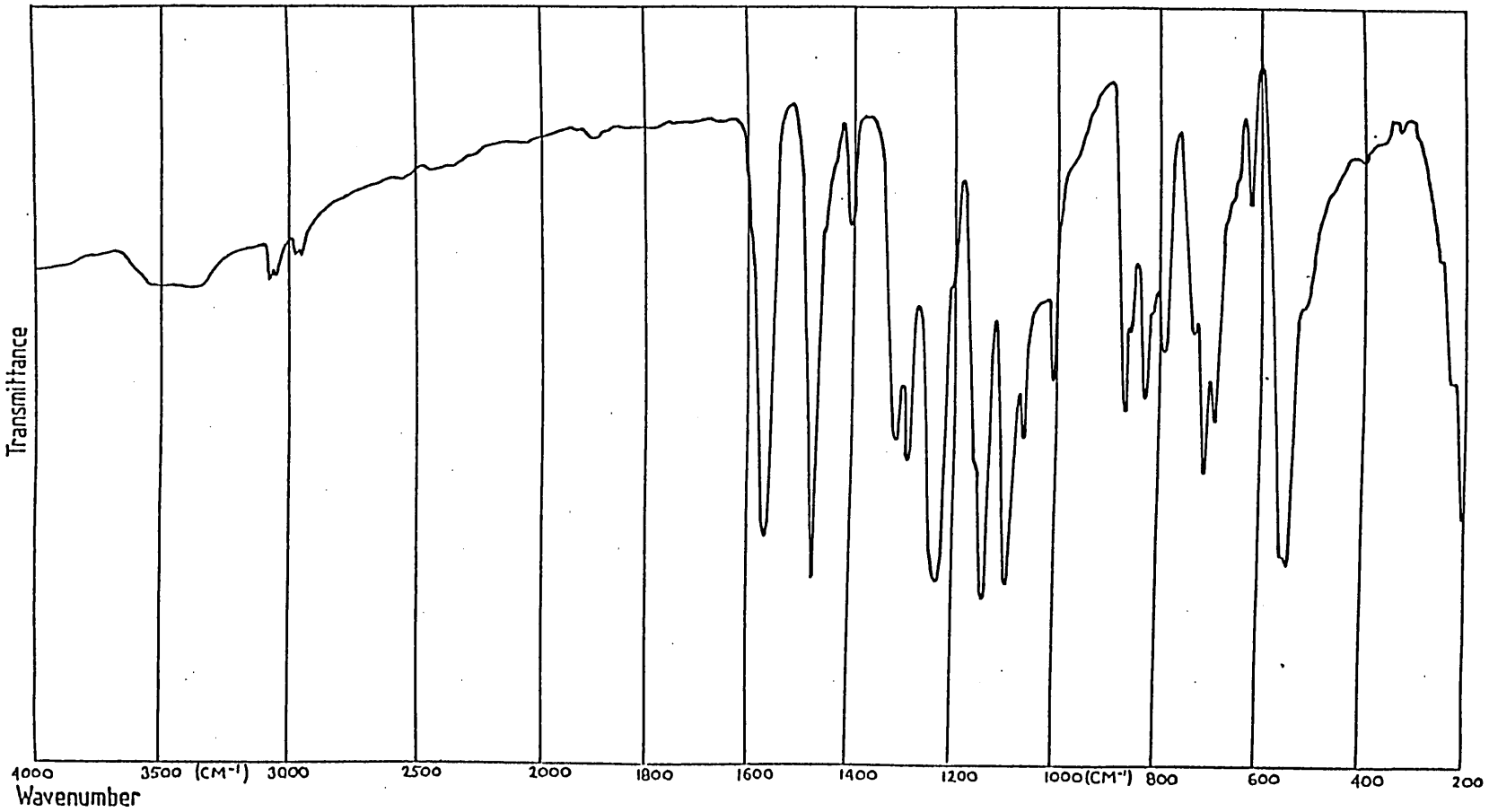

Figure 53: Infra-red spectrum of a PES/epoxy PDMS solution copolymerisation product after toluene extraction.

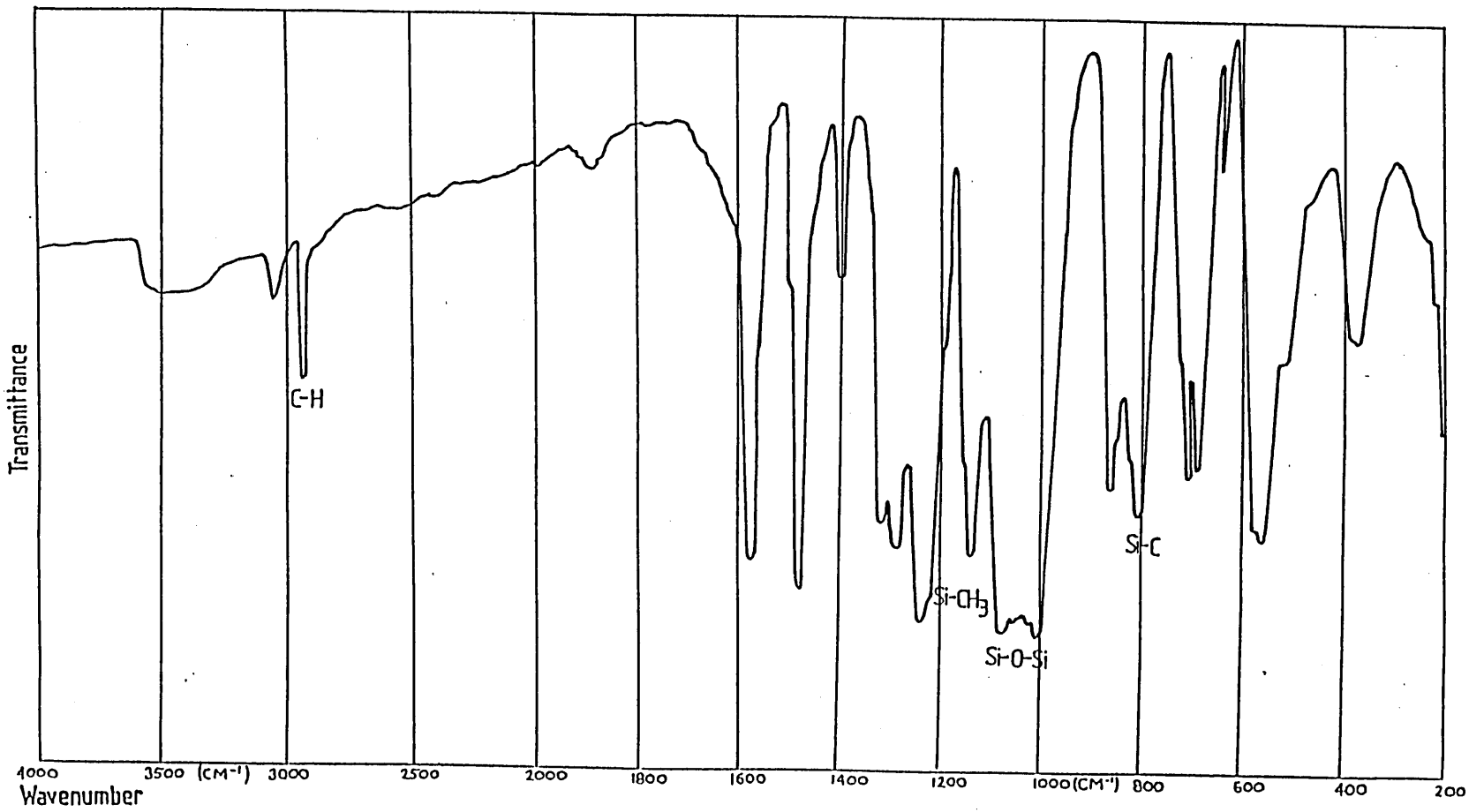

Figure 54: Infra-red spectrum of a blend of PES and 30% w/w PDMS.

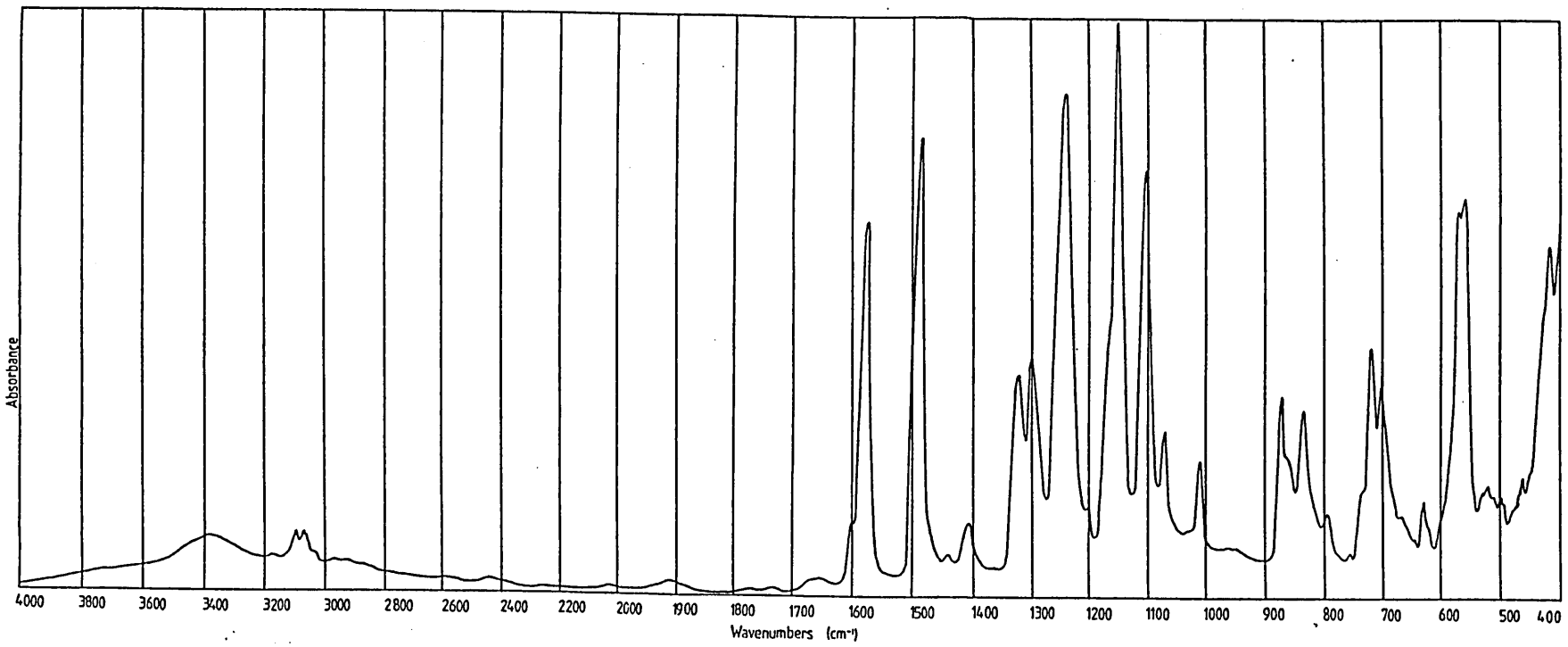

Figure 55: Infra-red spectrum of a PES/epoxy PDMS solution copolymerisation product after toluene extraction (Nicolet FT-IR instrument).

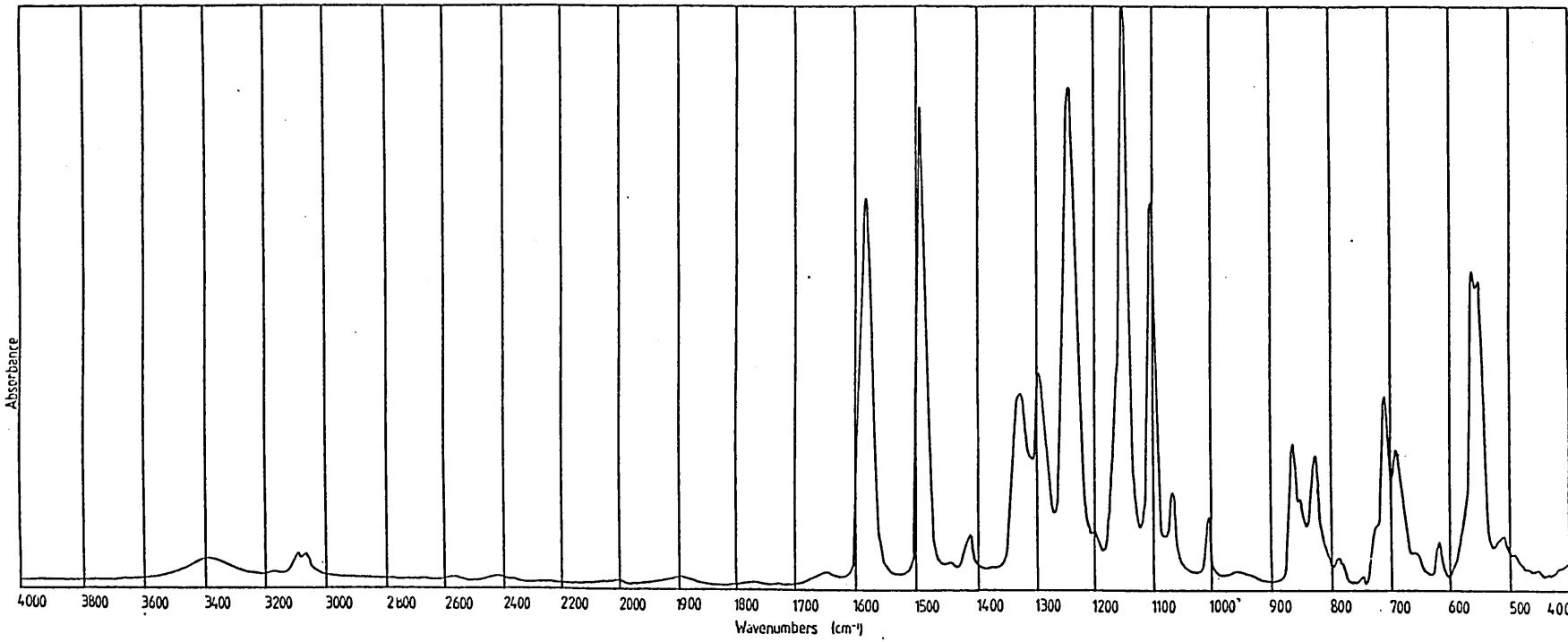

Figure 56: Infra-red spectrum of hydroxyl PES (Nicolet FT-IR instrument).

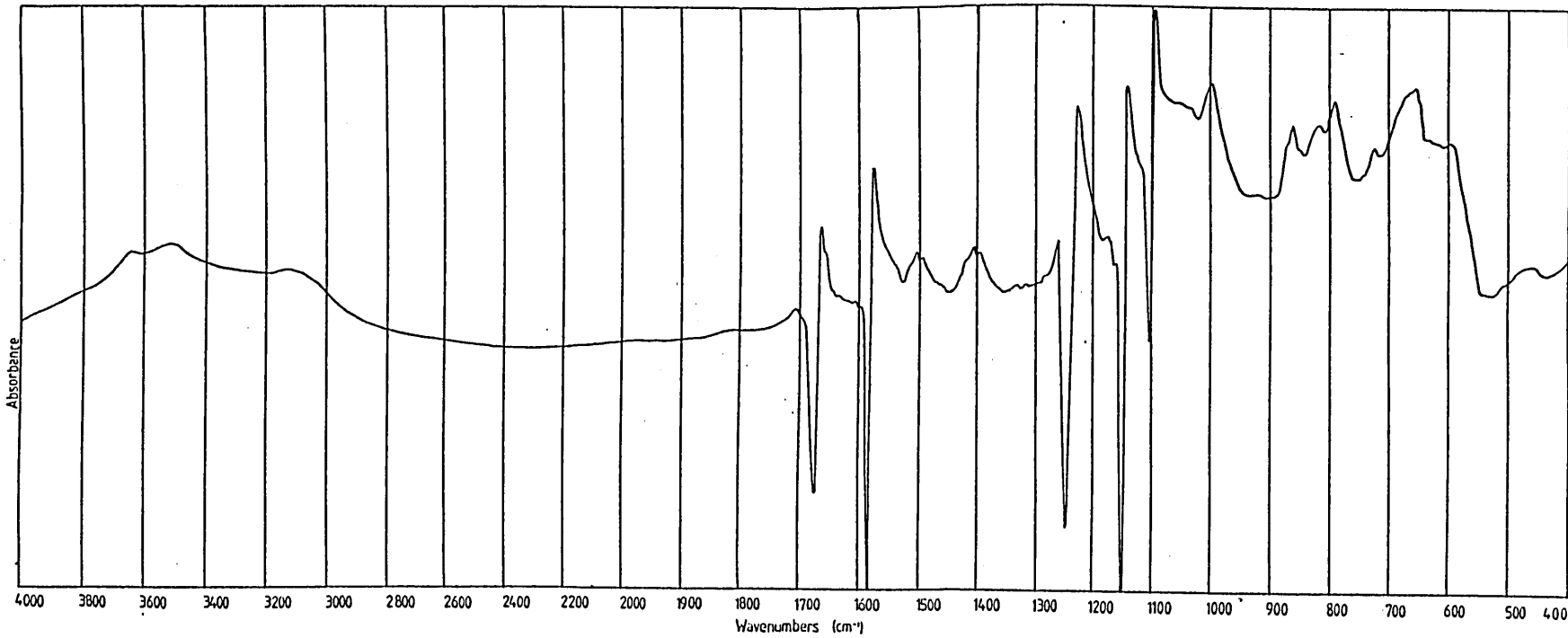

Figure 57: Infra-red spectrum prepared by subtracting the ir spectrum of hydroxyl PES (Figur 56) from the spectrum of PES/epoxy copolymer product (Figure 55); Mattson-Cygnus data handlir system.

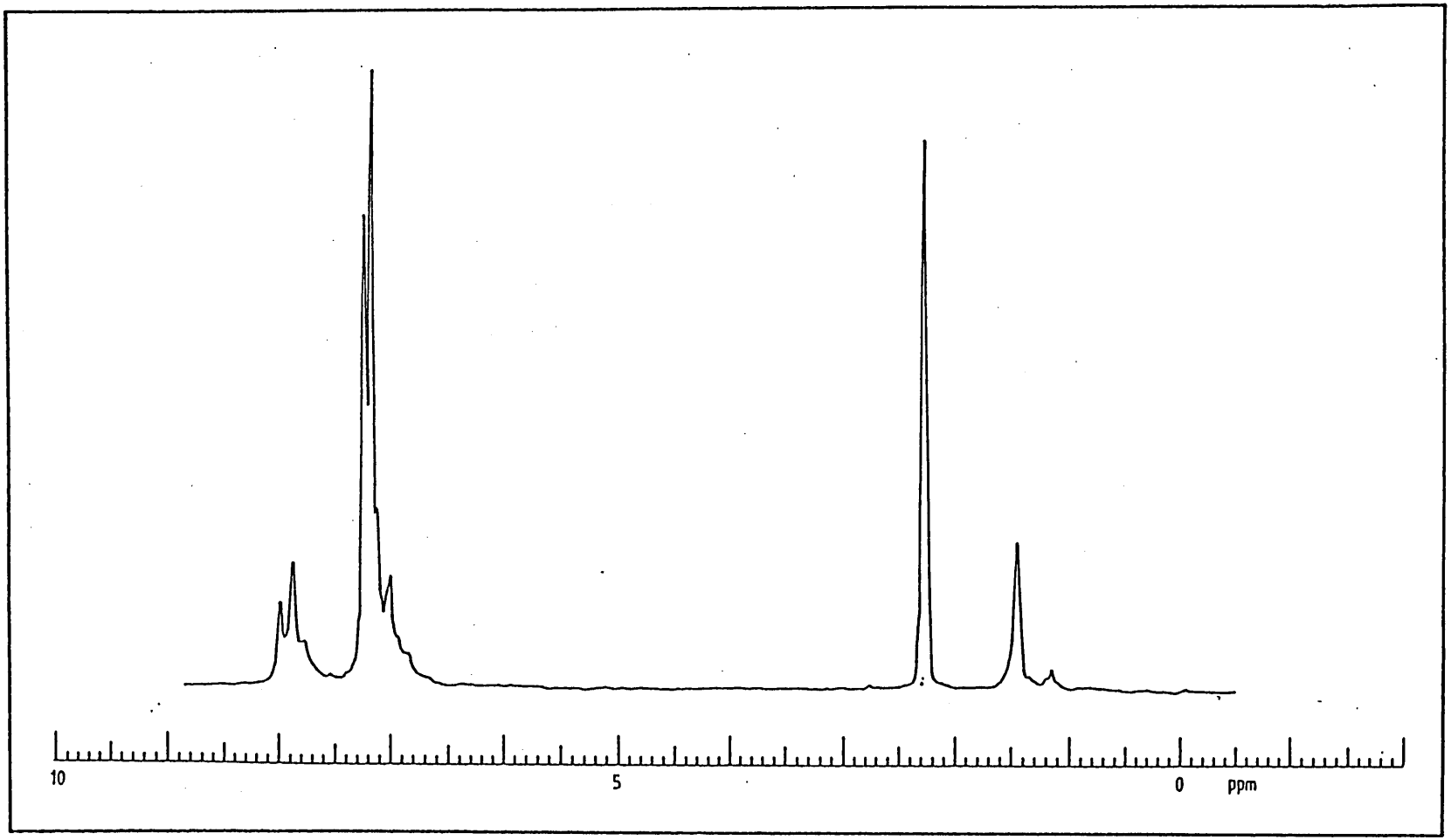

Figure 58: 80MHz ^{1}H nmr spectrum of a blend of PES and 30% w/w PDMS after toluene extraction ($CDCl_3$ solvent).

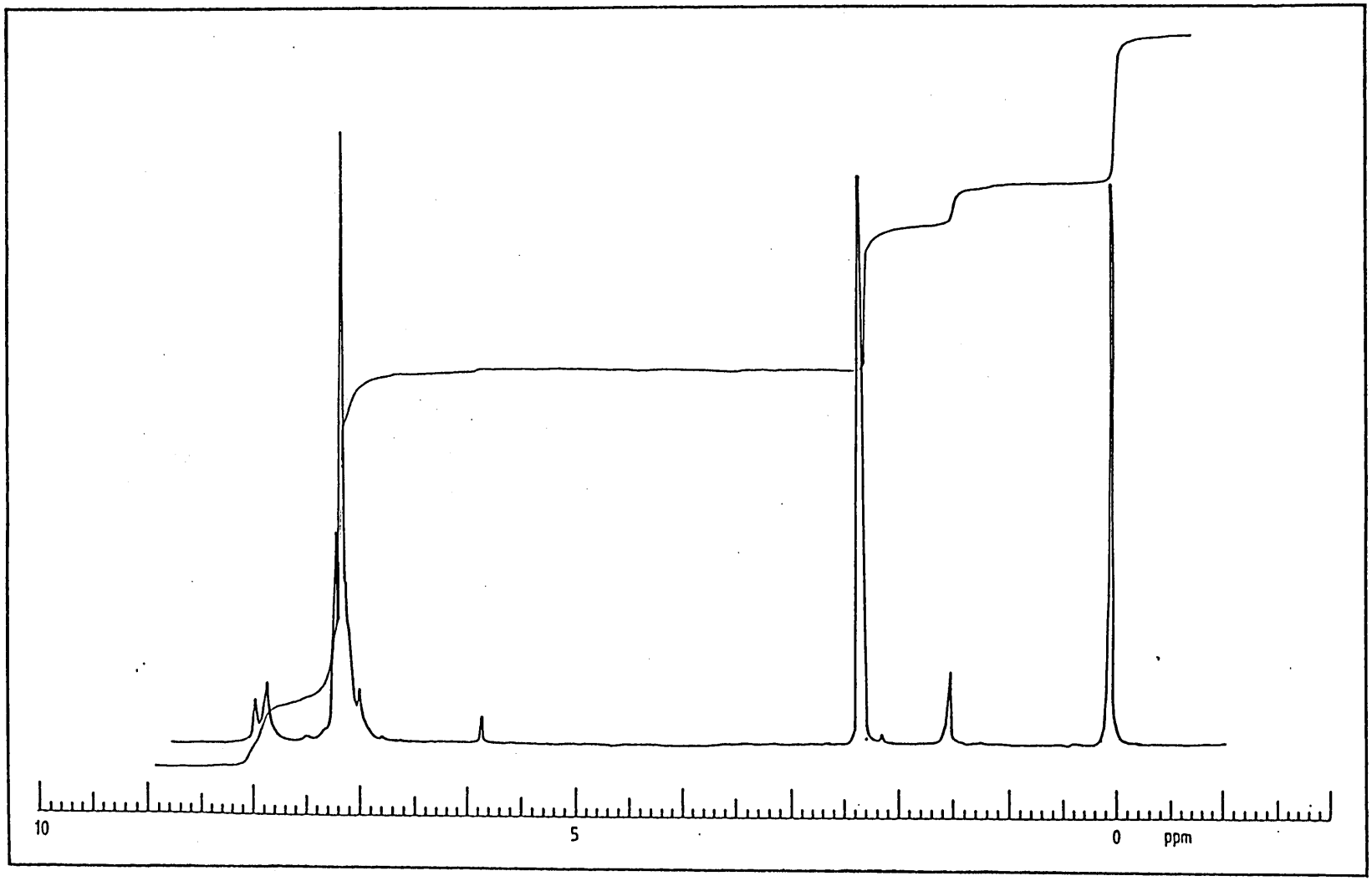

Figure 59: 80MHz ^{1}H nmr spectrum of the PES/epoxy PDMS solution copolymer product with the highest PDMS content (30%) after toluene extraction ($CDCl_3$ solvent).

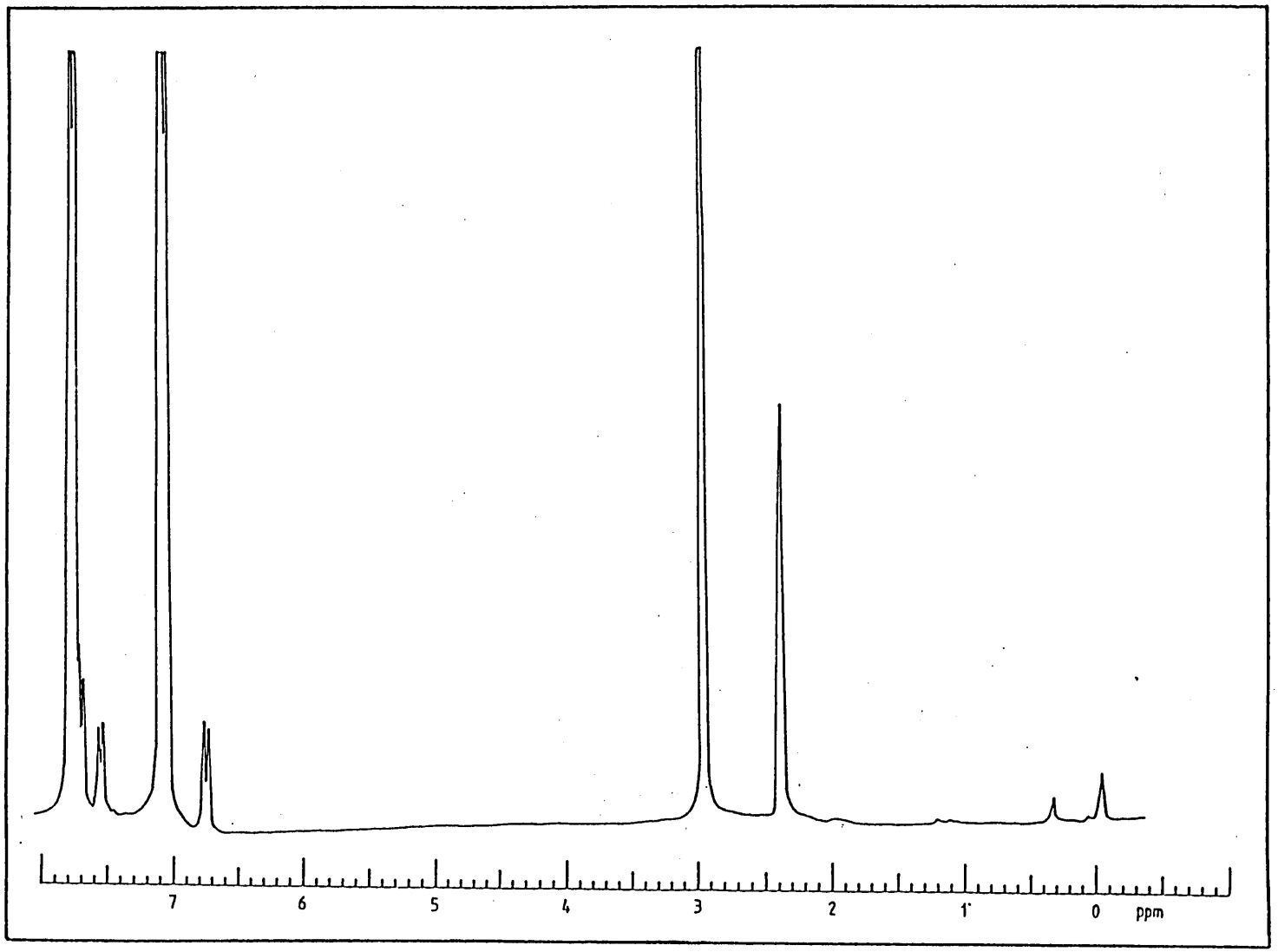

Figure 60: 270Mhz ^{1}H nmr spectrum of the PES/epoxy PDMS solution copolymer product with the highest PDMS content after toluene extraction (d-DMSO solvent).

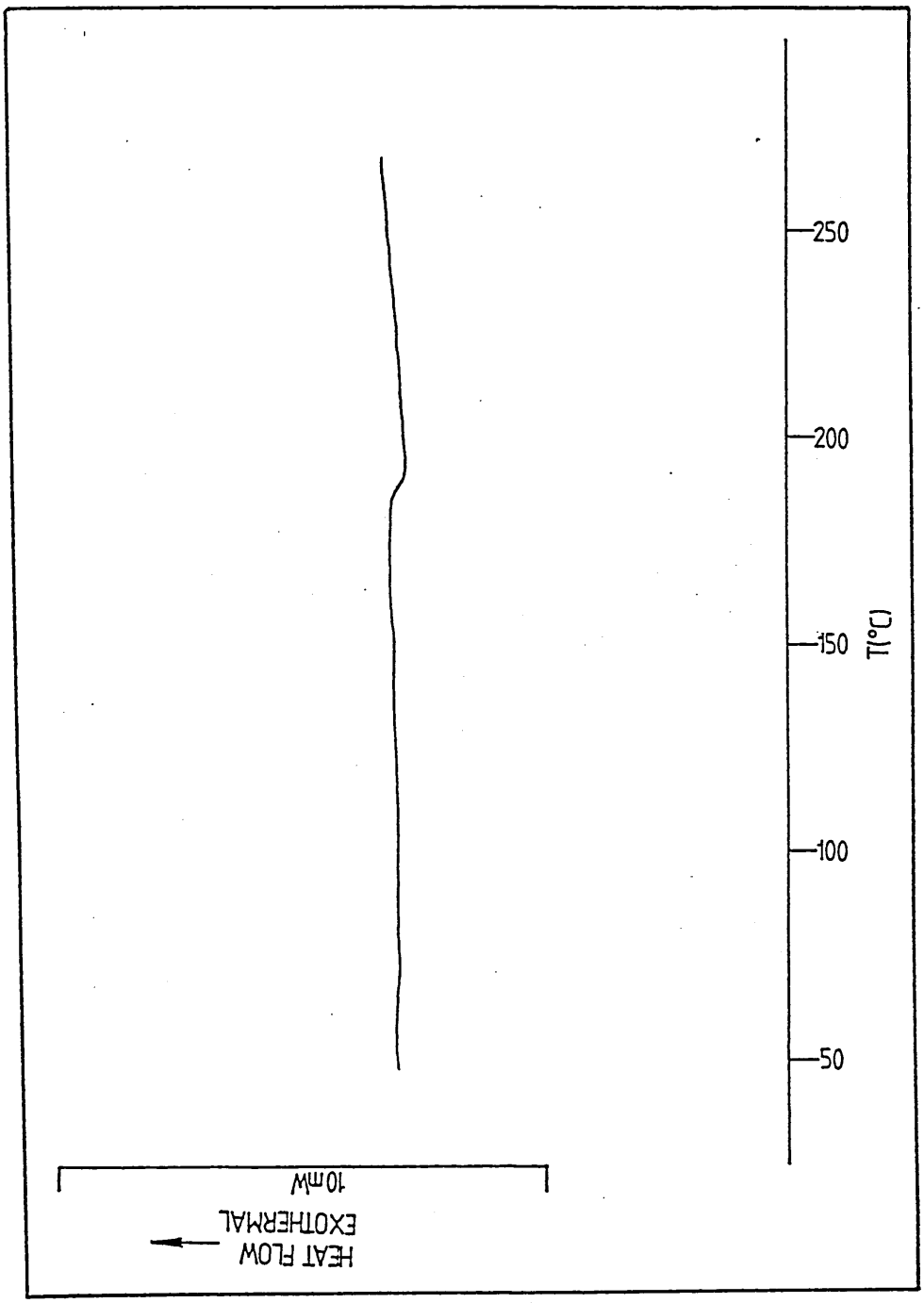

Figure 61: dsc trace of hydroxyl PES (RMM=4,370), Tg=189.4°C.

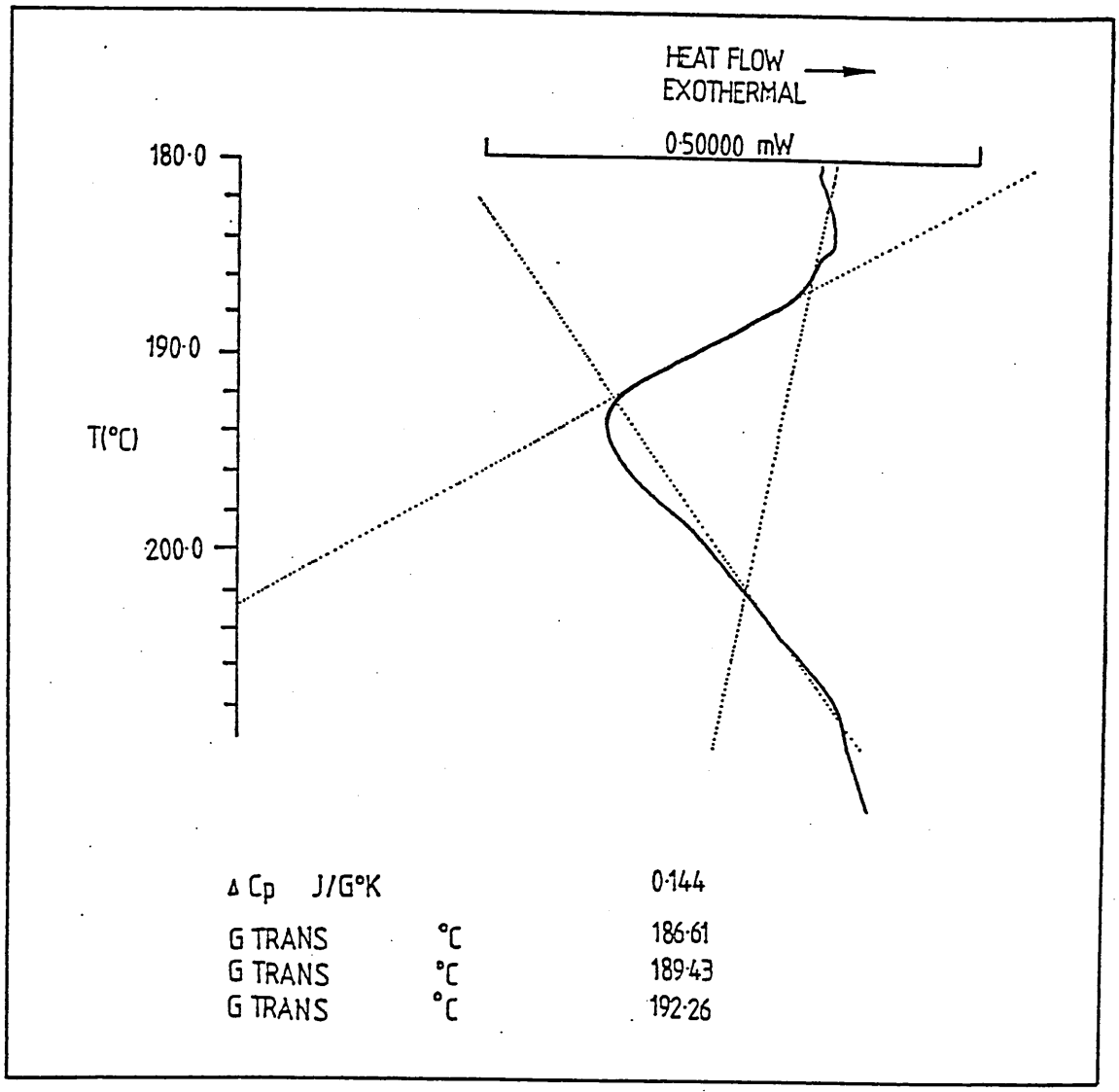

Figure 62: Microprocessor construction of the Tg calculation for hydroxyl PES (RMM=4,370).

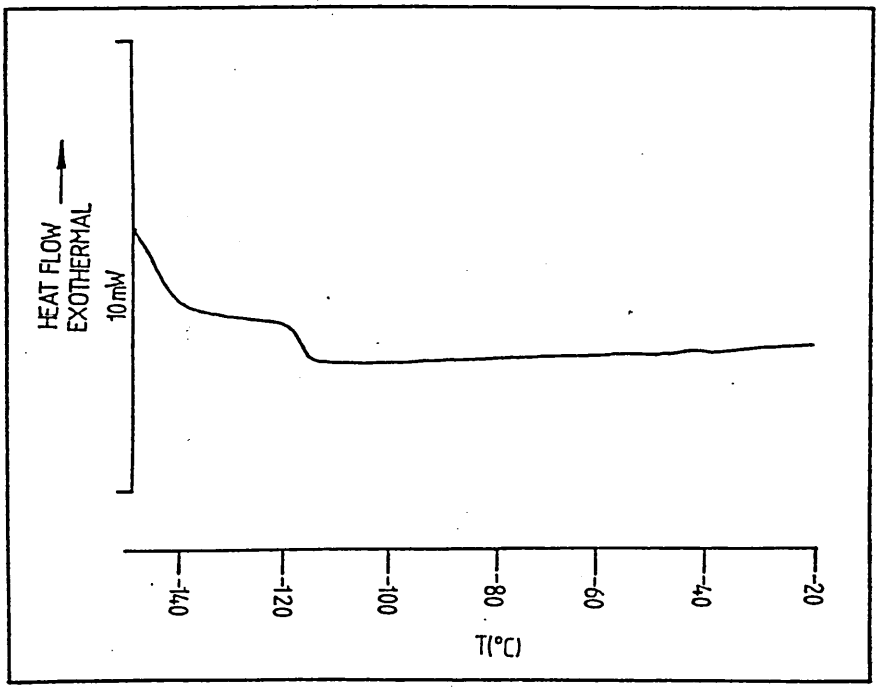

Figure 63: Dsc trace of epoxy functionalised PDMS (RMM=2,600), Tg=-116.5°C.

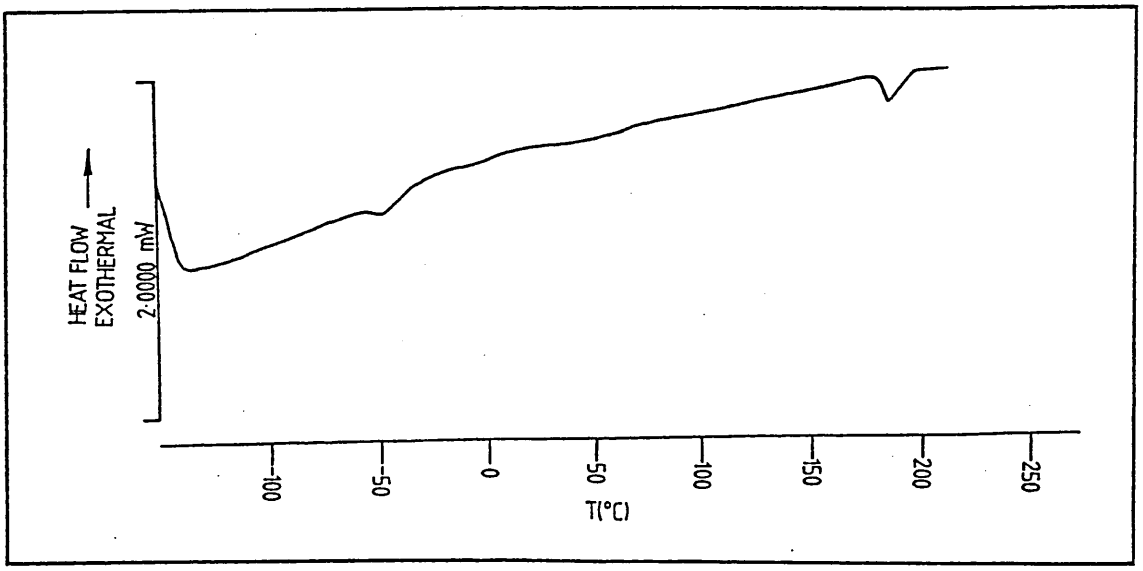

Figure 64: Dsc trace of PES/epoxy PDMS copolymer sample (30% PDMS by ^1H nmr analysis).

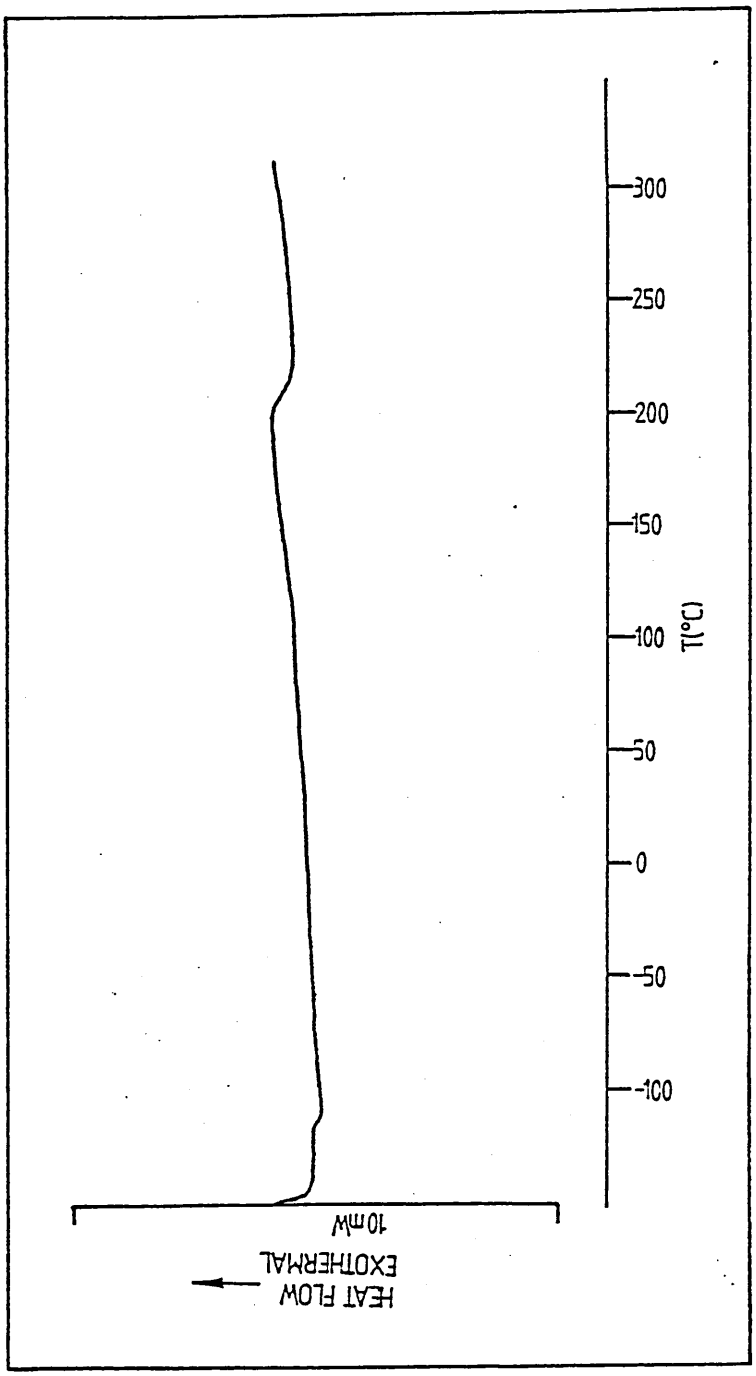

Figure 65: Dsc trace of a 30% w/w epoxy PDMS (RMM=2,600)/PES (RMM=4,370) blend.

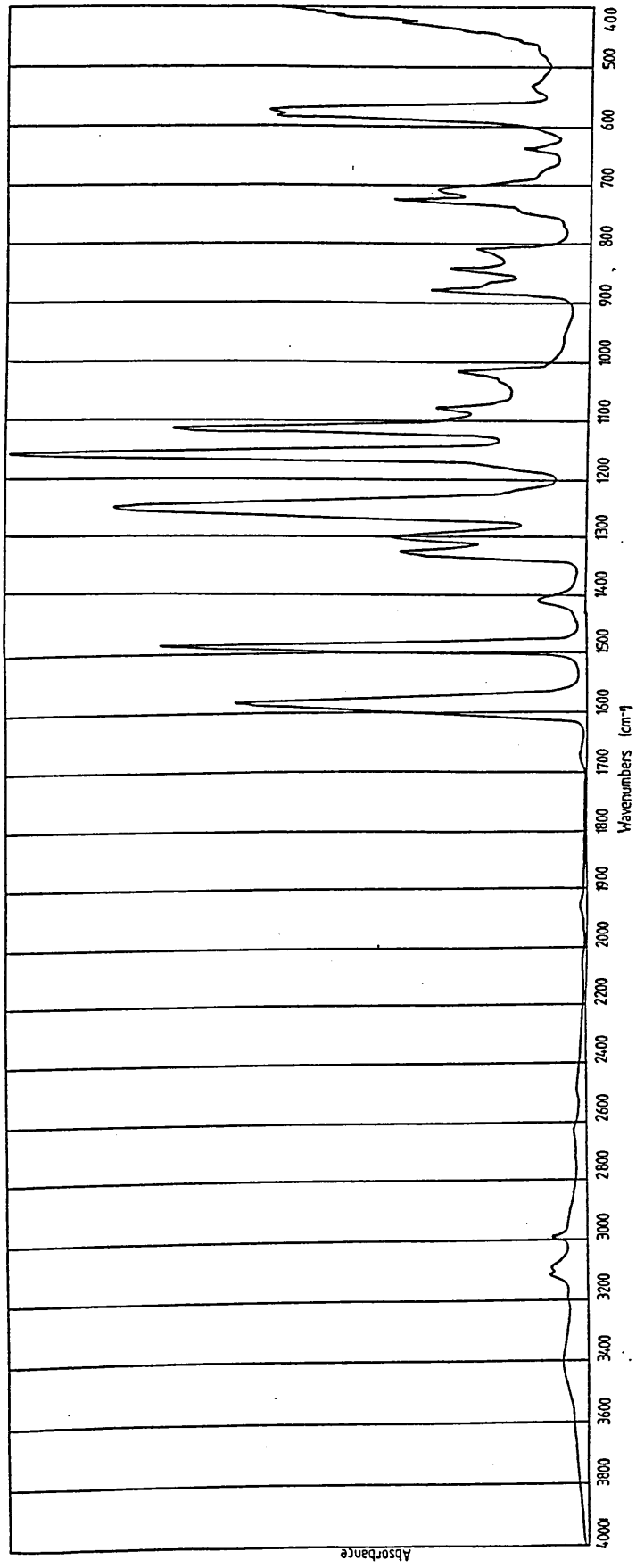

Figure 66: Infra-red spectrum of a v-PES/PDMS vinyl (11% PDMS) addition product after toluene extraction (Nicolet FT-IR instrument).

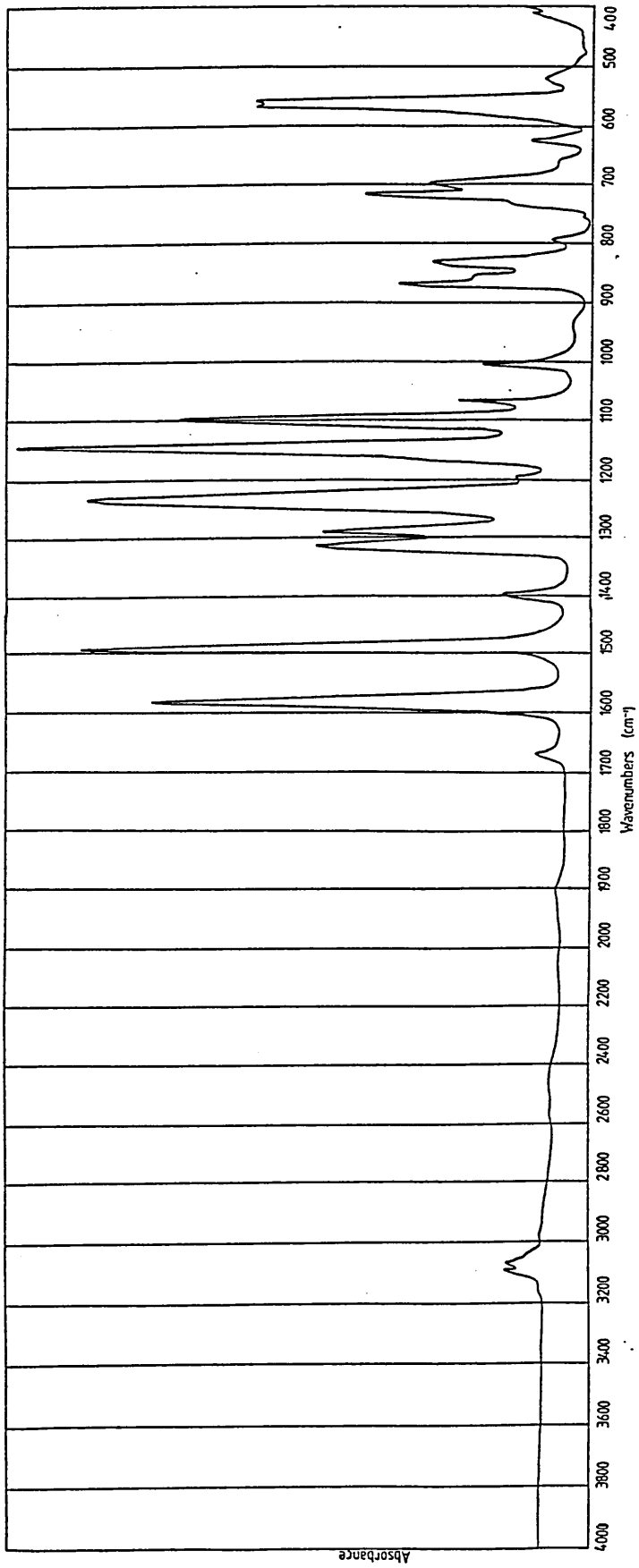

Figure 67: Infra-red spectrum of v-PES (Nicolet FT-IR instrument).

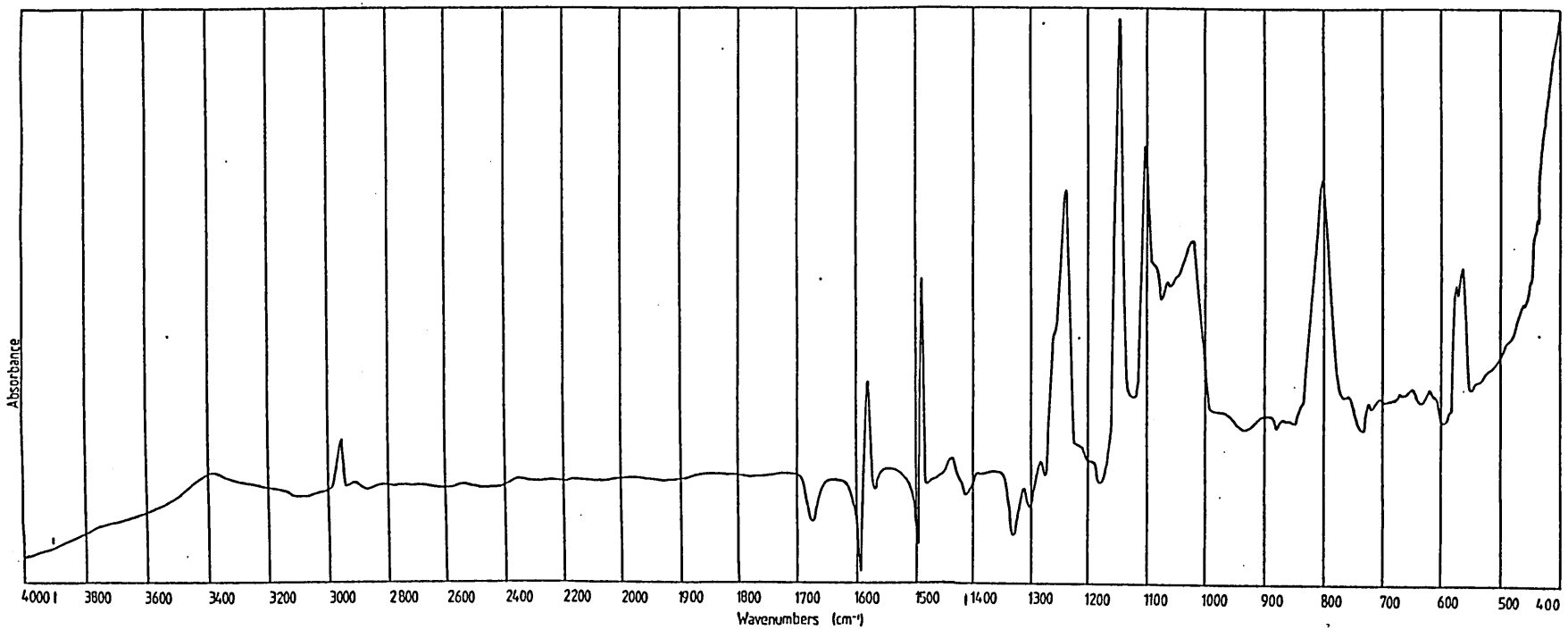

Figure 68: Infra-red spectrum prepared by subtracting the ir spectrum of v-PES (Figure 67) from the spectrum of v-PES/PDMS copolymerisation product (Figure 66), Mattson-Cygnus data handling system.

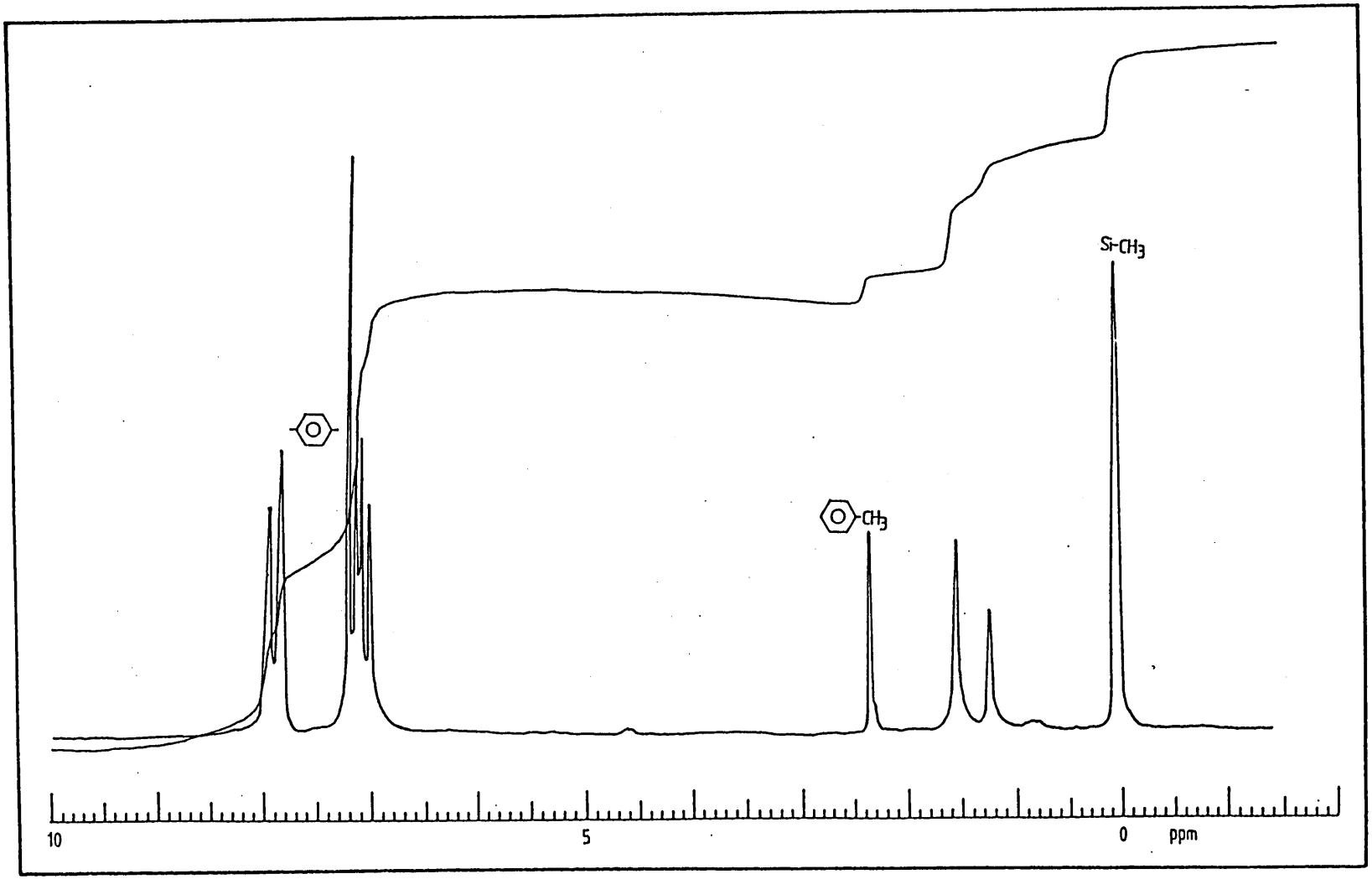

Figure 69: 80MHz ^1H nmr spectrum of v-PES/PDMS vinyl addition copolymer product with the highest PDMS content (11%) after toluene extraction ($CDCl_3$ solvent).

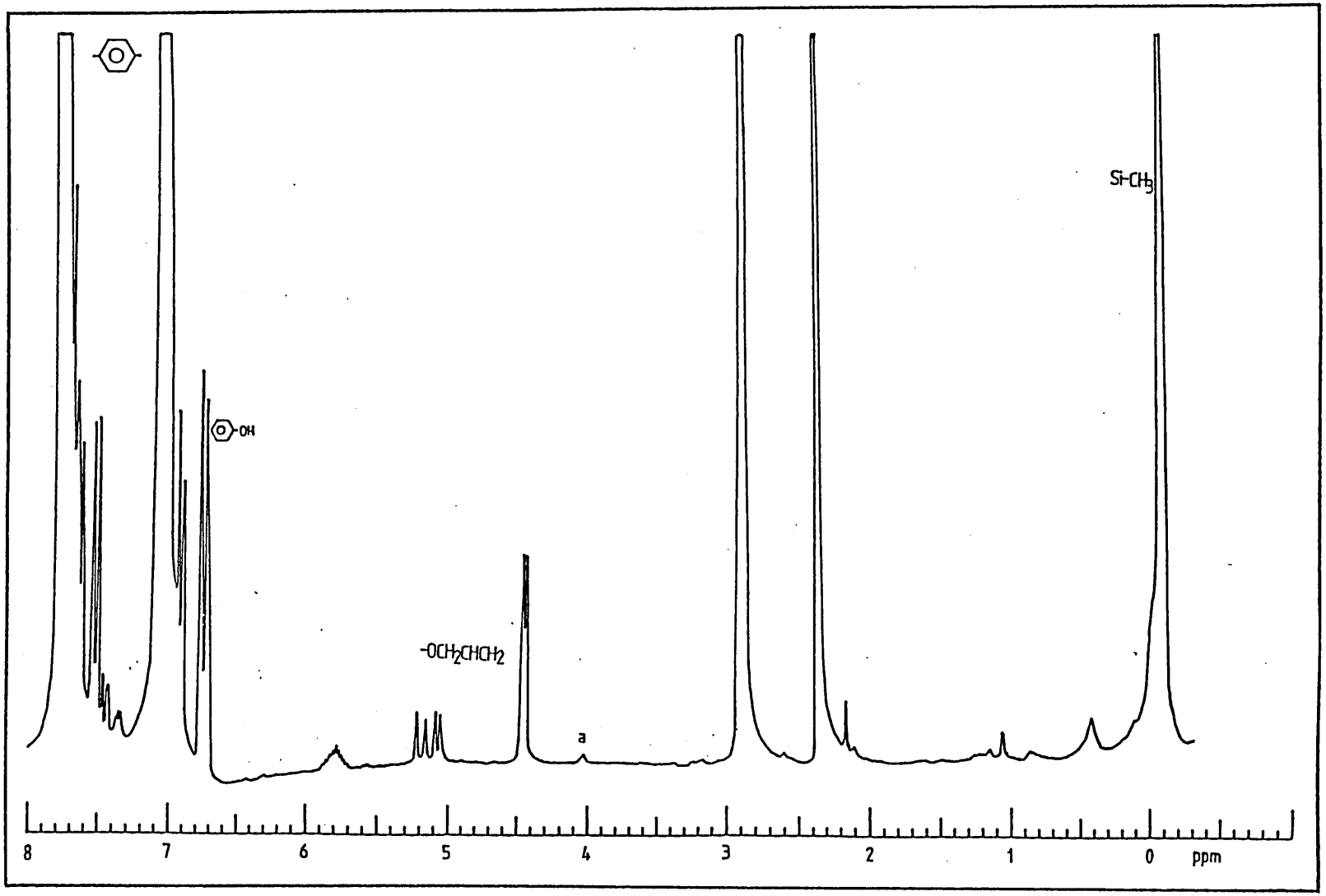

Figure 70: 270MHz ^{1}H nmr spectrum of v-PES/PDMS vinyl addition copolymer product with the highest PDMS content (11%) after toluene extraction (d-DMSO solvent).

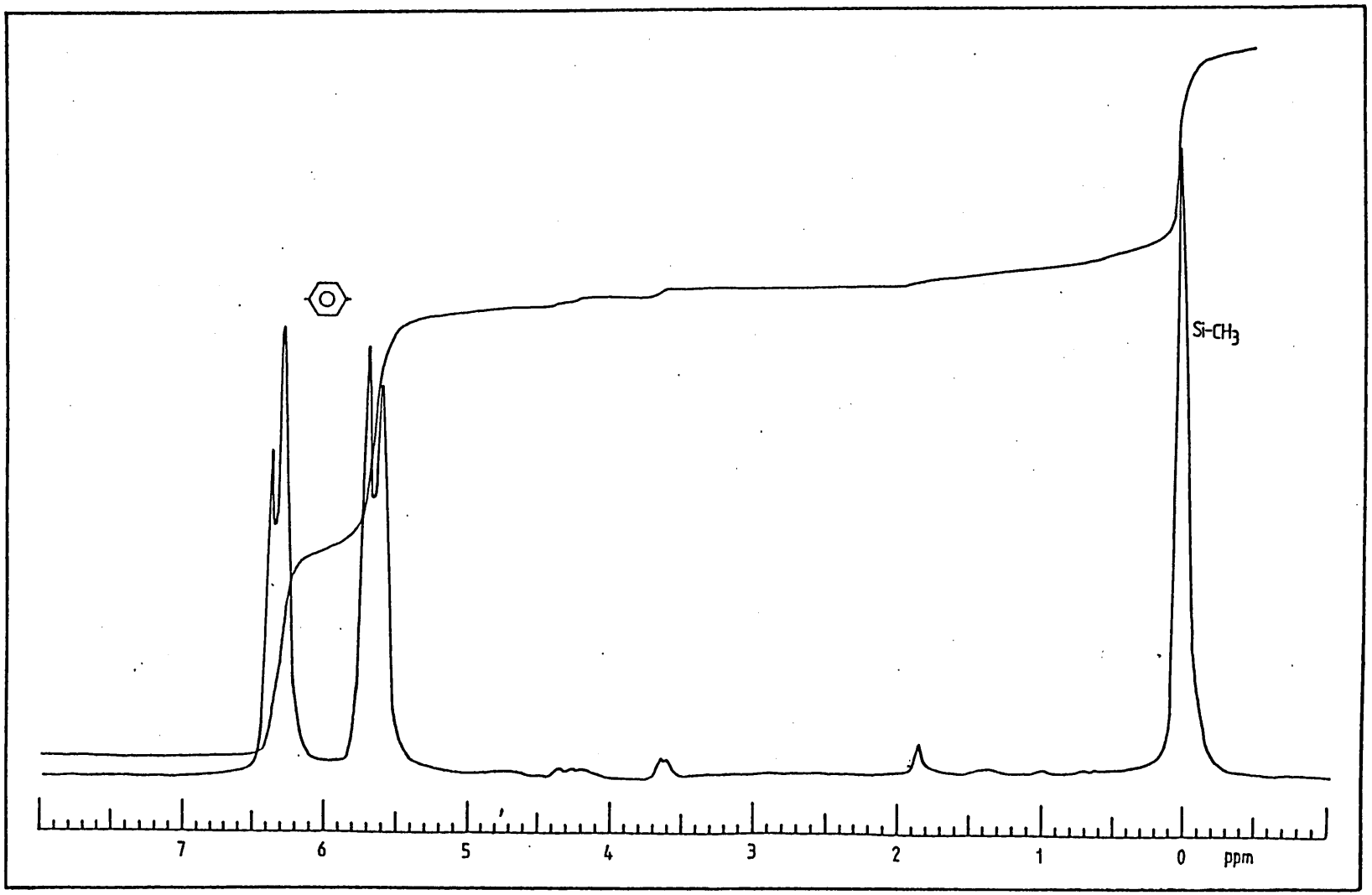

Figure 71: 80MHz ^1H nmr spectrum v-PES (RMM=4,450)/PDMS (RMM=4,370) vinyl addition product after toluene extraction ($CDCl_3$ solvent).

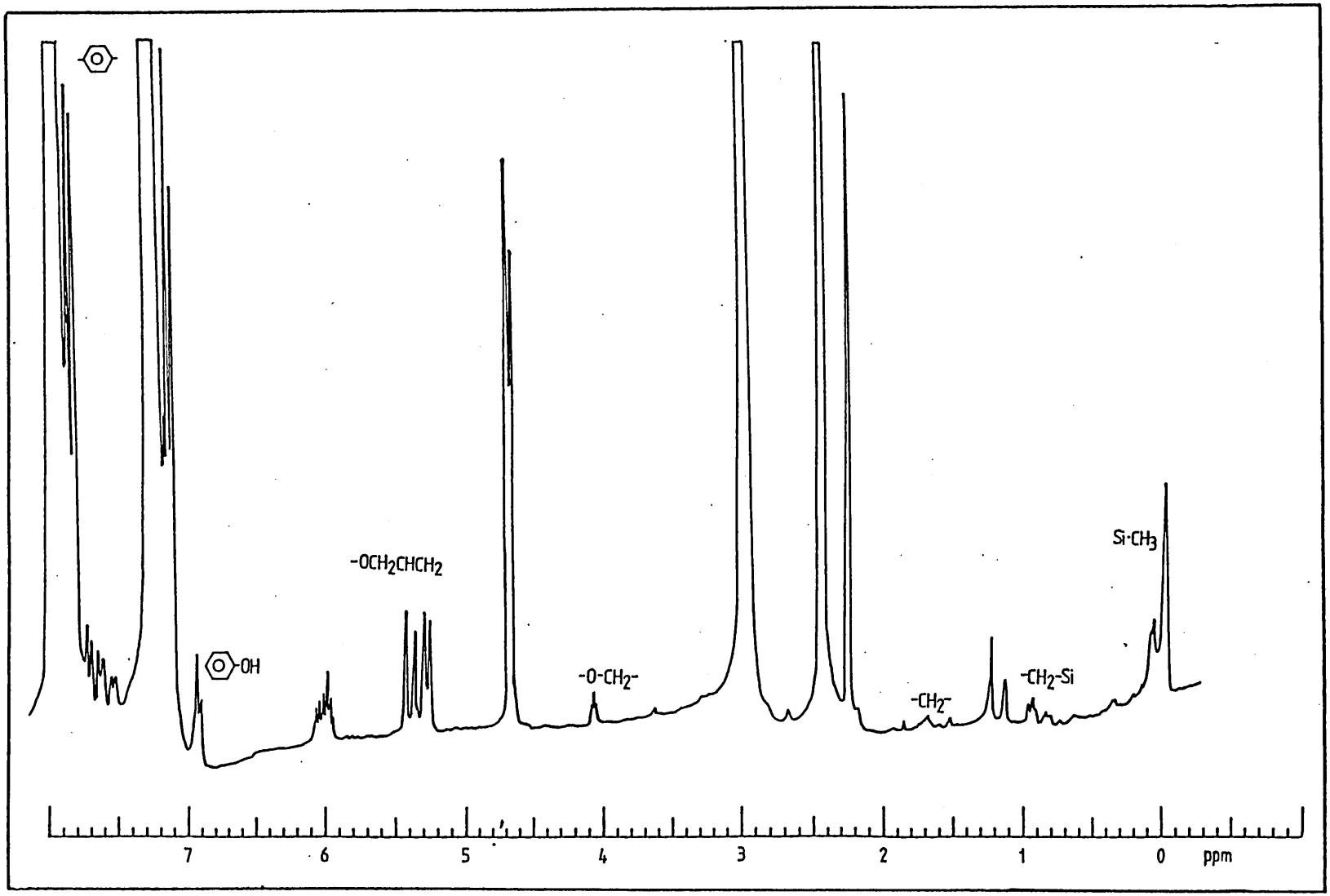

Figure 72: 270MHz ^1H nmr spectrum v-PES (RMM=4,450)/PDMS (RMM=4,370) vinyl addition product after toluene extraction (d-DMSO solvent).

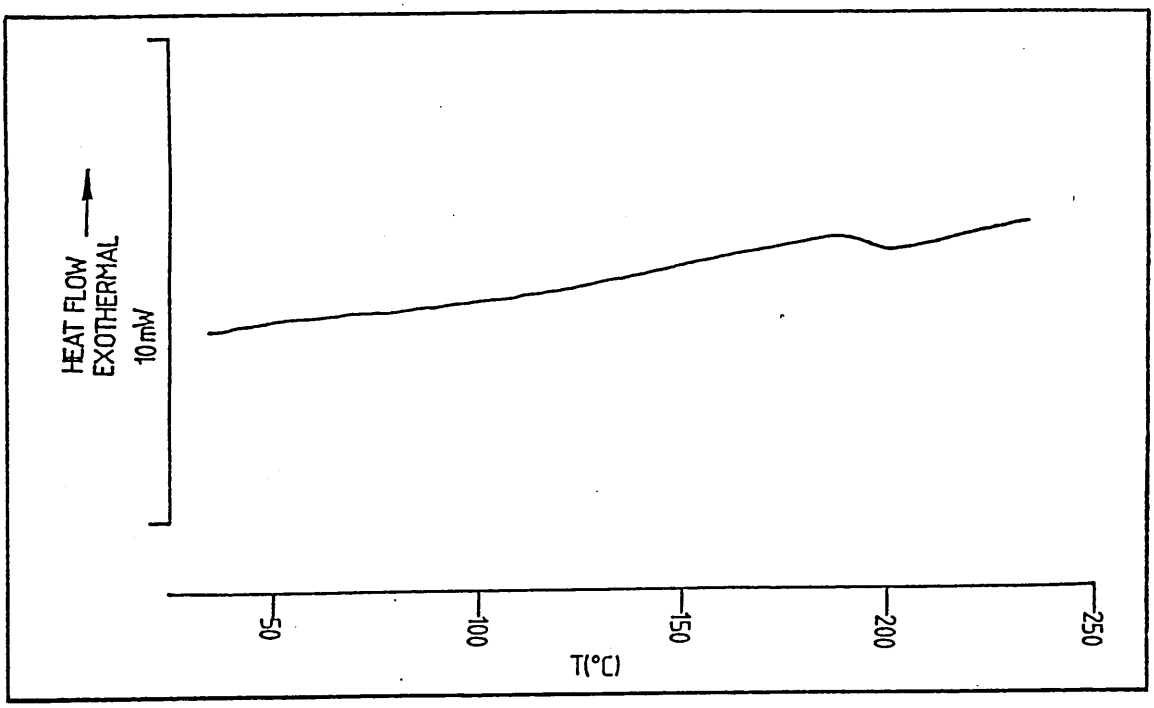

Figure 73: Dsc trace of v-PES (RMM=4,450), Tg=195.75°C.

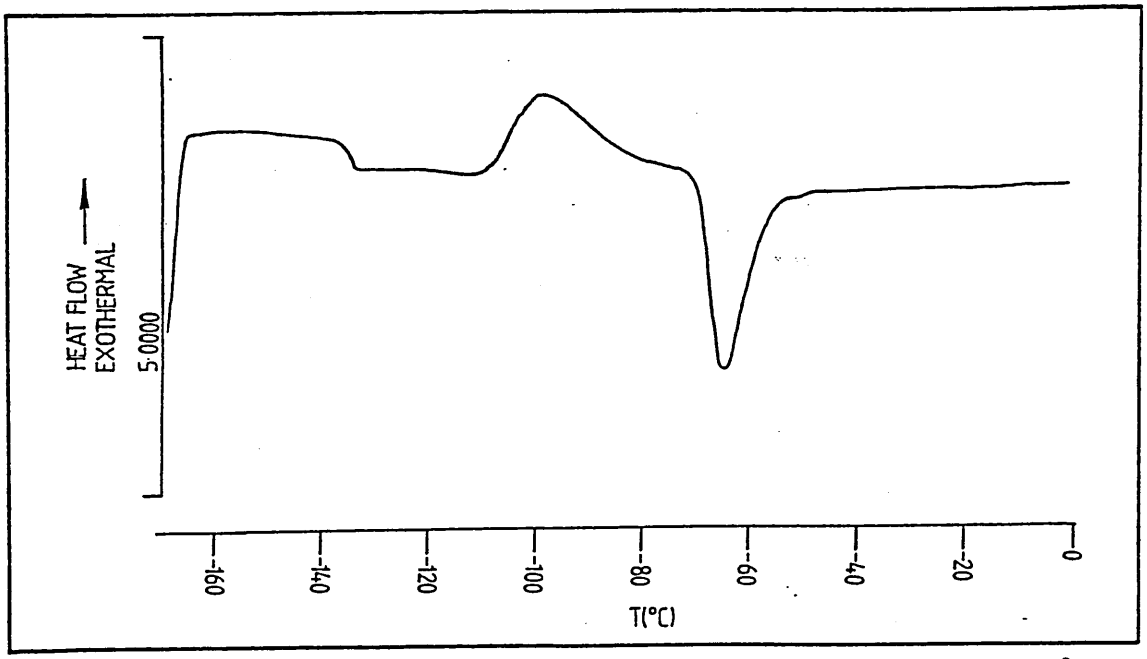

Figure 74: Dsc trace of hydride PDMS (RMM=700), Tg=136.5°C.

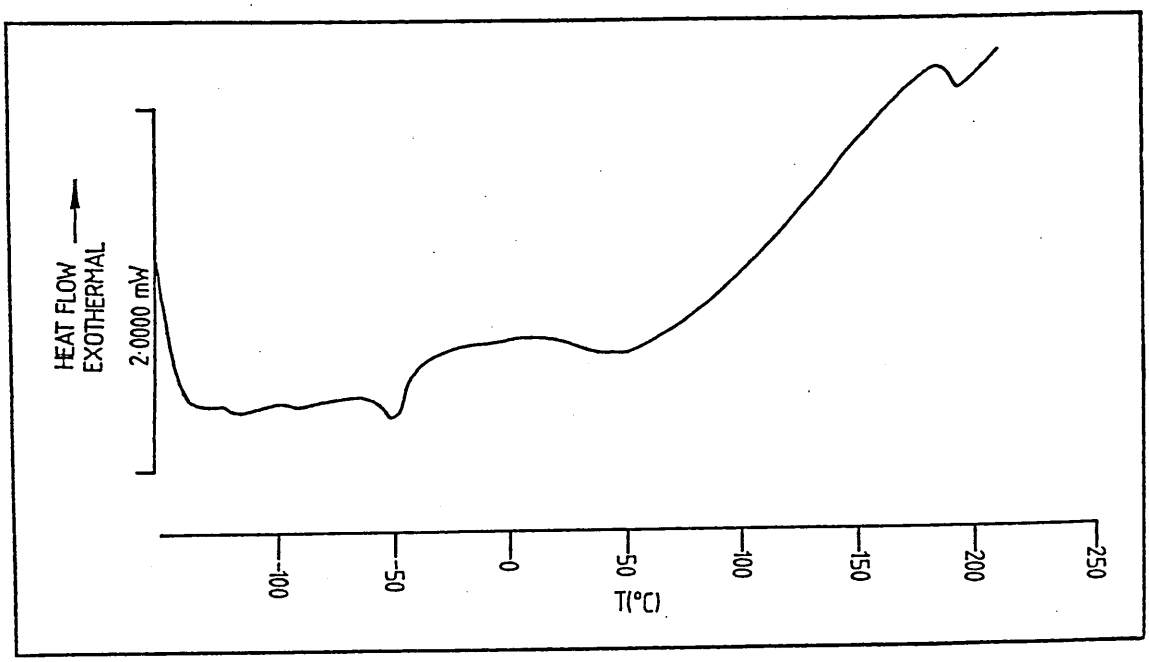

Figure 75: Dsc trace of v-PES (RMM=4,450)/PDMS (RMM=700) vinyl addition product after toluene extraction.

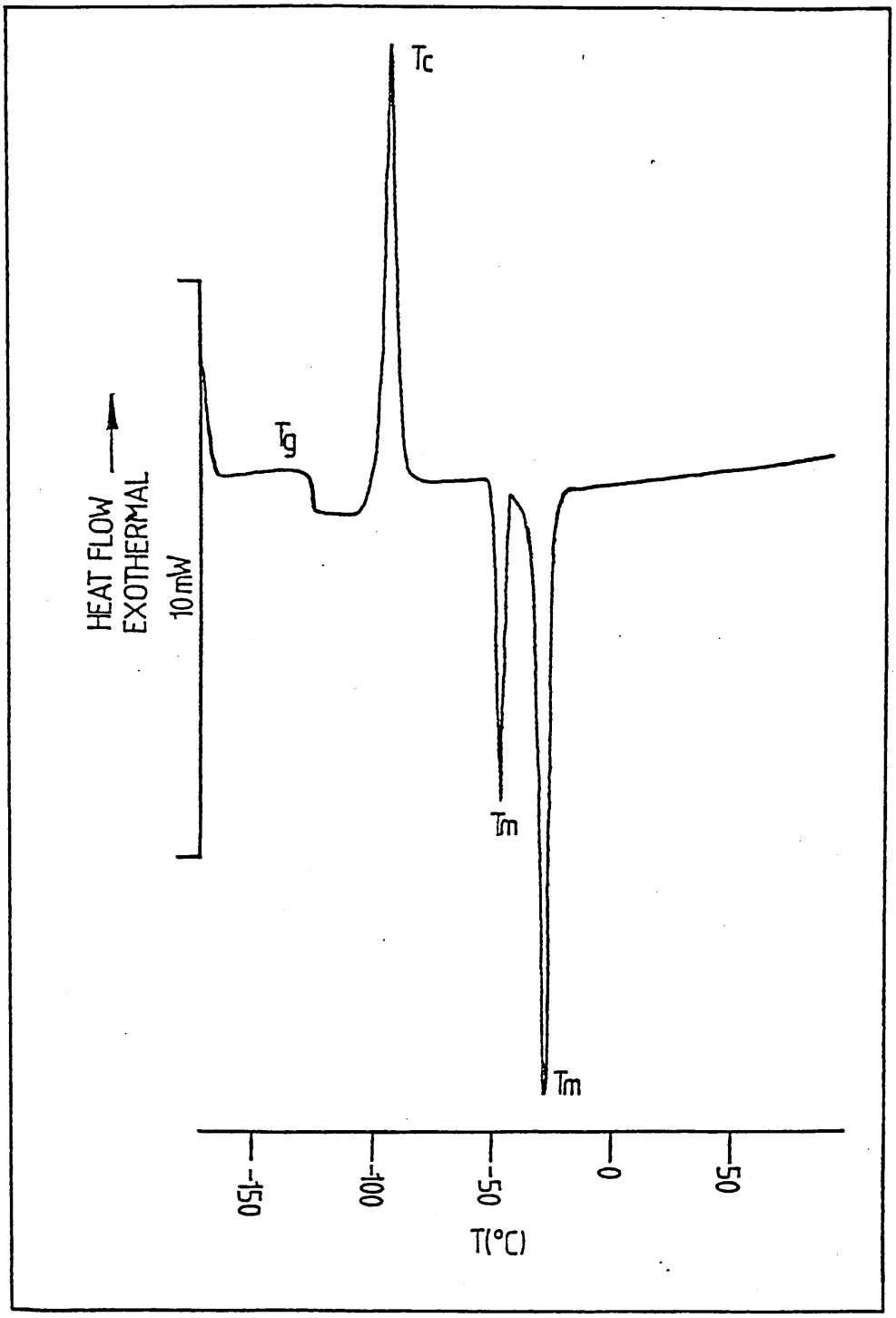

Figure 76: Dsc trace of hydride PDMS (RMM=4,370).

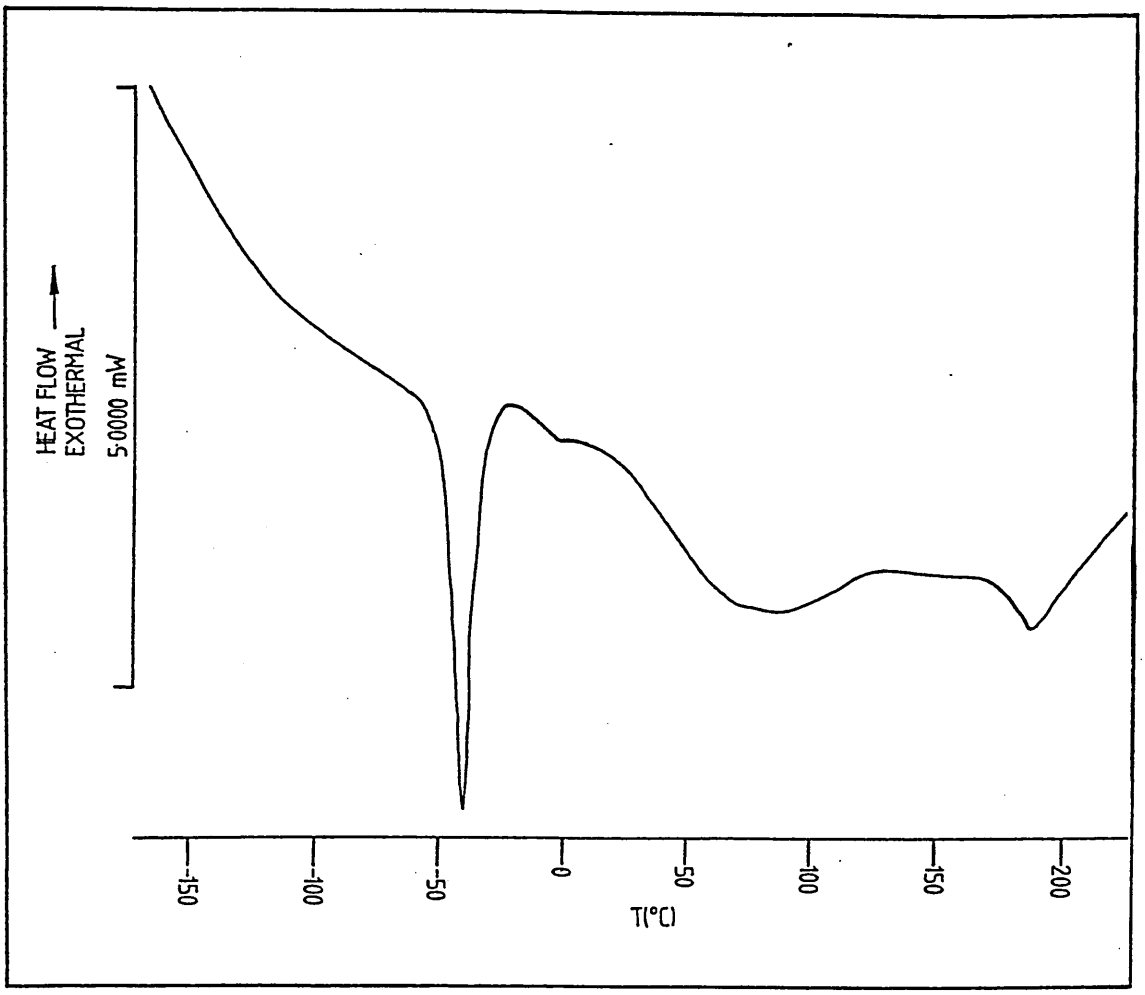

Figure 77: Dsc trace of v-PES (RMM=4,450)/PDMS (RMM=4,370) vinyl addition product after toluene extraction.

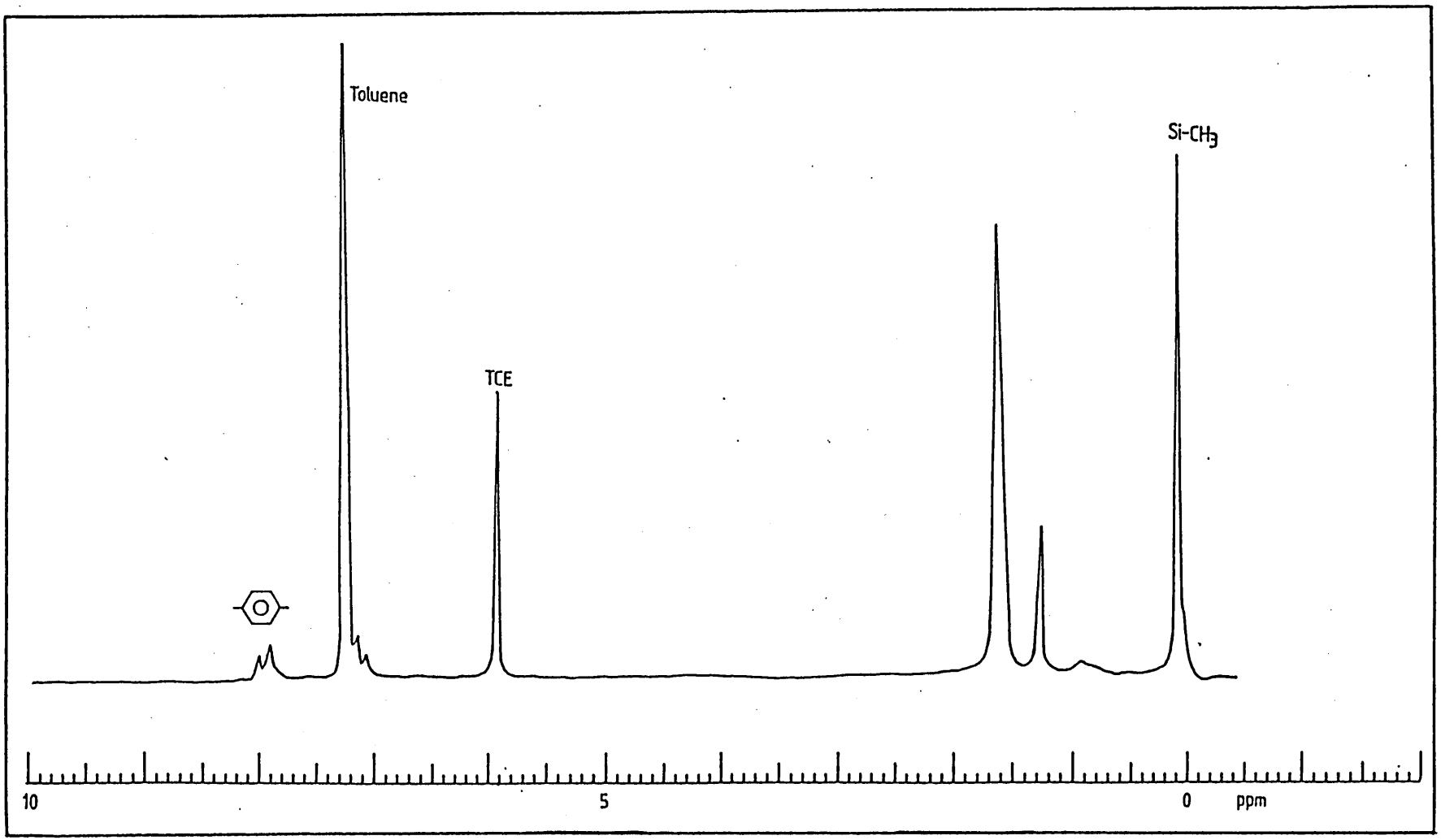

Figure 78: 80MHz ^1H nmr spectrum of the melt reaction between epoxy PDMS/hydroxyl PES after TCE extraction ($CDCl_3$ solvent).

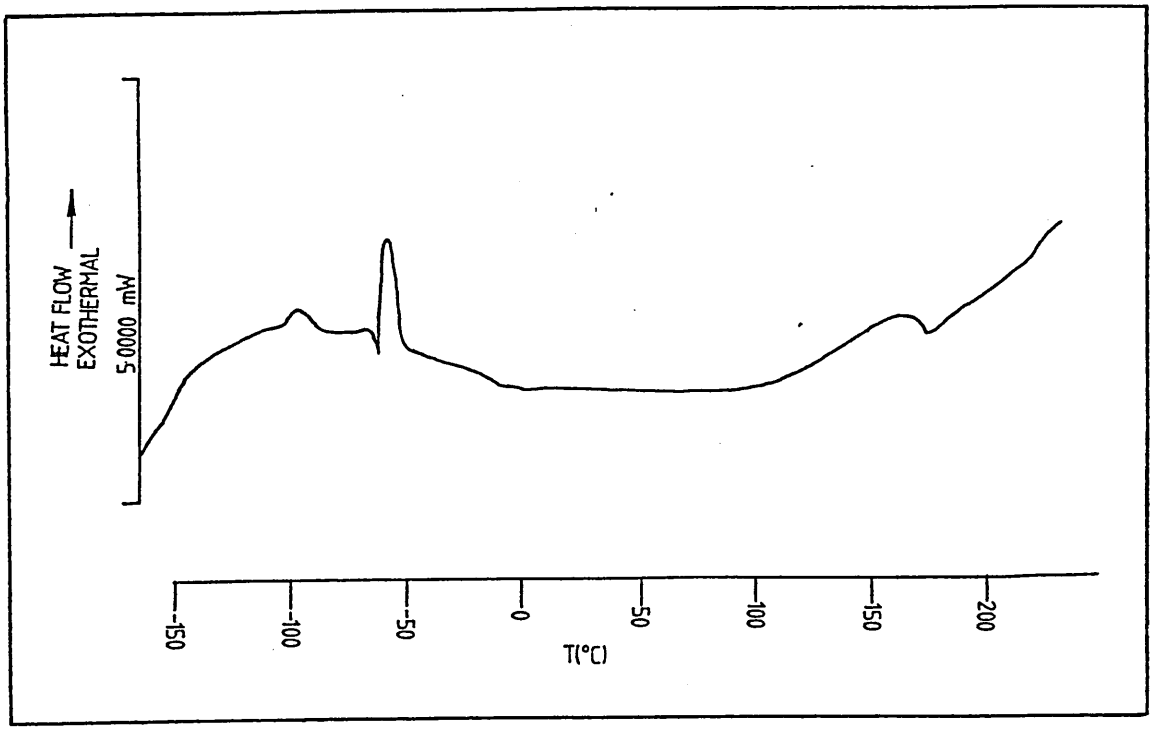

Figure 79: Dsc trace of melt reaction EB1 after toluene extraction, no catalyst.

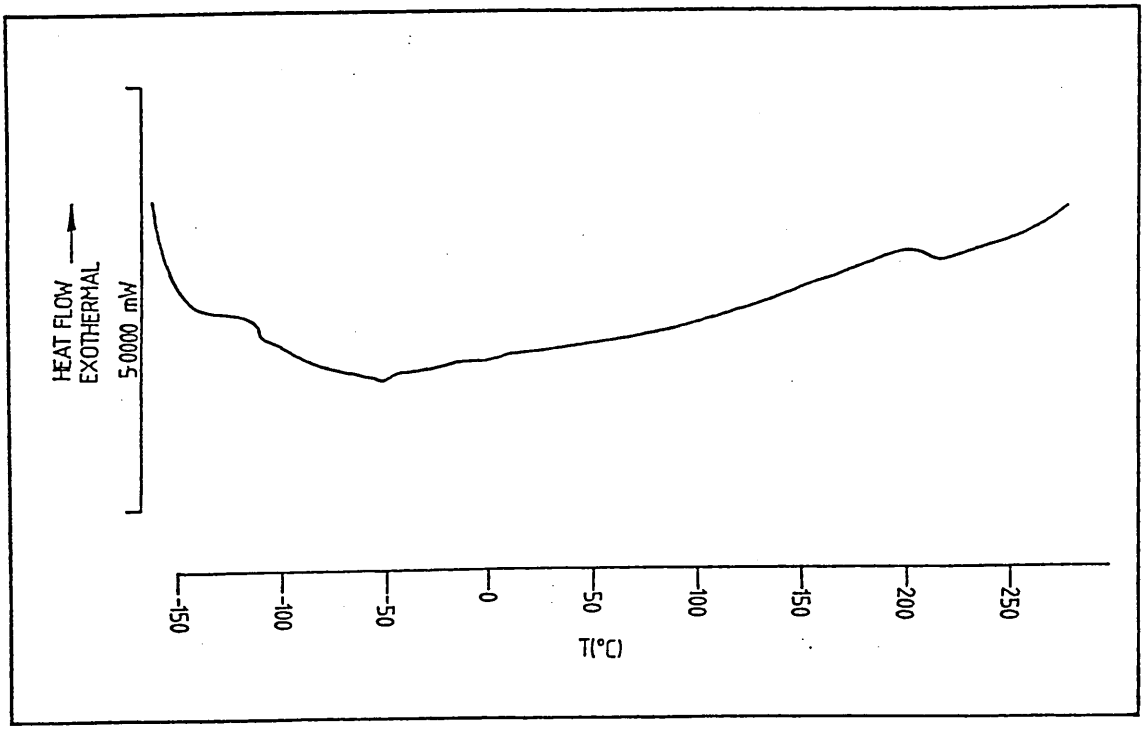

Figure 80: Dsc trace of melt reaction EB3 after TCE extraction, DDS catalyst.

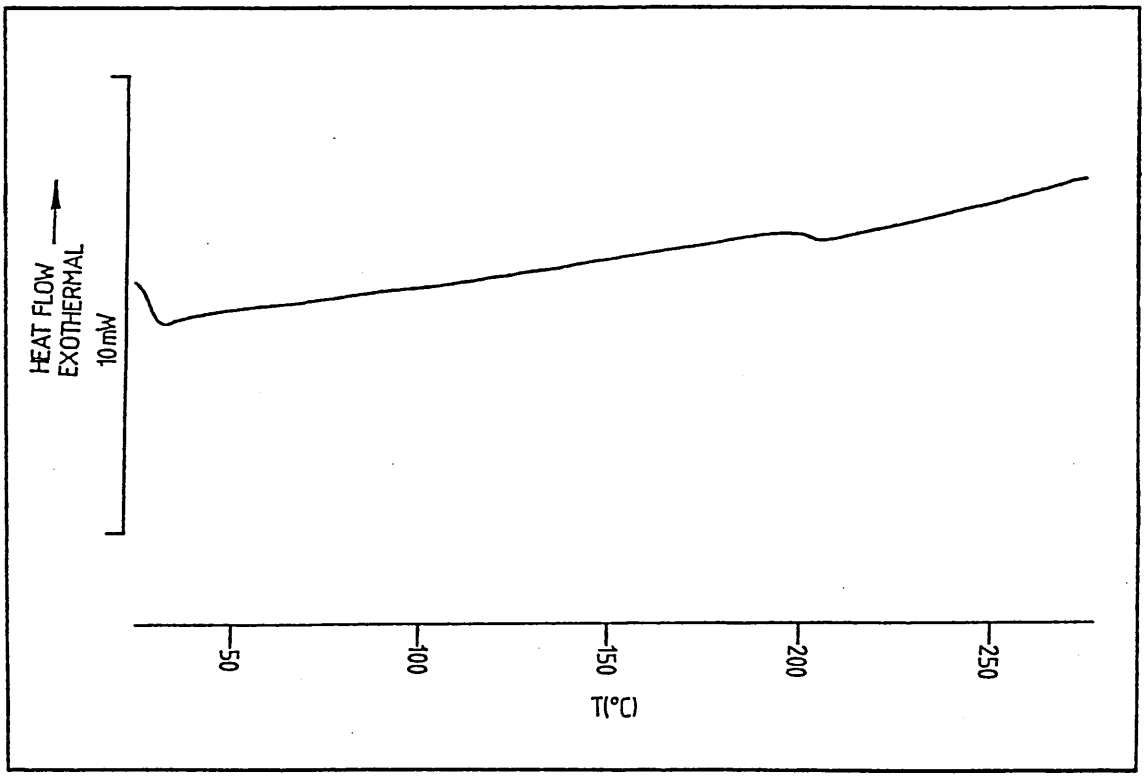

Figure 81: Dsc trace of hydroxyl PES (RMM=3,709), Tg=203.7°C.

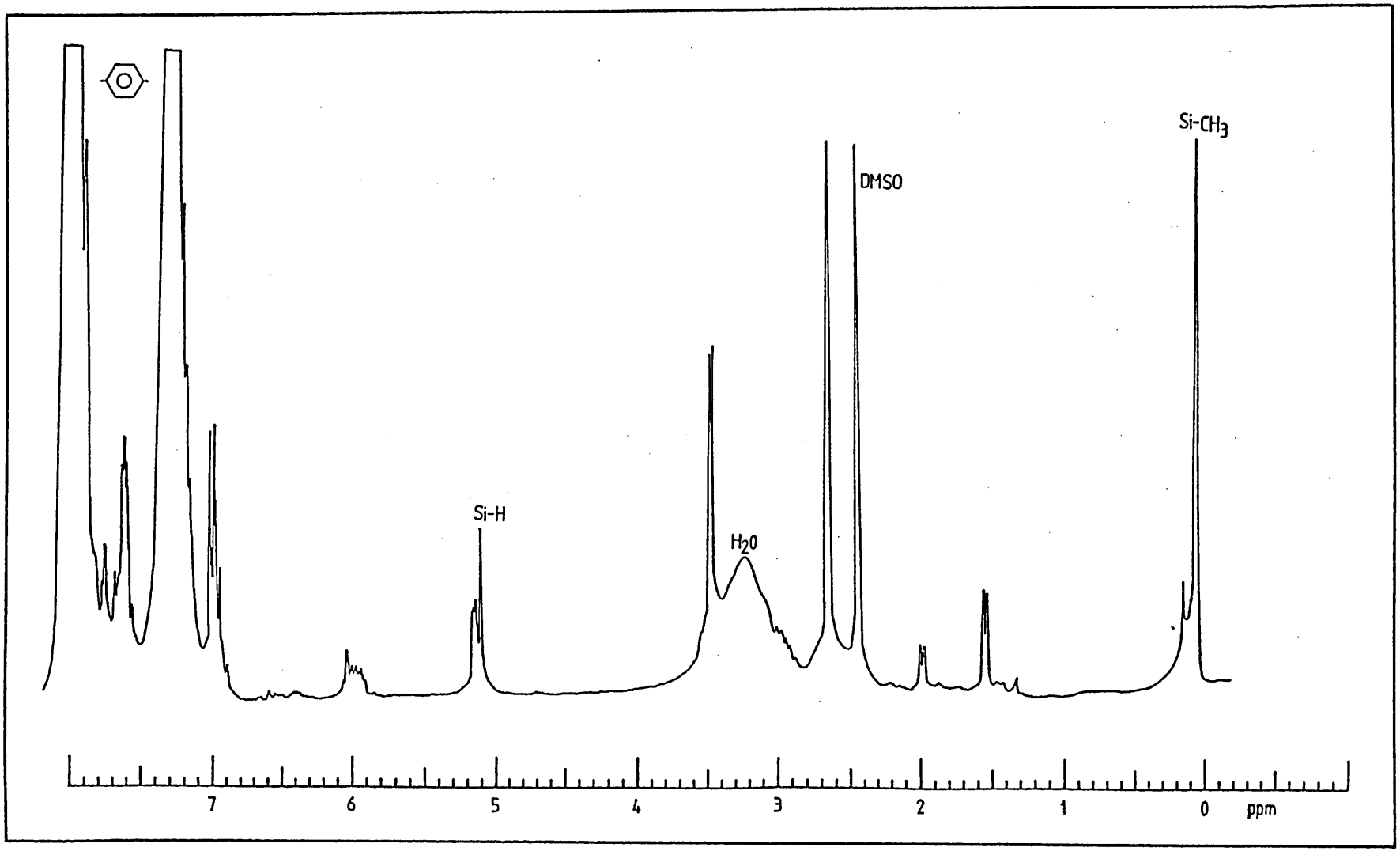

Figure 82: 400MHz ^1H nmr spectrum of melt reaction VB3 after toluene extraction (d-DMSO solvent).

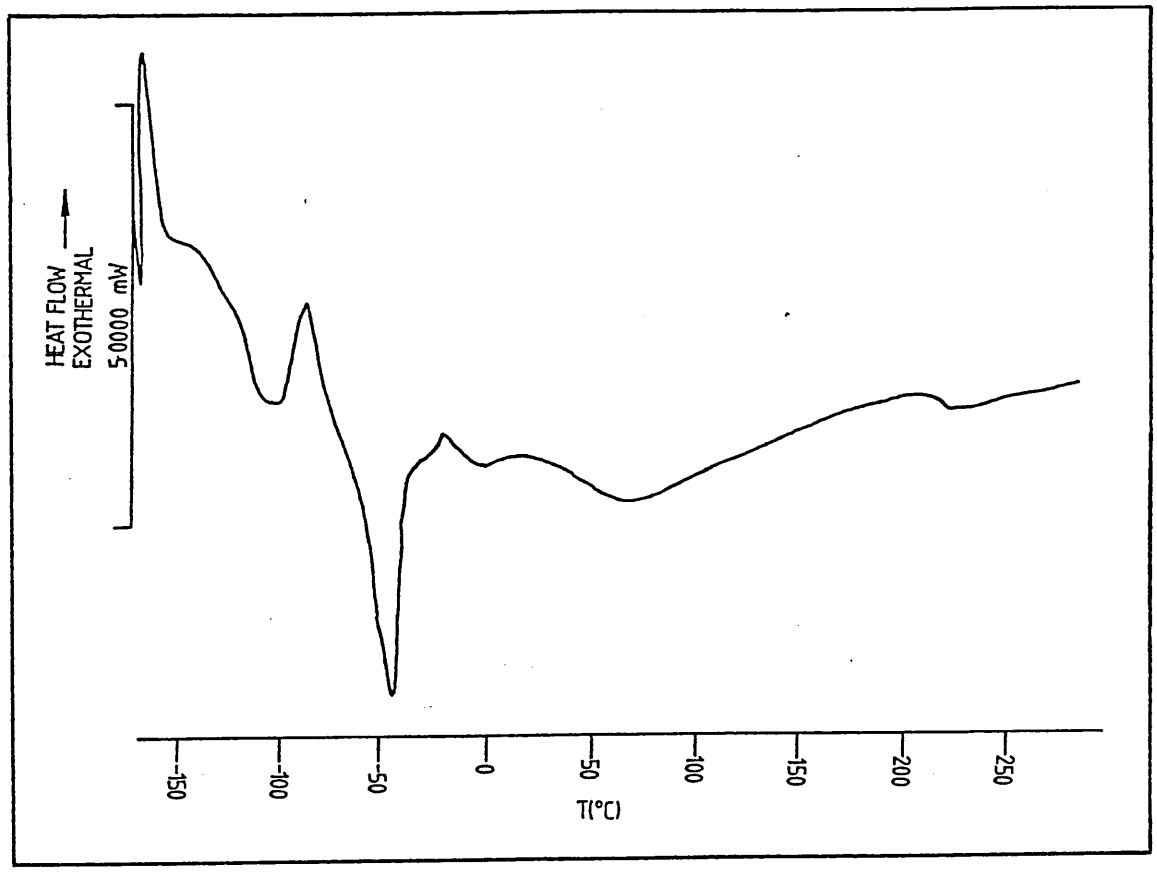

Figure 83: Dsc trace of melt reaction VB1 after toluene extraction. (Chloroplatinic acid catalyst in solution).

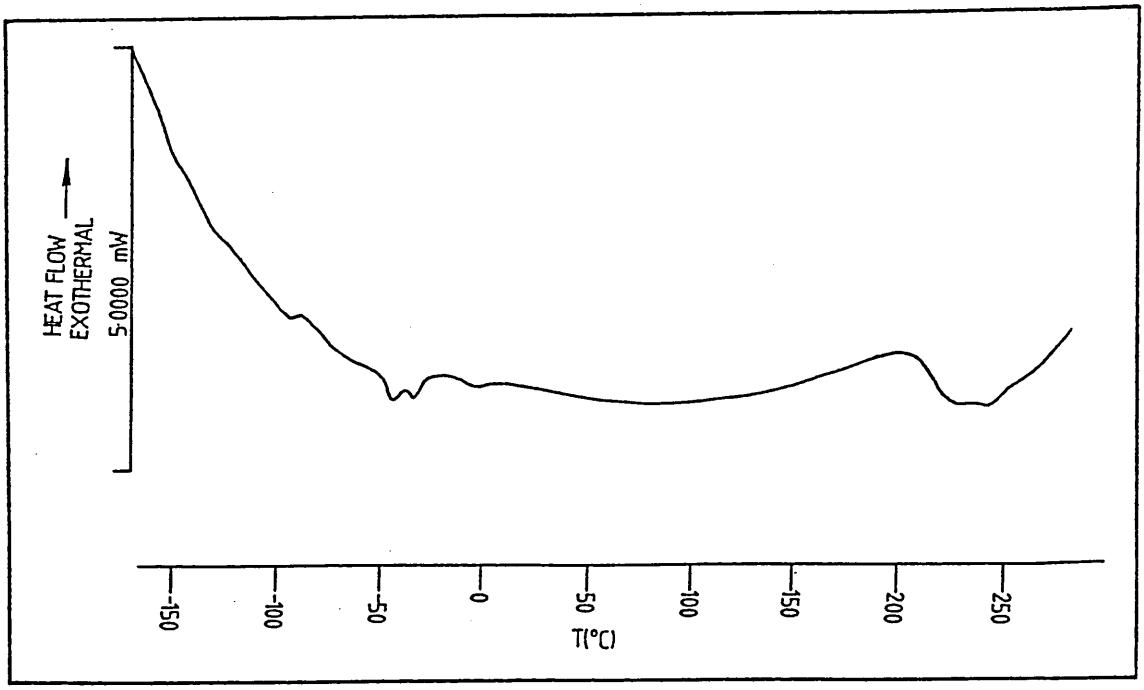

Figure 84: Dsc trace of melt reaction VB2 after toluene extraction. (Solid chloroplatinic acid catalyst).

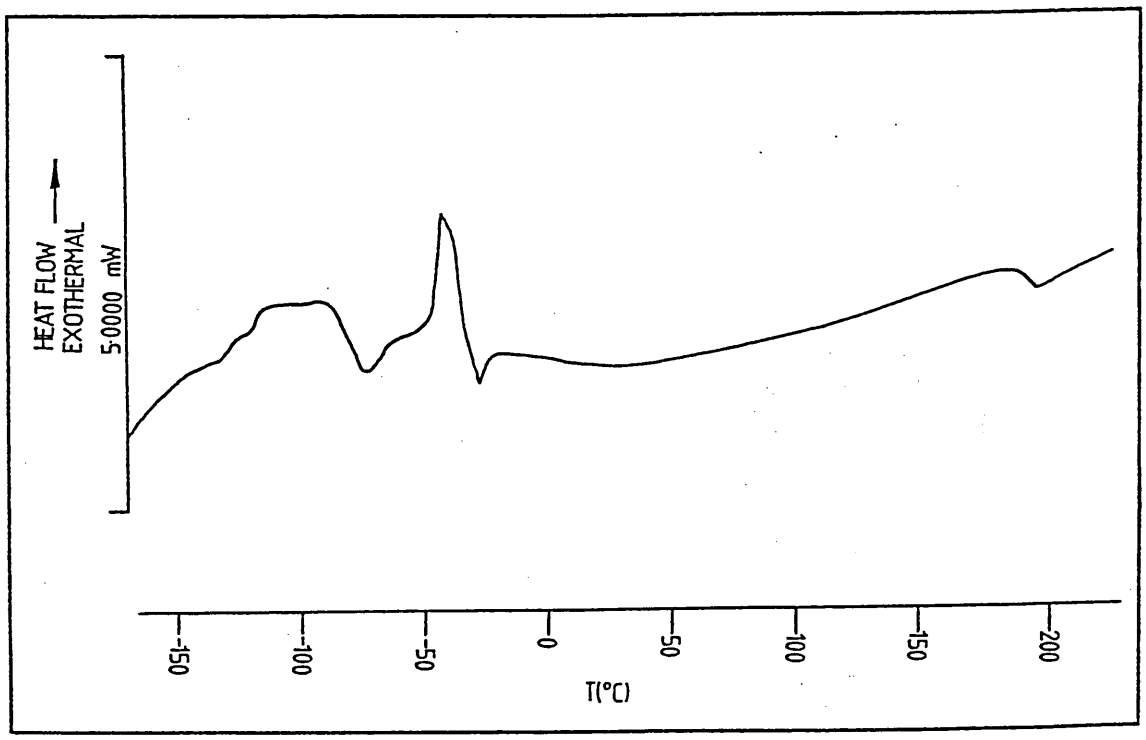

Figure 85: Dsc trace of melt reaction VB3 after toluene extraction. (Cumene hydroperoxide catalyst).

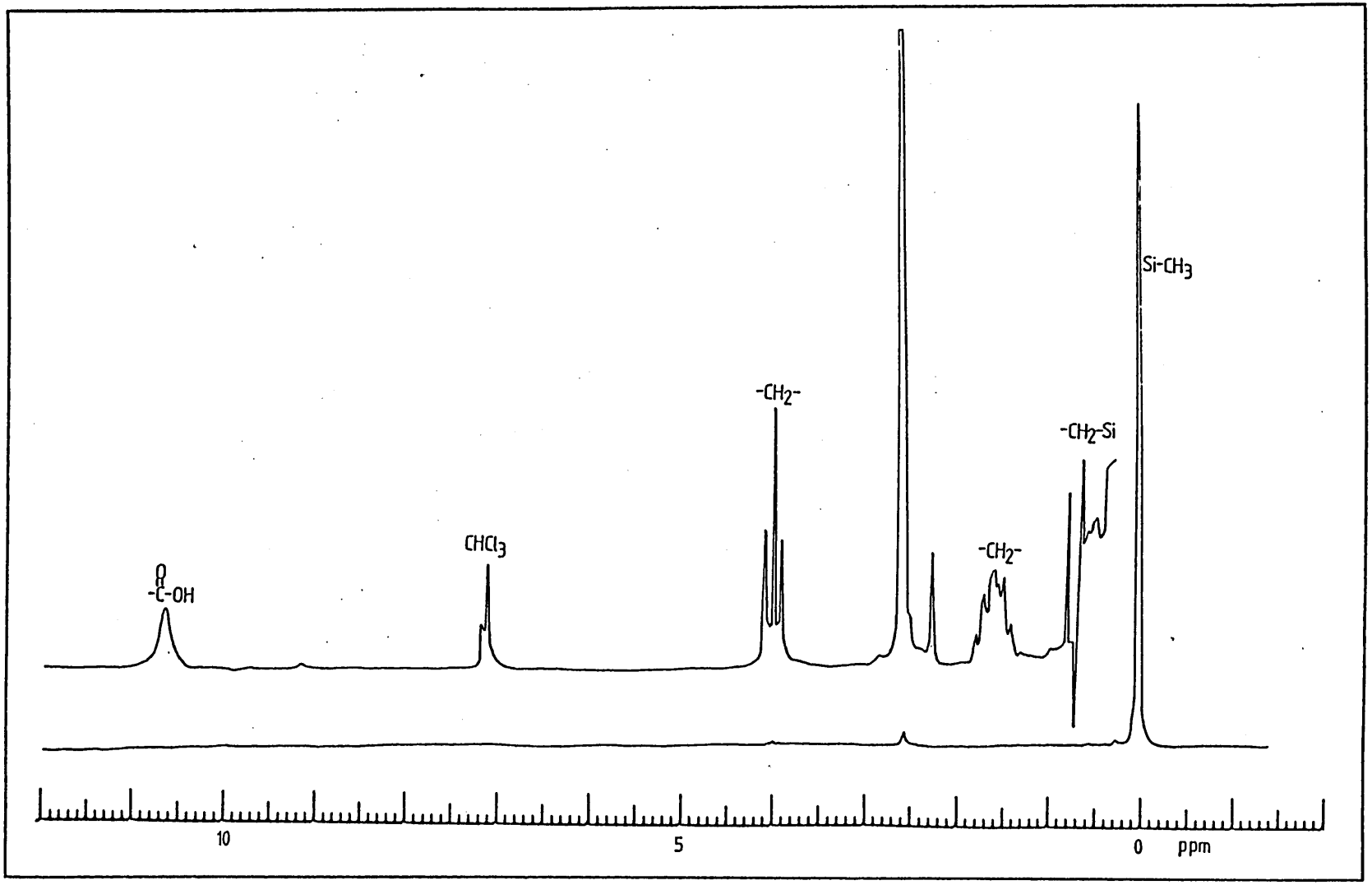

Figure 86: 80MHz ^1H nmr spectrum of carboxy propyl PDMS, RMM=2,000 ($CDCl_3$ solvent).

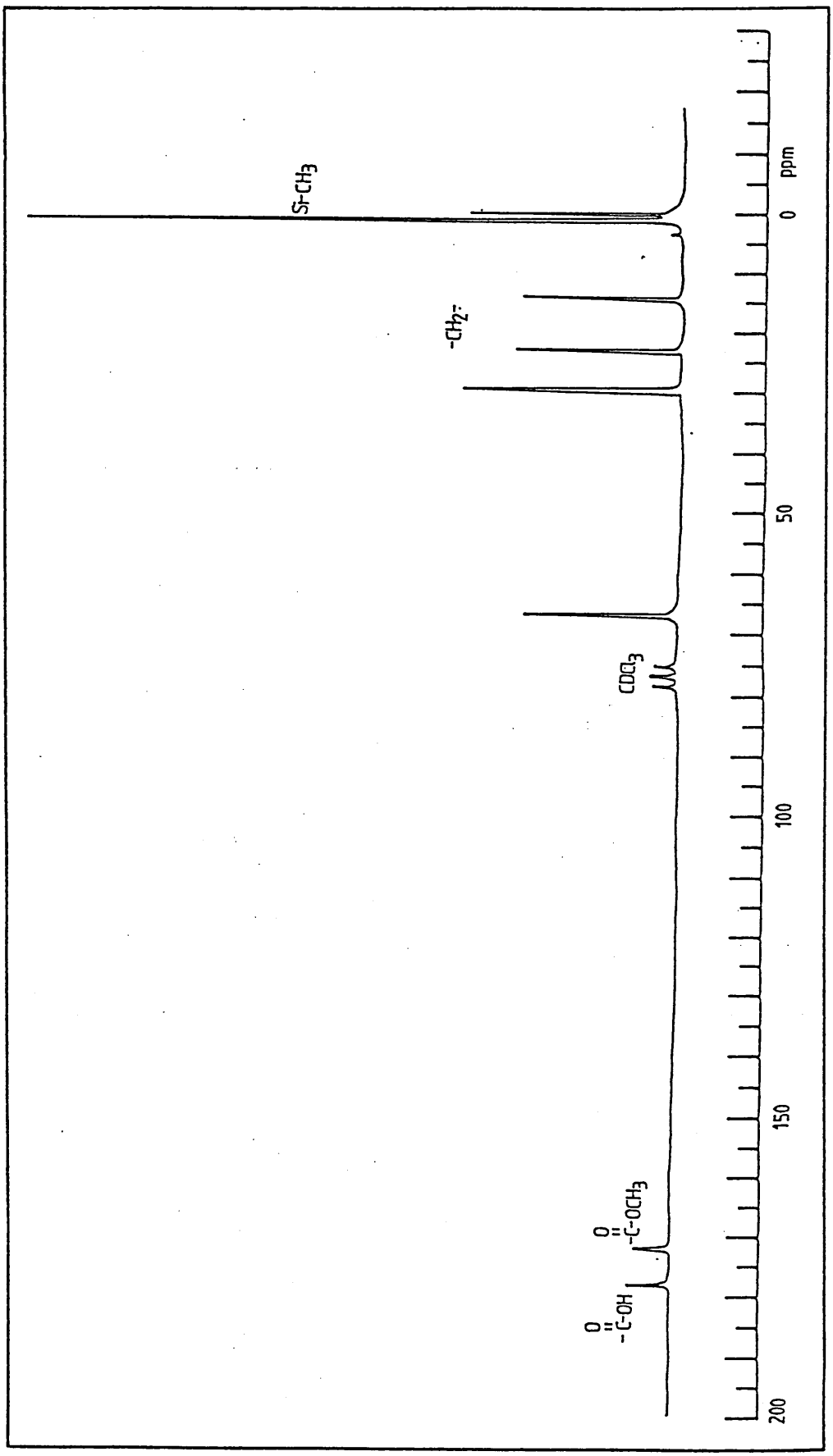

Figure 87: 80MHz ^{13}C nmr spectrum of carboxy propyl PDMS, RMM=1,000 ($CDCl_3$ solvent).

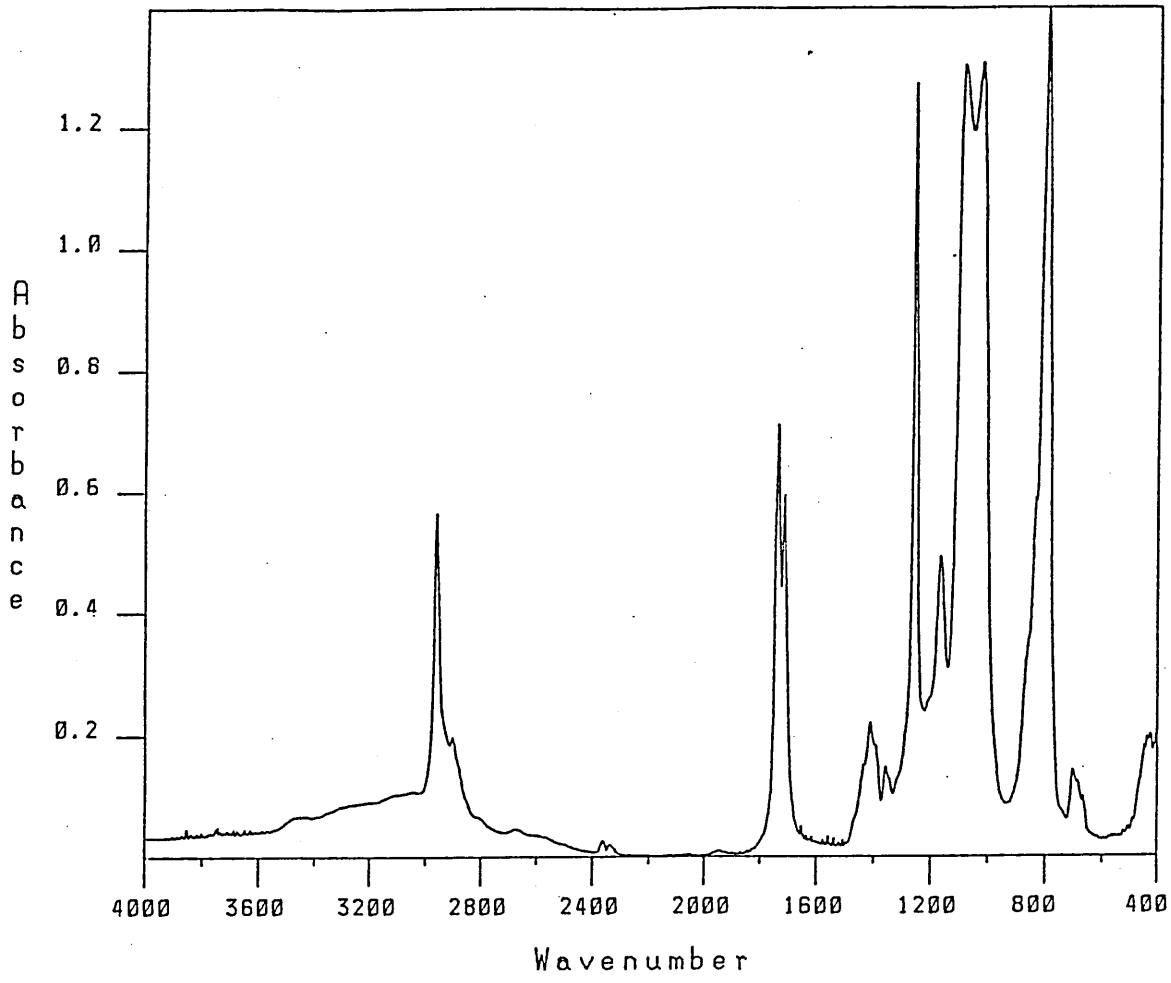

Figure 88: Infra-red spectrum of carboxy propyl PDMS (RMM=900).

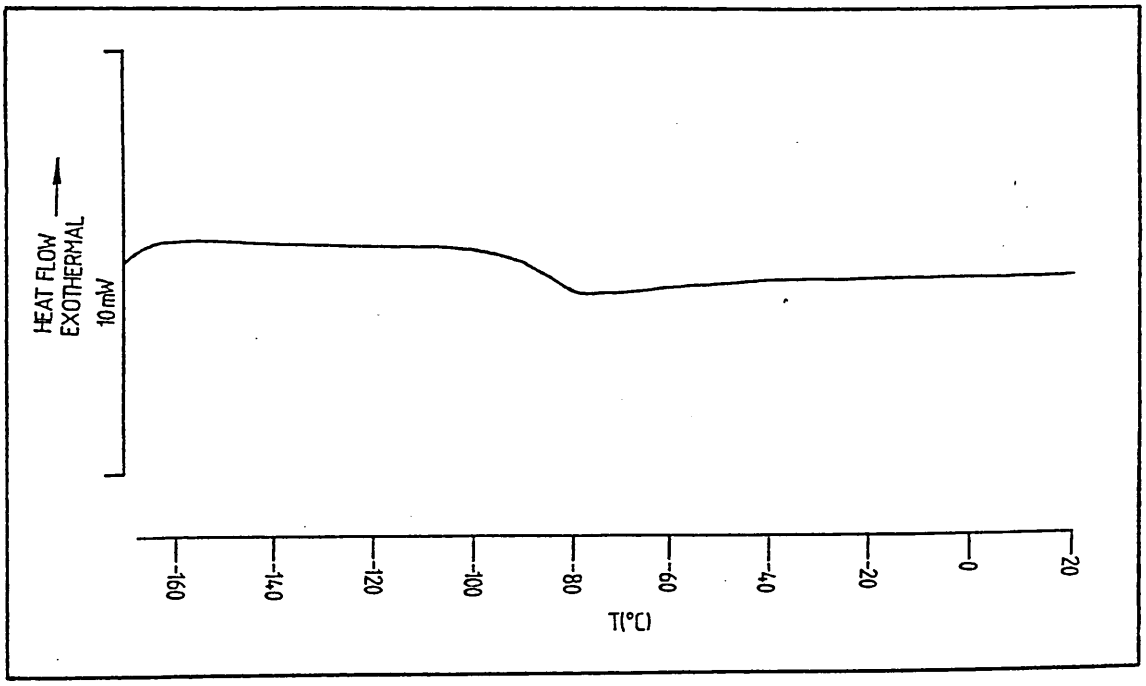

Figure 89: Dsc trace of carboxy propyl PDMS (RMM=900), Tg=-85.6°C.

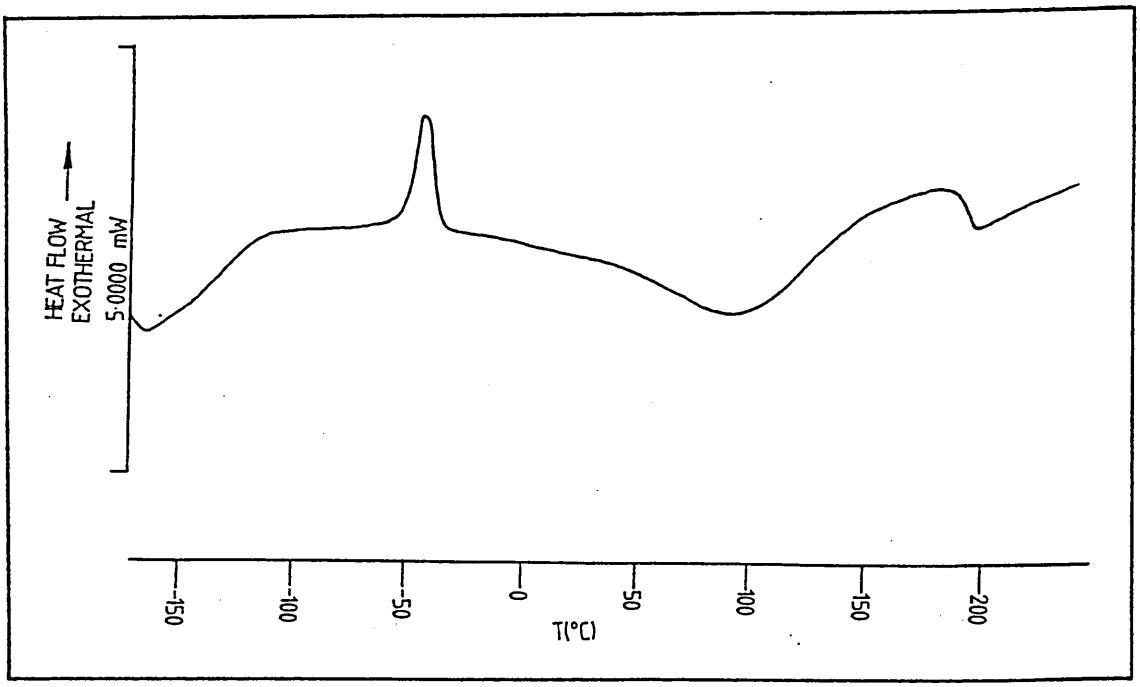

Figure 90: Dsc trace of melt reaction CB1 after toluene extraction. PES (RMM=4,370)/carboxy propyl PDMS (RMM=900).

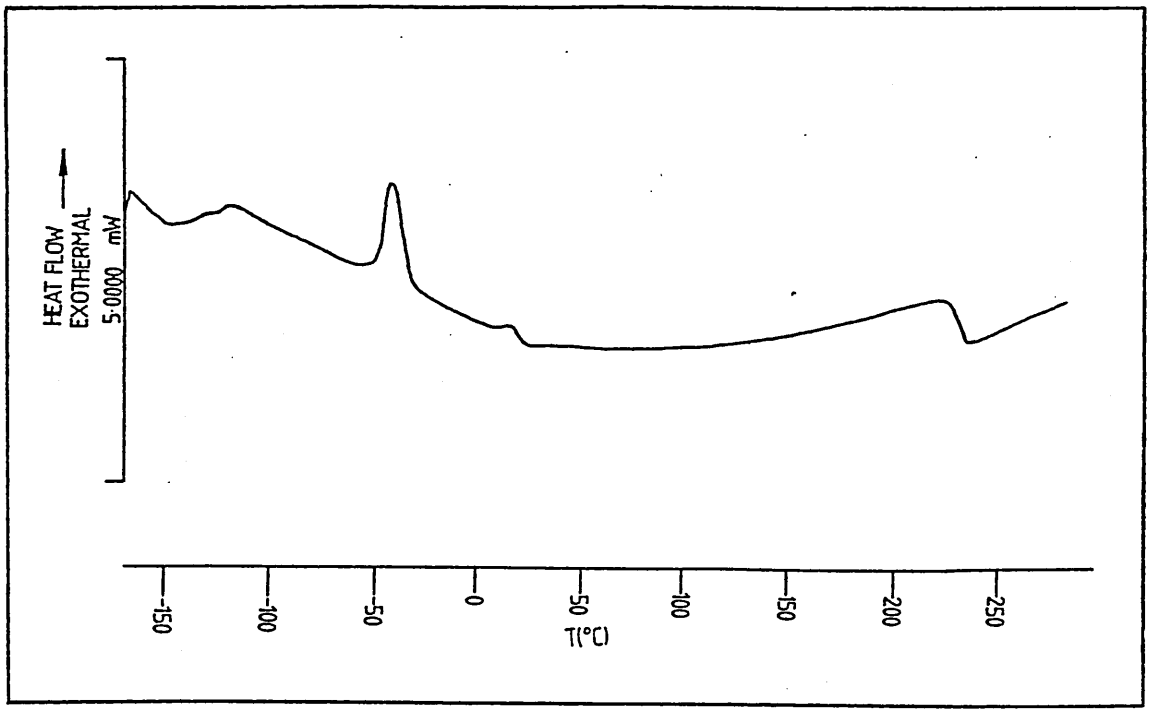

Figure 91: Dsc trace of melt reaction CB5 after toluene extraction. PES (RMM=22,124)/carboxy propyl PDMS (RMM=2,500).

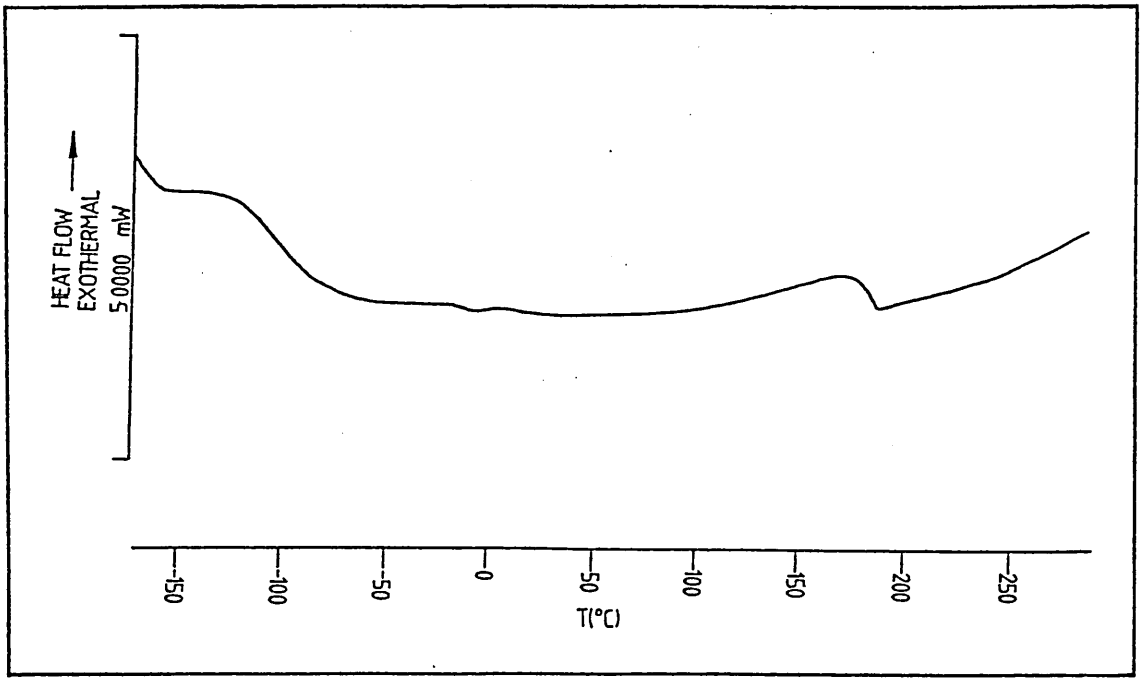

Figure 92: Dsc trace of melt reaction CB6 after toluene extraction. PES (RMM=2,112)/carboxy propyl PDMS (RMM=900).

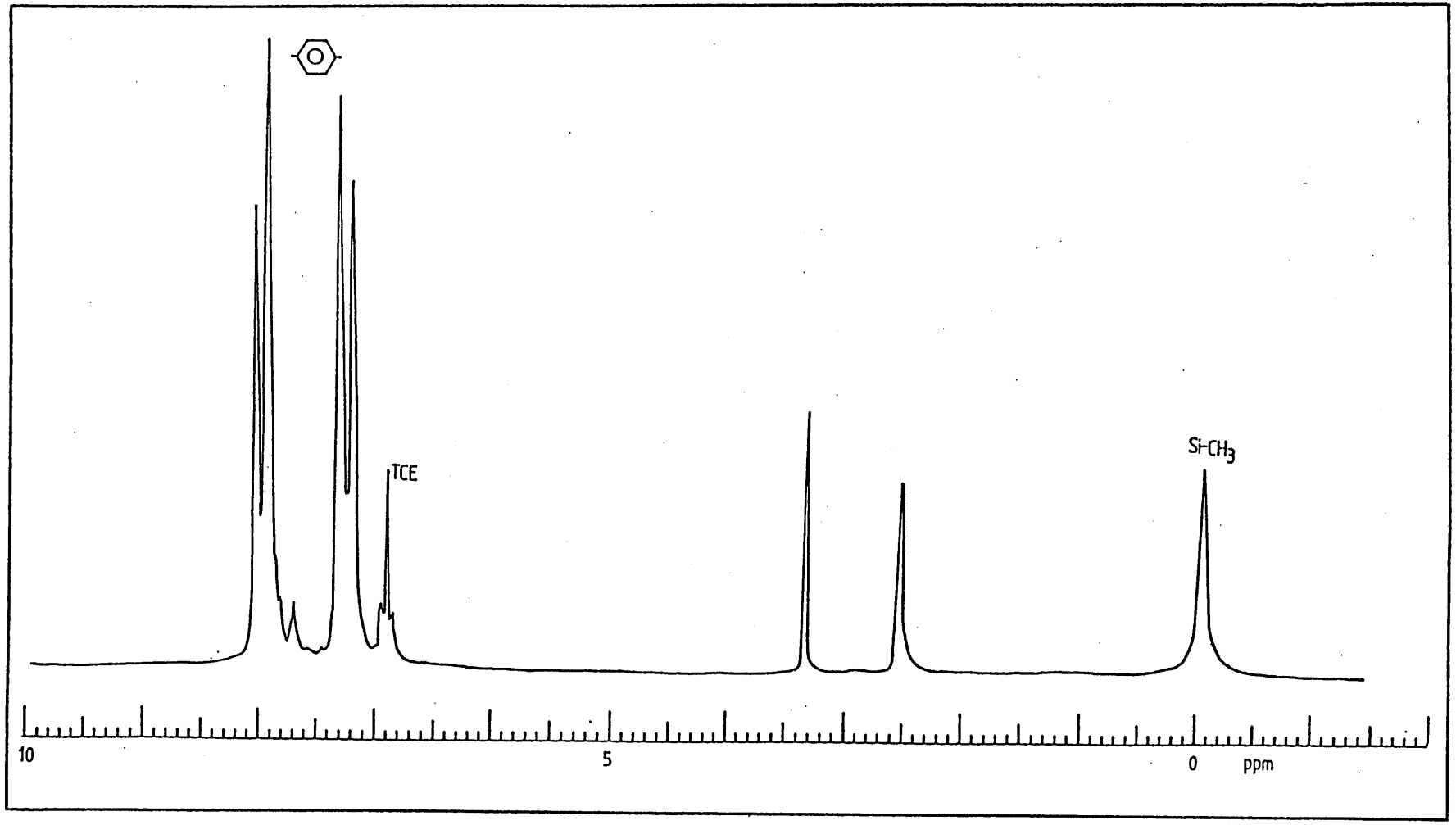

Figure 93: 80MHz ^1H nmr spectrum of hydroxyl PES (RMM=3,709)/hydride PDMS melt blend (BN1) after toluene extraction (d-DMSO) solvent).

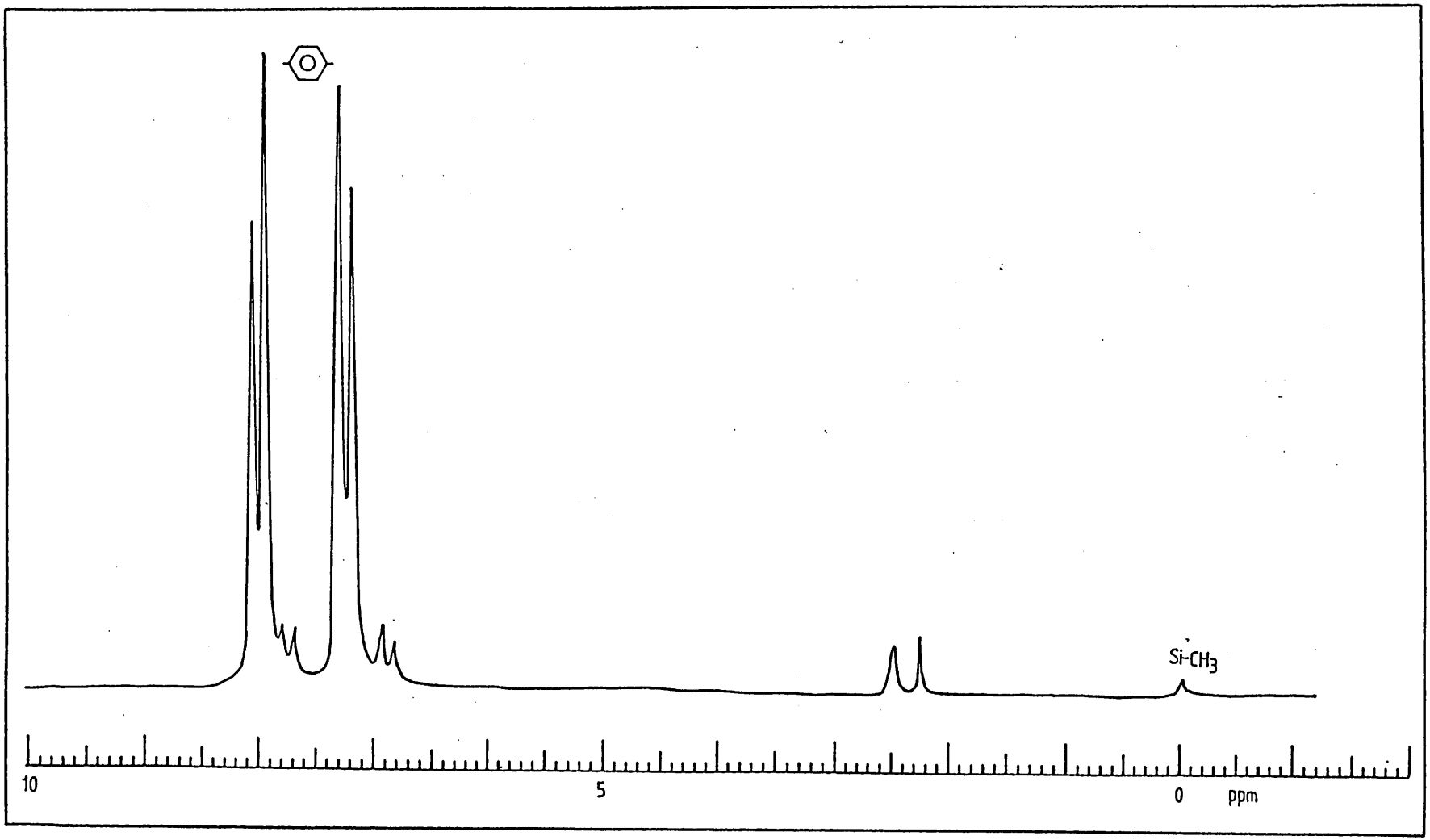

Figure 94: 80MHz ^{1}H nmr spectrum of hydroxyl PES (RMM=3,709)/trimethyl PDMS (DC200/200) melt blend (BN2) after toluene extraction (d-DMSO solvent).

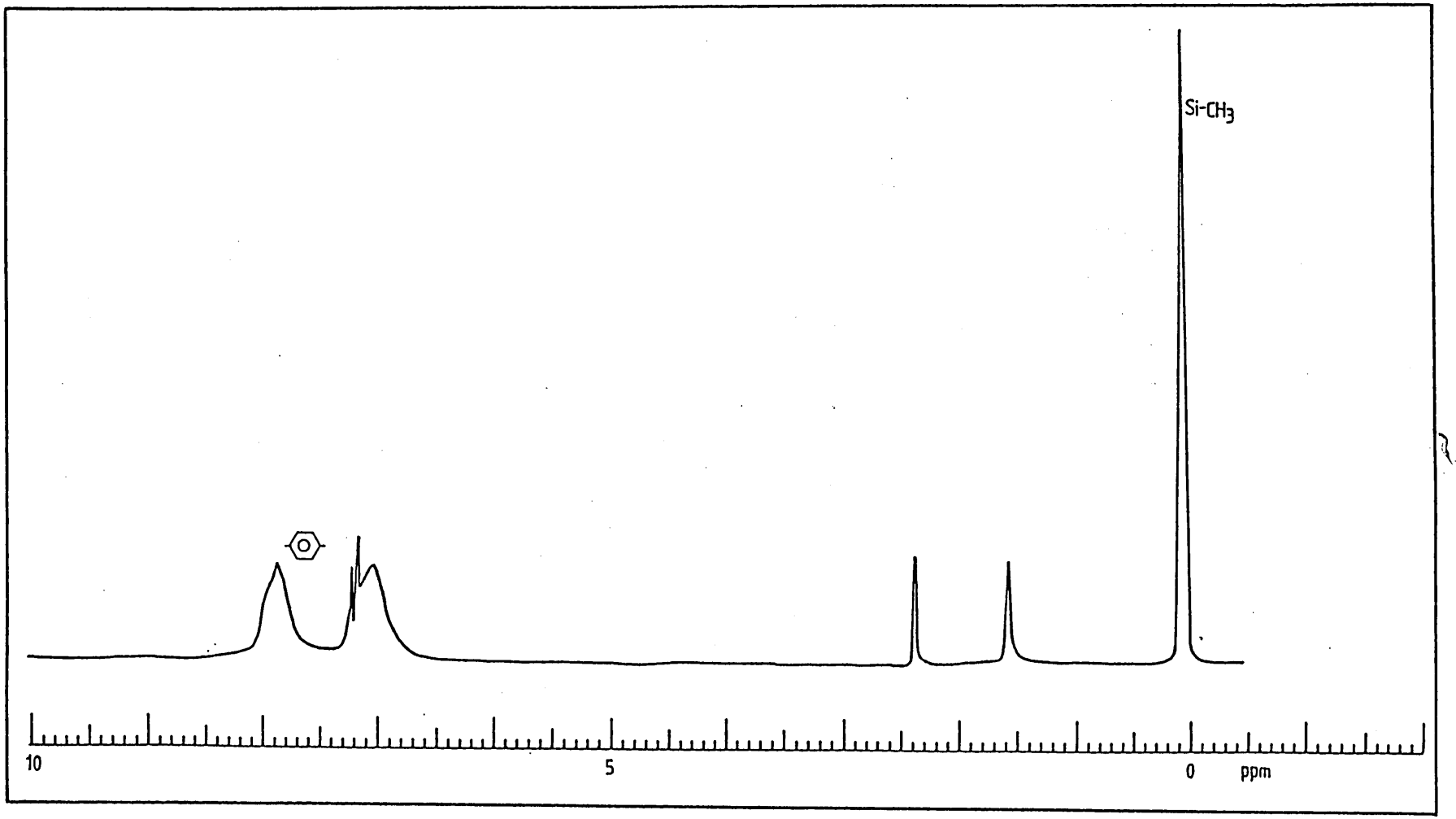

Figure 95: 80MHz ^{1}H nmr spectrum of hydroxyl PES (RMM=3,709)/trimethyl PDMS (DC200/200) melt blend (BN2) after toluene extraction ($CDCl_3$ solvent).

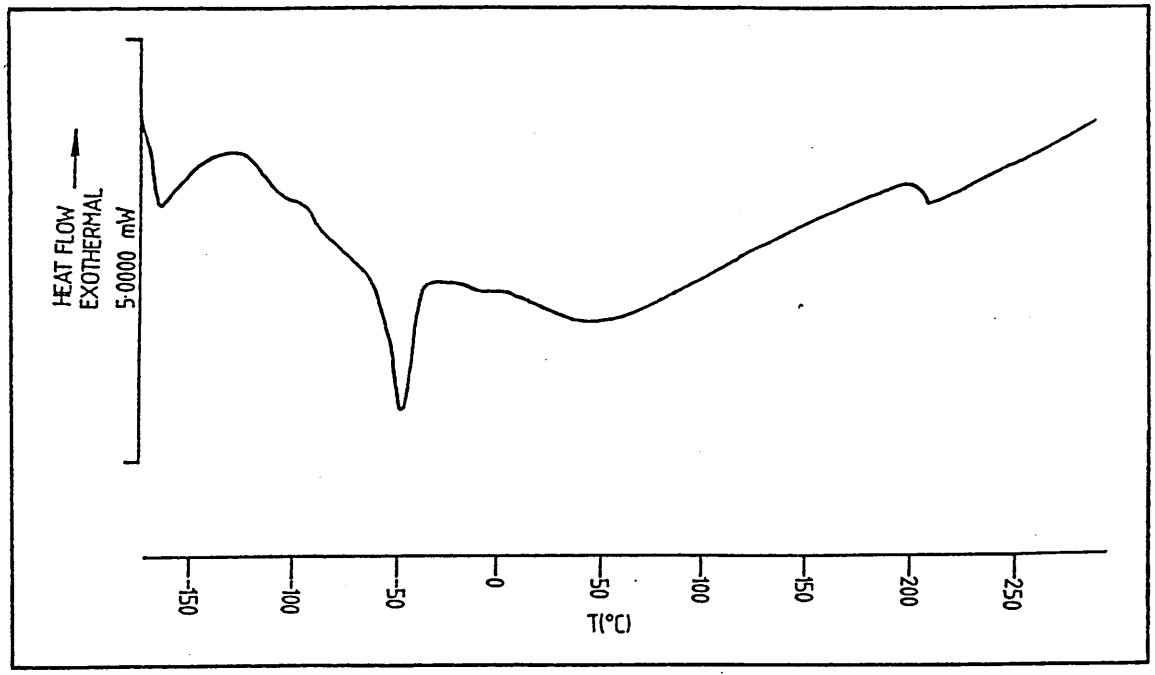

Figure 96: Dsc trace of hydroxyl PES (RMM=3,709)/hydride PDMS melt blend (BN1) after toluene extraction.

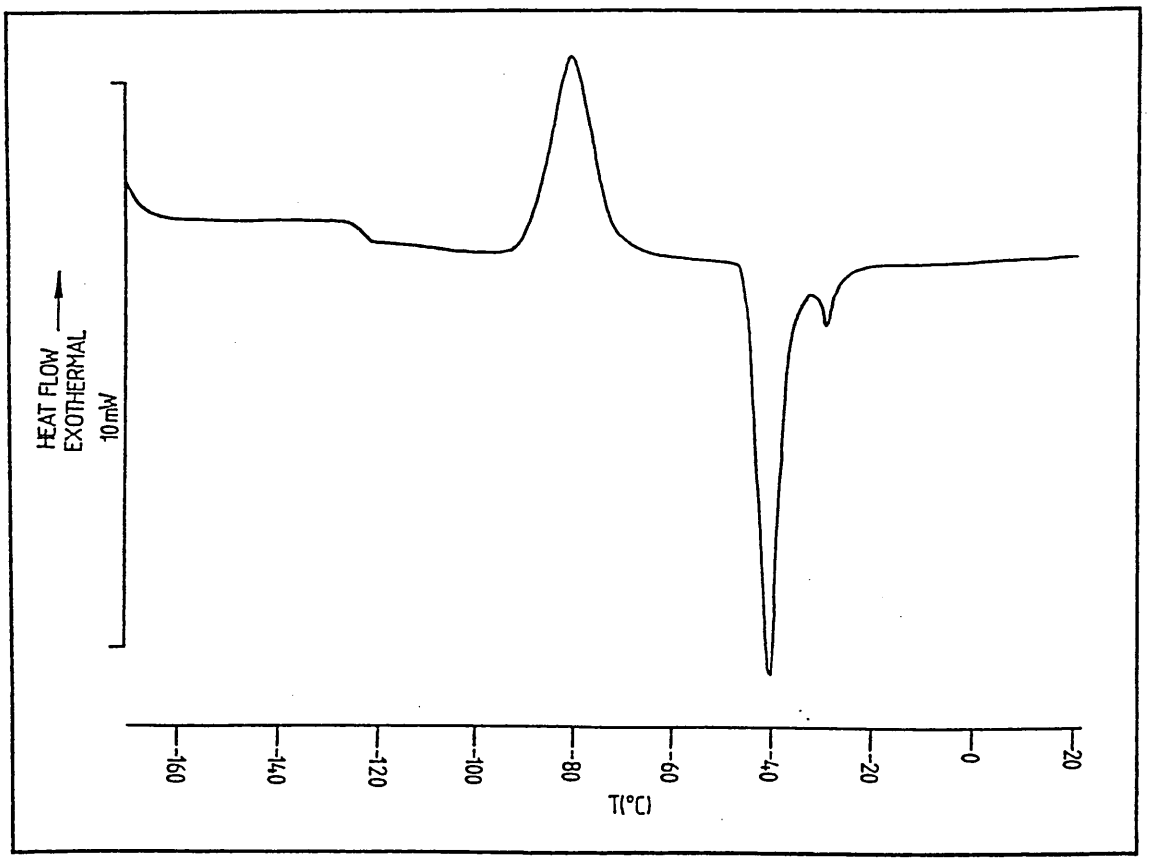

Figure 97: Dsc trace of hydride PDMS used in experiment BN1.

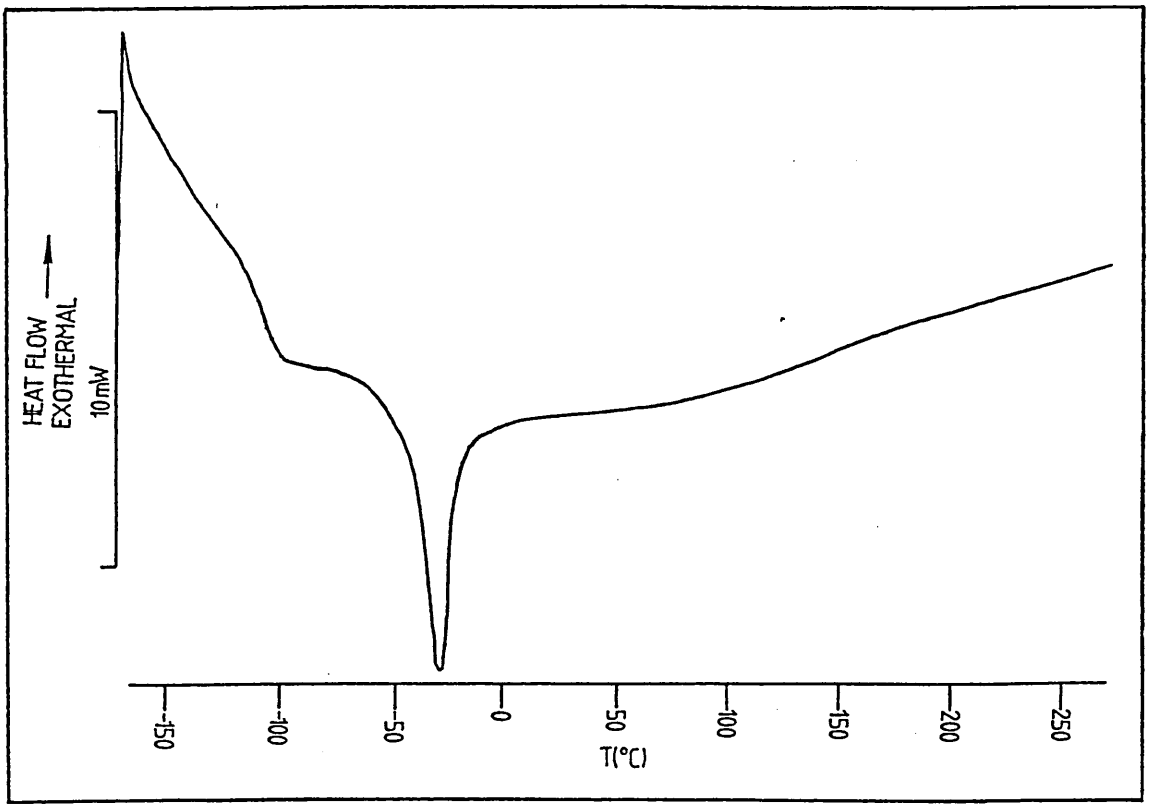

Figure 98: Dsc trace of hydroxyl PES (RMM=3,709)/hydride PDMS melt blend (BN1) after TCE extraction.

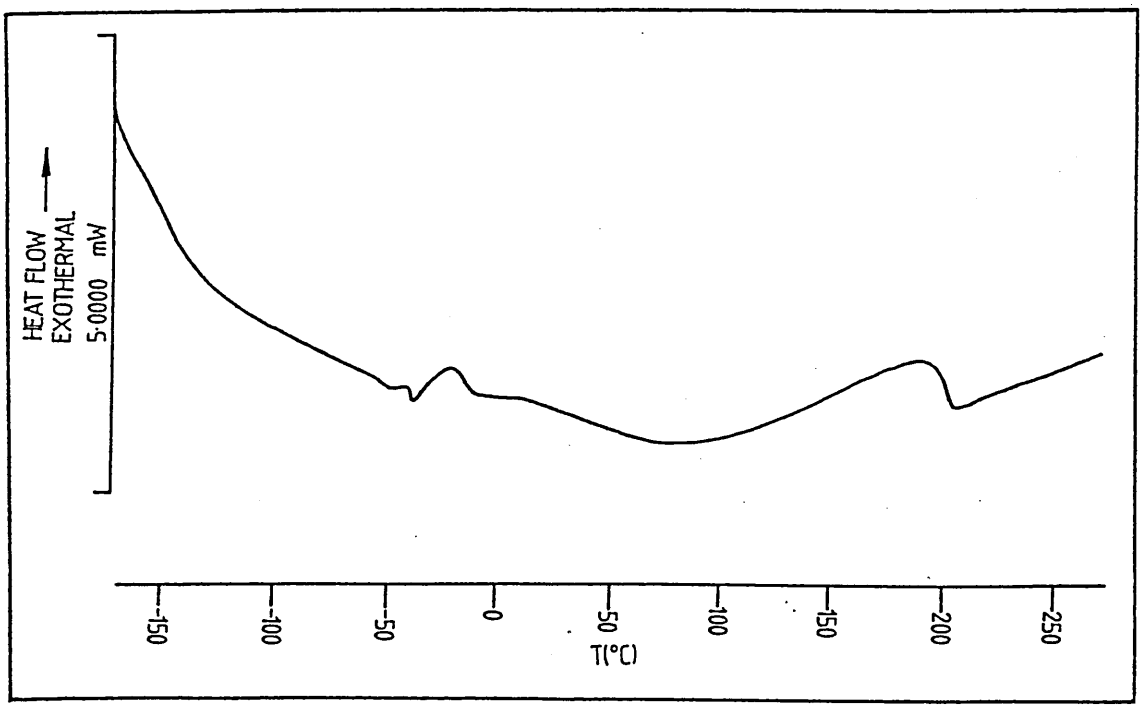

Figure 99: Dsc trace of hydroxyl PES (RMM=3,709)/trimethyl PDMS (DC200/200) melt blend (BN2) after toluene extraction.

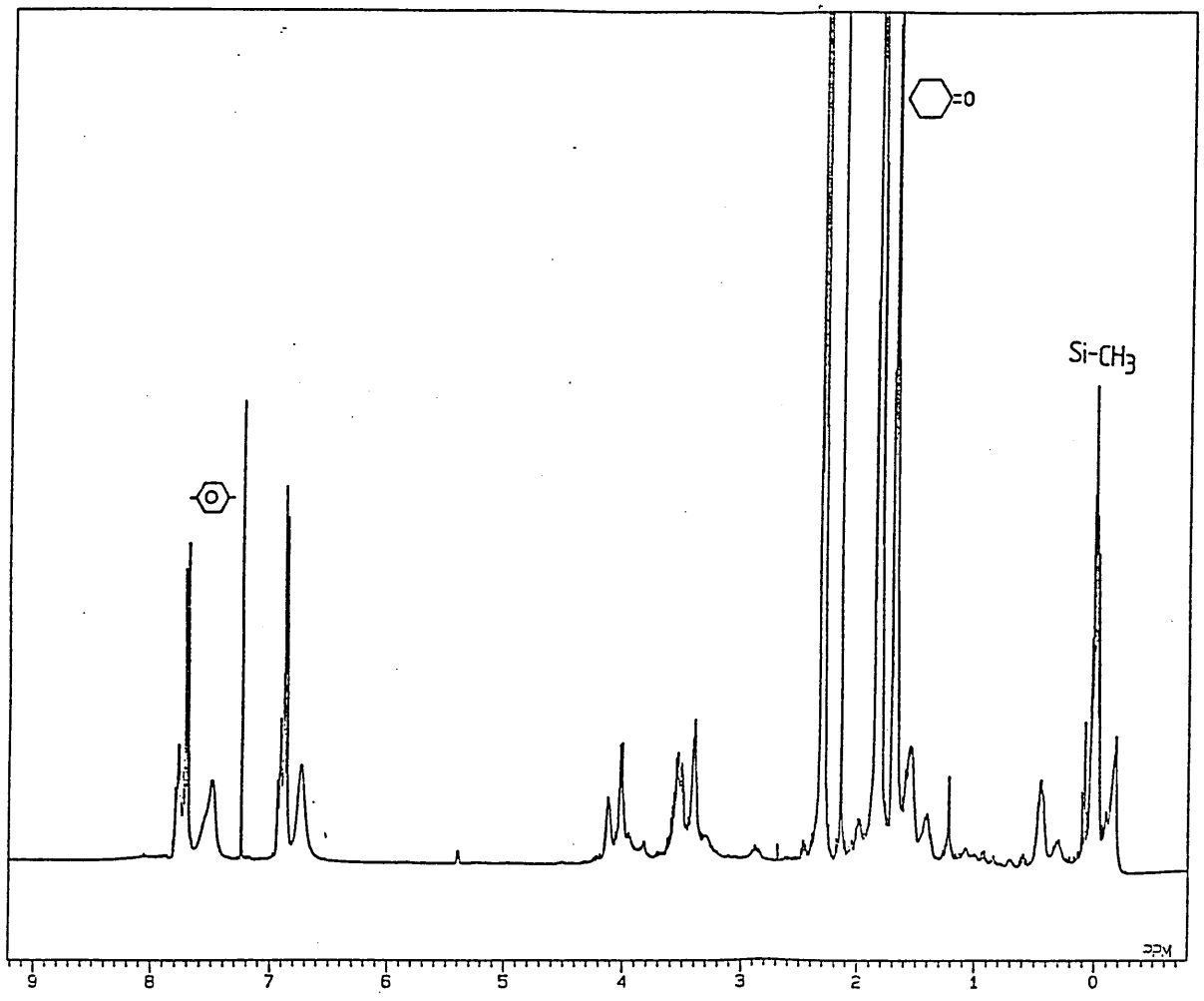

Figure 100: 400MHz ^1H nmr spectrum of reaction E1, Bisphenol"S"/epoxy PDMS (d-DMSO solvent).

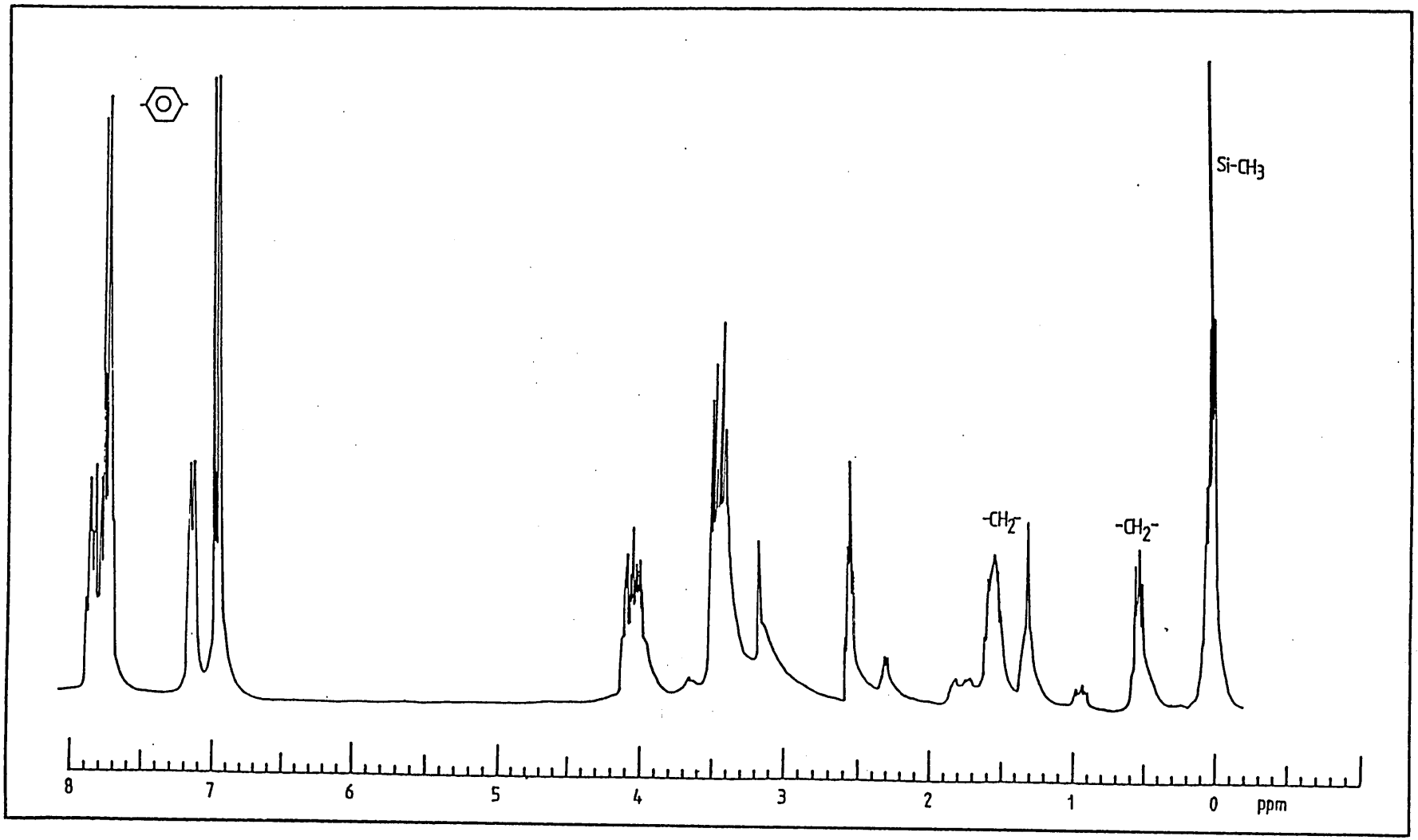

Figure 101: 400MHz ^1H nmr spectrum of reaction E1 (Bispenol"S"/epoxy PDMS) material soluble in $CDCl_3$.

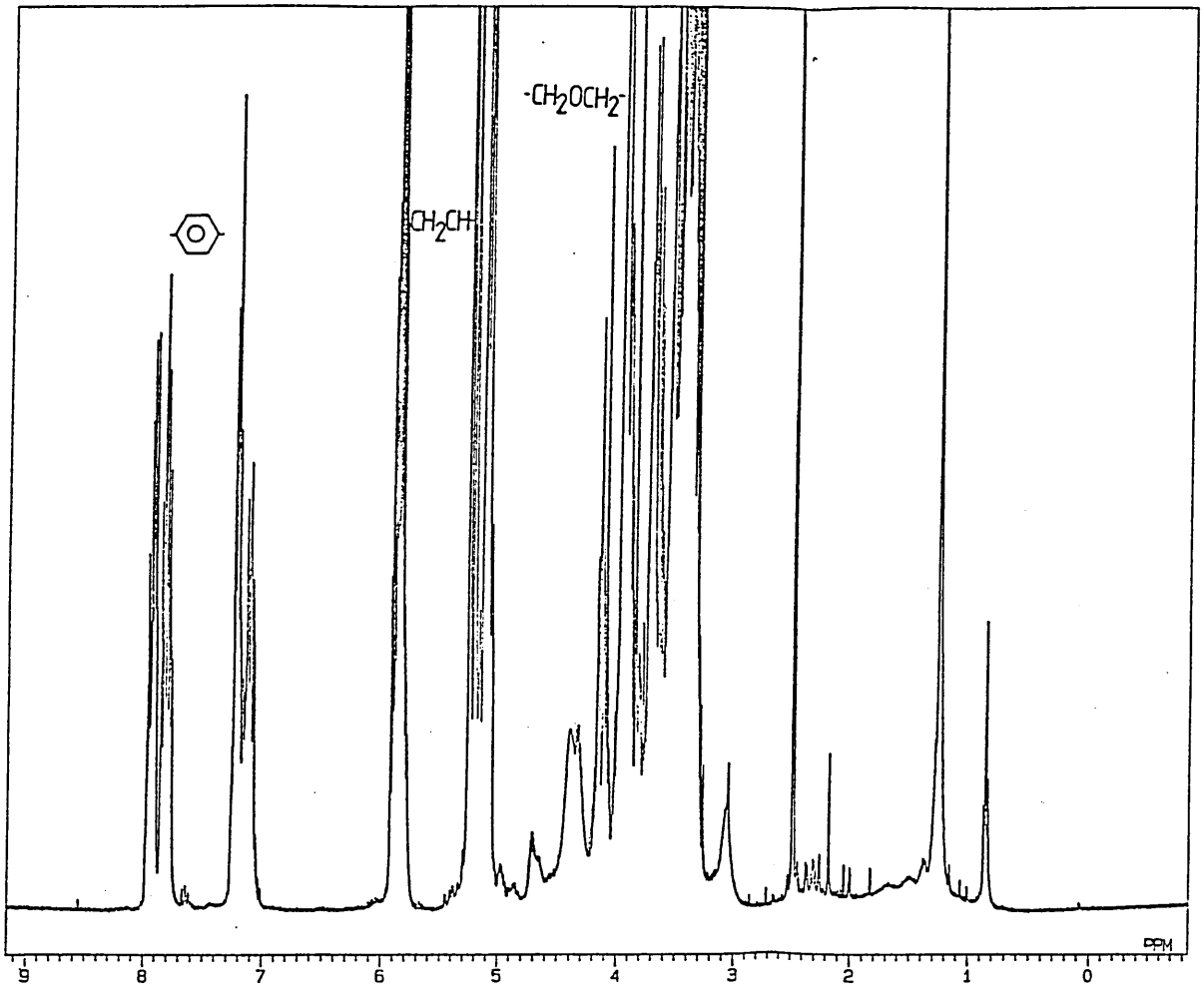

Figure 102: 400MHz ^1H nmr spectrum of reaction E2, hydroxy PES/allyl glycidyl ether (d-DMSO solvent).

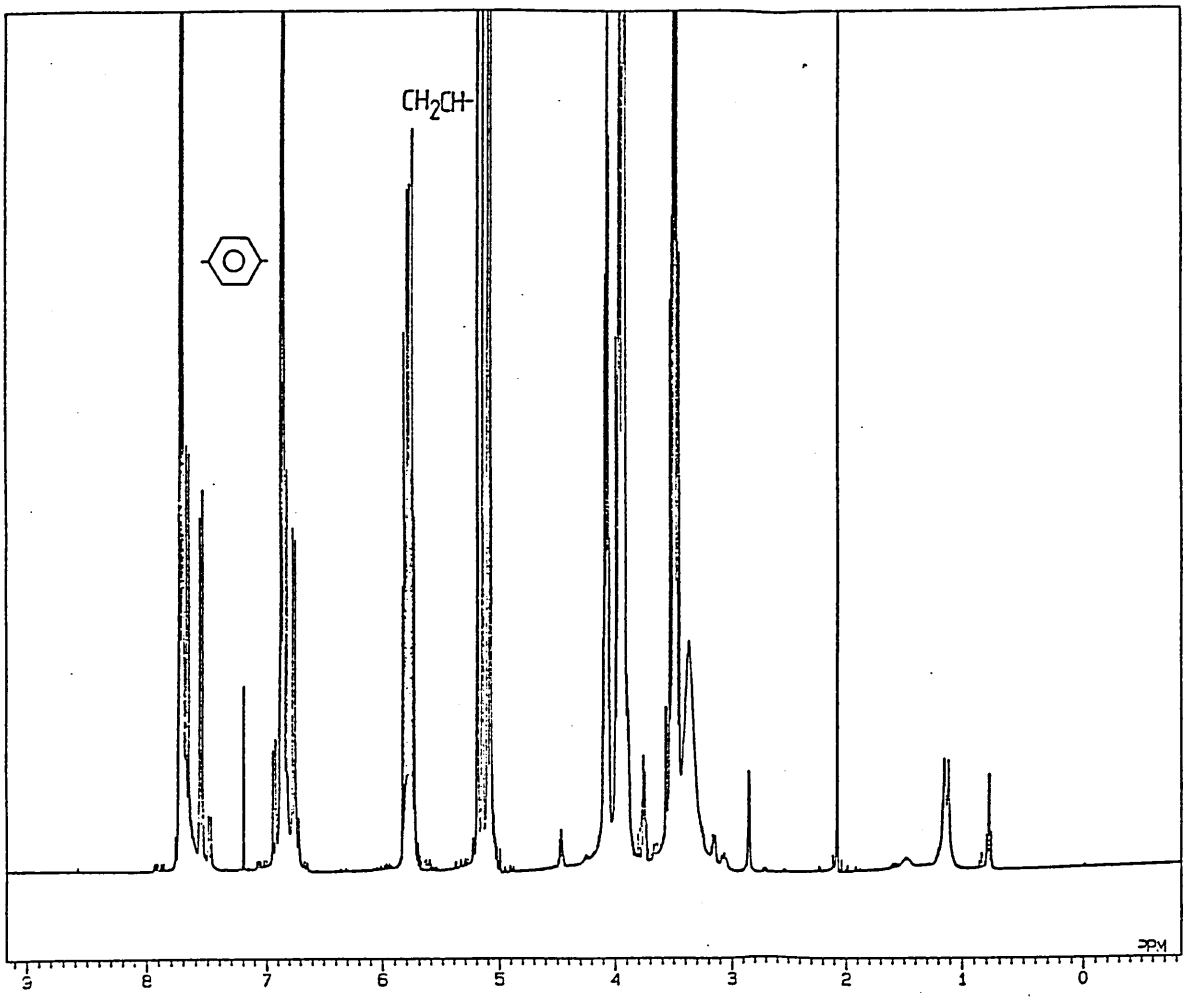

Figure 103: 400MHz ^{1}H nmr spectrum of the reaction product of allyl glycidyl ether and Bisphenol"S" (d-DMSO solvent).

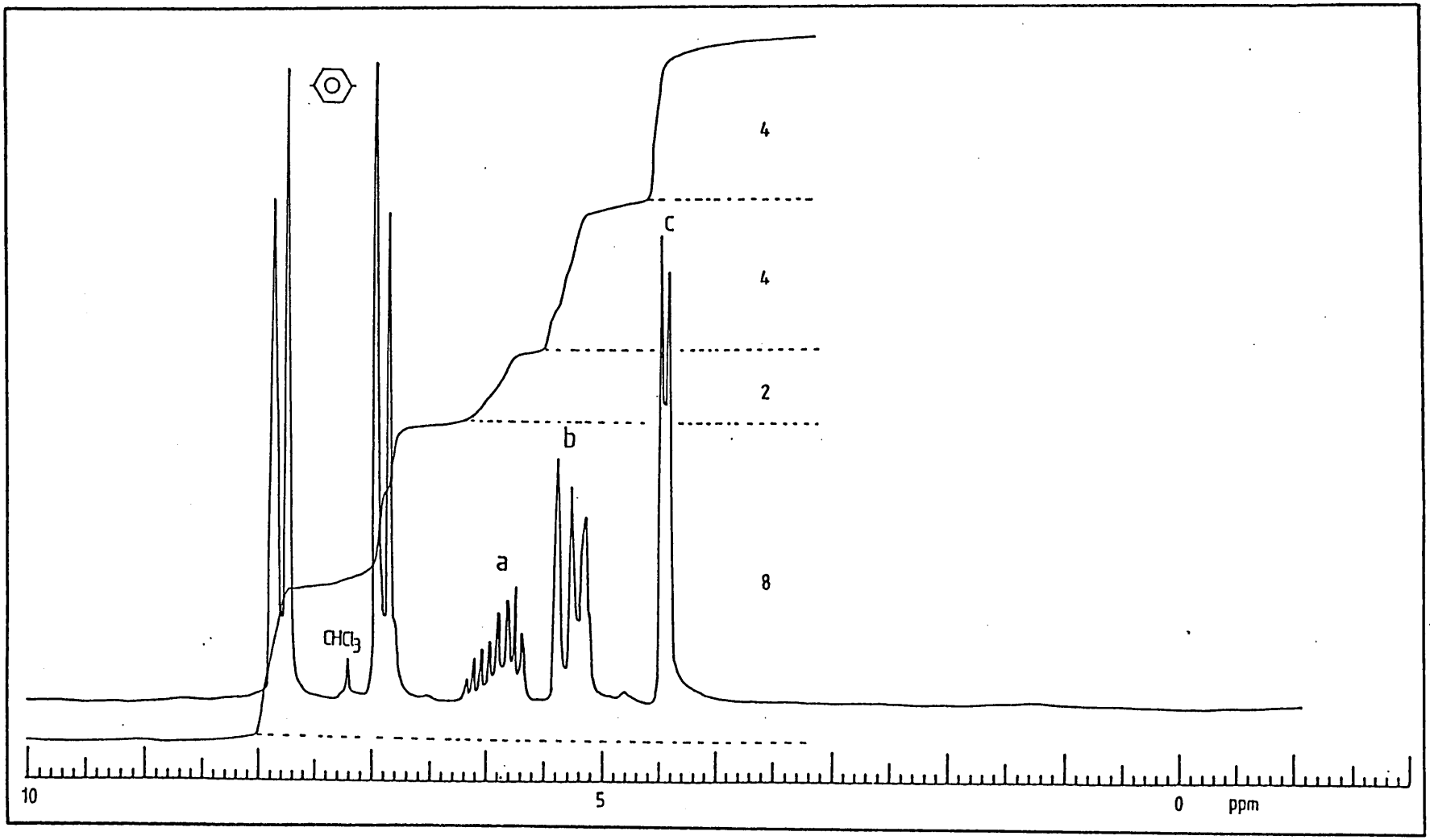

Figure 104: 80MHz ^1H nmr spectrum of vinyl Bisphenol"S" ($CDCl_3$ solvent).

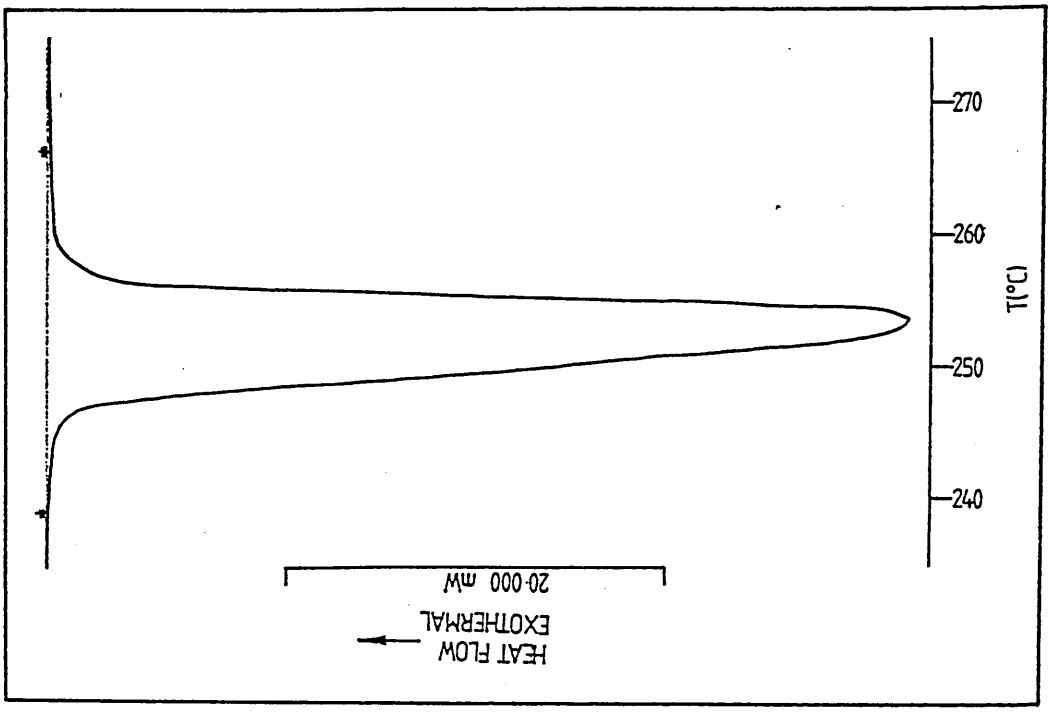

Figure 106: Dsc trace of Bisphenol"S".

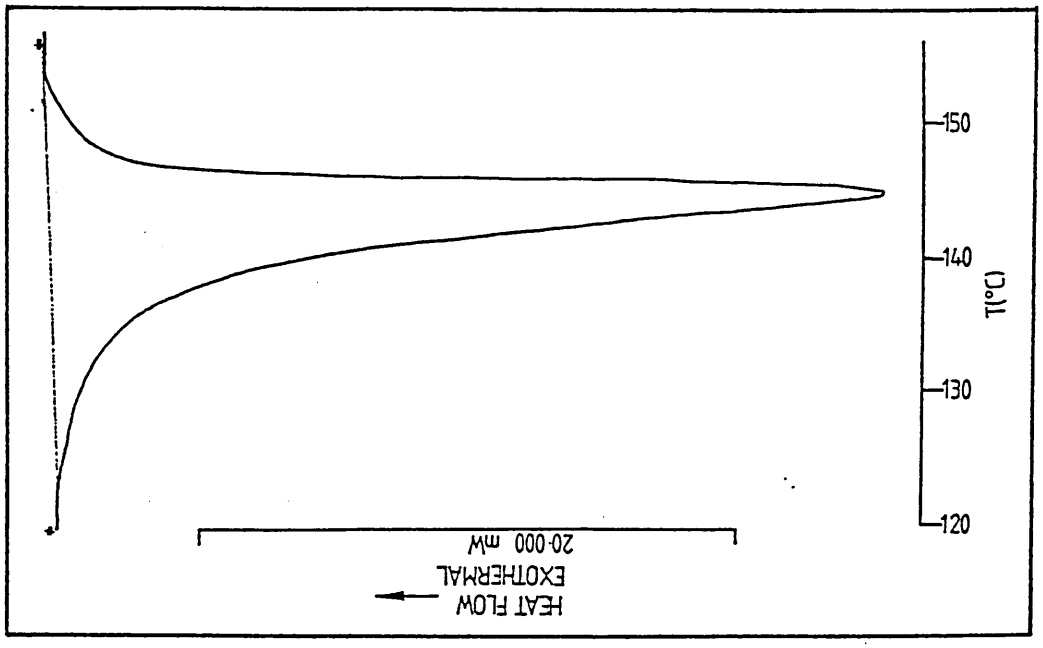

Figure 105: Dsc trace of vinyl Bisphenol"S".

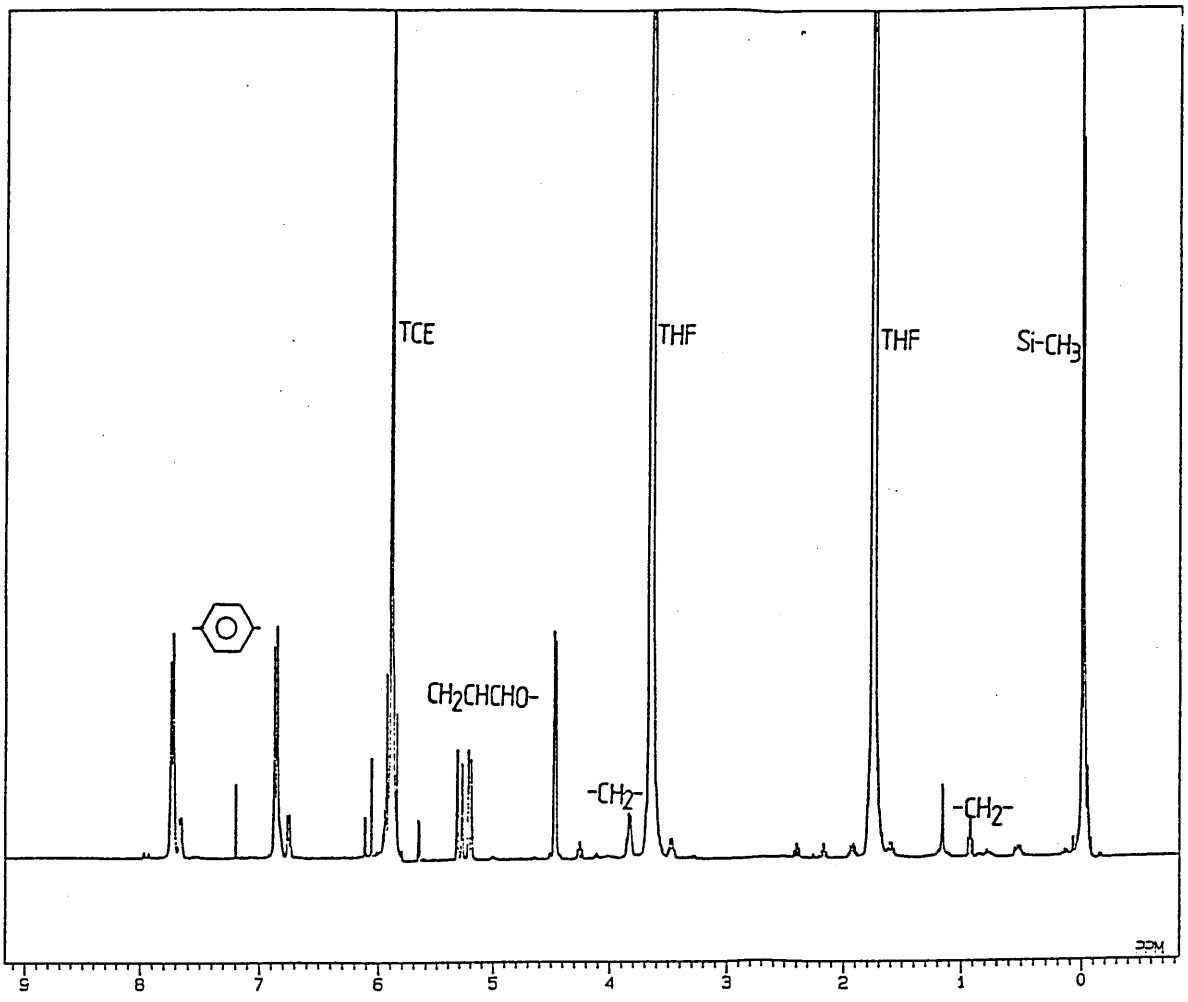

Figure 107: 400MHz ^{1}H nmr spectrum of the solution vinyl addition product of v-Bisphenol"S"/disiloxane in TCE, VS1 ($CDCl_3$ solvent).

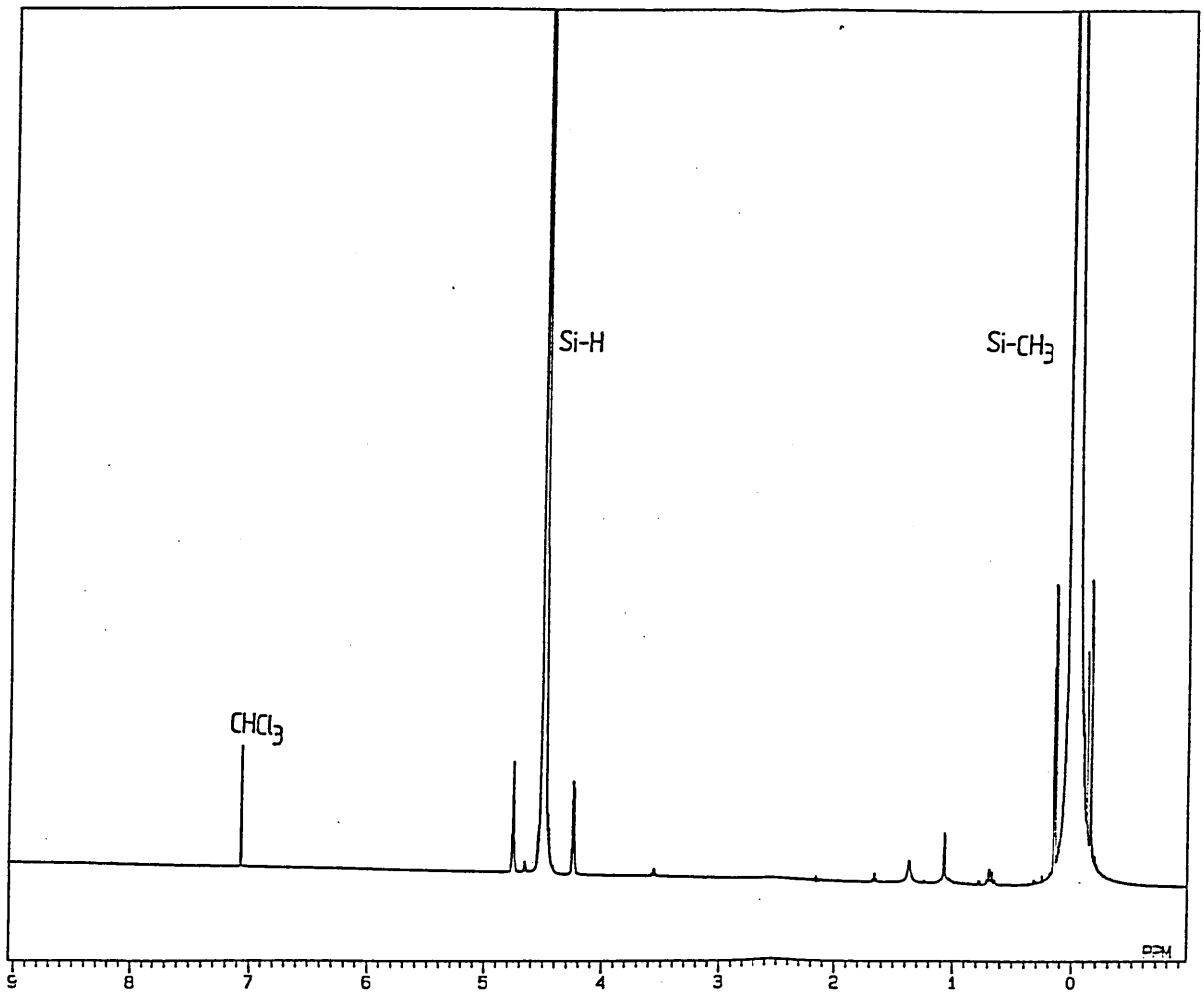

Figure 108: 400MHz ^1H nmr spectrum of 1,1,3,3-tetramethyldisiloxane ($CDCl_3$ solvent).

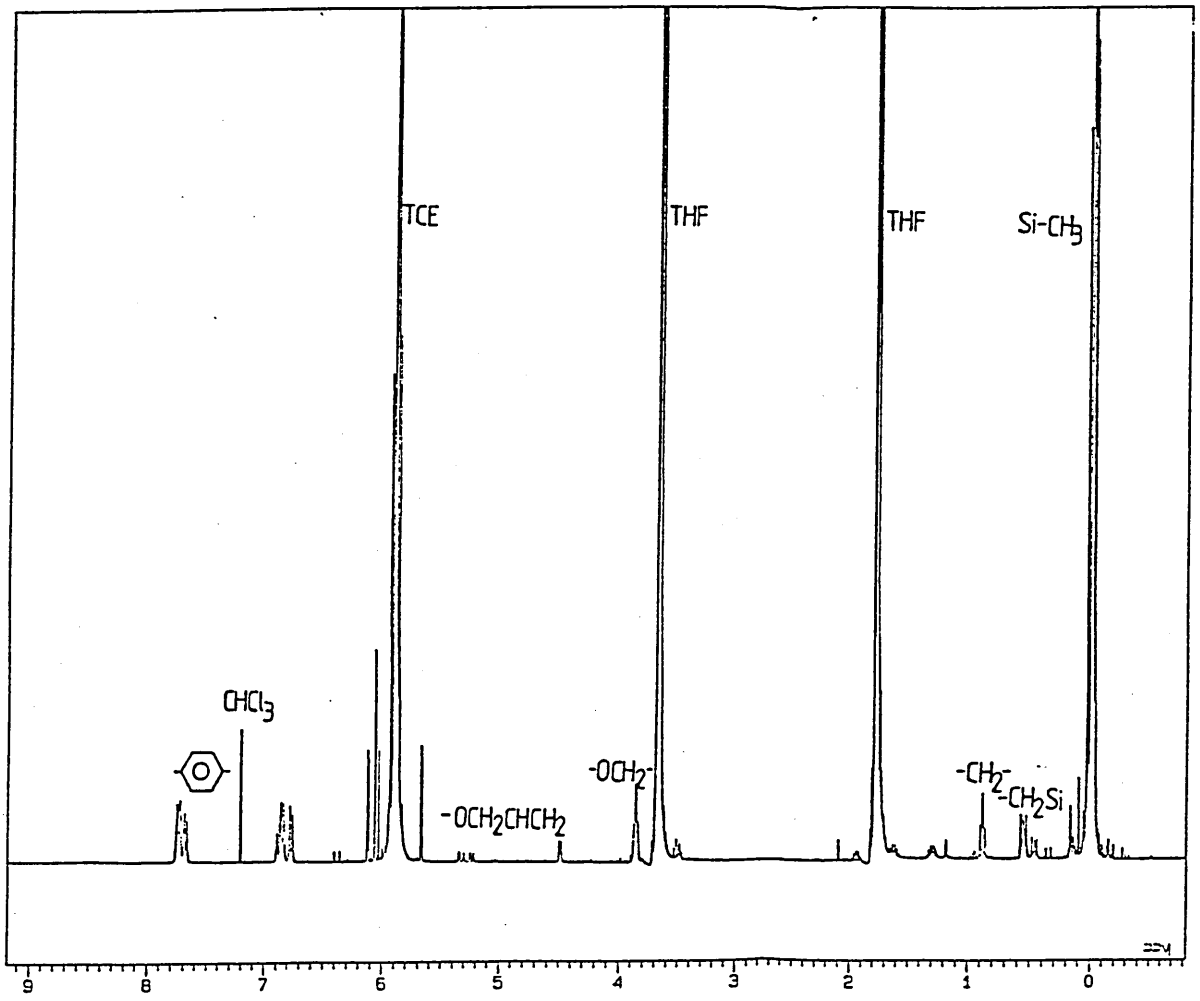

Figure 109: 400MHz ^1H nmr spectrum of the solution vinyl addition product of v-Bisphenol"S"/hydride PDMS in TCE, VS2 ($CDCl_3$ solvent).

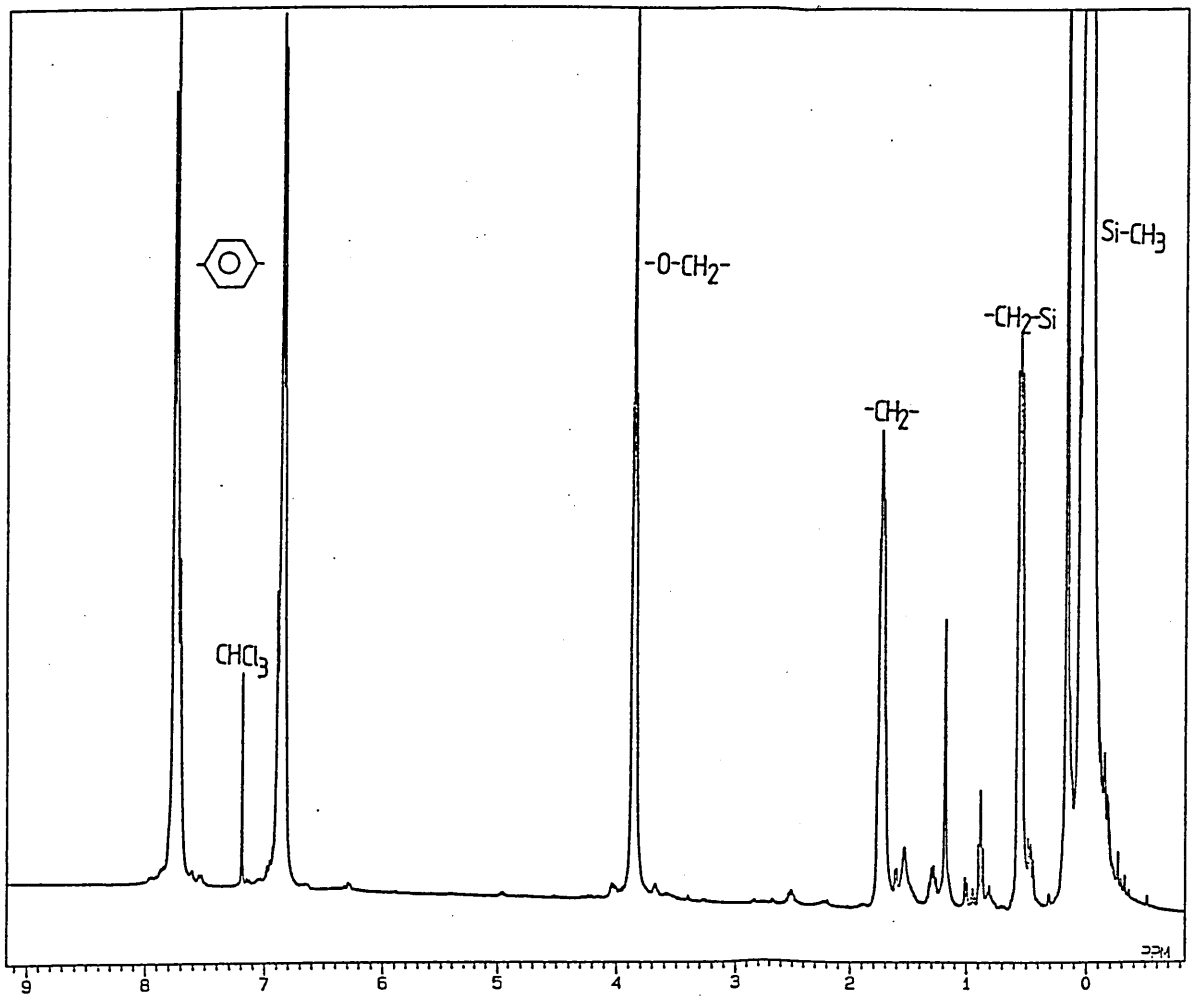

Figure 110: 400MHz ^1H nmr spectrum of the melt reaction product of vinyl Bisphenol"S"/hydride PDMS ($CDCl_3$ solvent).

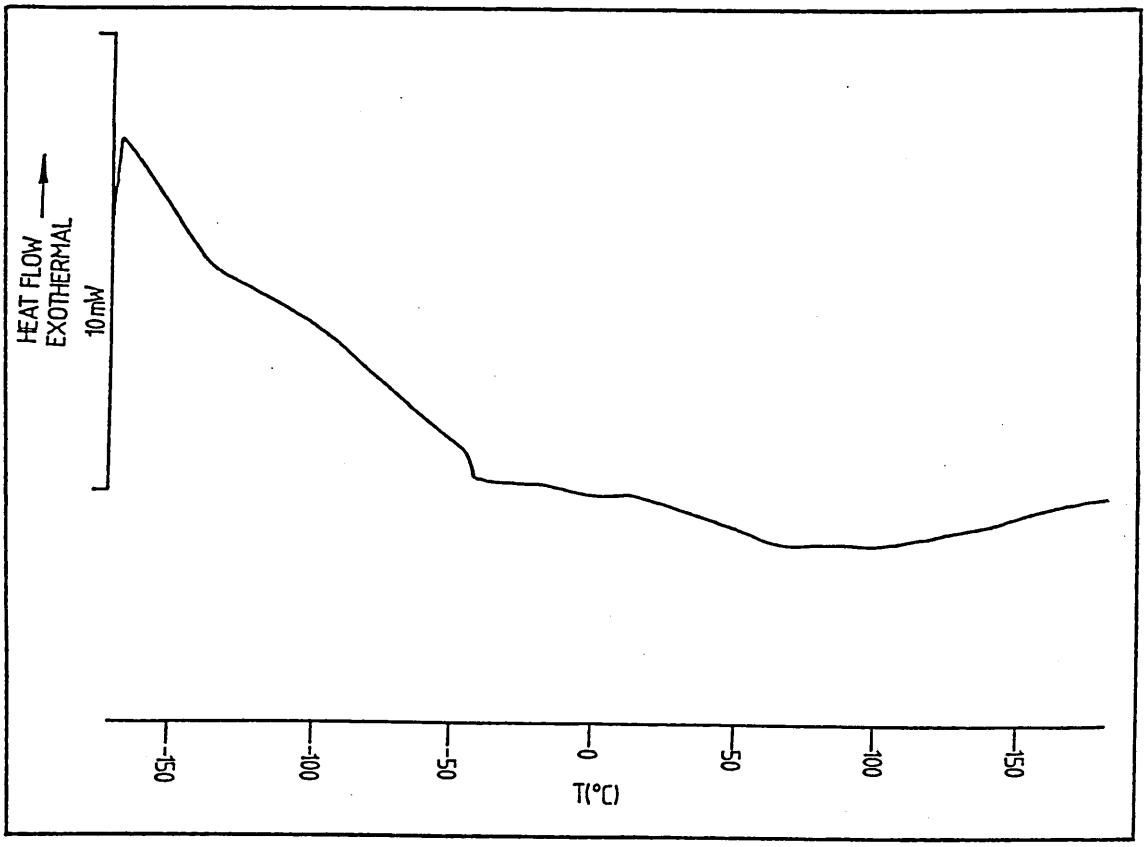

Figure 111: Dsc trace of the melt reaction product of v-Bisphenol"S"/hydride PDMS.

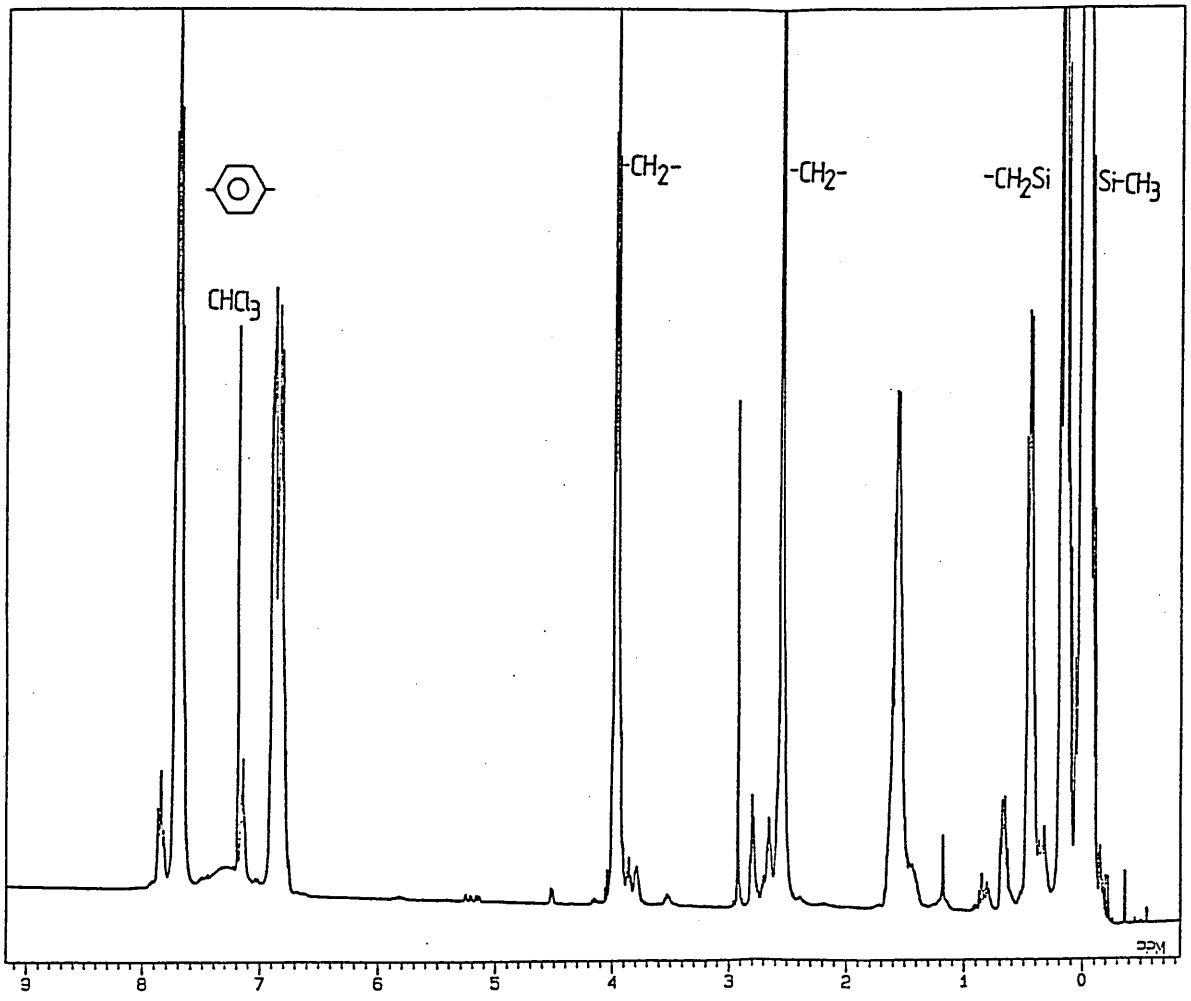

Figure 112: 400MHz ^1H nmr spectrum of the melt reaction product of Bisphenol"S"/carboxy propyl PDMS ($CDCl_3$ solvent).

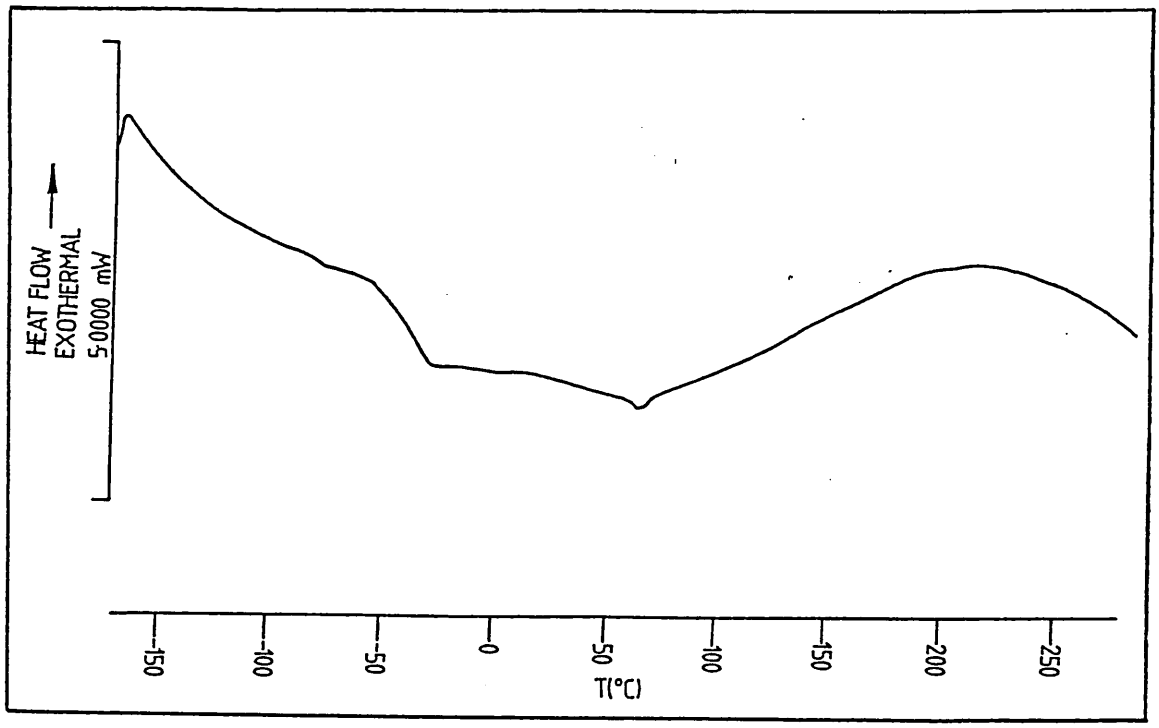

Figure 113: Dsc trace of the melt reaction product of Bisphenol"S"/carboxy propyl PDMS.

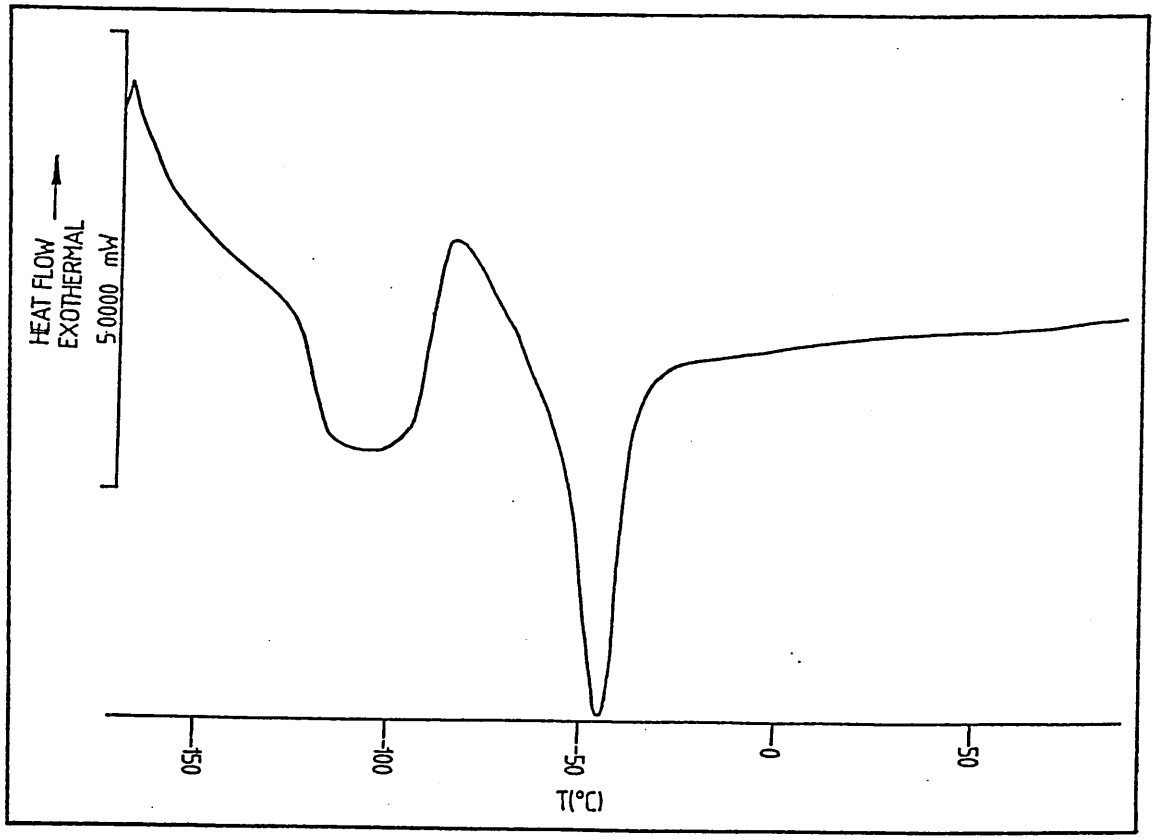

Figure 114: Dsc trace of carboxy propyl PDMS chain extension product.

TABLE 1.

Interpretation of the infra-red spectrum of PES oligomers.

Absorption Peak (cm^{-1})	Bond Stretch
3430	OH
3090	C-H aromatic
1585	C-H aromatic
1495	C-H aromatic
1325	SO_2 assymetrical stretch
1300	SO_2 assymetrical stretch
1250	C-O-C
1125	SO_2 assymetrical stretch
870	para-substituted aromatic
830	para-substituted aromatic
695	out of plane ring bending

TABLE 2.

Polymer	%xs monomer	Calculated Value	RMM RV	RMM Gpc	RMM ^{1}H nmr	%HMS
1	1.5	31,206	19,635	16,900	33,186	8.5
2	1.5	31,206	20,995	13,700	22,124	9.4
3	4	11,847	7,380	9,300	16,593	7.8
4	6	7,976	6,902	10,500	6,733	5.2
5	1.5	31,206	8,880	9,790	10,324	11.8
6	4	11,847	8,370	10,800	9,292	8.2
7	1.5	31,206	20,312	16,100	35,739	17.2
8	3	15,719	10,476	10,200	19,358	9.4
9	4	11,847	7,380	9,940	14,519	7.2
10	6	7,976	----	8,310	14,519	5.5
11	9.8	5,205	----	7,230	11,913	7.2
12	20.43	2,500	----	4,370	5,881	4.0
13	15.98	3,140	----	----	3,709	5.9
14	30	1,781	----	----	2,112	6.5
5003P	1.5	31,206	24,532	----	37,756	-

TABLE 3

Interpretation of the infra-red spectra of linear hydride PDMS oligomers.

Absorption Peak (cm^{-1})	Bond Stretch
2960	C-H aliphatic
2120	Si-H
1260	$Si-CH_3$
1090 and 1020	Si-O-Si
800	Si-C

TABLE 4

RMM determined by ^1H nmr and gpc for hydride PDMS.

Sample	RMM	
	^1H nmr	gpc
1	575	501
2	4,246	4,466
3	4,420	4,121
4	5,673	5,370
5	4,160	4,315
6	3,495	3,935